

ABSTRACT

Title of dissertation: PROBING SUPERSYMMETRIC GRAND
UNIFICATION WITH CP AND
FLAVOR VIOLATIONS

Parul Rastogi
Doctor of Philosophy, 2006

Dissertation directed by: Professor J. C. Pati
Department of Physics

A major part of my thesis is devoted to explore certain issues of CP and flavor violations in conjunction with those of fermion masses and neutrino oscillations in the context of supersymmetric grand unification. An attempt is made to present a *unified description* of four phenomena: (i) fermion masses and mixings, (ii) neutrino oscillations, (iii) CP non conservation and (iv) flavor violations in both the quark and the lepton sectors, in accord with observations, within a single predictive framework based on supersymmetric SO(10) or an effective $G(224)$ symmetry.

Including standard model and supersymmetric contributions, it is shown that the framework correctly accounts for Δm_K , Δm_{B_d} , $S(B_d \rightarrow J/\psi K_s)$ and ϵ_K . While SUSY-contribution is small (few%) for the first three quantities, that to ϵ_K is found to be sizable ($\sim 20\text{-}25\%$) and negative relative to the standard model as desired. The model predicts $S(B_d \rightarrow \phi K_s)$ to be in the range $+(0.65\text{--}0.73)$, close to the standard model prediction; it yields $Re(\epsilon'/\epsilon)_{SUSY} \approx +(4 - 14) \times 10^{-4}$. The model also predicts that the electric dipole moments of the neutron and the electron

should be discovered with improvements in current limits by factors of 10 to 100.

Assuming SUSY-messenger scale to be higher than the GUT scale, it is found that post-GUT physics, which has commonly been neglected in the literature, contributes significantly to CP and flavor violating processes. Including such contributions, the model predicts enhanced rates for $\mu \rightarrow e\gamma$, $\tau \rightarrow \mu\gamma$ and $\mu N \rightarrow eN$ which should be seen in forthcoming experiments.

A comparison of two promising SO(10) models, one with hierarchical fermion mass matrices (by Babu, Pati and Wilczek), and the other with lop-sided mass matrices (by Albright and Barr) is done, as regards their predictions regarding CP and flavor violations. Crucial tests are noted which would sharply distinguish between the models.

Envisaging string origin of the effective unification symmetry in 4D, the second part of my thesis will explore the issue of gauge coupling unification at the string scale when supersymmetric standard model and an extension is embedded in an effective G(224) or $G(214) \equiv SU(2)_L \times U(1)_{I_{3R}} \times SU(4)^c$ symmetry near the GUT scale.

PROBING SUPERSYMMETRIC GRAND UNIFICATION WITH
CP AND FLAVOR VIOLATIONS

by

Parul Rastogi

Dissertation submitted to the Faculty of the Graduate School of the
University of Maryland, College Park in partial fulfillment
of the requirements for the degree of
Doctor of Philosophy
2004

Advisory Committee:
Professor Jogesh C. Pati, Chair/Advisor
Professor Sylvester J. Gates
Professor Nicholas J. Hadley
Professor Rabrindra N. Mohapatra
Professor M. Coleman Miller

© Copyright by
Parul Rastogi
2006

Acknowledgements

I would like to thank my advisor Professor Jogesh C. Pati for his continued guidance and encouragement without which this project would have been impossible. I would also like to thank Professor Kaladi S. Babu for giving me a chance to collaborate with him and for answering a lot of my questions.

I am grateful to Professors Rabindra Mohapatra, Markus Luty, S. James Gates, and O. W. Greenberg, from whom I have learnt a lot.

I would also like to thank my colleague and friend Ram Sriharsha who has taught me a lot of things, not just Physics. I also want to thank my fellow graduate students Ken Hsieh, Haibo Yu and Willie Merrell for many discussions and conversations and for being great office mates.

Finally, I would like to thank my parents and my sister for their love and support.

CONTENTS

1. <i>Introduction</i>	1
2. <i>Supersymmetry and Supersymmetry Breaking</i>	15
2.1 Motivations for Low Energy Supersymmetry	15
2.2 The Minimal Supersymmetric Standard Model (MSSM)	19
2.2.1 Soft SUSY Breaking	22
2.2.2 Flavor and CP problems of MSSM	24
2.2.3 The μ -problem of MSSM	30
2.2.4 The fine tuning problem of SUSY	31
2.3 Supersymmetry Breaking Mechanisms	33
2.3.1 Gravity mediated SUSY breaking	33
2.3.2 Gauge mediated SUSY breaking	35
2.3.3 Supersymmetry breaking via anomalous U(1)	36
2.3.4 Anomaly mediated SUSY breaking	38
2.3.5 Gaugino mediated SUSY breaking	39
2.3.6 Constrained MSSM	42
3. <i>Grand Unification and the choice of the gauge group</i>	43
3.1 The need for SU(4)-color	45
3.2 Similarities and Differences between G(224) and SO(10)	52
3.3 SO(10) and its breaking into the standard model	55
4. <i>Fermion Masses and Neutrino Oscillations in a SO(10)/G(224) Framework: A Review of the BPW model</i>	59
5. <i>Tying in CP and Flavor Violations with Fermion Masses and Neutrino Os- cillations</i>	79
5.1 Introduction	79
5.2 Phases in the Fermion Mass Matrices: The Origin of CP violation	83
5.3 SUSY CP and Flavor Violations	88
5.4 Compatibility of CP and Flavor Violations with Fermion Masses and Neutrino Oscillations in SO(10)/G(224): Our Results	100
5.5 Summary and Concluding Remarks	132

Appendix	140
.1 Appendix: Approximate diagonalization of mass matrices and the CKM matrix for the BPW model	141
.2 Appendix: Renormalization group running of A-terms from the SUSY messenger scale M^* to M_{GUT}	149
.3 Appendix: CP Violation in the K Meson system	154
.3.1 ϵ_K and ΔM_K	154
.3.2 ϵ'_K/ϵ_K	157
.4 Appendix: CP Violation in the B Meson system	159
.4.1 Calculation of $S(B_d \rightarrow \phi K_S)$	160
.5 Appendix: Renormalization Group Analysis of the CKM Elements . .	162
6. <i>Lepton Flavor Violation within a Realistic $SO(10)/G(224)$ Framework</i> . . .	169
6.1 Introduction	169
6.2 Lepton Flavor Violation in the $SO(10)/G(224)$ Framework	173
6.3 Results	181
Appendix	196
.1 Appendix: Lepton Flavor violation: Amplitudes	197
7. <i>Distinguishing Between Hierarchical and Lop-sided $SO(10)$ Models.</i>	206
7.1 Introduction	206
7.2 A brief description of the BPW and the AB models	211
7.3 The Three Sources of Lepton Flavor Violation	221
7.4 Results on Lepton Flavor Violation	227
7.5 Results on Fermion Masses, CKM Elements and CP Violation	239
7.6 Conclusions	254
7.7 Figures	259
8. <i>Coupling Unification for An Effective $G(224)$ or $G(214)$ Symmetry: Compatibility with String Unification</i>	263
8.1 Introduction	263
8.2 The Extended Supersymmetric Standard Model and its embedding in $G(224)$	272
8.2.1 Yukawa couplings in ESSM and inter family mass hierarchy . .	274
8.2.2 Gauge coupling unification with ESSM embedded into $G(224)$. .	275
8.2.3 Results for the case of ESSM embedded in $G(224)$	282
8.3 Gauge Coupling Unification with ESSM embedded into $G(214)$	293
8.3.1 Yukawa couplings in $G(214)$	294
8.3.2 Results for the case of ESSM embedded in $G(214)$	296
8.4 Gauge Coupling Unification with MSSM embedded into $G(224)$	302
8.4.1 Threshold corrections to $\alpha_3(m_Z)$ due to gauge and Higgs multiplets of $G(224)$	304
8.5 Conclusion	307

<i>Appendix</i>	313
.1 Renormalization group analysis of ESSM	314
.2 G(224) renormalization group equations	317
.3 G(214) renormalization group equations	319
<i>I. Appendix: Renormalization group analysis of MSSM</i>	322
I.1 Renormalization Group Equations of Gauge Couplings and Gaugino masses with softly broken supersymmetry	322
I.2 Renormalization group equations of Yukawa couplings and A-terms	324
I.3 Renormalization group equations of scalar (mass) ² terms	325
<i>II. Appendix: Wolfenstein parameterization of the CKM matrix and the Unitary Triangle</i>	328
II.1 Wolfenstein Parametrization of the CKM Matrix	329
II.1.1 Wolfenstein Parametrization beyond the leading order	329
II.2 The Unitarity Triangle	330
<i>III. Appendix: CP Violation in the K Meson system</i>	334
III.1 $K^0 - \overline{K}^0$ mixing	334
III.2 ϵ_K and ΔM_K	336
III.3 ϵ'_K/ϵ_K	339
<i>IV. Appendix: CP Violation in the B Meson system</i>	342
IV.1 $B_d - \overline{B}_d$ mixing	342
IV.2 CP violation in decay	344
IV.3 Three types of CP violations in meson decays	345
IV.3.1 CP violation in mixing	345
IV.3.2 CP violation in decay	346
IV.3.3 CP violation in the interference between decays, with and without mixing	346
IV.3.4 Application to the specific case of $B_d \rightarrow \phi K_S$	347
IV.4 Calculation of $S(B_d \rightarrow \phi K_S)$	348

1. INTRODUCTION

The last four decades have brought forth great progress in the quest for a unification of the fundamental particles and their forces. The standard model of particle physics based on the gauge symmetry $SU(2)_L \times U(1)_Y \times SU(3)^c$, comprising the notions of electroweak unification [1] and quantum chromodynamics [2], together with that of spontaneous symmetry breaking (hidden symmetry) [3], is a major step in this direction. It received a strong boost through the realization that spontaneously broken gauge theories are renormalizable [4]. The standard model serves to clarify the nature of three of the basic forces of nature: the strong nuclear, electromagnetic and weak. It has turned out to be spectacularly successful empirically [5]. The missing ingredient of this model is the Higgs boson which will be searched for at the forthcoming LHC. Despite the successes of the standard model, there exist observations which clearly suggest the existence of

new physics beyond the standard model. These include: (1) neutrino oscillation [6, 7], (2) evidence for cold dark matter [5, 8], (3) baryon asymmetry of the universe [8, 9], and (4) the need for an inflationary expansion of the early universe that serves to explain the observed gross homogeneity and isotropy as well as flatness of the universe [10]¹.

The second major step in the unification ladder is the hypothesis of grand unification [11–14], which proposes an underlying unity of quarks and leptons and of their three gauge forces. This idea was motivated in the 1970s purely on aesthetic grounds, in part to remove some of the shortcomings of the standard model, such as the arbitrariness in the assignment of the hypercharge, Y_W and the lack of quantization of electric charge. Over the years, the evidence in favor of this idea has become strong. It includes: (1) the quantum numbers of the members of a family, (2) quantization of electric charge, (3) the meeting of the three gauge couplings which occurs at a scale $M_U \sim 10^{16}$ GeV, in the context of supersymmetry (see be-

¹ In addition, there is, of course, the discovery of dark energy [8], which cannot be understood within the standard model, nor in the presently available ideas *beyond* those of the standard model.

low), (4) neutrino oscillations, (5) certain fermion mass relations (to be discussed in Chapters 2 and 4), and (6) baryogenesis via leptogenesis [15, 16]. These features lend strong support in favor of the basic idea of grand unification being relevant at a scale of 10^{16} GeV, as well as low energy supersymmetry. As I will discuss in Chapter 2, the last three features (4), (5) and (6) go well with the so-called seesaw mechanism [17], and simultaneously serve to select out the nature of the underlying symmetry, favoring the class that possesses the symmetry $SU(4)$ -color [12] in 4D. This in turn suggests that the effective symmetry in 4D at short distances ($\lesssim 10^{-30}$ cm) should maximally be either $SO(10)$ [18] (or possibly E_6 [19] and minimally perhaps a string-derived $G(224) \equiv SU(2)_L \times SU(2)_R \times SU(4)^c$ [12, 20] or $G(214) \equiv SU(2)_L \times U(1)_{I_{3R}} \times SU(4)^c$, with coupling unification holding at the string scale (see discussions in Chapters 2 and 8), as opposed to other alternatives such as $SU(5)$ [13] or $[SU(3)]^3$ [21].

Referring to supersymmetry mentioned above, it is an idea that evolved in the early 1970s [22] simultaneously with the idea of grand unification. It is a symmetry that transforms a fermion into a boson

and vice versa. It turns out that supersymmetry is needed for the consistency of string theory [23]. It also seems to be the best candidate for avoiding large quantum corrections to the Higgs mass and thereby unnatural extreme fine tuning. The latter feature, however, requires the existence of the supersymmetric partners of the standard model particles at the electroweak scale with masses of $\mathcal{O}(1 \text{ TeV})$. As mentioned above, the same SUSY spectrum leads to the meeting of the three gauge couplings that occurs at a scale $M_U \sim 2 \times 10^{16} \text{ GeV}$ [24]. Such a meeting thus provides strong support for both grand unification and low energy supersymmetry. As an additional bonus, such a SUSY spectrum provides a natural candidate for cold dark matter that is needed to account for large scale observations [8]. Fortunately, the supersymmetric particles with masses of order 1 TeV can be searched for at the forthcoming LHC.

The discussion above suggests that the idea of grand unification based on $\text{SO}(10)$ or a string derived effective $\text{G}(224)$ -symmetry, together with low energy supersymmetry, is well motivated both on theoretical and on experimental grounds.

A major part of my thesis will therefore probe into some issues pertaining to the supersymmetric SO(10)/G(224)-framework with a view to confronting this framework as far as possible with existing and forthcoming experiments. In particular, I plan to explore how CP and flavor violations in the quark as well as the lepton sectors (as in $K^{\circ} \leftrightarrow \overline{K}^{\circ}$, $B_{d,s}^{\circ} \leftrightarrow \overline{B}_{d,s}^{\circ}$, $b \rightarrow s\gamma$, $\mu \rightarrow e\gamma$, $\tau \rightarrow \mu\gamma$, $\tau \rightarrow e\gamma$ and the EDMs of the neutron and the electron) can arise within a predictive supersymmetric SO(10)/G(224) framework in accord with observations and *in conjunction with* the observed masses and mixings of the charged fermions and neutrino oscillations.

In particular, my goal would be to obtain a *unified description* of all four phenomena: (i) CP non-conservation, (ii) flavor violation, (iii) masses and mixings of quarks and leptons, as well as (iv) neutrino oscillations, within a single predictive framework based on SUSY grand unification as mentioned above.

A predictive framework based on the symmetry SO(10) or G(224), and a minimal Higgs system was proposed by Babu, Pati and Wilczek in Ref. [25], which we refer to as the BPW model. This model describes

the masses and mixings of all fermions including neutrinos by making the simplifying assumption that the fermion mass matrices are real and thus CP-conserving. Notwithstanding this assumption, the framework is found to be remarkably successful. In particular, it makes seven predictions involving fermion masses, CKM elements and neutrino oscillations, all in good accord with observations, to within 10%.

Now in general one would of course expect the entries in the fermion mass matrices to have phases either because the VEVs of the relevant Higgs fields, and/or the effective Yukawa couplings are complex. These in turn can induce CP and flavor violation through the standard model/CKM interactions as well as through SUSY interactions involving sfermion/gaugino loops [26, 27].

The question arises: Can the BPW-framework of Ref. [25], based on the supersymmetric $SO(10)$ or $G(224)$ -symmetry, be extended, by allowing for phases in the fermion mass matrices, so as to yield net CP and flavor-violations, arising through both standard model and SUSY interactions, in accord with observations, while still preserving its successes as regards fermion masses and neutrino oscillations?

As we will see, these four phenomena - (i) fermion masses, (ii) neutrino oscillations, (iii) CP non-conservation, and (iv) flavor violations in quarks and leptons- get intimately linked to each other within the SUSY SO(10)/G(224) framework. Satisfying simultaneously the observed features of all four phenomena within such a predictive framework turns out, therefore, to be a non-trivial challenge to meet. One aspect of my study is to show that the answer to the question raised above is in the affirmative.

The dissertation is organized as follows. In Chapter 2, I discuss motivations for supersymmetry and certain mechanisms for supersymmetry breaking. The minimal supersymmetric standard model is discussed along with its associated problems such as that of flavor changing neutral currents, the SUSY CP problem, the μ -problem and the need for matter parity.

In Chapter 3, I discuss some salient features of SO(10)/G(224) grand unification and its breaking into the standard model.

In Chapter 4, I review the BPW framework [25], and its predictions regarding fermion masses and neutrino oscillations. This model

provides a basis for my study of the issues of SUSY CP and flavor violations in conjunction with the phenomena of neutrino oscillations and fermion masses, which is done in the following two chapters.

In Chapter 5, I extend this model to include CP violation by introducing phases in the mass matrices [28], and examine if this extension preserves the successes of the model regarding fermion masses and mixings, and neutrino oscillations. A detailed study of CP and flavor violations in the quark sector is done in this chapter. Assuming that SUSY breaking parameters are flavor universal at a scale $M^* \gtrsim M_{GUT}$, and that CP violation arises through phases in the fermion mass matrices, I show (based on collaborative work with Babu and Pati [28]) how the presence of GUT threshold induces new and calculable CP and flavor violations. Including standard model and SUSY contributions, we find that the extended BPW framework can correctly account for the observed flavor and/or CP violations in Δm_K , Δm_{B_d} , $S(B_d \rightarrow J/\psi K_S)$ and ϵ_K . While SUSY-contribution is small (\lesssim few%) for the first three quantities, that to ϵ_K is found to be sizable (\sim 20-25%) and *negative* (as desired) compared to that

of the standard model. The model predicts $S(B_d \rightarrow \phi K_S)$ to be in the range $+(0.65-0.73)$, close to the standard model prediction. The model yields $Re(\epsilon'/\epsilon)_{SUSY} \approx +(4 - 14) \times 10^{-4}$; the relevance of this contribution can be assessed only when the associated matrix elements are known reliably. The model also predicts that the electric dipole moments of the neutron and the electron should be discovered with improvements in the current limits by factors of 10 to 100.

Chapter 6 deals with lepton flavor violation in the supersymmetric $SO(10)/G(224)$ -framework mentioned above. We study the processes $\mu \rightarrow e\gamma$, $\tau \rightarrow \mu\gamma$, $\tau \rightarrow e\gamma$ and $\mu N \rightarrow eN$ within this framework [29] by including contributions *both* from the presence of the right handed neutrinos as well as those arising from renormalization group running in the post-GUT regime ($M^* \rightarrow M_{GUT}$). Typically the latter, though commonly omitted in the literature, is found to dominate. Our predicted rates for $\mu \rightarrow e\gamma$ show that while some choices of the universal SUSY parameters ($m_o, m_{1/2}$) are clearly excluded by the current empirical limit, this decay should be seen with an improvement of the current sensitivity by a factor of 10–100, even if sleptons are

moderately heavy ($\lesssim 800$ GeV, say). For the same reason, $\mu - e$ conversion ($\mu N \rightarrow e N$) should show in the planned MECO experiment. Implications of WMAP and $(g - 2)_\mu$ -measurements are noted, as also the significance of the measurement of parity-odd asymmetry in the decay of polarized μ^+ into $e^+\gamma$. Continuing searches at BaBar will be sensitive to $\tau \rightarrow \mu\gamma$ decay for a large part of the SUSY parameter space (i.e. choice of $(m_0, m_{1/2})$).

One of the goals of my thesis is to study some generic properties of SO(10)/G(224) unification, for example, those arising from post-GUT physics ($M^* \rightarrow M_{GUT}$), which can be applied to other models as well. In particular, I study the SUSY CP and flavor violations within another promising SO(10) model proposed by Albright and Barr [30].

In chapter 7, I make a comparative study [31] of two promising SO(10) models, namely the BPW model (proposed by Babu, Pati and Wilczek) and the AB model [30], based on their predictions regarding CP and flavor violations. There is a significant difference in the structure of the fermion mass-matrices in the two models (which are hierarchical for the BPW case and lop-sided for the AB model) which

gives rise to different CP and flavor violating effects. I include both SM and SUSY contributions to these processes. Assuming flavor universality of SUSY breaking parameters at a messenger scale $M^* \gtrsim M_{GUT}$, I find that renormalization group based post-GUT physics gives rise to large CP and flavor violations. While these effects were calculated for the BPW model in [28,29] as described above, my paper [31] is the first work (to my knowledge) that includes post-GUT contributions for the AB model. The values of $\Delta m_K, \epsilon_K, \Delta m_{B_d}$ and $S(B_d \rightarrow J/\psi K_S)$ are found, in both models, to be close to SM predictions, in good agreement with data. Both models predict that $S(B_d \rightarrow \phi K_S)$ should lie in the range +0.65–0.74, close to the SM prediction. Both also predict that the EDM of the neutron $\approx (few \times 10^{-26})\text{e-cm}$, should be observed in upcoming experiments. The lepton sector, however, brings out marked differences between the two models. It is found that $Br(\mu \rightarrow e\gamma)$ in the AB model is generically much larger than that in the BPW model, being consistent with the experimental limit only with a rather heavy SUSY spectrum with $(m_o, m_{1/2}) \sim (1000, 1000)$ GeV. The BPW model, on the other hand, is consistent with the SUSY

spectrum being as light as $(m_o, m_{1/2}) \sim (600, 300)$ GeV. Another distinction arises in the prediction for the EDM of the electron. In the AB model d_e should lie in the range $10^{-27} - 10^{-28}$ e-cm, and should be observed by forthcoming experiments. The BPW model gives d_e to be typically 100 times lower than that in the AB case. Thus the two models can be distinguished based on their predictions regarding CP and flavor violations, and can be tested in future experiments.

Most of my work holds for the effective gauge symmetry above the GUT scale being either $SO(10)$ or $SU(2)_L \times SU(2)_R \times SU(4)^c$. Several authors [32–34] have noted the advantages of a string derived $G(224)$ solution in 4D over an $SO(10)$ solution as regards the problem of doublet triplet splitting. For a $G(224)$ solution, the undesired color-triplets, which could induce rapid proton decay, can be naturally projected out through the process of string compactification. On the other hand for the case of supersymmetric $SO(10)$ being effective in 4D, one would need a suitable doublet-triplet splitting mechanism, like the Dimopoulos-Wilczek mechanism [35] or something analogous to it, to be operative in 4D. Such a mechanism has not been shown to

emerge consistently from string theory for the case of $SO(10)$.

The case of $SO(10)$, however, has an *a priori* advantage over an effective $G(224)$ -solution as regards the issue of the observed gauge coupling unification. While for a string derived $SO(10)$ solution, coupling unification would hold in the region spanning from M_{st} to M_{GUT} (regardless of the gap between them), for the case of a string derived $G(224)$ solution, however, coupling unification ($g_{2L} = g_{2R} = g_4$) can hold only at the string scale $M_{st} \gtrsim M_{GUT}$ through the constraints of string theory even though $G(224)$ is semi-simple [36]. In Chapter 8, I therefore examine how the gauge couplings α_1 , α_2 and α_3 observed at the LEP energies can be compatible with unification at the string scale when the standard model is embedded in either $G(224)$ or $G(214)$ at about the GUT scale $\sim 2 \times 10^{16}$ GeV. In this context I will consider two alternative low energy spectra: (i) that of the Minimal Supersymmetric Standard Model (MSSM), as well as (ii) that of an extension of the MSSM, known as the Extended Supersymmetric Standard Model (ESSM) [37]. The latter introduces two vector like families at the TeV scale, in addition to the spectrum of MSSM, and has been mo-

tivated on several grounds [37]. In exploring the issue of coupling unification it is required that the following constraints be also simultaneously satisfied: (a) consistent electroweak symmetry breaking, (b) non-violation of color and charge, (c) lightest neutralino and the Higgs mass limits, and (d) the masses and mixings of the second and third generation fermions. It is shown that including GUT-scale threshold corrections, one can consistently obtain gauge couplings unification at a scale $\sim 10^{17}$ GeV which can plausibly be identified with the string scale; and the constraints mentioned above can also be satisfied simultaneously.

Lastly, some useful formulae and derivations are included in the appendices at the end.

2. SUPERSYMMETRY AND SUPERSYMMETRY BREAKING

2.1 *Motivations for Low Energy Supersymmetry*

Supersymmetry is a symmetry that transforms a boson into a fermion and vice versa [22, 38]. The generators of such transformations are fermionic operators that obey graded Lie Algebra. The single particle states of a supersymmetric theory are the irreducible representations of the supersymmetry algebra, called the supermultiplets. Each supermultiplet contains both fermion and boson states, known as superpartners of each other. Thus superpartners of spin-1/2 quarks and leptons would be spin-0 squarks (\tilde{q}) and sleptons (\tilde{l}); likewise for spin-1 gluons, W-bosons and photons, the partners would be spin-1/2 gluinos (\tilde{g}), Winos (\tilde{W}) and photinos ($\tilde{\gamma}$). If supersymmetry is exact, these superpartners have the same masses and charges (electric, weak and color). Since in nature we do not yet see spin-0 squarks and sleptons *etc.*, they must be considerably heavier than quarks and leptons.

Thus supersymmetry, even if it holds at some level, cannot be exact.

It must be broken.

It turns out that supersymmetry is needed for consistency of string theory which is the only existing candidate for a unified theory of gauge interactions and gravity. On the practical side, supersymmetry is needed to avoid the problem of extreme fine-tuning in the Higgs mass. While fermion masses are protected by chiral symmetry, there is no symmetry that protects the scalar masses. Quantum corrections to fermion mass terms are proportional to the fermion mass itself and the logarithm of the cut-off scale. However, quantum corrections to scalars at one and higher loop orders are quadratically divergent. The standard model requires a Higgs scalar to break the electroweak symmetry. If the loop integrals are cut-off at the scale of new physics $\Lambda \gg m_W$, then the Higgs mass gets a correction of order Λ^2 . For example, if the Higgs couples to a Dirac fermion f with the coupling $-\lambda_f H \bar{f} f$, one loop corrections to Higgs mass yield

$$\Delta m_H^2 = \frac{|\lambda_f|^2}{16\pi^2} [-2\Lambda^2 + 6m_f^2 \ln(\Lambda/m_f)]. \quad (2.1)$$

Thus quantum gravity or GUT-scale physics characterized by

$\Lambda \sim M_{\text{Planck}}$ or M_{GUT} would give a correction to Higgs (mass)² which is too large by some 30–24 orders of magnitude compared to the desired Higgs (mass)² of order (1/10 to 1 TeV)². This would need extreme fine tuning through counter terms to obtain the desired Higgs mass via large cancellation. On the other hand, in a supersymmetric theory, each Weyl fermion is accompanied by a scalar partner. If this scalar couples to the Higgs with the interaction $-\lambda_S |H|^2 |S|^2$, then the correction to the Higgs mass due to this coupling is:

$$\Delta m_H^2 = \frac{|\lambda_S|}{16\pi^2} [\Lambda^2 - 2m_S^2 \ln(\Lambda/m_S)]. \quad (2.2)$$

With supersymmetry, for each Dirac fermion there are two scalars whose couplings to the Higgs are related as $|\lambda_f|^2 = |\lambda_S|$. This ensures a cancellation of the quadratic divergence (see Eqs. (2.1) and (2.2)), leaving only a logarithmic dependence on the cut-off scale in the Higgs mass.

$$|\Delta m_H^2| \sim \left| \frac{\lambda}{16\pi^2} [(m_f^2 - m_S^2) \ln(\Lambda/m)] \right|. \quad (2.3)$$

Electroweak symmetry breaking implies that the Higgs mass must

be $\lesssim 1$ TeV. To avoid large fine-tuning, $\sqrt{|\Delta m_H^2|} \lesssim \mathcal{O}(1 \text{ TeV})$. With this constraint, if supersymmetry is the cause of avoidance of large quantum corrections to the Higgs mass, it follows that SUSY partners of the standard model particles (i.e. squarks, sleptons, gluinos *etc.*) should have masses less than or of order 1 TeV.

As mentioned in the introduction, an independent strong motivation for weak scale supersymmetry is gauge coupling unification. In the minimal supersymmetric extension of the standard model (discussed below), the three gauge couplings neatly unify at a scale $M_{\text{GUT}} \approx 2 \times 10^{16}$ GeV, supporting the ideas of Grand Unification as well as low energy supersymmetry. Finally, supersymmetry contains a viable cold dark matter candidate. It turns out that in the supersymmetric standard model, to prevent rapid proton decay, one has to impose a discrete symmetry known as R-parity or matter-parity on the supersymmetric Lagrangian, which does arise naturally in a large class of models (see below). This has the consequence that the lightest supersymmetric particle is completely stable, and can serve as cold dark matter. These arguments provide strong motivations in favor of low

energy (i.e. weak-scale) supersymmetry. Fortunately, SUSY particles with masses of order 1 TeV can be searched for at the LHC.

2.2 *The Minimal Supersymmetric Standard Model (MSSM)*

In the minimal supersymmetric extension of the standard model (see e.g. [39]), all fermions of the standard model are embedded into chiral superfields and all gauge fields into vector superfields [38]. The matter content of the MSSM along with its $(SU(3) \times SU(2) \times U(1)_Y)$ quantum

numbers is given below:

$$\begin{aligned}
Q &= \begin{pmatrix} u_L & \tilde{u}_L \\ d_L & \tilde{d}_L \end{pmatrix}_i & (3^c, 2_L, +1/6) \\
L &= \begin{pmatrix} \nu_{eL} & \tilde{\nu}_{eL} \\ e_L^- & \tilde{e}_L^- \end{pmatrix}_i & (1^c, 2_L, -1/2) \\
\bar{U} &= (u_L^c, \tilde{u}_L^c)_i & (3^{*c}, 1_L, -2/3) \\
\bar{D} &= (d_L^c, \tilde{d}_L^c)_i & (3^{*c}, 1_L, +1/3) \\
\bar{E} &= (e_L^c, \tilde{e}_L^c)_i & (1^c, 1_L, +1) \\
H_u &= \begin{pmatrix} H_u^+ & \tilde{H}_u^+ \\ H_u^0 & \tilde{H}_u^0 \end{pmatrix} & (1^c, 2_L, +1/2) \\
H_d &= \begin{pmatrix} H_d^0 & \tilde{H}_d^0 \\ H_d^- & \tilde{H}_d^- \end{pmatrix} & (1^c, 2_L, -1/2)
\end{aligned} \tag{2.4}$$

The SUSY partners of the standard model particles are denoted by a tilde on the top. Here Q , L , \bar{U} , \bar{D} , \bar{E} , H_u and H_d stand for positive chiral superfields with left chiral fermions [38]. The $i = 1, 2, 3$ is the generation index. Note that for the supersymmetric standard model, two Higgs doublets with opposite hypercharges: H_u , H_d are needed in order to cancel the anomalies, as fermionic components of the Higgs

scalars contribute to the triangle anomaly. These two doublets are also needed to give masses to up and down type quarks; hence the subscript u and d on them. The gauge bosons also come along with their fermionic partners:

$$(g, \tilde{g}), \quad (W, \tilde{W}) \quad (B, \tilde{B}) \quad (2.5)$$

The Yukawa superpotential along with the mass term for the Higgs fields is given by:

$$W = h_u Q H_u \bar{U} + h_d Q H_d \bar{D} + h_e L H_d \bar{E} + \mu H_u H_d \quad (2.6)$$

Since there are three generations, h_u , h_d and h_e are 3×3 matrices with, in general, complex entries. The following gauge invariant, renormalizable terms are also allowed in the superpotential:

$$W' = \lambda_1 Q L \bar{D} + \lambda_2 \bar{U} D \bar{D} + \lambda_3 L L \bar{E} + \mu' L H_u \quad (2.7)$$

These couplings violate lepton and baryon number symmetries and can induce rapid proton decay. These terms are forbidden by a discrete symmetry known as R-parity or an equivalent matter parity, which arises in a large class of models (see remarks later). The R-

parity can be defined by

$$R = (-1)^{3(B-L)+2S} \tag{2.8}$$

All standard model particles are even under this symmetry, while all superpartners are odd. Such a parity forbids the W' superpotential and thus the dangerous rapid proton decay operators. In the process, it also ensures that all superpartners are produced in pairs. This would mean that the lightest supersymmetric particle (LSP) is absolutely stable as it cannot decay into the standard model particles. As mentioned above, such a particle can serve as a candidate for cold dark matter.

2.2.1 *Soft SUSY Breaking*

Supersymmetry introduces two complex scalar fields for every Dirac fermion, or one complex scalar field for every Weyl fermion. As noted above, this can bring about a cancellation of the quadratically divergent contribution to the Higgs mass², if the coupling of the fermion to the Higgs ($\lambda_f H f \bar{f}$) and the coupling of the scalar to the Higgs ($\lambda_s H^2 s^2$) are related as $\lambda_s = |\lambda_f|^2$. Such relationships indeed oc-

cur in unbroken supersymmetry. Supersymmetry guarantees that the quadratic divergences in scalar squared masses must vanish to all orders in perturbation theory. If broken supersymmetry is to still provide a solution to the Higgs mass fine-tuning problem, then the relationship between the dimensionless couplings λ_s and λ_f must be maintained. This means that the couplings in the Lagrangian that break supersymmetry must be “soft”, i.e. of positive mass dimension (e.g. mass terms for scalars and scalar cubic coupling terms with couplings of mass dimension one and spin-1/2 gaugino mass terms). In this case the corrections to the Higgs mass squared are proportional to $m_{\text{soft}}^2/(16\pi^2) \ln(\Lambda_{\text{UV}}/m_{\text{soft}})$, where $m_{\text{soft}} \sim 1$ TeV. The effective soft SUSY breaking Lagrangian is given by:

$$\begin{aligned}
-\mathcal{L}_{\text{soft}} = & M_{\tilde{Q}}^2 \tilde{Q}^\dagger \tilde{Q} + M_{\tilde{U}}^2 \tilde{U}^\dagger \tilde{U} + M_{\tilde{D}}^2 \tilde{D}^\dagger \tilde{D} + M_{\tilde{L}}^2 \tilde{L}^\dagger \tilde{L} + M_{\tilde{E}}^2 \tilde{E}^\dagger \tilde{E} \\
& + m_{H_u}^2 H_u^\dagger H_u + m_{H_d}^2 H_d^\dagger H_d + (B\mu H_u H_d + h.c.) \\
& + M_1 \tilde{B}\tilde{B} + M_2 \tilde{W}\tilde{W} + M_3 \tilde{g}\tilde{g} \\
& + (A_u \tilde{Q} H_u \tilde{U} + A_d \tilde{Q} H_d \tilde{D} + A_e \tilde{L} H_d \tilde{E} + h.c.)
\end{aligned} \tag{2.9}$$

The $M_{\tilde{Q}, \tilde{U}, \tilde{D}, \tilde{L}, \tilde{E}}^2$ are 3×3 hermitian matrices. The $A_{u,d,e}$ are also 3×3 matrices with complex entries. The renormalization group equa-

tions of the soft SUSY parameters in MSSM are given in Appendix I.

2.2.2 Flavor and CP problems of MSSM

The mass matrices $M_{\tilde{Q},\tilde{U},\tilde{D},\tilde{L},\tilde{E}}^2$, and the A-terms $A_{u,d,e}$ can in general have complex off-diagonal entries in the bases in which the mass matrices of quarks and leptons are diagonal. These can give rise to large contributions to flavor changing and CP violating processes, in addition to those present in the standard model (see e.g. [26, 27]). For example, the $K^\circ - \overline{K^\circ}$ mixing, which is explained very well within the standard model, can have a contribution from the squark loops as shown in figure 1.

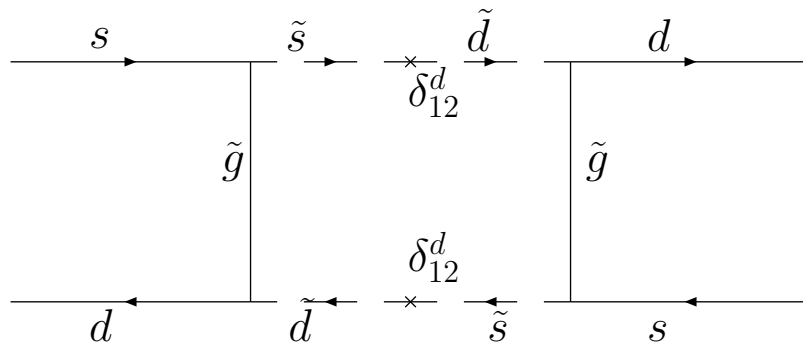


Figure 1.

The $\delta_{ij} = \Delta_{ij}/\tilde{m}^2$ where Δ_{ij} are the off-diagonal terms in the sfermion mass² matrices defined in the so called SUSY basis where all couplings of the fermion and sfermion states to neutral gauginos are flavor diagonal. From the gauge basis, the scalars are transformed by the same matrices that diagonalize the fermion mass matrices. The \tilde{m}^2 is an average sfermion mass². The contribution to Δm_K from box diagrams involving superpartners is given by:

$$(\Delta m_K)_{SUSY} \sim \frac{g_3^4}{16\pi^2} m_K f_k^2 \frac{(\Delta m_{\tilde{s}\tilde{d}}^2)^2}{m_{\tilde{q}}^6} \quad (2.10)$$

Constraints from experiments, for $m_{\tilde{q}} \approx 500$ GeV and $m_{\tilde{g}}^2/m_{\tilde{q}}^2 \approx 1$ yield [40]:

$$\begin{aligned} \sqrt{|\operatorname{Re}(\delta_{12}^d)_{LL}^2|} &\lesssim 4 \times 10^{-2}; & \sqrt{|\operatorname{Re}(\delta_{12}^d)_{LR}^2|} &\lesssim 4.4 \times 10^{-3}; & (2.11) \\ \sqrt{|\operatorname{Re}(\delta_{12}^d)_{LL}(\delta_{12}^d)_{RR}|} &\lesssim 2.5 \times 10^{-3}. \end{aligned}$$

Constraints on the imaginary parts of δ_{12}^d come from measurements of ϵ_K , and for $m_{\tilde{q}} \approx 500$ GeV and $m_{\tilde{g}}^2/m_{\tilde{q}}^2 \approx 1$, are given below [40]:

$$\begin{aligned} \sqrt{|\operatorname{Im}(\delta_{12}^d)_{LL}^2|} &\lesssim 3.2 \times 10^{-3}; & \sqrt{|\operatorname{Im}(\delta_{12}^d)_{LR}^2|} &\lesssim 3.5 \times 10^{-4}; & (2.12) \\ \sqrt{|\operatorname{Im}(\delta_{12}^d)_{LL}(\delta_{12}^d)_{RR}|} &\lesssim 2.2 \times 10^{-4}. \end{aligned}$$

Similarly, there can be supersymmetric contributions (shown in figure 2) to lepton flavor violating processes such as $\mu \rightarrow e\gamma$, which are forbidden in the standard model or are highly suppressed. Experiments have put an upper bound on the branching ratios of these processes, setting an upper bound on the magnitude of the off-diagonal elements in the slepton mass² matrices. For example, for $m_{\tilde{l}} \approx 100$ GeV and $m_{\tilde{\chi}}^2/m_{\tilde{l}}^2 = 1$ where $m_{\tilde{\chi}}$ is the average neutralino mass, [40]:

$$|(\delta_{12}^l)_{LL}| \lesssim 7.7 \times 10^{-3}; \quad |(\delta_{12}^l)_{LR}| \lesssim 1.7 \times 10^{-6}. \quad (2.13)$$

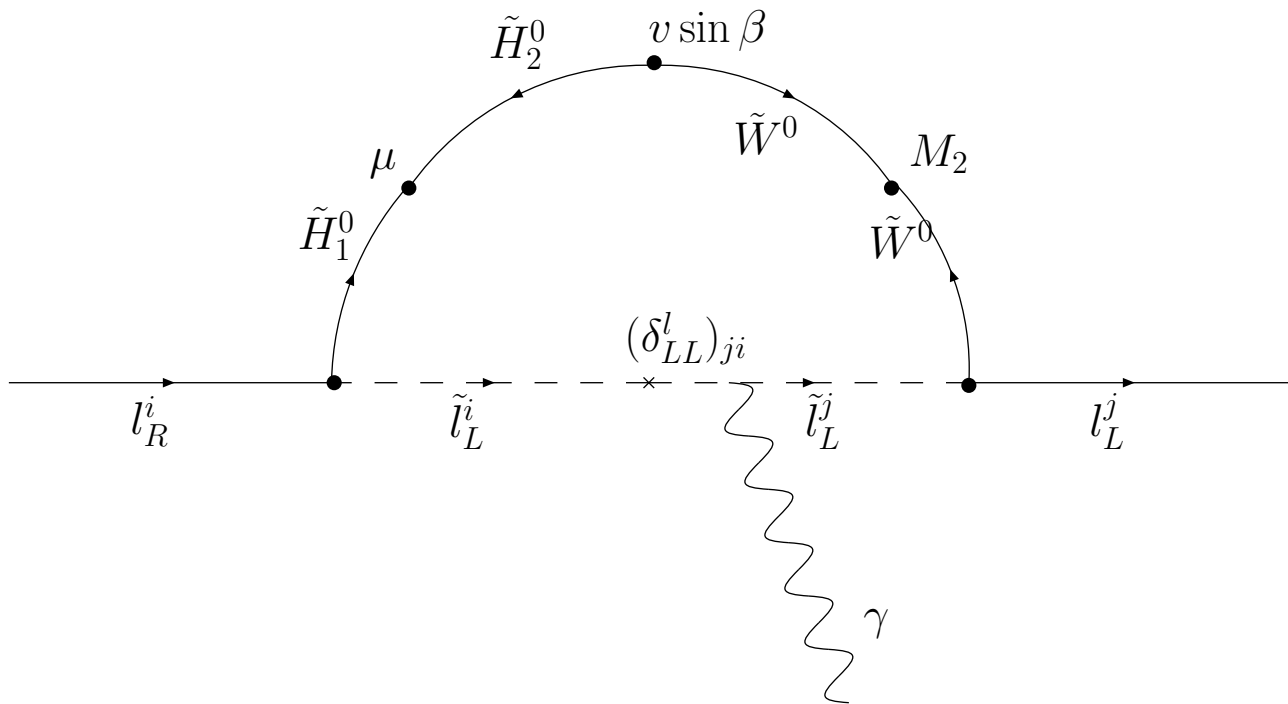


Figure 2.

Phases in squark and slepton masses can give rise to electric dipole moments (EDMs) of electron and neutron as shown in figure 3. These have not been observed and there are stringent bounds on the values of these EDMs from experiments. For $m_{\tilde{q}} \approx 500$ GeV, $m_{\tilde{g}}^2/m_{\tilde{q}}^2 \approx 1$, $m_{\tilde{l}} \approx 100$ GeV and $m_{\tilde{B}}^2/m_{\tilde{l}}^2 = 1$, the constraints on the imaginary parts of δ_{ij} are given below [40]:

$$|\text{Im}(\delta_{11}^d)_{LR}| \lesssim 3.0 \times 10^{-6}; \quad |\text{Im}(\delta_{11}^u)_{LR}| \lesssim 5.9 \times 10^{-6}; \quad (2.14)$$

$$|\text{Im}(\delta_{11}^l)_{LR}| \lesssim 3.7 \times 10^{-7}.$$

For the same choice of sfermion and gaugino masses as above, the constraints on the real parts of the δ_{11}^a are [40]:

$$|\text{Re}(\delta_{11}^d)_{LR}| \lesssim 1.6 \times 10^{-3}; \quad |\text{Re}(\delta_{11}^l)_{LR}| \lesssim 7.3 \times 10^{-1} \quad (2.15)$$

From Eqs. (2.14) and (2.15), one can see that the phases, ϕ , of these parameters have to be extremely small, $\phi_{11}^d \lesssim 10^{-3}$ and $\phi_{11}^l \lesssim 10^{-4} - 10^{-5}$.

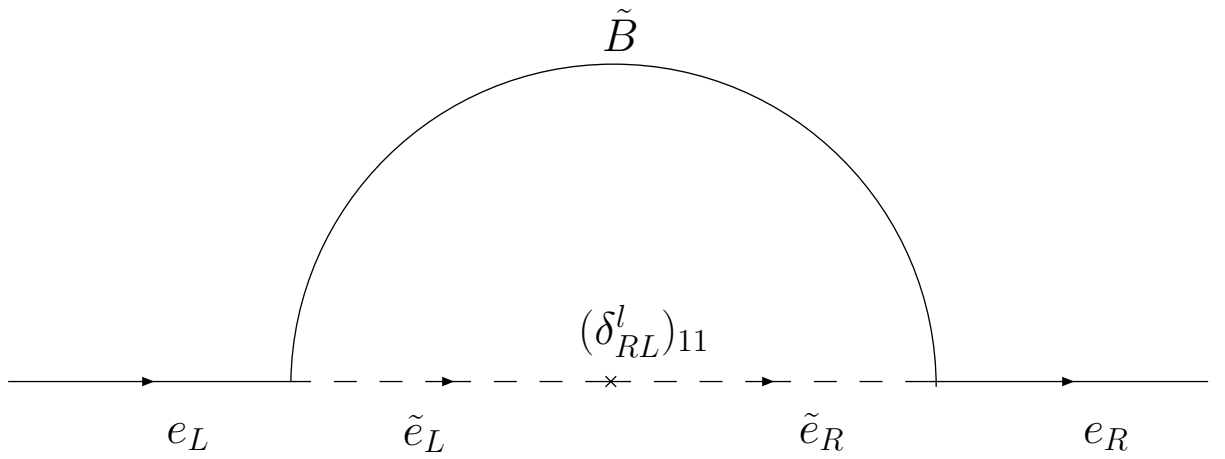


Figure 3.

A detailed review of FCNC and CP constraints in supersymmetric extensions of the standard model can be found in [40]. The bottom-line is that if supersymmetry exists at the TeV scale, then to avoid large FCNCs, a very high degree of degeneracy (to about one part in 100-1000)¹ between the three families of squarks (and also sleptons) is needed. The soft mass parameters must be almost real with phases $\lesssim 10^{-3}$ for squark and slepton masses of 100 GeV– 1 TeV, so as to avoid constraints from CP violations. Understanding the smallness of these phases in the so called SUSY CP problem. We study several such

¹ Strictly speaking the high degree of degeneracy of squarks and sleptons is needed on empirical grounds (involving Δm_K , ϵ_K etc.) only for the first two families, assuming that their masses are $\lesssim 1$ TeV.

CP and flavor violating processes within a specific $SO(10)/G(224)$ framework in Chapters 5, 6 and 7.

These dangerous flavor changing neutral currents in supersymmetry can be avoided if one assumes that supersymmetry breaking is flavor blind at least at some high scale, that is the squark and slepton mass² matrices are proportional to the unit matrix in family space:

$$M_{\tilde{Q},\tilde{U},\tilde{D},\tilde{L},\tilde{E}}^2 = (M_{\tilde{Q},\tilde{U},\tilde{D},\tilde{L},\tilde{E}}^2) 1_{3\times 3} \quad (2.16)$$

In this case all squark and slepton mixing angles are rendered trivial and supersymmetric contributions to FCNC processes will be very small, modulo the mixing due to the A-terms. To suppress undesirable mixing due to the A-terms, one can further assume that the A matrices are proportional to the corresponding Yukawa coupling matrices:

$$A_{u,d,e} = h_{u,d,e} A_{u,d,e}^0 \quad (2.17)$$

Finally, large CP violation can be avoided with the assumption that the soft mass parameters are real or almost real at a high scale. I will shortly mention a few supersymmetry breaking mechanisms which

naturally yield the desired flavor-blindness and reality properties of SUSY breaking parameters.

2.2.3 The μ -problem of MSSM

The minimization of the Higgs potential for electroweak symmetry breaking gives rise to the following condition (see e.g. [39]):

$$\mu^2 = \frac{m_Z^2}{2} - \frac{m_{H_u}^2 \tan^2 \beta - m_{H_d}^2}{\tan^2 \beta - 1} \quad (2.18)$$

where $\tan \beta$ is the ratio of the vacuum expectation values of H_u° and H_d° . Since $m_Z, m_{H_u}^2$ and $m_{H_d}^2$ are all of order the weak scale, the above condition implies that *the μ -parameter must also be of order the weak scale*. But μ is a supersymmetry respecting parameter, while $m_{H_{u,d}}^2$ are soft SUSY breaking parameters. There is no reason for μ to be the scale of SUSY breaking. This is the so called μ -problem which has led to various models that extend the MSSM at very high energies to include a mechanism which relates the effective value of μ to the supersymmetry breaking mechanism [41,42]. Thus a favorable supersymmetry breaking mechanism should be accompanied with a resolution to the μ -problem.

2.2.4 The fine tuning problem of SUSY

Including the soft terms, the Higgs potential in MSSM is given by the following equation:

$$\begin{aligned}
 V_{\text{Higgs}} = & (m_{H_u}^2 + |\mu|^2)|H_u|^2 + (m_{H_d}^2 + |\mu|^2)|H_d|^2 - B\mu(H_u H_d + h.c.) \\
 & + \frac{1}{8}(g_1^2 + g_2^2)(|H_u|^2 - |H_d|^2)^2 + \frac{1}{2}g_2^2|H_u^\dagger H_d|^2.
 \end{aligned}
 \tag{2.19}$$

With this potential, the physical mass of the neutral CP even Higgs, h^0 computed at tree level is bounded by

$$m_{h^0} \leq m_Z |\cos 2\beta| \tag{2.20}$$

where $\tan \beta$ is the ratio of the VEVs of H_u and H_d . The experimental limit from LEP II, $m_{h^0} \geq 114$ GeV, rules out a Higgs lighter than the Z boson. The bound in Eq. (2.20) does not include loop corrections. The largest corrections to the Higgs mass come from top-stop loops, giving

$$\Delta m_{h^0}^2 = \frac{3y_t^4}{4\pi^2} v_u^2 \sin^4 \beta \ln \frac{m_{\tilde{t}_1} m_{\tilde{t}_2}}{m_t^2}. \tag{2.21}$$

This correction grows logarithmically, so a large Higgs mass can be obtained by having a large stop mass. However, the Higgs mass parameter $m_{H_u}^2$ gets loop correction that grow quadratically with the

stop mass.

$$\Delta m_{H_u}^2 = -\frac{3y_t^2}{4\pi^2} m_{\tilde{t}}^2 \ln \frac{\Lambda}{m_{\tilde{t}}^2}. \quad (2.22)$$

If Eq. (2.21) is to account for the current LEP bound, we must have

$$\Delta m_{h^0}^2 \geq (114 \text{ GeV})^2 - m_Z^2 = (69 \text{ GeV})^2 \quad (2.23)$$

setting $|\cos 2\beta| = 1$ which enhances the Higgs mass. The above relation is satisfied for the stop mass $\gtrsim 650 \text{ GeV}$ (inverting Eq. (2.21) and using Eq. (2.23)). A natural scale for the Higgs mass parameter is order m_Z , therefore an approximate measure of fine-tuning, Δ , is

$$\Delta \sim \frac{\Delta m_{H_u}^2}{m_Z^2} \simeq \frac{3y_t^2 m_{\tilde{t}}^2}{4\pi^2 m_Z^2} \ln \frac{\Lambda}{m_{\tilde{t}}^2}. \quad (2.24)$$

For $m_{\tilde{t}} \approx 650 \text{ GeV}$ (as obtained from the Higgs mass bound), and a UV scale $\Lambda \approx 100 \text{ TeV}$, the above expression gives a fine-tuning of one part in 16. A more detailed calculation including full one-loop and the largest two loop corrections push $m_{\tilde{t}}$ to the 1 TeV range if the A-terms are small, increasing fine-tuning to about a percent level. This is the fine-tuning problem of supersymmetry. However, this fine-tuning of order 1 to few % is considerably better than the case of extreme fine-tuning (to one part in $10^{24} - 10^{30}$) that would be needed if there was no

low energy supersymmetry (or other mechanisms such as large extra dimensions either [43] either). Some extensions of MSSM have been suggested [44] to address this problem.

We now proceed to discuss a few supersymmetry breaking mechanisms.

2.3 Supersymmetry Breaking Mechanisms

In this section we briefly discuss a few mechanisms of breaking supersymmetry. A review can be found in Ref. [45].

2.3.1 Gravity mediated SUSY breaking

A general strategy for breaking supersymmetry is to assume that supersymmetry is broken in a hidden sector, which does not involve any of the matter or the forces of the standard model (the visible sector). Supersymmetry breaking is communicated to the visible sector, i.e. the standard model fields through messenger interactions. A natural way of avoiding additional flavor violation in MSSM is to have messenger interactions that are flavor blind. One possible candidate for such a

messenger is gravity [46]. In this case the hidden sector communicates with the visible sector through gravitational strength interactions. In an effective field theory language this means that the supergravity Lagrangian contains non-renormalizable terms which communicate between the two sectors that are suppressed by powers of the Planck scale. If X is a chiral superfield in the hidden sector which breaks SUSY by its F-component getting a VEV $\langle F_X \rangle$, then the soft SUSY breaking parameters can be written in terms of the following four quantities:

$$m_{1/2} = f \frac{\langle F_X \rangle}{M_{Pl}}, \quad m_0^2 = k \frac{\langle F_X \rangle^2}{M_{Pl}^2}, \quad A_0 = \alpha \frac{\langle F_X \rangle}{M_{Pl}}, \quad B_0 = \beta \frac{\langle F_X \rangle}{M_{Pl}} \quad (2.25)$$

This simplification is done with the aim of avoiding the SUSY FCNC and CP problems and is achieved by assuming that the Kähler Potential respects flavor-blindness at the Planck scale. In terms of these

four parameters, the soft terms in Eq. (2.9) are given by:

$$\begin{aligned}
M_1 &= M_2 = M_3 = m_{1/2} \\
m_{\tilde{Q}}^2 &= m_{\tilde{U}}^2 = m_{\tilde{D}}^2 = m_{\tilde{L}}^2 = m_{\tilde{E}}^2 = m_0^2 \mathbf{1}_{3 \times 3} \\
m_{H_u}^2 &= m_{H_d}^2 = m_0^2 \\
A_{u,d,e} &= A_0 h_{u,d,e} \\
b &= B_0 \mu
\end{aligned} \tag{2.26}$$

This parameterization, known as the minimal SUGRA or the MSUGRA model has been widely used in the literature. Its main virtue is its simplicity, though on theoretical grounds there is no obvious reason why the Kähler Potential should be flavor blind [47].

2.3.2 Gauge mediated SUSY breaking

Another simple framework is to assume that SUSY breaking in a hidden sector is communicated to the visible sector by standard model gauge interactions via heavy chiral supermultiplets that are charged under the standard model gauge symmetries [48]. Since gauge interactions are family-universal, the induced SUSY breaking becomes family universal in the visible sector.

The gauginos and scalars get masses from loops involving the

messenger fields (of mass M):

$$m_{\text{gaugino}} \sim \frac{g^2}{16\pi^2} \frac{\langle F \rangle}{M}; \quad m_{\text{scalar}}^2 \sim \left(\frac{g^2}{16\pi^2} \right)^2 \frac{\langle F \rangle^2}{|M|^2} \quad (2.27)$$

Thus the gaugino and the scalar masses are of the same order, which is important for a realistic model of SUSY breaking. The A-terms arise at two loops and are further suppressed by a factor of $\alpha_i/4\pi$, therefore are very small compared to the gaugino masses. Since the scalar masses depend only on gauge quantum numbers, they are flavor blind providing a natural solution to the SUSY flavor problem.

2.3.3 Supersymmetry breaking via anomalous $U(1)$

Anomalous $U(1)$ gauge groups often appear in effective theories after string compactification. Since the original string theory is anomaly free, anomaly cancellation happens via the Green-Schwarz mechanism.

Consider a pair of fields ϕ^+ and ϕ^- with $U(1)$ charges ± 1 , and assume that there are other charged fields Q_i such that $\text{Tr } Q > 0$.

Then the Fayet-Illiopoulos term is given by

$$\xi = \frac{g^2 \text{Tr } Q}{192\pi^2} M_{Pl}^2. \quad (2.28)$$

The D-term contribution to the effective potential is:

$$V_D = \frac{g^2}{2} \left(\sum_i q_i |Q_i|^2 + |\phi^+|^2 + |\phi^-|^2 + \xi \right)^2 \quad (2.29)$$

where q_i is the U(1) charge of the field Q_i . If the ϕ^\pm fields have a non-zero mass m , then the minimization of the potential leads to

$$\begin{aligned} \langle \phi^+ \rangle &= 0, & \langle \phi^- \rangle &= \xi - \frac{m^2}{g^2}, & \langle F_{\phi^+} \rangle &= m \sqrt{\xi - \frac{m^2}{g^2}}, \\ \langle F_{\phi^-} \rangle &= 0; & \langle D \rangle &= \frac{m^2}{g^2}. \end{aligned} \quad (2.30)$$

The supersymmetry breaking is communicated by gravity from the hidden sector, ϕ^\pm , to the observable sector, Q_i . The superparticle spectrum is given by (see Refs. [49–51]):

$$m_Q^2 = \frac{\langle F_{\phi^+} \rangle^2}{M_{Pl}^2} \approx \frac{m^2 \xi}{M_{Pl}^2}; \quad m_\lambda \simeq \frac{\langle F_{\phi^+} \phi^- \rangle}{M_{Pl}^2}. \quad (2.31)$$

The contributions to scalar masses, in principle, are non-universal. Extra contributions to the scalar masses arise, however, from the D-term for fields that transform under the anomalous U(1). These are given by

$$\Delta m_{Q_i}^2 = q_i m^2. \quad (2.32)$$

These contributions can be much larger than the F-term contributions

if $\epsilon \equiv \frac{\xi}{M_{Pl}^2} \ll 1$. Thus a hierarchy of soft masses is achieved:

$$\Delta m_{Q_i}^2 > m_Q^2 > m_\lambda^2. \quad (2.33)$$

This allows a solution to the SUSY flavor problem if the U(1) charges of the relevant Q_i fields are family universal. Precisely such family-universality arises automatically for a class of three family string models as shown in Ref. [50]. The soft trilinear couplings, i.e. the A-terms turn out to be small in a class of string models as discussed in Ref. [50], as also the B-term. We will make use of such a scenario of supersymmetry breaking in our study of CP and flavor violation. As noted in Refs. [50] and [51], the anomalous U(1) D-term SUSY breaking must, however, be combined with dilaton F-term SUSY breaking that gives desired masses to squarks, sleptons as well as gauginos.

2.3.4 *Anomaly mediated SUSY breaking*

In the absence of mass terms, a supergravity coupled Yang-Mills theory is classically conformally invariant. This symmetry is broken by quantum effects, i.e. renormalization, which introduces a mass scale into the theory. This leads to conformal anomaly, which leads to soft

SUSY breaking terms with a very definite pattern [52]:

$$\begin{aligned}
m_\lambda &= -\frac{\beta(g^2)}{2g^2}m_{3/2} \\
m_{\tilde{f}}^2 &= -\frac{1}{4}\left(\frac{d\gamma}{dg}\beta(g) + \frac{d\gamma}{dy}\beta(y)\right)m_{3/2}^2 \\
\text{and } A_{ijk} &= -y_{ijk}\frac{(\gamma_i+\gamma_j+\gamma_k)}{2}m_{3/2}
\end{aligned}
\tag{2.34}$$

where $m_{3/2}$ is the gravitino mass, $\beta(g)$ is the beta function of the gauge coupling g , and γ_i are the anomalous dimension of the field. An important consequence is that in the absence of Yukawa interactions, i.e. $y = 0$, the sfermion masses are family degenerate, thus alleviating the SUSY flavor problem. One problem with this mechanism of SUSY breaking is that the slepton mass squared are negative since they do not get the SU(3)-color contributions. Some attempts have been made to solve this problem in recent years, for example, by combining anomaly mediated SUSY breaking with other mechanisms of SUSY breaking [53].

2.3.5 Gaugino mediated SUSY breaking

This mechanism of supersymmetry breaking [54] makes use of an extra-dimensional setup. The standard model gauge fields are assumed to propagate in the bulk, while the matter fields are localized

on the visible brane. The gauginos get a mass from contact terms on the hidden brane:

$$\Delta\mathcal{L} \sim \int d^2\theta \frac{X}{M} W^\alpha W_\alpha + h.c. \quad (2.35)$$

where X is a hidden sector field that breaks supersymmetry. Thus the gaugino gets a mass at the tree level, while the visible matter fields get mass at the one-loop order, leading to gaugino masses being much larger at the compactification scale, M^* , than the scalar masses. At the 1 TeV scale, these masses are of the same order due to renormalization group running. The gaugino masses are unified at the compactification scale i.e. $M_1 = M_2 = M_3$ at the compactification scale. The quantity M_i/g_i^2 is RG invariant at one loop, therefore at the weak scale we get:

$$\frac{M_1}{g_1^2} \simeq \frac{M_2}{g_2^2} \simeq \frac{M_3}{g_3^2} \quad (2.36)$$

The scalar masses and A-terms are generated by loops involving gauginos, hence the name of the mechanism. These masses are suppressed by a loop factor relative to the gaugino masses at the compactification scale.

The soft SUSY breaking spectrum at the compactification scale with gaugino mediated SUSY breaking is found to be:

$$\begin{aligned}
M_1 &= M_2 = M_3 = m_{1/2} \\
m_{H_u}^2, m_{H_d}^2 &\sim m_{1/2}^2 \\
m_{\tilde{q}}^2, m_{\tilde{l}}^2 &\sim \frac{m_{1/2}^2}{16\pi^2} \\
A &\sim \frac{m_{1/2}}{16\pi^2}
\end{aligned}
\tag{2.37}$$

This model can also address the SUSY CP problem. CP violating phases can appear in μ , B and $M_{1/2}$ from higher dimensional operators. The phases in B and μ can be rotated away by $U(1)_{PQ}$ and $U(1)_R$ transformations, leaving a single phase in $m_{1/2}$. This phase can naturally vanish if CP is violated only by terms in the Lagrangian localized on the visible brane. This situation can arise if CP is broken spontaneously on the visible brane.

Thus gaugino mediated SUSY breaking is capable of yielding a realistic SUSY spectrum together with providing a solution of the SUSY CP and flavor problems.

These mechanisms illustrate that family universality or flavor blindness and reality of soft SUSY parameters can arise plausibly

within viable models of SUSY-breaking.

2.3.6 Constrained MSSM

One extreme form of universality is the so called Constrained MSSM (CMSSM) which is characterized by five universal parameters at a high scale M^* :

$$\begin{aligned}
 m_{\tilde{Q}, \tilde{U}, \tilde{D}, \tilde{L}, \tilde{E}, H_u, H_d}^2 &= m_0^2 \\
 M_1 &= M_2 = M_3 = m_{1/2} \\
 A_{u,d,e} &= A_0 \\
 \mu \text{ and } \tan \beta &\equiv v_u/v_d
 \end{aligned}
 \tag{2.38}$$

We should stress, however, that there is no strong theoretical or phenomenological reason to impose squark-slepton-Higgs mass universality. For example, in the anomalous U(1) D-term SUSY breaking model, family universality can hold (with $q_1 = q_2 = q_3$) but squark-Higgs universality does not hold if $q_1 = q_2 = q_3 \neq q_{H_u} \neq q_{H_d}$ (see [50])

3. GRAND UNIFICATION AND THE CHOICE OF THE GAUGE GROUP

The idea of grand unification was initiated in Refs. [11–14]. A comprehensive review can be found in Ref. [55]. Much of my thesis work deals with the issues of CP and flavor violations and coupling unification in the context of supersymmetric SO(10) [18] or an effective string-derived G(224) symmetry [12,20]. Therefore, I first list some evidence in favor of supersymmetric grand unification, especially that based on SO(10) or an effective G(224)-symmetry. As we will see, the advantages of these two symmetries over alternatives such as SU(5) [13] or $[SU(3)]^3$ [21], arise because they both possess the symmetry SU(4)-color.

As mentioned in the introduction, the evidence (including old and new) in favor of supersymmetric grand unification has become strong over the years. This includes:

(a) the quantum numbers of quarks and leptons in a family, which are predicted precisely by grand unification in accord with observations;

(b) quantization of electric charge;

(c) $Q_{e^-}/Q_p = -1$;

(d) the meeting of the three gauge couplings at a scale $M_U \sim 2 \times 10^{16}$ GeV in the context of low energy supersymmetry [24];

(e) neutrino oscillations with a (mass)² splitting $\sqrt{\Delta m^2(\nu)_{23}} \sim 1/20$ eV [6];

(f) the success of two mass relations (i) $m_b(\text{GUT}) \approx m_\tau$, and (ii) $m(\nu_{\text{Dirac}}^\tau) \approx m_{\text{top}}(\text{GUT})$ (needed for the success of the seesaw mechanism [17]);

(g) successful baryogenesis via leptogenesis leading to $Y_B \sim 10^{-10}$ [15, 16].

While the first four features (a)–(d) provide strong support, on empirical grounds, in favor of grand unification, they leave open the question of the choice of the effective symmetry G in 4D near the GUT-scale. In particular, they do not make a sharp distinction between the

alternatives of (i) $SU(5)$ [13], (ii) $SO(10)$ [18], (iii) E_6 [19], (iv) $[SU(3)]^3$ [21], or (v) a string-derived semi-simple group like $G(224)$ [12,20], with coupling unification being ensured in this case by string theory at the string scale (see remarks below), or (vi) flipped $SU(5) \times U(1)$ [56]. Of these, the symmetries $G(224)$, $SO(10)$ and E_6 possess the symmetry $SU(4)$ -color, while $SU(5)$, $[SU(3)]^3$ and flipped $SU(5) \times U(1)$ do not.

One can argue that the last three features, involving: (e) neutrino oscillations, (f) the success of the two mass relations $m_b(\text{GUT}) \approx m_\tau$, and $m(\nu_{\text{Dirac}}^\tau) \approx m_{\text{top}}(\text{GUT})$, and (g) the success of baryogenesis via leptogenesis, clearly suggest that the effective symmetry G in 4D should possess the symmetry $SU(4)$ -color. I will mention below the common advantages shared by $SO(10)$ and a string-derived $G(224)$ -symmetry as well as the distinctions between them.

3.1 *The need for $SU(4)$ -color*

To see the need for having $SU(4)$ -color as a component of the higher gauge symmetry, it is useful to recall the family-multiplet structure of $G(224)$, which is retained by $SO(10)$ as well. The symmetry $G(224) =$

$SU(2)_L \times SU(2)_R \times SU(4)^c$, subject to left-right discrete symmetry which is natural to $G(224)$, organizes members of a family into a single left-right self-conjugate multiplet $(F_L^e \oplus F_R^e)$ given by:

$$F_{L,R}^e = \begin{bmatrix} u_r & u_g & u_b & \nu_e \\ d_r & d_g & d_b & e^- \end{bmatrix}_{L,R} \quad (3.1)$$

The multiplets F_L^e and F_R^e are left-right conjugates of each other transforming respectively as $(\mathbf{2}, \mathbf{1}, \mathbf{4})$ and $(\mathbf{1}, \mathbf{2}, \mathbf{4})$ of $G(224)$; likewise for the muon and the tau families. Note that each family of $G(224)$, subject to left-right symmetry, must contain sixteen two-component objects as opposed to fifteen for $SU(5)$ or the standard model. While the symmetries $SU(2)_{L,R} \subset G(224)$ treat each column of $F_{L,R}^e$ as doublets, the symmetry $SU(4)$ -color unifies quarks and leptons by treating each row of F_L^e and F_R^e as a quartet. Thus both $SU(4)$ -color and $SU(2)_R$ predict the existence of the right-handed neutrino as an essential member of each family, with non-trivial $SU(4)^c$ and $SU(2)_R$ quantum numbers [12]. In particular, $SU(4)$ -color treats the left and right-handed neutrinos $(\nu_L^e$ and $\nu_R^e)$ as the fourth color-partners of the left and right-handed up quarks $(u_L$ and $u_R)$ respectively; likewise

for the μ and the τ families.

The familiar $SU(3)^c$, $SU(2)_L$, Y_W as well as $SU(2)_R$ and $B - L$ quantum numbers of all the members of any multiplet are fully determined by the symmetry $G(224)$, once the representation of the multiplet is specified. In particular, the charge formula for any multiplet (matter, Higgs or gauge) is given by the elegant formula [12, 57]:

$$Q = I_{3L} + I_{3R} + \frac{B - L}{2}. \quad (3.2)$$

where I_{3L} , I_{3R} and $B - L$ have familiar meanings. The hypercharge is thus determined by the formula:

$$Y_W = I_{3R} + \frac{B - L}{2}. \quad (3.3)$$

Because of the symmetry $SU(4)$ -color, we have at the GUT scale the following two mass relations for the third family: $m_b(\text{GUT}) \approx m_\tau$, and $m(\nu_{\text{Dirac}}^\tau) \approx m_{\text{top}}(\text{GUT})$. The first relation is empirically favored. The second relation is needed for the success of the seesaw mechanism in yielding the scale of the (mass)²-splitting for atmospheric neutrino oscillations [6].

An important feature of $SU(4)$ -color is that it introduces $B - L$ as a local symmetry. This protects the Majorana masses of the right-

handed neutrinos from acquiring Planck-scale values. The symmetry, SO(10) or a string-derived G(224) should break into the standard model symmetry at the GUT scale $M_U \approx 2 \times 10^{16}$ GeV to account for the observed gauge coupling unification. This implies that $B - L$ should break spontaneously at a scale M_{B-L} near the GUT scale (i.e. $M_{B-L} \sim M_{GUT}$) rather than at a low or intermediate scale like $10^3 - 10^{13}$ GeV. This in turn implies that the mass of the heaviest right-handed Majorana neutrino should be close to the GUT scale rather than being arbitrarily light (like 1–10 TeV) or of the Planck scale. This is needed for the seesaw mechanism to give to give desired masses to neutrinos and for the success of baryogenesis via leptogenesis [15, 16].

I will now argue (see e.g. [58]) that (i) the seesaw mechanism, (ii) the symmetry SU(4)-color, and (iii) the SUSY unification-scale M_U , *together* provide a simple understanding of the neutrino (mass)²-splitting observed at SuperK i.e. $\sqrt{\Delta m^2(\nu)_{23}} \equiv \sqrt{|m^2(\nu_3) - m^2(\nu_2)|} \sim 1/20$ eV [6]. Ignoring inter-family mixing for simplicity, for a moment, the seesaw mechanism [17] combines the super heavy Majorana mass, $M(\nu_R)$ of the right-handed neutrino with the Dirac mass of the

neutrino to give a light mass for the left handed neutrino (through diagonalization):

$$m(\nu_L) \approx m(\nu)_{\text{Dirac}}^2/M(\nu_R) \quad (3.4)$$

For the third family, the Dirac mass of ν_τ is related to the top mass at the GUT scale through the SU(4)-color relation $m(\nu_{\text{Dirac}}^\tau) \approx m_{\text{top}}(\text{GUT}) \approx 120 \text{ GeV}$. The Majorana mass of the right-handed neutrino is related, again, by SU(4)-color to the scale of $B - L$ breaking i.e. M_{B-L} . In the context of a minimal Higgs sector which breaks $B - L$ by one unit (see Chapter 4), $M(\nu_R^\tau) \sim M_{B-L}^2/M \approx M_{\text{GUT}}^2/M \approx (2 \times 10^{16} \text{ GeV})^2 / (10^{18} \text{ GeV})(1/2 - 2) \approx (4 \times 10^{14} \text{ GeV})(1/2 - 2)$, say, where M denotes the scale of an effective non-renormalizable operator induced by Planck or string-scale physics and therefore has the magnitude $(10^{18} \text{ GeV})(1/2 - 2)$. Substituting these values into Eq. (4.8), we get

$$m(\nu_L^3) \approx (120 \text{ GeV})^2 / (4 \times 10^{14} \text{ GeV})(1/2 - 2) \approx (1/28)(1/2 - 2) \text{ eV} \quad (3.5)$$

Following the hierarchical pattern of fermion masses (see Chapter 4), one naturally expects $m(\nu_L^2) \ll m(\nu_L^3)$. Thus $\sqrt{\Delta m^2(\nu)_{23}} \approx m(\nu_L^3) \sim$

$(1/28)(1/2 - 2)eV$, which is in very good agreement with the Super Kamiokande data [6].

Let us contrast this with the case of $SU(5)$ unification. In this case, the fermions of one generation belong to $\bar{\mathbf{5}} + \mathbf{10}$ of $SU(5)$; these do not, however, contain a right-handed neutrino. Even if one introduces the right-handed neutrino by hand as a singlet of $SU(5)$, there is no $B - L$ symmetry to protect its Majorana mass from acquiring either Planck scale values or being as light as even 1 TeV. Also, while $m_b(\text{GUT}) \approx m_\tau$ holds for $SU(5)$, there is no relation between $m(\nu_{\text{Dirac}}^\tau)$ and m_{top} unlike the case of $G(224)$. The Dirac mass term is therefore arbitrary, except for being bounded from above by the electroweak scale. It can thus vary from say 1 MeV to 100 GeV. With such large arbitrariness in $M(\nu_R^\tau)$ and $m(\nu_{\text{Dirac}}^\tau)$, $m(\nu_L^3)$ can vary from about 10^{-14} eV to as high as about 10 GeV. This arbitrariness is drastically reduced, however, as shown above, if ν_R is related to the other fermions in a family by $SU(4)$ -color symmetry. Thus $m(\nu_L^3)$ cannot be determined in the case of $SU(5)$.

Symmetries like $G(2213) = SU(2)_L \times SU(2)_R \times U(1)_{B-L} \times SU(3)^c$

[59] and $[SU(3)]^3$ [21] possess $B - L$ and the right handed neutrino, and therefore the Majorana mass $M(\nu_R)$ is constrained. The Dirac mass term, on the other hand, is arbitrary as there is no relation between the top mass and the neutrino Dirac mass. And, there is no $b - \tau$ unification either. In the case of flipped $SU(5) \times U(1)$ [56], both $B - L$ and the right handed neutrino exist, and the relation $m(\nu_{\text{Dirac}}^\tau) \approx m_{\text{top}}$ holds, but there is no symmetry relating the b and τ masses.

Thus we see that the observed neutrino oscillations and the success of certain fermion mass relations clearly support (a) the idea of the seesaw, (b) SUSY unification, *and* (c) the route to higher unification based on the symmetry $SU(4)$ -color. This says as mentioned in the introduction, that the effective symmetry in 4D above the GUT-scale should either be $SO(10)$ (possibly E_6), or minimally a string-derived $G(224)$ or $G(214)$ symmetry, as opposed alternative symmetries.

Although I will not discuss baryogenesis in my thesis, it turns out that baryogenesis via leptogenesis [15, 16], which again requires the existence of the right handed neutrino as above, clearly support

an effective symmetry like $SO(10)$ or $G(224)$ or $G(214)$ symmetry.

I will now briefly mention some similarities and distinctions between an effective SUSY $SO(10)$ and $G(224)$ symmetry.

3.2 Similarities and Differences between $G(224)$ and $SO(10)$

As partly noted above, the effective symmetry $G(224)$ together with left-right discrete symmetry offers some attractive features including :

- (i) unification of all sixteen members of a family within one left-right self-conjugate multiplet;
- (ii) quantization of electric charge;
- (iii) quark lepton unification through $SU(4)$ -color;
- (iv) conservation of parity at a fundamental level [59,60];
- (v) right-handed neutrinos as a compelling feature;
- (vi) $B-L$ as a local symmetry, and
- (vii) the desired mass relations for the third family.

As noted above, some of these features are needed on empirical grounds. Any simple or semi-simple group that contains $G(224)$ as a sub-group would of course possess these seven features, so does therefore $SO(10)$, which is the smallest simple group containing $G(224)$. $SO(10)$ even preserves the family multiplet structure of $G(224)$, where the L-R conjugate 16-plet = $(F_L \oplus F_R)$

corresponds to the spinorial $16 = (F_L \oplus (F_R)^c)$ of $SO(10)$. The group $G(224)$, with $SU(4)$ -color being vectorial, is anomaly free; $SO(10)$ is anomaly-free as a group.

In addition to sharing these features, $SO(10)$ and $G(224)$ lead essentially to the same predictions for fermion masses and neutrino oscillations in the context of a minimal Higgs system (see Chapter 4).

Despite these similarities, there are, however, two notable distinctions between $SO(10)$ and $G(224)$, as regards the issues of (a) gauge coupling unification, and (b) doublet-triplet splitting. For this discussion, I will assume that either $SO(10)$ or $G(224)$ emerges as an effective symmetry in 4D through compactification of string/M theory defined in $D = 10/11$ to four dimensions. (For attempts at obtaining string- $SO(10)$ solution see Ref. [61] and a string $G(224)$ solution see Ref. [20]).

For the case of a string derived $G(224)$ solution, coupling unification ($g_{2L} = g_{2R} = g_4$) can hold at the string scale M_{st} through the constraints of string theory, even though $G(224)$ is a semi-simple group [36]. One may then hope to explain the observed gauge cou-

pling unification by assuming that the string scale is not far above the GUT scale ($M_{st} \approx (2 - 3)M_{GUT}$), where $G(224)$ breaks into the standard model. I will explore this issue concretely in Chapter 8. On the other hand, for $SO(10)$, coupling unification is ensured above the GUT scale regardless of the gap between M_{st} and M_{GUT} .

A string derived $G(224)$ solution, however, possesses a distinct advantage over a SUSY $SO(10)$ -solution as regards the problem of doublet-triplet splitting. As noted by several authors (see e.g. [20,34]), the undesired color triplets which induce rapid proton decay can naturally be projected out in this case by the process of string compactification. For the case of SUSY- $SO(10)$, one would need a suitable mechanism in 4D to make the color triplets super heavy while keeping the $SU(2)$ doublets light. Such a mechanism has been constructed in 4D [35], but it is not clear if it can emerge consistently from a string theory.

In view of the relative advantages of $G(224)$ and $SO(10)$ over each other, and the fact that the possible disadvantage in each case has at least a plausible solution, I will consider both interchangeably

as they share the advantages (i)–(vii), and lead essentially to the same predictions for fermion masses and neutrino oscillations (see Chapter 4), and also baryogenesis via leptogenesis (see e.g. Ref. [16]). I will point out in Chapters 5 and 6 that the two symmetries can in fact be distinguished empirically through experiments involving CP and flavor violations¹. In the next section, I will describe some group properties of SO(10) and its breaking into the standard model.

3.3 *SO(10) and its breaking into the standard model*

It would be useful to enlist the decomposition of some representations of SO(10) under G(224) and SU(5). As mentioned earlier, the **16** of SO(10) contains the standard model fermions including the right handed neutrino. The rest of the representations, including the **16**,

¹ Although I will not discuss it here, it has been shown that the symmetries SO(10) and G(224) can also be distinguished through proton decay searches, especially the decay $p \rightarrow e^+\pi^0$. See e.g. [62]

are often used as Higgs to break $SO(10)$ down to smaller groups.

$$10 \quad G(224) : (1, 1, 6) + (2, 2, 1)$$

$$SU(5) : 5 + \bar{5}$$

$$16 \quad G(224) : (2, 1, 4) + (1, 2, \bar{4})$$

$$SU(5) : 10 + \bar{5} + 1$$

$$45 \quad G(224) : (3, 1, 1) + (2, 2, 6) + (1, 1, 15) + (1, 3, 1)$$

$$SU(5) : 24 + 10 + \bar{10} + 1$$

$$54 \quad G(224) : (1, 1, 1) + (2, 2, 6) + (1, 1, 20) + (3, 3, 1)$$

$$SU(5) : 24 + 15 + \bar{15}$$

$$120 \quad G(224) : (1, 1, 20) + (2, 2, 15) + (1, 3, \bar{6}) + (3, 1, 6) + (2, 2, 1)$$

$$SU(5) : 5 + \bar{5} + 10 + \bar{10} + 45 + \bar{45}$$

$$126 \quad G(224) : (3, 1, 10) + (2, 2, 15) + (1, 3, \bar{10}) + (1, 1, \bar{6})$$

$$SU(5) : 1 + \bar{5} + 10 + \bar{15} + 45 + \bar{50}$$

$$210 \quad G(224) : (1, 1, 1) + (1, 1, 15) + (1, 3, 15) + (3, 1, 15)$$

$$+ (2, 2, 20) + (2, 2, 6)$$

$$SU(5) : 1 + 5 + \bar{5} + 10 + \bar{10} + 24 + 40 + \bar{40} + 75$$

Depending on choice of the Higgs, $SO(10)$ can break into the standard model in several different ways. Some $SO(10)$ breaking chains are presented below.

(1) $SO(10) \xrightarrow{\langle 16_H \rangle / \langle 126_H \rangle} SU(5) \xrightarrow{\langle 45_H \rangle} SM$, where SM stands for the $G(213) \equiv SU(2)_L \times U(1)_Y \times SU(3)^c$ symmetry. In the case of the 16_H the scalar field with the quantum numbers of the right handed neutrino i.e. $(\tilde{\nu}_R^c)_H$ gets a VEV. For the 126_H it is the one with the quantum numbers of $(\tilde{\nu}_R^c)_H(\tilde{\nu}_R^c)_H$ that gets a VEV. It must be noted that because supersymmetry is broken only at the electroweak scale, the Higgs multiplets that reduce the rank of the gauge group must occur in pairs e.g. $16 + \overline{16}$ or $126 + \overline{126}$, so that the D-terms due to these cancel each other.

$$(2) SO(10) \xrightarrow{\langle 54_H \rangle} G(224) \times Z_2 \xrightarrow{\langle 16_H \rangle / \langle 126_H \rangle} SM.$$

$$(3) SO(10) \xrightarrow{\langle 45_H \rangle^{B-L}} SU(2)_L \times SU(2)_R \times U(1)_{B-L} \times SU(3) \xrightarrow{\langle 16_H \rangle = \langle (\tilde{\nu}_R^c)_H \rangle} SM.$$

$$(4) SO(10) \xrightarrow{\langle 210_H \rangle} G(224) \xrightarrow{\langle 16_H \rangle / \langle 126_H \rangle} SM.$$

To summarize, in this chapter, we show that any unification symmetry above the GUT scale should possess $SU(4)$ -color. This symme-

try could minimally be $G(224)$ or maximally $SO(10)$. We have described a general form of $SO(10)$ unification and its breaking to the standard model. This can be done by using low dimensional Higgs multiplets including $(16 + \overline{16})$ or large dimensional Higgs- multiplets including $(126 + \overline{126})$. In chapter 4, I will describe in detail, a specific $SO(10)$ model proposed by Babu, Pati and Wilczek [25], that uses a minimal set of low dimensional Higgs-multiplets.

4. FERMION MASSES AND NEUTRINO OSCILLATIONS IN A SO(10)/G(224) FRAMEWORK: A REVIEW OF THE BPW MODEL

To set the background for my work on CP and flavor violations, I will first review a predictive framework based on the SO(10) or G(224) symmetry proposed by Babu, Pati and Wilczek [25] (to be referred to as the BPW model henceforth). This framework has been shown to be remarkably successful in describing fermion masses and neutrino oscillations. It introduces a minimal Higgs system containing low dimensional multiplets to break SO(10) to the standard model and the same multiplets are used also to generate fermion masses. In the following, only the case of SO(10) is presented. The discussion would remain essentially unaltered for the symmetry G(224), if one uses the corresponding G(224) Higgs-submultiplets instead.

The minimal Higgs system used in the BPW model consists of

the set:

$$H_{\text{minimal}} = \{ \mathbf{45}_H, \mathbf{16}_H, \overline{\mathbf{16}}_H, \mathbf{10}_H \} \quad (4.1)$$

Of these, the VEV of $\langle \mathbf{45}_H \rangle \sim M_X$ breaks $SO(10)$ in the B-L direction to $G(2213) = SU(2)_L \times SU(2)_R \times U(1)_{B-L} \times SU(3)^c$, and those of $\langle \mathbf{16}_H \rangle = \langle \overline{\mathbf{16}}_H \rangle$ along $\langle \tilde{\nu}_{RH} \rangle$ and $\langle \tilde{\nu}_{RH} \rangle$ break $G(2213)$ into the SM symmetry $G(213)$ at the unification-scale M_X . Now $G(213)$ breaks at the electroweak scale by the VEV of $\langle \mathbf{10}_H \rangle$ to $SU(3)^c \times U(1)_{em}$.

Before discussing fermion masses and mixings, some advantages and disadvantages of using low dimensional Higgs multiplets (as listed in Eq. (4.1) above) versus large-dimensional ones are noted below. Large-dimensional tensorial multiplets of $SO(10)$ including $(126_H, \overline{126}_H)$, 210_H and possibly 120_H , have been used widely in the literature [63] to break $SO(10)$ to the SM symmetry and give masses to the fermions. In the BPW model, the use of low-dimensional Higgs multiplets (45_H , 16_H and $\overline{16}_H$) was preferred over the large dimensional ones like $(126_H, \overline{126}_H, 210_H$ and possibly $120_H)$ in part because the latter tend to give too large GUT-scale threshold corrections to $\alpha_3(m_Z)$ from split sub-multiplets (typically exceeding 15–20% with ei-

ther sign), which would render observed gauge coupling unification fortuitous. By contrast, with the low-dimensional multiplets (45_H , 16_H and $\overline{16}_H$), the threshold corrections to $\alpha_3(m_Z)$ are smaller and are found, for a large range of the relevant parameters, to have the right sign and magnitude (nearly -5 to -8%) so as to account naturally for the observed gauge coupling unification [25].

Another possible disadvantage of 126_H , which contributes to EW symmetry breaking through its (2, 2, 15) component of $G(224)$, is that it gives $B - L$ dependent contribution to family-diagonal fermion masses. Such a contribution, barring adjustment of parameters against the contribution of $\langle 10_H \rangle$ could in general make the success of the relation $m_b(GUT) \approx m_\tau$ fortuitous. By contrast, the latter relation emerges as a robust prediction of the minimal Higgs system ($45_H, 16_H, \overline{16}_H$ and 10_H), subject to a hierarchical pattern, because the only ($B - L$) dependent contribution in this case can come effectively through $\langle 10_H \rangle \langle 45_H \rangle / M$ which is family-antisymmetric and cannot contribute to diagonal entries (see below).

For what it is worth, it has also been shown that weakly interact-

ing heterotic string theories do yield the low-dimensional multiplets as in Eq. (4.1), but not the high dimensional ones such as 126 and 120 [64].

Balancing against these advantages of the minimal Higgs system, the large-dimensional system $(126_H, \overline{126}_H)$ has an advantage over the minimal system, because 126 and $\overline{126}$ break $B - L$ by two units and thus automatically preserve the familiar R-parity $= (-1)^{3(B-L)+2S}$. By contrast, 16 and $\overline{16}$ break $B - L$ by one unit and thereby break the familiar R-parity. This possible drawback is, however, easily avoided, because for a large class of models based on low dimensional Higgs multiplets (see e.g. [25] and [30]) one can still define consistently a matter-parity (i.e. $16_i \rightarrow -16_i$, $16_H \rightarrow 16_H$, $\overline{16}_H \rightarrow \overline{16}_H$, $45_H \rightarrow 45_H$, $10_H \rightarrow 10_H$), which serves the desired purpose by allowing all desired interactions but forbidding the dangerous $d = 4$ proton decay operators and yielding stable LSP to serve as CDM. Taking into account the net advantages as noted above, the BPW model makes use of the minimal Higgs system. The structure of the fermion mass matrices obtained with this set of Higgs is given below.

The 3×3 Dirac mass matrices for the four sectors (u, d, l, ν) proposed in Ref. [25] were motivated in part by the notion that flavor symmetries [65] are responsible for the hierarchy among the elements of these matrices (i.e., for “33” \gg “23” \gg “22” \gg “12” \gg “11”, etc.), and in part by the group theory of $SO(10)/G(224)$, relevant to a minimal Higgs system (see below). Up to minor variants,¹ they are

¹ The zeros in “11”, “13”, and “31” elements signify that they are relatively small quantities (specified below). While the “22” elements were set to zero in Ref. [25], because they are meant to be $<$ “23” “32” / “33” $\sim 10^{-2}$ (see below), and thus unimportant for purposes of Ref. [25], they are retained here, because such small ζ_{22}^u and ζ_{22}^d [$\sim (1/3) \times 10^{-2}$ (say)] can still be important for CP violation and thus leptogenesis.

as follows:²

$$M_u = \begin{bmatrix} 0 & \epsilon' & 0 \\ -\epsilon' & \zeta_{22}^u & \sigma + \epsilon \\ 0 & \sigma - \epsilon & 1 \end{bmatrix} \mathcal{M}_u^0 \quad (4.2a)$$

$$M_d = \begin{bmatrix} 0 & \eta' + \epsilon' & 0 \\ \eta' - \epsilon' & \zeta_{22}^d & \eta + \epsilon \\ 0 & \eta - \epsilon & 1 \end{bmatrix} \mathcal{M}_d^0 \quad (4.2b)$$

$$M_\nu^D = \begin{bmatrix} 0 & -3\epsilon' & 0 \\ 3\epsilon' & \zeta_{22}^u & \sigma - 3\epsilon \\ 0 & \sigma + 3\epsilon & 1 \end{bmatrix} \mathcal{M}_u^0 \quad (4.2c)$$

$$M_l = \begin{bmatrix} 0 & \eta' - 3\epsilon' & 0 \\ \eta' + 3\epsilon' & \zeta_{22}^d & \eta - 3\epsilon \\ 0 & \eta + 3\epsilon & 1 \end{bmatrix} \mathcal{M}_d^0$$

² A somewhat analogous pattern, also based on $SO(10)$, has been proposed by C. Albright and S. Barr [AB] [30]. One major difference between the work of AB and that of BPW [25] is that the former introduces the so-called “lop-sided” pattern in which some of the “23” elements are even greater than the “33” element; in BPW on the otherhand, the pattern is consistently hierarchical with individual “23” elements (like η , ϵ and σ) being much smaller in magnitude than the “33” element of 1. For a comparative study of some of the $SO(10)$ -models for fermion masses and neutrino oscillations and the corresponding references, see C.H. Albright, talk presented at the Stony Brook conf. (Oct. 2002), Ed. by R. Shrock, publ. by World Scientific (page 201). A comparative study of the AB and the BPW models based on their predictions regarding CP and flavor violations is presented in chapter 7.

These matrices are defined in the gauge basis and are multiplied by $\bar{\Psi}_L$ on left and Ψ_R on right. For instance, the row and column indices of M_u are given by $(\bar{u}_L, \bar{c}_L, \bar{t}_L)$ and (u_R, c_R, t_R) respectively. Note the group-theoretic up-down and quark-lepton correlations: the same σ occurs in M_u and M_ν^D , and the same η occurs in M_d and M_l . It will become clear that the ϵ and ϵ' entries are proportional to $B-L$ and are antisymmetric in the family space (as shown above). Thus, the same ϵ and ϵ' occur in both $(M_u$ and $M_d)$ and also in $(M_\nu^D$ and $M_l)$, but $\epsilon \rightarrow -3\epsilon$ and $\epsilon' \rightarrow -3\epsilon'$ as $q \rightarrow l$. Such correlations result in enormous reduction of parameters and thus in increased predictiveness. Such a pattern for the mass-matrices can be obtained, using a minimal Higgs system $\mathbf{45}_H$, $\mathbf{16}_H$, $\overline{\mathbf{16}}$, and $\mathbf{10}_H$ and a singlet S of $SO(10)$ carrying

flavor charges (see below), through effective couplings as follows [66]:

$$\begin{aligned}
\mathcal{L}_{\text{Yuk}} = & \\
& h_{33} \mathbf{16}_3 \mathbf{16}_3 \mathbf{10}_H \\
& + h_{23} \mathbf{16}_2 \mathbf{16}_3 \mathbf{10}_H (S/M) \\
& + a_{23} \mathbf{16}_2 \mathbf{16}_3 \mathbf{10}_H (\mathbf{45}_H / M') (S/M)^p \\
& + g_{23} \mathbf{16}_2 \mathbf{16}_3 \mathbf{16}_H^d (\mathbf{16}_H / M'') (S/M)^q \\
& + h_{22} \mathbf{16}_2 \mathbf{16}_2 \mathbf{10}_H (S/M)^2 \tag{4.3} \\
& + g_{22} \mathbf{16}_2 \mathbf{16}_2 \mathbf{16}_H^d (\mathbf{16}_H / M'') (S/M)^{q+1} \\
& + g_{12} \mathbf{16}_1 \mathbf{16}_2 \mathbf{16}_H^d (\mathbf{16}_H / M'') (S/M)^{q+2} \\
& + a_{12} \mathbf{16}_1 \mathbf{16}_2 \mathbf{10}_H (\mathbf{45}_H / M') (S/M)^{p+2}
\end{aligned}$$

Typically we expect M' , M'' and M to be of order M_{string} [67]. The VEV's of $\langle \mathbf{45}_H \rangle$ (along $B-L$), $\langle \mathbf{16}_H \rangle = \langle \overline{\mathbf{16}}_H \rangle$ (along standard model singlet sneutrino-like component) and of the $SO(10)$ -singlet $\langle S \rangle$ are of the GUT-scale, while those of $\mathbf{10}_H$ and of the down type $SU(2)_L$ -doublet component in $\mathbf{16}_H$ (denoted by $\mathbf{16}_H^d$) are of the electroweak scale [25, 68]. The powers of (S/M) are determined by flavor charges (see below). Depending upon whether $M'(M'') \sim M_{\text{GUT}}$ or M_{string}

(see [69]), the exponent $p(q)$ is either one or zero [69].

The entries 1 and σ arise respectively from h_{33} and h_{23} couplings, while $\hat{\eta} \equiv \eta - \sigma$ and η' arise respectively from g_{23} and g_{12} -couplings. The (B-L)-dependent antisymmetric entries ϵ and ϵ' arise respectively from the a_{23} and a_{12} couplings. [Effectively, with $\langle \mathbf{45}_H \rangle \propto B - L$, the product $\mathbf{10}_H \times \mathbf{45}_H$ contributes as a $\mathbf{120}$, whose coupling is family-antisymmetric.] The small entry ζ_{22}^u arises from the h_{22} -coupling, while ζ_{22}^d arises from the joint contributions of h_{22} and g_{22} -couplings. As discussed in [25], using some of the observed masses as inputs, one obtains $|\hat{\eta}| \sim |\sigma| \sim |\epsilon| \sim \mathcal{O}(1/10)$, $|\eta'| \approx 4 \times 10^{-3}$ and $|\epsilon'| \sim 2 \times 10^{-4}$. The success of the framework presented in Ref. [25] (which set $\zeta_{22}^u = \zeta_{22}^d = 0$) in describing fermion masses and mixings remains essentially unaltered if $|(\zeta_{22}^u, \zeta_{22}^d)| \leq (1/3)(10^{-2})$ (say).

Such a hierarchical form of the mass-matrices, with h_{33} -term being dominant, is attributed in part to flavor gauge symmetry(ies) that distinguishes between the three families, and in part to higher dimensional operators involving for example $\langle \mathbf{45}_H \rangle / M'$ or $\langle \mathbf{16}_H \rangle / M''$, which are suppressed by $M_{\text{GUT}} / M_{\text{string}} \sim 1/10$, if M' and/or $M'' \sim M_{\text{string}}$.

The basic presumption here is that effective dimensionless couplings allowed by $SO(10)/G(224)$ and flavor symmetries are of order unity [i.e., $(h_{ij}, g_{ij}, a_{ij}) \approx 1/3$ -3 (say)]. The need for appropriate powers of (S/M) with $\langle S \rangle/M \sim M_{\text{GUT}}/M_{\text{string}} \sim (1/10$ – $1/20)$ in the different couplings leads to a hierarchical structure. As an example, introduce just one $U(1)$ -flavor symmetry, together with a discrete symmetry D , with one singlet S . The hierarchical form of the Yukawa couplings exhibited in Eqs. (4.2) and (4.3) would follow, for the case of $p = 1$, $q = 0$, if, for example, the $U(1)$ flavor charges are assigned as follows (see e.g. [62]:

$$\begin{array}{cccc}
\mathbf{16}_3 & \mathbf{16}_2 & \mathbf{16}_1 & \mathbf{10}_H \\
a & a + 1 & a + 2 & -2a \\
\mathbf{16}_H & \overline{\mathbf{16}}_H & \mathbf{45}_H & \mathbf{S} \\
-a - 1/2 & -a & 0 & -1
\end{array} \tag{4.4}$$

The value of a would get fixed by the presence of other operators (see later). All the fields are assumed to be even under a discrete symmetry D , except for $\mathbf{16}_H$ and $\overline{\mathbf{16}}_H$ which are odd. It is assumed that other fields are present as in a string solution that would make

the U(1) symmetry anomaly-free. With this assignment of charges, one would expect $|\zeta_{22}^{u,d}| \sim (\langle S \rangle / M)^2$; one may thus take, for example, $|\zeta_{22}^{u,d}| \sim (1/3) \times 10^{-2}$ without upsetting the success of Ref. [25]. In the same spirit, one would expect $|\zeta_{13}, \zeta_{31}| \sim (\langle S \rangle / M)^2 \sim 10^{-2}$, and $|\zeta_{11}| \sim (\langle S \rangle / M)^4 \sim 10^{-4}$ (say). where ζ_{11} , ζ_{13} , and ζ_{31} denote the “11,” “13,” and “31,” elements respectively. These elements were dropped (ζ_{11} , ζ_{13} , ζ_{31} , and even ζ_{22}) as a first in Ref. [25] for the sake of economy of parameters. But these elements can in general be relevant in a more refined analysis (e.g. $\zeta_{11}^{u,d}$, though small, can make small contributions to $m_{u,d}$ of order few MeV without altering significantly the mixing angles, and ζ_{22} can be relevant for considerations of CP violation).

To discuss the neutrino sector one must specify the Majorana mass-matrix of the RH neutrinos as well. These arise from effective couplings of the form [70]:

$$\mathcal{L}_{\text{Maj}} = f_{ij} \mathbf{16}_i \mathbf{16}_j \overline{\mathbf{16}}_H \overline{\mathbf{16}}_H / M \quad (4.5)$$

where the f_{ij} 's include appropriate powers of $\langle S \rangle / M$, in accord with flavor charge assignments of $\mathbf{16}_i$ (see Eq. (4.4)), and M is expected to be of order string or reduced Planck scale. For the f_{33} -term to be

leading (~ 1), we must assign the charge $-a$ to $\overline{\mathbf{16}}_H$. This leads to a hierarchical form for the Majorana mass-matrix [25]:

$$M_R^\nu = \begin{bmatrix} x & 0 & z \\ 0 & 0 & y \\ z & y & 1 \end{bmatrix} M_R \quad (4.6)$$

Following the flavor-charge assignments given in Eq. (4.4), we expect $|y| \sim \langle S/M \rangle \sim 1/10$, $|z| \sim (\langle S/M \rangle)^2 \sim (1/200)(1 \text{ to } 1/2, \text{ say})$, $|x| \sim (\langle S/M \rangle)^4 \sim (10^{-4}\text{--}10^{-5})$ (say). The “22” element (not shown) is $\sim (\langle S/M \rangle)^2$ and its magnitude is taken to be $< |y^2/3|$, while the “12” element (not shown) is $\sim (\langle S/M \rangle)^3$. In short, with the assumption that the “33”-element is leading, the hierarchical pattern of M_R^ν is identical to that of the Dirac mass matrices (Eq. (4.2)). We expect

$$M_R = \frac{f_{33} \langle \overline{\mathbf{16}}_H \rangle^2}{M} \approx (4 \times 10^{14} \text{ GeV})(1/2\text{--}2) \quad (4.7)$$

where we have put $\langle \overline{\mathbf{16}}_H \rangle \approx 2 \times 10^{16} \text{ GeV}$, and $f_{33} \approx 1$. The effective scale M should lie between $M_{\text{string}} \approx 4 \times 10^{17} \text{ GeV}$ and $(M_{\text{Pl}})_{\text{reduced}} \approx 2 \times 10^{18} \text{ GeV}$. Thus we take $M \approx 10^{18} \text{ GeV}$ (1/2–2) [71]. These lead to an expected central value of M_R of around $4 \times 10^{14} \text{ GeV}$. Allowing for 2-3 family-mixing in the Dirac and the Majorana sectors as in Eqs.

(4.2) and (4.6), the seesaw mechanism leads to ([25]):

$$m(\nu_3) \approx B \frac{m(\nu_{\text{Dirac}}^\tau)^2}{M_R} \quad (4.8)$$

The quantity B represents the effect of 2-3 family-mixing and is given by $B = (\sigma + 3\epsilon)(\sigma + 3\epsilon - 2y)/y^2$ (see [25]). Thus B is fully calculable within the model once the parameters σ , η , ϵ , and y are determined in terms of inputs involving some quark and lepton masses (as noted below). In this way, one obtains $B \approx (2.9 \pm 0.5)$. The Dirac mass of the tau-neutrino is obtained by using the $SU(4)$ -color relation (see Chapter 3): $m(\nu_{\text{Dirac}}^\tau) \approx m_{\text{top}}(M_X) \approx 120$ GeV. One thus obtains from Eq. (4.7) :

$$\begin{aligned} m(\nu_3) &\approx \frac{(2.9)(120 \text{ GeV})^2}{10^{15} \text{ GeV}} (1/2-2) \\ &\approx (1/24 \text{ eV})(1/2-2) \end{aligned} \quad (4.9)$$

Noting that for hierarchical entries — i.e. for $(\sigma, \epsilon, \text{ and } y) \sim 1/10$ — one naturally obtains a hierarchical spectrum of neutrino-masses: $m(\nu_1) \lesssim m(\nu_2) \sim (1/10)m(\nu_3)$, we thus get:

$$\left[\sqrt{\Delta m_{23}^2} \right]_{\text{Th}} \approx m(\nu_3) \approx (1/24 \text{ eV})(1/2-2) \quad (4.10)$$

This agrees remarkably well with the SuperK value of $(\sqrt{\Delta m_{23}^2})_{\text{SK}} (\approx$

1/20 eV), which lies in the range of nearly (1/15 to 1/30) eV. As mentioned in the introduction and Chapter 3, the success of this prediction provides clear support for (i) the existence of ν_R , (ii) the notion of $SU(4)$ -color symmetry that gives $m(\nu_{\text{Dirac}}^\tau)$, (iii) the SUSY unification-scale that gives M_R , and (iv) the seesaw mechanism.

For simplicity, the parameters in the mass matrices in the BPW model, were chosen to be real, and for the sake of economy of parameters, ζ_{22}^d and ζ_{22}^u were set to zero in Ref. [25]. The parameters $(\sigma, \eta, \epsilon, \epsilon', \eta', \mathcal{M}_u^0, \mathcal{M}_D^0, y)$ can be determined by using, for example, $m_t^{\text{phys}} = 174$ GeV, $m_c(m_c) = 1.37$ GeV, $m_s(1 \text{ GeV}) = 110\text{--}116$ MeV, $m_u(1 \text{ GeV}) = 6$ MeV, the observed masses of e, μ , and τ and $m(\nu_2)/m(\nu_3) \approx 1/(6 \pm 1)$ (as suggested by a combination of atmospheric and solar neutrino data, the latter corresponding to the LMA MSW solution, see below) as inputs. One is thus led, for this CP conserving case (as the mass matrices are real), to the following fit for the parameters, and the associated predictions [25]. [In this fit, the small quantities x and z in M_R' are left undetermined. It is assumed that they have the magnitudes suggested by flavor symmetries

(i.e., $x \sim (10^{-4}\text{--}10^{-5})$ and $z \sim (1/200)(1 \text{ to } 1/2)$ (see remarks below Eq. (4.6))]:

$$\sigma \approx 0.110 \quad (4.11a)$$

$$\eta \approx 0.151 \quad (4.11b)$$

$$\epsilon \approx -0.095 \quad (4.11c)$$

$$|\eta'| \approx 4.4 \times 10^{-3} \quad (4.11d)$$

$$\epsilon' \approx 2 \times 10^{-4} \quad (4.11e)$$

$$\mathcal{M}_u^0 \approx m_t(M_X) \approx 120 \text{ GeV} \quad (4.11f)$$

$$\mathcal{M}_D^0 \approx m_b(M_X) \approx 1.5 \text{ GeV} \quad (4.11g)$$

$$y \approx -1/17. \quad (4.11h)$$

These output parameters remain stable to within 10% corresponding to small variations ($\lesssim 10\%$) in the input parameters of m_t , m_c , m_s , and m_u . These in turn lead to the following predictions for the quarks

and light neutrinos [25, 62]:

$$\begin{aligned}
m_b(m_b) &\approx (4.7\text{--}4.9) \text{ GeV}, \\
\sqrt{\Delta m_{23}^2} &\approx m(\nu_3) \approx (1/24 \text{ eV})(1/2\text{--}2), \\
V_{cb} &\approx \left| \sqrt{\frac{m_s}{m_b} \left| \frac{\eta+\epsilon}{\eta-\epsilon} \right|} - \sqrt{\frac{m_c}{m_t} \left| \frac{\sigma+\epsilon}{\sigma-\epsilon} \right|} \right| \\
&\approx 0.044, \\
\left\{ \begin{aligned}
\theta_{\nu_\mu\nu_\tau}^{\text{osc}} &\approx \left| \sqrt{\frac{m_\mu}{m_\tau} \left| \frac{\eta-3\epsilon}{\eta+3\epsilon} \right|}^{1/2} + \sqrt{\frac{m_{\nu_2}}{m_{\nu_3}}} \right| \\
&\approx |0.437 + (0.378 \pm 0.03)|, \\
\text{Thus, } \sin^2 2\theta_{\nu_\mu\nu_\tau}^{\text{osc}} &\approx 0.993, \\
\text{(for } \frac{m(\nu_2)}{m(\nu_3)} &\approx 1/6),
\end{aligned} \right. \quad (4.12) \\
V_{us} &\approx \left| \sqrt{\frac{m_d}{m_s}} - \sqrt{\frac{m_u}{m_c}} \right| \approx 0.20, \\
\left| \frac{V_{ub}}{V_{cb}} \right| &\approx \sqrt{\frac{m_u}{m_c}} \approx 0.07, \\
m_d(1 \text{ GeV}) &\approx 8 \text{ MeV}.
\end{aligned}$$

It is rather striking that all seven predictions in Eq. (4.12) agree with observations, to within 10%. Particularly intriguing is the $(B - L)$ -dependent group-theoretic correlation between the contribution from the first term in V_{cb} and that in $\theta_{\nu_\mu\nu_\tau}^{\text{osc}}$, which explains simultaneously why one is small (V_{cb}) and the other is large ($\theta_{\nu_\mu\nu_\tau}^{\text{osc}}$) [62]. That in turn provides some degree of confidence in the pattern of the mass-matrices.

The Majorana masses of the RH neutrinos ($N_{iR} \equiv N_i$) are given by [62]:

$$\begin{aligned}
M_3 &\approx M_R \approx 4 \times 10^{14} \text{ GeV (1/2-1),} \\
M_2 &\approx |y^2| M_3 \approx 10^{12} \text{ GeV(1/2-1),} \\
M_1 &\approx |x - z^2| M_3 \sim (1/4-2) 10^{-4} M_3 \\
&\sim 4 \times 10^{10} \text{ GeV(1/8-2).}
\end{aligned} \tag{4.13}$$

Note that we necessarily have a hierarchical pattern for the light as well as the heavy neutrinos (see discussions below on m_{ν_1}).

As regards ν_e - ν_μ and ν_e - ν_τ oscillations, the standard seesaw mechanism would typically lead to rather small angles (e.g. $\theta_{\nu_e \nu_\mu}^{\text{osc}} \approx \sqrt{m_e/m_\mu} \approx 0.06$), within the framework presented above [25]. It has, however, been noted subsequently [72] that small intrinsic (non-seesaw) masses $\sim 10^{-3}$ eV of the LH neutrinos can arise quite plausibly through higher dimensional operators of the form [62]: $W_{12} \supset \kappa_{12} \mathbf{16}_1 \mathbf{16}_2 \mathbf{16}_H \mathbf{16}_H \mathbf{10}_H \mathbf{10}_H / M_{\text{eff}}^3$, without involving the standard seesaw mechanism [17]. Such a term leads to an intrinsic Majorana mixing mass term of the form $m_{12}^0 \nu_L^e \nu_L^\mu$, with a strength given by $m_{12}^0 \approx \kappa_{12} \langle \mathbf{16}_H \rangle^2 (175 \text{ GeV})^2 / M_{\text{eff}}^3 \sim (1.5-6) \times 10^{-3}$ eV, for $\langle \mathbf{16}_H \rangle \approx (1-2) M_{\text{GUT}}$ and $\kappa_{12} \sim 1$, if $M_{\text{eff}} \sim M_{\text{GUT}} \approx$

2×10^{16} GeV [62]. Such an intrinsic Majorana $\nu_e\nu_\mu$ mixing mass \sim few $\times 10^{-3}$ eV, though small compared to $m(\nu_3)$, is still much larger than what one would generically get for the corresponding term from the standard seesaw mechanism (as in Ref. [25]). Now, the diagonal $(\nu_\mu\nu_\mu)$ mass-term, arising from standard seesaw can naturally be \sim (3-8) $\times 10^{-3}$ eV for $|y| \approx 1/20$ - $1/15$ [25]. Thus, taking the net values of $m_{22}^0 \approx (6 - 7) \times 10^{-3}$ eV, $m_{12}^0 \sim 3 \times 10^{-3}$ eV as above and $m_{11}^0 \ll 10^{-3}$ eV, which are all plausible, we obtain $m_{\nu_2} \approx (6 - 7) \times 10^{-3}$ eV, $m_{\nu_1} \sim (1 \text{ to few}) \times 10^{-3}$ eV, so that $\Delta m_{12}^2 \approx (3.6\text{-}5) \times 10^{-5}$ eV² and $\sin^2 2\theta_{\nu_e\nu_\mu}^{\text{osc}} \approx 0.6\text{-}0.7$. These go well with the LMA MSW solution of the solar neutrino puzzle.

Thus, the intrinsic non-seesaw contribution to the Majorana masses of the LH neutrinos can possibly have the right magnitude for $\nu_e\text{-}\nu_\mu$ mixing so as to lead to the LMA solution within the G(224)/SO(10)-framework, without upsetting the successes of the seven predictions in Eq. (4.12). [In contrast to the near maximality of the $\nu_\mu\text{-}\nu_\tau$ oscillation angle, however, which emerges as a compelling prediction of the framework [25], the LMA solution, as obtained above, should, be

regarded as a consistent possibility, rather than as a compelling prediction, within this framework.]

It is worth noting at this point that in a theory leading to Majorana masses of the LH neutrinos as above, one would expect the neutrinoless double beta decay process (like $n + n \rightarrow ppe^-e^-$), satisfying $|\Delta L| = 2$ and $|\Delta B| = 0$, to occur at some level. The crucial parameter which controls the strength of this process is given by $m_{ee} \equiv |\sum_i m_{\nu_i} U_{ei}^2|$. With a non-seesaw contribution leading to $m_{\nu_1} \sim \text{few} \times 10^{-3} \text{ eV}$, $m_{\nu_2} \approx 7 \times 10^{-3} \text{ eV}$, $\sin^2 2\theta_{12} \approx 0.6 - 0.7$, and an expected value for $\sin \theta_{13} \sim m_{13}^0/m_{33}^0 \sim (1 - 5) \times 10^{-3} \text{ eV} / (5 \times 10^{-2} \text{ eV}) \sim (0.02 - 0.1)$, one would expect $m_{ee} \approx (1 - 5) \times 10^{-3} \text{ eV}$ [72]. Such a strength, though compatible with current limits [73], would be accessible if the current sensitivity is improved by about a factor of 50–100.

In summary, it is remarkable that the simple pattern of fermion mass matrices, motivated in large part by the group theory of the $G(224)$ or $SO(10)$ symmetry and the minimality of the Higgs system, and in part by the assumption of flavor symmetry, leads to seven pre-

dictions in agreement with observations. Particularly significant are the predictions for $m(\nu_L^3)$ (to within a factor of 2 or 3, say), together with that of m_b/m_τ , which help select out the route to higher unification based on $G(224)$ or $SO(10)$ as the effective symmetry in 4D; so also are the predictions for the extreme smallness of V_{cb} together with the near maximality of $\theta_{\nu_\mu\nu_\tau}^{\text{osc}}$, all in accord with observations.

In the next two chapters, given the success of the BPW framework, it is extended to include CP and flavor violations by allowing for phases in the mass matrices. A set of processes involving CP and flavor violations are studied within the extended framework.

5. TYING IN CP AND FLAVOR VIOLATIONS WITH FERMION MASSES AND NEUTRINO OSCILLATIONS

5.1 Introduction

In this chapter, following work done in collaboration with Babu and Pati [28], I address the issues of CP and flavor violations in conjunction with those of fermion masses and neutrino oscillations, in the context of SUSY grand unification based on a SO(10) or an effective G(224) symmetry. On the experimental side there are now four well measured quantities reflecting CP and/or $\Delta F = 2$ flavor violations. They are:¹

$$\Delta m_K, \epsilon_K, \Delta m_{B_d} \text{ and } S(B_d \rightarrow J/\Psi K_S) \quad (5.1)$$

where $S(B_d \rightarrow J/\Psi K_S)$ denotes the asymmetry parameter in (B_d versus $\overline{B_d}$) $\rightarrow J/\Psi K_S$ decays. It is indeed remarkable that the observed values including the signs of all four quantities as well as the empirical

¹ ϵ'_K reflecting direct $\Delta F = 1$ CP violation is well measured, but its theoretical implications are at present unclear due to uncertainties in the matrix element. We discuss this later.

lower limit on Δm_{B_s} can consistently be realized within the standard CKM model for a single choice of the Wolfenstein parameters (see Appendix II) [74]:

$$\bar{\rho}_W = 0.178 \pm 0.046; \bar{\eta}_W = 0.341 \pm 0.028 . \quad (5.2)$$

This fit is obtained using the observed values of $\epsilon_K = 2.27 \times 10^{-3}$, $V_{us} = 0.2240 \pm 0.0036$, $|V_{ub}| = (3.30 \pm 0.24) \times 10^{-3}$, $|V_{cb}| = (4.14 \pm 0.07) \times 10^{-2}$, $|\Delta m_{B_d}| = (3.3 \pm 0.06) \times 10^{-13}$ GeV and $\Delta m_{B_d}/\Delta m_{B_s} > 0.035$, and allowing for uncertainties in the hadronic matrix elements of up to 15%. One can then predict the asymmetry parameter $S(B_d \rightarrow J/\Psi K_S)$ in the SM to be $\approx 0.685 \pm 0.052$ [74, 75]. This agrees remarkably well with the observed value $S(B_d \rightarrow J/\Psi K_S)_{expt.} = 0.687 \pm 0.032$ representing an average of the BABAR and BELLE results [76]. This agreement of the SM prediction with the data in turn poses a challenge for physics beyond the SM, especially for supersymmetric grand unified (SUSY GUT) models, as these generically possess new sources of CP and flavor violations beyond those of the SM.

In particular, our goal would be to obtain a unified description,

in accord with observations, of all four phenomena: (i) CP non-conservation, (ii) flavor violation, (iii) masses and mixings of quarks and leptons, as well as (iv) neutrino oscillations, within a single predictive framework based on SUSY $SO(10)/G(224)$ unification.

In chapter 4, I described a predictive framework (which I refer to as the BPW model [25]), based on the symmetry $SO(10)$ or $G(224)$, and a minimal Higgs system. This model describes the masses and mixings of all fermions including neutrinos by making the simplifying assumption that the fermion mass matrices are real and thus CP-conserving. Notwithstanding this assumption, the framework is found to be remarkably successful. In particular, it makes seven predictions involving fermion masses, CKM elements and neutrino oscillations, all in good accord with observations, to within 10% (see Chapter 4).

Now in general one would of course expect the entries in the fermion mass matrices to have phases because the VEVs of the relevant Higgs fields, and/or the effective Yukawa couplings, can well be complex. These in turn can induce CP violation through the SM/CKM interactions as well as through SUSY interactions involving

sfermion/gaugino loops.

The question arises: Can the BPW-framework of Ref. [25], based on the supersymmetric $SO(10)$ or $G(224)$ -symmetry, be extended, by allowing for phases in the fermion mass matrices, so as to yield net CP and flavor-violations, arising through both SM and SUSY interactions, in accord with observations, while still preserving its successes as regards fermion masses and neutrino oscillations?

As we will see, these four phenomena - (i) fermion masses, (ii) neutrino oscillations, (iii) CP non-conservation, and (iv) flavor violations - get intimately linked to each other within the SUSY $SO(10)/G(224)$ framework. Satisfying simultaneously the observed features of all four phenomena within such a predictive framework turns out, however, to be a non-trivial challenge to meet. The main purpose of this chapter is to show that the answer to the question raised above is in the affirmative.

violation

In this section the BPW model [25] is extended to include CP violation. This model was reviewed in Chapter 4. For completeness and future reference, the 3×3 Dirac mass matrices for the four sectors (u, d, l, ν) proposed in the model of Ref. [25] are given below:

$$M_u = \begin{bmatrix} 0 & \epsilon' & 0 \\ -\epsilon' & \zeta_{22}^u & \sigma + \epsilon \\ 0 & \sigma - \epsilon & 1 \end{bmatrix} \mathcal{M}_u^0; \quad M_d = \begin{bmatrix} 0 & \eta' + \epsilon' & 0 \\ \eta' - \epsilon' & \zeta_{22}^d & \eta + \epsilon \\ 0 & \eta - \epsilon & 1 \end{bmatrix} \mathcal{M}_d^0 \quad (5.3)$$

$$M_\nu^D = \begin{bmatrix} 0 & -3\epsilon' & 0 \\ 3\epsilon' & \zeta_{22}^u & \sigma - 3\epsilon \\ 0 & \sigma + 3\epsilon & 1 \end{bmatrix} \mathcal{M}_u^0; \quad M_l = \begin{bmatrix} 0 & \eta' - 3\epsilon' & 0 \\ \eta' + 3\epsilon' & \zeta_{22}^d & \eta - 3\epsilon \\ 0 & \eta + 3\epsilon & 1 \end{bmatrix} \mathcal{M}_d^0$$

These matrices are defined in the gauge basis and are multiplied by $\bar{\Psi}_L$ on left and Ψ_R on right.

In the BPW model, the parameters $(\sigma, \epsilon, \eta, \epsilon', \eta'$ etc.) entering into the fermion mass matrices were assumed to be real, for simplicity, and thereby (at least) the SM interactions were rendered

CP-conserving². Noting that the VEVs of the Higgs fields³ and/or the effective Yukawa couplings can well be complex, however, we now propose to extend the SO(10)/G(224) framework reviewed above to include CP violation by allowing for these parameters to have phases.

Given the empirical constraints on (i) CP and flavor violations, as well as (ii) fermion masses and (iii) neutrino oscillations, on the one hand, and (iv) the group-theoretical constraints of the SO(10)/G(224) framework on the other, it is of course not at all clear, a priori, whether any choice of phases and variations in the parameters of the fermion mass matrices presented above can yield *observed* CP and flavor-violations, and simultaneously preserve the successes of the framework of [25] as regards fermion masses and neutrino oscillations. That is the issue we now explore. We choose to diagonalize the quark mass matrices M_u and M_d at the GUT scale $\sim 2 \times 10^{16}$ GeV, by bi-unitary

² modulo the contribution from the strong CP parameter Θ

³ For instance, consider the superpotential for $\mathbf{45}_H$ only: $W(\mathbf{45}_H) = M_{\mathbf{45}}(\mathbf{45}_H)^2 + \lambda(\mathbf{45}_H)^4/M$, which yields (setting $F_{\mathbf{45}_H} = 0$), either $\langle \mathbf{45}_H \rangle = 0$, or $\langle \mathbf{45}_H \rangle^2 = -(2M_{\mathbf{45}}M/\lambda)$. Assuming that “other physics” would favor $\langle \mathbf{45}_H \rangle \neq 0$, we see that $\langle \mathbf{45}_H \rangle$ would be pure imaginary, if the quantity in the brackets is positive with all parameters being real. In a coupled system, it is conceivable that $\langle \mathbf{45}_H \rangle$ in turn would induce phases (other than 0 and π) in some of the other VEVs as well, and may itself become complex rather than pure imaginary.

transformations - i.e.

$$M_d^{diag} = X_L^{d\dagger} M_d X_R^d \text{ and } M_u^{diag} = X_L^{u\dagger} M_u X_R^u \quad (5.4)$$

with phases of $q_{L,R}^i$ chosen such that the eigenvalues are real and positive and that the CKM matrix V_{CKM} (defined below) has the Wolfenstein form [77]) (see Appendix II on Wolfenstein parametrization of the CKM matrix). Utilizing the hierarchical nature of the mass matrices, one can obtain (approximate) analytic expressions for the diagonalizing matrices (see Appendix .1 at the end of the chapter). They are:

$$X_L^d \simeq \begin{bmatrix} e^{-i(\phi_{\eta-\epsilon})} & |\eta'/X_d| e^{-i(\phi_{\eta-\epsilon}+\zeta_{us})} & \eta'|\eta-\epsilon| e^{-i(\phi_{\eta-\epsilon}-\zeta_{33}^d)} \\ -|\eta'/X_d| e^{i(\phi_{\eta+\epsilon}+\phi_{X_d})} & e^{i(\phi_{\eta+\epsilon}+\phi_{X_d}-\zeta_{us})} & |\eta+\epsilon| e^{i(\phi_{\eta+\epsilon}+\zeta_{33}^d)} \\ |\eta'/X_d||\eta+\epsilon| e^{i(\phi_{X_d})} - Y & -|\eta+\epsilon| e^{i(\phi_{X_d}-\zeta_{us})} & e^{i\zeta_{33}^d} \end{bmatrix} \quad (5.5)$$

$$X_R^d \simeq \begin{bmatrix} e^{i(\phi_{\eta+\epsilon}+\phi_{X_d})} & |\eta'/X_d| e^{i(\phi_{\eta+\epsilon}+\phi_{X_d}-\zeta_{us})} & \eta'|\eta+\epsilon| e^{i(\phi_{\eta+\epsilon}+\zeta_{33}^d)} \\ -|\eta'/X_d| e^{-i(\phi_{\eta-\epsilon})} & e^{-i(\phi_{\eta-\epsilon}+\zeta_{us})} & |\eta-\epsilon| e^{-i(\phi_{\eta-\epsilon}-\zeta_{33}^d)} \\ |\eta'/X_d||\eta-\epsilon| & -|\eta-\epsilon| e^{-i\zeta_{us}} & e^{i\zeta_{33}^d} \end{bmatrix} \quad (5.6)$$

Here $\phi_{\eta\pm\epsilon} \equiv \arg(\eta \pm \epsilon)$, that is, $(\eta \pm \epsilon \equiv |\eta \pm \epsilon| e^{i\phi_{\eta\pm\epsilon}})$; $Y \equiv \eta'|\eta-\epsilon| e^{-i\zeta_{ud}}$ and

$$X_d \equiv -|\eta^2 - \epsilon^2| + |\zeta_{22}^d| e^{-i(\phi_{\eta+\epsilon}+\phi_{\eta-\epsilon}-\phi_{\zeta_{2d}})} \equiv |X_d| e^{i\phi_{X_d}}, \text{ where } \zeta_{22}^d \equiv$$

$|\zeta_{22}^d|e^{i\phi_{\zeta_{2d}}}$. The corresponding matrices $X_{L,R}^u$ for diagonalizing the up sector are obtained from above with the substitutions : $\eta \rightarrow \sigma$; $\zeta_{22}^d \rightarrow \zeta_{22}^u$; $(\eta' \pm \epsilon') \rightarrow \pm\epsilon'$. Thus $\phi_{\eta\pm\epsilon}$ are replaced by $\phi_{\sigma\pm\epsilon} \equiv \text{arg}(\sigma \pm \epsilon)$; and X_d by $X_u \equiv -|\sigma^2 - \epsilon^2| + |\zeta_{22}^u|e^{-i(\phi_{\sigma+\epsilon} + \phi_{\sigma-\epsilon} - \phi_{\zeta_{2u}})} \equiv |X_u|e^{i\phi_{X_u}}$. Given the definitions of ϕ_{X_d} and ϕ_{X_u} as above, we have

$$\zeta_{33}^d \simeq (\phi_{X_d} - \phi_{\eta-\sigma} + \phi_{\eta+\epsilon}) + R \sin \Omega; \quad \gamma \equiv (\phi_{\eta+\epsilon} + \phi_{\eta-\epsilon}) - (\phi_{\sigma+\epsilon} + \phi_{\sigma-\epsilon}) + \phi_{\epsilon'},$$

where

$$R \equiv |\epsilon'/X_u|/|\eta'/X_d| \approx \sqrt{m_u/m_c}\sqrt{m_s/m_d} \approx 0.3;$$

$$\beta_\Omega \approx R(\sin \Omega/\Omega), \quad \Omega \equiv (\phi_{X_d} - \phi_{X_u}) + \gamma;$$

$$\zeta_{cb} \simeq \text{arg}[e^{i(\gamma - \phi_{X_u})}\{|\eta + \epsilon| - |\sigma + \epsilon|e^{i(\phi_{\sigma+\epsilon} - \phi_{\eta+\epsilon})}\}];$$

$$\zeta_{us} \approx -R \sin \Omega [1 - R \cos \Omega]^{-1}.$$

As mentioned above, using observed fermion masses and mixings [25], we obtain: $|\epsilon'| \sim 1/10 |\eta'|$, with $|\eta'| \sim (\text{few}) \times 10^{-3} \ll (|\eta| \sim |\epsilon| \sim |\sigma| \sim 1/10) \ll 1$. In writing Eqns. (5.5) and (5.6), we have not displayed for simplicity of writing, small correction terms ($\mathcal{O}(\epsilon^2, \eta^2)$), which are needed to preserve unitarity. We have also not displayed small phases of order $|\eta'\epsilon'/X_u X_d| \times \sin \Omega \sim 1/100$, $|\epsilon'/\eta'| \sim 1/10$ and

$R \sin \Omega \sim 1/10$. Our results to be presented, that are based on exact numerical calculations, however incorporate these small corrections.

The CKM elements in the Wolfenstein basis are given by the matrix $V_{CKM} = e^{-i\alpha}(X_L^{u\dagger} X_L^d)$, where $\alpha = (\phi_{\sigma-\epsilon} - \phi_{\eta-\epsilon}) - (\phi_{\epsilon'} - \phi_{\eta'+\epsilon'})$, where without loss of generality (given $|\eta'| \gg |\epsilon'|$), we can choose $\phi_{\eta'+\epsilon'} \approx 0$. To a good approximation, the CKM elements are given by (these expressions are derived in the appendix .1):

$$\begin{aligned}
V_{ud} &\approx V_{cs} \approx V_{tb} \approx 1 \\
V_{us} &\approx | |\eta'/X_d| - |\epsilon'/X_u| e^{i\Omega} | \approx -V_{cd} \\
V_{cb} &\approx | e^{i(\gamma-\phi_{X_u})} \{ |\eta + \epsilon| - |\sigma + \epsilon| e^{i(\phi_{\sigma+\epsilon} - \phi_{\eta+\epsilon})} \} | \approx -V_{ts} \\
V_{ub} &\approx [|\eta'| |\eta - \epsilon| - |\epsilon'/X_u| e^{i(\gamma-\phi_{X_u})} \{ |\eta + \epsilon| - |\sigma + \epsilon| e^{-i(\phi_{\sigma+\epsilon} - \phi_{\eta+\epsilon})} \}] \quad (5.7) \\
&\quad \times e^{i[\Omega(1+\beta\Omega) - \zeta_{cb}]} \\
V_{td} &\approx [| |\eta'/X_d| e^{i(\phi_{X_d})} \{ |\epsilon + \eta| - |\sigma + \epsilon| e^{-i(\phi_{\sigma+\epsilon} - \phi_{\eta+\epsilon})} \} - \eta' |\eta - \epsilon|] \\
&\quad \times e^{-i[\Omega(1+\beta\Omega) - \zeta_{cb}]}
\end{aligned}$$

Note that the CKM elements have the desired Wolfenstein form with only V_{ub} and V_{td} being complex and the others being real to a good approximation. ζ_{cb} defined above is just the argument of the expression within the bars for V_{cb} . One can check that to a good approximation, (neglecting the $\eta'|\eta - \epsilon|$ term for V_{td} that causes $< 10\%$ error), the

phase of V_{td} is given by

$$\phi_{td} \equiv \text{Arg}(V_{td}) \approx -R \sin \Omega, \text{ and } |V_{td}| \approx |\eta'/X_d| |V_{cb}^*| \approx \sqrt{m_d/m_s} |V_{cb}|,$$

and similarly $|V_{ub}| \approx \sqrt{m_u/m_c} |V_{cb}|$.

Before presenting the results of a certain fit and the corresponding predictions, we need to first discuss SUSY CP and flavor violations in the presence of phases in the fermion mass matrices. This is done in the next section.

5.3 SUSY CP and Flavor Violations

Our procedure for dealing with SUSY CP and flavor violations may be summarized by the following set of considerations:

- 1) As is well known, since the model is supersymmetric, non-standard CP and flavor violations would generically arise in the model through sfermion/gaugino quantum loops involving scalar $(mass)^2$ transitions [26, 27]. The latter can either preserve chirality (as in $\tilde{q}_{L,R}^i \rightarrow \tilde{q}_{L,R}^j$) or flip chirality (as in $\tilde{q}_{L,R}^i \rightarrow \tilde{q}_{R,L}^j$). Subject to our assumption on SUSY breaking (specified below), it would turn out that these scalar $(mass)^2$ parameters get completely determined within our

model by the fermion mass-matrices, and the few parameters of SUSY breaking.

2) **SUSY Breaking** : We assume that SUSY breaking is communicated to the SM sector by messenger fields which have large masses of order M^* , where $M_{GUT} \lesssim M^* \approx M_{string}$, such that the soft parameters are flavor-blind, and family-universal at the scale M^* . A number of well motivated models of SUSY breaking, e.g., those based on mSUGRA [46], gaugino-mediation [54], anomalous $U(1) - D$ term [49, 50], combined with dilaton-mediation [50, 51], or possibly a combination of some of these mechanisms, do in fact induce such a breaking. While for the first two cases [46, 54] we would expect extreme squark degeneracy (ESD) i.e. $\kappa \equiv |m^2(\tilde{q}_i) - m^2(\tilde{q}_j)|/m^2(\tilde{q})_{AV} \ll 10^{-3}$ (say) at the scale M^* , for the third case [49, 50], one would expect intermediate squark degeneracy (ISD) i.e. $\kappa \sim 10^{-2}(1 - 1/3)$ at M^* . For the sake of generality, we would initially allow both possibilities, $\kappa = 0$ (ESD), and $\kappa \sim 10^{-2}(1 - 1/3)$ (ISD) at M^* .

In an extreme version of universality, analogous to CMSSM, the SUSY sector of the model would introduce only five parameters at the

scale M^* :

$$m_o, m_{1/2}, A_o, \tan \beta \text{ and } \text{sgn}(\mu).$$

In some cases, A_o can be zero or extremely small ($\lesssim 1\text{GeV}$) at M^* as in [54] and [50]. For most purposes we will adopt this restricted version of SUSY breaking, including the vanishing of A_o at M^* . However, our results will be essentially unaffected even if A_o is non-zero ($\sim 500\text{ GeV}$, say) but real (see remarks later). We will not insist on, but will allow for, Higgs-squark-slepton universality, which does not hold, for example, in the string-derived model of [50]. In spite of flavor-preservation at a high scale M^* , SUSY-induced flavor-violation would still arise at the electroweak scale through renormalization group running of the sfermion masses and the A -parameters from $M^* \rightarrow M_{GUT} \rightarrow m_W$, as specified below. Although the premises of our model as regards the choice of universal SUSY parameters coincide with that of CMSSM, as we will see, owing to the presence of GUT-scale physics in the interval $M^* \rightarrow M_{GUT}$, SUSY CP and flavor violations in our model (evaluated at the electroweak scale) would be significantly enhanced compared to that in CMSSM (or even CMSSM with right-handed neutrinos). This

difference provides some distinguishing features of our model.

3) Flavor Violation due to RG Running of Scalar Masses from M^* to M_{GUT}

For MSSM embedded into SO(10) above the GUT scale, there necessarily exist heavy color-triplet Higgs fields which couple to fermions through the coupling $h_t \mathbf{16}_3 \mathbf{16}_3 \mathbf{10}_H$, while there exist heavy doublets for both SO(10) and G(224) which also couple to fermions owing to the mixing of $\mathbf{10}_H$ with $\mathbf{16}_H$ (see [25]). These couple to \tilde{b}_L and \tilde{b}_R with the large top quark Yukawa coupling h_t . The heavy triplets and doublets possess masses of order M_{GUT} . One can verify (see [26, 78]) that the evolution of RG equations for squark masses involving such couplings suppress \tilde{b}_L and \tilde{b}_R masses significantly compared to those of $\tilde{d}_{L,R}$ and $\tilde{s}_{L,R}$. Note that left–right symmetry implies equal shifts in \tilde{b}_L and \tilde{b}_R masses arising from GUT scale physics in the momentum range $M_{GUT} \leq \mu \leq M^*$. Such differential mass shifts i.e.- $(\hat{m}_3^2 - \hat{m}_{1,2}^2)_{L,R} \equiv \Delta \hat{m}_{\tilde{b}_{L,R}}^2$, for the embedding of MSSM into SO(10), are found to be (with $A_o = 0$) [26]:

$$\Delta \hat{m}_{\tilde{b}_R}^2 = \Delta \hat{m}_{\tilde{b}_L}^2 \approx -\left(\frac{30m_o^2}{16\pi^2}\right) h_t^2 \ln(M^*/M_{GUT}) \equiv -(m_o^2/4)\xi . \quad (5.8)$$

The hat signifies GUT scale values. Here m_o denotes the (approximately) degenerate mass of squarks at the scale M^* . We have set $h_t^2 = 1/2$; we expect $M^*/M_{GUT} \sim (3 \text{ to } 10)$, say, and thus, $\xi \equiv \ln(M^*/M_{GUT})/2.6 \approx (0.4 \text{ to } 0.9)$. For the case of MSSM embedded into G(224), which provides the heavy doublet, but not the triplets, the factor 30 in Eq. (5.8) should be replaced by 12.

Having diagonalized the quark mass-matrices $M_d^{(0)}$ and $M_u^{(0)}$ at the GUT scale by matrices as in Eq. (5.4), SUSY flavor violation may be assessed by imposing the parallel transformations on the squark (*mass*)² matrices $((\tilde{M}_d^{(0)})_{LL/RR})$ defined in the gauge basis, i.e., by evaluating $X_L^{d\dagger}(\tilde{M}_d^{(0)})_{LL}X_L^d$ and $X_R^{d\dagger}(\tilde{M}_d^{(0)})_{RR}X_R^d$, and similarly for the up sector. Following discussion on SUSY breaking, the off-diagonal elements (in the gauge basis) and all chirality flipping elements are set to be zero - i.e $(\tilde{M}_{ij}^{(0)})_{LL/RR} = 0$ ($i \neq j$) and $(A_{ij}^0)_{LR} = 0$ - at the scale M^* . Once squarks are non degenerate at M_{GUT} owing to the mass-shift of $\tilde{b}_{L,R}$ as in Eq. (5.8), the transformations mentioned above induce off-diagonal elements with squarks being in the SUSY basis⁴. For the down squark mass matrices (evaluated at the GUT

⁴ The SUSY basis is one where all couplings of the fermion and sfermion states to neutral

scale), these off diagonal elements are found to be:

gauginos are flavor diagonal. From the gauge basis, the scalars are transformed by the same matrices that diagonalize the fermion mass matrices. The \tilde{m}^2 is an average sfermion mass².

$$\begin{aligned}
\hat{\delta}_{LL}^{12}(M_{GUT}) &\simeq [\kappa_{ISD}^{12} + (\Delta\hat{m}_{\tilde{b}_L}^2/m_{sq}^2)(-|\eta'/X_d||\epsilon + \eta|^2 \\
&\quad + \eta'|\epsilon^2 - \eta^2|e^{i\phi_{X_d}})]e^{-i\phi_{td}} \\
&\approx [\kappa_{ISD}^{12} + 1.5 \times 10^{-4}\xi](m_o^2/m_{sq}^2)e^{-i\phi_{td}}
\end{aligned}$$

$$\begin{aligned}
\hat{\delta}_{RR}^{12}(M_{GUT}) &\simeq [\kappa_{ISD}^{12} + (\Delta\hat{m}_{\tilde{b}_R}^2/m_{sq}^2)(-|\eta'/X_d||\epsilon - \eta|^2 \\
&\quad + \eta'|\epsilon^2 - \eta^2|e^{-i\phi_{X_d}})]e^{-i\phi_{td}} \\
&\approx [\kappa_{ISD}^{12} + 3\xi \times 10^{-3} - 10^{-5}(\xi)e^{-i\phi_{X_d}}](m_o^2/m_{sq}^2)e^{-i\phi_{td}}
\end{aligned}$$

$$\begin{aligned}
\hat{\delta}_{LL}^{13}(M_{GUT}) &\simeq (\Delta\hat{m}_{\tilde{b}_L}^2/m_{sq}^2)[- \eta'|\eta - \epsilon|e^{i\zeta_{33}^d} + |\eta'/X_d||\eta + \epsilon|e^{i(\zeta_{33}^d - \phi_{X_d})}] \\
&\approx [(2.5\xi) \times 10^{-4}e^{i\zeta_{33}^d} - (2.5\xi) \times 10^{-3}e^{i(\zeta_{33}^d - \phi_{X_d})}](m_o^2/m_{sq}^2) \quad (5.9)
\end{aligned}$$

$$\begin{aligned}
\hat{\delta}_{RR}^{13}(M_{GUT}) &\simeq (\Delta\hat{m}_{\tilde{b}_R}^2/m_{sq}^2)[- \eta'|\eta + \epsilon|e^{i(\zeta_{33}^d - \phi_{X_d})} + |\eta'/X_d||\eta - \epsilon|e^{i\zeta_{33}^d}] \\
&\approx -[(1.25\xi) \times 10^{-2}e^{i\zeta_{33}^d}](m_o^2/m_{sq}^2)
\end{aligned}$$

$$\begin{aligned}
\hat{\delta}_{LL}^{23}(M_{GUT}) &\simeq (\Delta\hat{m}_{\tilde{b}_L}^2/m_{sq}^2)[-|\eta + \epsilon|e^{i(\zeta_{33}^d - \phi_{X_d} + \phi_{td})}] \\
&\approx [(1.25\xi) \times 10^{-2}e^{i(\zeta_{33}^d - \phi_{X_d} + \phi_{td})}](m_o^2/m_{sq}^2)
\end{aligned}$$

$$\begin{aligned}
\hat{\delta}_{RR}^{23}(M_{GUT}) &\simeq (\Delta\hat{m}_{\tilde{b}_R}^2/m_{sq}^2)[-|\eta - \epsilon|e^{i(\zeta_{33}^d + \phi_{td})}] \\
&\approx [(6.2\xi) \times 10^{-2}e^{i(\zeta_{33}^d + \phi_{td})}](m_o^2/m_{sq}^2)
\end{aligned}$$

Here $\kappa_{ISD}^{12} \equiv [(m_1^{(0)2} - m_2^{(0)2})]/m_{sq}^2(|\eta'/X_d|) \sim \pm(2 \times 10^{-3})(1 - 1/3)$; this term would be present for the case of intermediate squark degeneracy (ISD), corresponding to small ($\sim 10^{-2}(1 - 1/3)$) squark non-degeneracy at the scale M^* , as in models of Ref. [49, 50]. From now on, for the sake of concreteness, we drop this term,⁵ setting $\kappa_{ISD}^{12} = 0$. In above $\phi_{td} \approx -|\epsilon'/X_u|/|\eta'/X_d| \sin \Omega \sim (-1/3) \sin \Omega \sim (-1/6)$ (say). The hat on top signifies GUT scale values, and $\hat{\delta}_{LL/RR}^{ij} \equiv (\hat{\Delta}_{LL/RR}^{ij})/m_{sq}^2$, where $\hat{\Delta}_{LL}^{ij}$ denotes the $(mass)^2$ parameter for $\tilde{q}_{jL} \rightarrow \tilde{q}_{iL}$ transition in the SUSY basis. Here, m_{sq} denotes the average mass of the $\tilde{d}_{L,R}$ and $\tilde{s}_{L,R}$ squarks, which remain nearly degenerate(to 1% or better) even at the weak scale. For each $\hat{\delta}_{LL/RR}^{ij}$ we have exhibited approximate numerical values by inserting values of the parameters $\eta, \sigma, \epsilon, \eta'$ etc. for some typical fits (as in Eq. (5.16), see also the fit in Chapter 4) to indicate their typical values.

Assuming for simplicity, universality of scalar masses m_o (of the first two families) and of the gaugino masses $m_{1/2}$ at the GUT scale, the physical masses of squarks of the first two families and of the

⁵ Note that the case of ISD ($\kappa_{ISD}^{12} \sim (2 \times 10^{-3})(1 - 1/3) \neq 0$) would make a difference only for the case of $K^o - \overline{K}^o$ transitions - that is, for Δm_K and ϵ_K .

gluino are given by:

$$m_{sq}^2 \approx m_o^2 + 7.2 m_{1/2}^2; \quad m_{\tilde{g}} \approx 2.98 m_{1/2} . \quad (5.10)$$

This result is rather insensitive to the mass shifts of $\tilde{b}_{L,R}$. Using the above relations we get $\rho_X \equiv (m_o^2/m_{sq}^2) \simeq 1 - 0.8x \approx (0.84, 0.76, 0.5$ and $0.2)$ for $x \equiv m_{\tilde{g}}^2/m_{sq}^2=(0.2, 0.3, 0.6$ and $1)$, which enters into all the $\hat{\delta}^{ij}$ -elements in Eq. (5.9).

We remind the reader that the elements $\hat{\delta}_{LL,RR}^{ij}$, induced solely through GUT scale physics being relevant in the interval $M^* \rightarrow M_{GUT}$, would be absent in a general CMSSM or MSSM, and so would the associated CP and flavor violations.

4) Flavor Violation Through RG Running From M_{GUT} to m_W in MSSM: It is well known that, even with universal masses at the GUT scale, RG running from M_{GUT} to m_W in MSSM, involving contribution from the top Yukawa coupling, gives a significant correction to the mass of $\tilde{b}'_L = V_{td}\tilde{d}_L + V_{ts}\tilde{s}_L + V_{tb}\tilde{b}_L$, which is not shared by the mass-shifts of $\tilde{b}_R, \tilde{d}_{L,R}$ and $\tilde{s}_{L,R}$. This in turn induces flavor violation. Here, \tilde{d}_L, \tilde{s}_L and \tilde{b}_L are the SUSY partners of the physical d_L, s_L and b_L respectively. The differential mass shift of \tilde{b}'_L arising as above, may

be expressed by an effective Lagrangian [79]: $\Delta\mathcal{L} = -(\Delta m_L'^2)\tilde{b}_L'^*\tilde{b}_L'$, where⁶

$$\begin{aligned} \Delta m_L'^2 = & -3/2m_o^2\eta_t + 2.3A_o m_{1/2}\eta_t(1 - \eta_t) \\ & -(A_o^2/2)\eta_t(1 - \eta_t) + m_{1/2}^2(3\eta_t^2 - 7\eta_t). \end{aligned} \quad (5.11)$$

Here $\eta_t = (h_t/h_f) \approx (m_t/v \sin\beta)^2(1/1.21) \approx 0.836$ for $\tan\beta = 3$. Numerically, setting⁷ $A_o = 0$, Eq. (5.11) yields: $(\Delta m_L'^2/m_{sq}^2) \approx -(0.40, 0.34, 0.26, 0.22)$ for $x = m_{\tilde{g}}^2/m_{sq}^2 \approx (0.1, 0.4, 0.8, 1.0)$. Expressing \tilde{b}_L' in terms of down-flavor squarks in the SUSY basis as above, Eq. (5.11) yields new contributions to off diagonal squark mixing. Normalizing to m_{sq}^2 , they are given by

$$\delta_{LL}'^{(12,13,23)} = \left(\frac{\Delta m_L'^2}{m_{sq}^2}\right)(V_{td}^*V_{ts}, V_{td}^*V_{tb}, V_{ts}^*V_{tb}) . \quad (5.12)$$

The net squark $(mass)^2$ off-diagonal elements at m_W are then obtained by adding the respective GUT-scale contributions from Eqs.

⁶ Note that strictly speaking Eq. (5.11) holds if the soft parameters are universal at the GUT-scale. However, the correction to this expression due to RG running from M^* to m_W would be rather small, being a correction to a correction.

⁷ Although we have put $A_o = 0$ (for concreteness), note that $\Delta m_L'^2$ would typically get only a small correction ($\lesssim 5\%$), even if A_o were non-zero ($\lesssim 1$ TeV), with $m_o \approx (0.7 - 1)$ TeV and $m_{1/2} \approx (200 - 300)$ GeV, say.

(5.9) to that from Eq. (5.12). They are:

$$\delta_{LL}^{ij} = \hat{\delta}_{LL}^{ij} + \delta'_{LL}{}^{ij}; \quad \delta_{RR}^{ij} = \hat{\delta}_{RR}^{ij} \quad (5.13)$$

From the expressions given above (Eqs. (5.9) and (5.12)), it follows that for a given choice of the SUSY-parameters (i.e. m_o , $m_{1/2}$ or equivalently m_{sq} and $m_{\tilde{g}}$), SUSY CP and flavor violations are *completely determined* within our model by parameters of the fermion mass-matrices. This is the reason why within a quark-lepton unified theory as ours, SUSY CP and flavor violations get intimately related to fermion masses and neutrino oscillations.

5) **A-Terms Induced Through RG Running from M^* to**

M_{GUT} : Even if A_o is zero at M^* (as we assume, for concreteness, see also [54] and [50]), RG running from M^* to M_{GUT} in the context of SO(10)/G(224) would still induce non-zero A parameters at the GUT scale [26]. For our case, the A terms are induced through loop diagrams involving the h_{33} , g_{23} , and a_{23} couplings and the SO(10) or G(224) gauginos. We find that if we take $M_{10_H} \approx M_{16_H} \approx M_{GUT}$, we can write the A_{LR} -matrix at the GUT-scale for the down squark sector in the SUSY basis for the case of SO(10) as follows (the details

are presented in Appendix .2):

$$A_{LR}^d = Z \begin{bmatrix} 0 & 95\epsilon' + 90\eta' & 0 \\ -95\epsilon' + 90\eta' & 90\zeta_{22}^d - 27\zeta_{22}^u & 95\epsilon + 90\eta - 27\sigma \\ 0 & -95\epsilon + 90\eta - 27\sigma & 63 \end{bmatrix} \quad (5.14)$$

where $Z = \left(\frac{1}{16\pi^2}\right)h_t g_{10}^2 M_\lambda \ln\left(\frac{M^*}{M_{GUT}}\right)$. This matrix has to be multiplied with $(X_L^d)^\dagger$ on the left and X_R^d on the right. The matrices $(X^d)_{L,R}$ are given in Eqs. (5.5) and (5.6). The g_{23} coupling does not contribute to the up-sector; thus the A -matrix for the up squarks, A_{LR}^u , can be obtained from above by setting $\eta' = 0$ and replacing $90\eta - 27\sigma$ by 63σ , $90\zeta_{22}^d - 27\zeta_{22}^u$ by $63\zeta_{22}^u$, and $X_{L,R}^d$ by $X_{L,R}^u$ in A^d . Similarly, the lepton A -matrix, A_{LR}^l is obtained by letting $(\epsilon, \epsilon') \rightarrow -3(\epsilon, \epsilon')$ and replacing $X_{L,R}^d$ by $X_{L,R}^l$ in A_{LR}^d . For the case of G(224), the matrix A_{LR}^d would be obtained by making the substitutions: $(90, 63, 95) \rightarrow (42, 27, 43)$ in Eq. (5.14), and likewise in A_{LR}^u and A_{LR}^l . It is sometimes convenient to define the sfermion transition mixing angles as

$$\begin{aligned} (\delta_{LR}^{d,l})_{ij} &\equiv (A_{LR}^{d,l})_{ij} \left(\frac{v_d}{m_{sq}^2}\right) = (A_{LR}^{d,l})_{ij} \left(\frac{v_u}{\tan\beta m_{sq}^2}\right); \\ (\delta_{LR}^u)_{ij} &\equiv (A_{LR}^u)_{ij} \left(\frac{v_u}{m_{sq}^2}\right). \end{aligned} \quad (5.15)$$

Note that these induced A_{LR} -terms for all three sectors, like the

squarks $(mass)^2$ elements $\delta_{LL,RR}^{ij}$ given in Eqs. (5.9)-(5.13), are completely determined within our model by the fermion mass matrices, for a given choice of $M_\lambda \approx m_{1/2}$ and $\ln(M^*/M_{GUT})$. We now utilize these SUSY CP and flavor-violating elements to predict the results of our model.

Once again, as in the case of $\hat{\delta}_{LL,RR}^{ij}$, these induced A -terms arising purely through GUT-physics, would be absent or negligibly small in CMSSM. As a result, some of the interesting predictions of our model as regards ϵ'_K and edm's (to be discussed below) and lepton flavor violations [29] (to be discussed in the next chapter) would be absent altogether in CMSSM.

5.4 *Compatibility of CP and Flavor Violations with Fermion*

Masses and Neutrino Oscillations in $SO(10)/G(224)$: Our

Results

It has been noted in Sec. 1 that (given about 15% uncertainty in the matrix elements) the SM agrees very well with all four entries of Eq. (5.1), for a single choice of the Wolfenstein parameters $\bar{\rho}_W$ and

$\bar{\eta}_W$ (Eq. (5.2)). The question then arises (as noted in Sec. 1): If a SUSY SO(10) or G(224) model is constrained by requiring that it should successfully describe fermion masses and neutrino oscillations (see Chapter 4), can it still yield (for some choice of phases in the parameters η , σ , ϵ etc.) values for $\bar{\rho}_W$ and $\bar{\eta}_W$ more or less in accord with the SM-based phenomenological values for the same, as listed in Eq. (5.2)? Anticipating that (for any given choice of the parameters η , σ , ϵ etc.) the SO(10)/G(224) model-based values of $\bar{\rho}_W$ and $\bar{\eta}_W$ would generically differ from the SM-based phenomenological values (given in Eq.(5.2)), we will denote the former by $\bar{\rho}'_W$ and $\bar{\eta}'_W$ and the corresponding contributions from the SM-interactions (based on $\bar{\rho}'_W$ and $\bar{\eta}'_W$) by SM' . The question that faces us then is this: When the SM' contributions are added to the SUSY contributions arising from the three sources listed in Sec. 3, can such a constrained SO(10) or G(224) model account for the observed values of all the four quantities listed in Eq. (5.1), and in addition is it consistent with the empirical upper limits on the edm's of the neutron and the electron?⁸.

⁸ We extend the same question to include lepton flavor violating processes (such as $\mu \rightarrow e \gamma$ and $\tau \rightarrow \mu \gamma$) in the next chapter.

Before presenting our results [28], we make some preliminary remarks. First of all one might have thought, given the freedom in the choice of phases in the parameters of the mass matrices, that it ought to be possible to get almost any set of values of $(\bar{\rho}_W$ and $\bar{\eta}_W)$, and in particular those in accord with the SM values (Eq. (5.2)). It turns out, however, that in general this is indeed not possible without running into a conflict with the fermion masses and/or neutrino oscillation parameters within a SO(10) or G(224)-model⁹. In other words, any predictive SO(10) or G(224)-model is rather constrained in this regard.

Second, one might think that even if the SO(10)/G(224) model-derived entities $\bar{\rho}'_W$ and $\bar{\eta}'_W$, constrained by the pattern of fermion masses and neutrino oscillations, are found to be very different in signs and/or magnitudes from the SM values shown in Eq. (5.2), perhaps the SUSY contributions added to the SM' contributions (based on $\bar{\rho}'_W$ and $\bar{\eta}'_W$) could possibly account for all four quantities listed in Eq. (5.1). It seems to us, however, that this is simply not a viable and

⁹ for a discussion of difficulties in this regard within a recently proposed SO(10)model, see e.g. [80]

natural possibility, unless one is willing to invoke MSSM and finely adjust its arbitrary (in general some 105) parameters, as needed. In the latter case, the good agreement between experiments and the SM predictions would appear to be fortuitous (see Sec. 1).

This is why it seems to us that the only viable and natural solution for any SUSY G(224) or SO(10) model for fermion masses and neutrino oscillations is that the model, allowing for phases in the fermion mass matrices, should not only yield the masses and mixings of all fermions including neutrinos in accord with observations, but it should yield $\bar{\rho}'_W$ and $\bar{\eta}'_W$ that are close to the SM values shown in Eq. (5.2). This, if achievable, would be a *major step in the right direction*. One then needs to ask: how does the combined ($SM' + \text{SUSY}$) contributions fare for such a solution as regards its predictions for the four quantities of Eq. (5.1) and other CP and/or flavor violating processes, for any given choice of the SUSY parameters (m_o , $m_{1/2}$, A_o , $\tan \beta$ and $\text{sgn}(\mu)$)? It should be stressed here that even if the CKM elements including $\bar{\rho}'_W$ and $\bar{\eta}'_W$ should turn out to be close to the SM values (Eq. (5.2)), the SUSY contributions can in general still have a marked ef-

fect, in accord with observations, at least on some of the processes where the SM (or SM')-contributions are naturally suppressed (as in the case for ϵ_K , edm's and lepton flavor violating transitions). Study of these processes, some of which we discuss below, can help distinguish between the SM versus the SUSY SO(10)/G(224)-models.

Without further elaboration, I now present our main results. Here I will present only two fits to the parameters which has the desired properties.¹⁰

Allowing for phases ($\sim 1/10$ to $1/2$) in the parameters η , σ , ϵ' and ζ_{22}^d of the G(224)/SO(10) framework (see Chapter 4) we find that there do exist solutions which yield masses and mixings of quarks and leptons, in accord with observations to within 10% for most part (see discussion below), and at the same time yield $\vec{\rho}'_W$ and $\vec{\eta}'_W$ close to the SM values, as given in Eq. (5.2). A desired fit to the parameters is given by:

¹⁰ We have verified that there actually exists a class of fits which nearly serve the same purpose. Two of these (Eq. (5.16) and Eq. (5.18)) are exhibited here for the sake of concreteness.

Fit A

$$\begin{aligned} \sigma &= 0.109 - 0.012i, \quad \eta = 0.122 - 0.0464i, \quad \epsilon = -0.103, \\ \eta' &= 2.4 \times 10^{-3}, \quad \epsilon' = 2.35 \times 10^{-4} e^{i(69^\circ)}, \quad \zeta_{22}^d = 9.8 \times 10^{-3} e^{-i(149^\circ)}, \quad (5.16) \\ (\mathcal{M}_u^0, \mathcal{M}_d^0) &\approx (100, 1.1) \text{ GeV}. \end{aligned}$$

For the sake of simplicity and economy, we have set $\zeta_{22}^u = 0$ in this fit; however, values of $|\zeta_{22}^u| \lesssim 10^{-3}$ can lead to similar results (see e.g. Fit B given below). Note that the magnitudes of the real parts of η , σ , ϵ , and ϵ' are nearly the same as those given in the CP-conserving case [25] (see Chapter 4); in particular the relative signs of these real parts are identical. The fit A shown above leads to the following values for the fermion masses and mixings, while preserving the predictions for the neutrino system (see Chapter 4):

$$\begin{aligned} (m_t^{\text{phys}}, m_b(m_b), m_\tau) &\approx (174, 4.97, 1.78) \text{ GeV} \\ (m_c(m_c), m_s(1\text{GeV}), m_\mu) &\approx (1320, 101, 109) \text{ MeV} \\ (m_u^\circ(1\text{GeV}), m_d^\circ(1\text{GeV}), m_e^\circ) &\approx (10.1, 3.7, 0.13) \text{ MeV} \quad (5.17) \\ (V_{us}, V_{cb}, |V_{ub}|, |V_{td}|)(\leq m_Z) &\approx (0.2250, 0.0412, 0.0037, 0.0086) \\ \bar{\rho}'_W &= 0.150, \quad \bar{\eta}'_W = 0.374 \end{aligned}$$

Fit B

$$\begin{aligned} \sigma &= 0.1 - 0.012i, & \eta &= 0.12 - 0.0464i, & \epsilon &= -0.0954, \\ \eta' &= 2.42 \times 10^{-3}, & \epsilon' &= 2.37 \times 10^{-4} e^{i(69^\circ)}, & \zeta_{22}^d &= 9.8 \times 10^{-3} e^{-i(149^\circ)} \quad (5.18) \\ \zeta_{22}^u &= 4.8 \times 10^{-3} e^{i(103^\circ)}, & (\mathcal{M}_u^0, \mathcal{M}_d^0) &\approx (100, 1.1) \text{ GeV}. \end{aligned}$$

Fit B leads to approximately the same values of fermion masses and CKM elements as Fit A, except that in this case $m_s(1 \text{ GeV}) \approx 110 \text{ MeV}$ and $m_c(m_c) \approx 1.30 \text{ GeV}$. Also, in the case of Fit B, the Wolfenstein parameters are found to be $(\bar{\rho}'_W, \bar{\eta}'_W) = (0.178, 0.327)$.

In obtaining the fermion masses at the low scales, we have not directly used \mathcal{M}_u^0 and \mathcal{M}_d^0 of Eq. (5.3). Instead, we have used: (a) $m_t(m_t) = 167 \text{ GeV}$ and $m_\tau(m_\tau) = 1.777 \text{ GeV}$ as inputs; (b) the GUT-scale predictions of our model for the ratios of masses - such as m_b/m_τ , $m_{u,c}/m_t$, $m_{d,s}/m_b$, m_μ/m_τ etc; (c) renormalization in 2-loop QCD of these ratios in going from the GUT-scale to an effective SUSY-scale $M_S = 500 \text{ GeV}$; and (d) the evolutions in 3-loop QCD and 1-loop QED of individual fermion masses as the effective momentum runs from M_S to the appropriate low energy scales [81]¹¹.

¹¹ Defining $\eta_{a/b} \equiv (m_a/m_b)_{GUT}/(m_a/m_b)_{M_S}$ and $\eta_f \equiv m_f(M_S)/m_f(\mu_{low})$, we get (for $\tan\beta =$

The primes on $\bar{\rho}'_W$ and $\bar{\eta}'_W$ signify that these values are obtained from the SO(10)/G(224) model based fermion mass matrices (as in Eq. (5.3)), in conjunction with fermion masses and neutrino oscillations, as opposed to SM-based phenomenological values (Eq. (5.2)).

Note that, except for the very light fermion masses (m_u° , m_d° , and m_e°) which would need corrections of order 1 to few MeV [82], all the other quark-lepton masses and especially the CKM mixings are in good accord with observations (see values quoted below Eq. (5.2) or Ref. [83]), to within 10%. (As alluded to before, we should not of course expect the very light fermion masses to be described adequately by the gross pattern of the mass-matrices exhibited in Eq. (5.3). In particular the “11” entries in Eq. (5.3) (expected to be of order $10^{-4} - 10^{-5}$) arising from higher dimensional operators, can quite plausibly lead to a needed reduction in m_u by about 6-8 MeV and an increase in (m_e and m_d)¹² by nearly (0.36 and 2-3) MeV respectively,

5 and $\alpha_3(M_Z)=0.118$): $\eta_{b/\tau} = 0.6430$, $\eta_{u,c/t} = 0.4456$, $\eta_{d,s/b} = 0.7660$, $\eta_{e,\mu/\tau} = 0.9999$, $\eta_u = 0.3954$, $\eta_{d,s} = 0.3982$, $\eta_c = 0.4418$, $\eta_b = 0.6053$, $\eta_{e,\mu} = 0.9894$, $\eta_\tau = 0.9914$, $\eta_t = 0.9427$. The CKM elements at low scales are given by $V_{\alpha\beta}(\leq m_Z) = V_{\alpha\beta}(GUT)/K_{\alpha\beta}$, where $K_{\alpha\beta} \approx 0.91$ for $\alpha\beta = ub, cb, td, \text{ and } ts$ and $K_{\alpha\beta} \approx 1$ for the other elements. (The renormalization group equations for the CKM elements are given in Appendix .5).

¹² Note that the “11” entry for the up sector can differ from that for the down sector even in

at the 1 GeV scale, *without* altering the CKM mixings).

The important point is that the SO(10)/G(224)-model presented in Sec. 2 has turned out to be capable of yielding values for $\bar{\rho}'_W$ and $\bar{\eta}'_W$ that are close to the SM values as desired, while simultaneously being able to yield fermion masses of the two heavy families, all the CKM elements and neutrino oscillations (see Chapter 4), in good accord with observations. This in itself is non-trivial.

Before presenting the results for CP and flavor violations some comments are in order as regards the parameters of the model versus its predictiveness. As expected, introduction of (in general four) phases in the Dirac mass matrices clearly increase the number of parameters compared to that for the CP-conserving case [25]. As a result, as long as we confine to the realm consisting of (a) the fermion masses and mixings, (b) CP and flavor violations induced *only by the SM interactions*, and (c) neutrino oscillations, the predictiveness of the model is reduced considerably (compare with the CP-conserving case of Ref. [25]), the number of parameters now being sign because of contribution through the operator $\mathbf{16}_1\mathbf{16}_1\mathbf{16}_H^d(\mathbf{16}_H/M'')(S/M)^n$ which contributes only to m_d and m_e (so that $\delta m_d = \delta m_e$ at M_{GUT}) but not to m_u .

comparable to the number of observables¹³. Nevertheless, some gross features of the predictions in fact survive, even in the realm mentioned above, simply because: (a) the entries in the mass-matrices, governed by flavor symmetries, are hierarchical with a pattern as in Eq. (5.3); (b) the phases are constrained¹⁴ to lie between 0 to 2π , and, (c) the system itself is constrained by the group theory of $SO(10)/SU(4)^c$. One can argue that these features in turn pretty much ensure the gross

¹³ A counting of parameters of the model versus the observables is as follows: The parameters of the model are: [7 for the Dirac mass matrices (Eq. (4.2)) + 5 additional including 4 phases and ζ_{22}^d (see Eq. (5.16)) + 2 higher dimensional operators needed to correct the masses of m_u , m_d and m_e + two (y,z) for the right hand neutrino sector (see Eq. (4.6)) + one higher dimensional operator to correct the value of $\theta_{\nu_e\nu_\mu}^{osc}$ (see discussion in Chapter 4)] = 17. The number of observables are as follows: Without SUSY CP and flavor violations, these are [9 charged fermion masses + 3 quark mixing angles + 1 CKM phase + 3 left handed neutrino masses + 3 left handed neutrino mixings + 3 right handed neutrino masses] = 22. However the number of observables increases enormously when additional ones arising due to SUSY CP and flavor violations are included; these include: Δm_K , ϵ_K , Δm_{B_d} , $S(B_d \rightarrow J/\psi K_S)$, ϵ'_K , Δm_{B_s} , $S(B_d \rightarrow \phi K_S)$, $S(B_d \rightarrow \eta' K_S)$, $S(B_s \rightarrow J/\psi \phi)$, $S(B_s \rightarrow \phi K_S)$, $B \rightarrow K\pi$, $B \rightarrow \pi\pi$, $b \rightarrow s\gamma$, electric dipole moments of (n, e, Hg, d), $\mu \rightarrow e\gamma$, $\tau \rightarrow \mu\gamma$, $\tau \rightarrow e\gamma$ and many more = 20 + many more. Thus the total number of observables = 22 + 20 + many more = 42 + many more, far outnumber the number of parameters (= 17) of the model.

¹⁴ For instance, consider the familiar relation $|V_{us}| = |\sqrt{m_d/m_s} - e^{i\phi}\sqrt{m_u/m_c}|$, that holds for a hierarchical pattern. Given $\sqrt{m_d/m_s} \approx 0.22$ and $\sqrt{m_u/m_c} \approx 0.07$, we cannot of course predict V_{us} precisely without knowing the phase angle ϕ . Yet, since ϕ can vary only between 0 to 2π , $|V_{us}|$ must lie between 0.15 and 0.29

nature of the following predictions: (i) $m_b^\circ/m_\tau^\circ \approx 1$, (ii) $|V_{us}| \sim 0.2$, (iii) $|V_{ub}| \approx \sqrt{m_u/m_c} |V_{cb}|$, (iv) $|V_{td}| \approx \sqrt{m_d/m_s} |V_{cb}|$, (v) $m_{\nu_2}/m_{\nu_3} \sim 1/10$, (vi) $m_{\nu_3} \sim 1/10$ eV, and, (vii) $\sin^2 2\theta_{\nu_\mu\nu_\tau}^{osc} \approx (0.8 - 0.99)$, despite large variations in the parameters.

The real virtue of the model (including the phases) emerges, once one includes SUSY CP and flavor violations. In this case, the realm of observables and thereby the predictiveness of the model expands enormously. The set of observables now includes not only the four entities listed in Eq. (5.1)-i.e., (i) Δm_K , (ii) ϵ_K (iii) Δm_{B_d} and (iv) $S(B_d \rightarrow J/\psi K_S)$ — *but also* a host of others, for which the predictions of the G(224)/SO(10) model including (SM'+ SUSY) contributions, can a priori differ significantly from those of the SM contributions. In particular, the set includes observables such as (v) ϵ'_K (vi) Δm_{B_s} , (vii) $S(B_d \rightarrow \phi K_S)$, (viii) $S(B_d \rightarrow \eta' K_S)$, (ix) $S(B_s \rightarrow J/\psi \phi)$, (x) $S(B_s \rightarrow \phi K_S)$, (xi) $B \rightarrow K\pi$, (xii) $B \rightarrow \pi\pi$ (rates and asymmetry parameters), (xiii) $b \rightarrow s\gamma$, (xiv) electric dipole moments of (n, e, Hg, d) and (xv) Lepton flavor violating processes ($\mu \rightarrow e\gamma$, $\tau \rightarrow \mu\gamma$, $\tau \rightarrow e\gamma$), and more.

Now, the SUSY contributions do of course depend in part on the flavor preserving SUSY-parameters (i.e. m_o , $m_{1/2}$, μ , and $\tan\beta$; we set $A_o = 0$ at M^*). But these few parameters should be regarded as *extraneous* to the present model, and hopefully, they would be determined through the discovery of SUSY at the LHC. *The interesting point is that for a given choice of these flavor-preserving SUSY parameters (essentially m_o and $m_{1/2}$) the SUSY contributions to all the CP and/or flavor-violating processes listed above get completely determined within our model, in magnitude as well as in phases.* This is because all the flavor and in general CP violating sfermion $(mass)^2$ -parameters $((\delta m^2)_{LL,RR,LR}^{ij})$, arising through SO(10)/G(224)-based RG running from M^* to M_{GUT} are completely fixed in the model in terms of the parameters of the fermion mass-matrices (see Eqs. (5.9), (5.14) and (5.15)). The latter are, however essentially fixed by fermion masses and mixings, for example, as shown in fit A given above (Eq. (5.16)), especially when we demand that the $\vec{\rho}'_W$ and $\vec{\eta}'_W$ be close to the SM-values. In short, the inclusion of SUSY CP and flavor violations, treated in conjunction with fermion masses and neu-

trino oscillations, encompasses a host of processes without introducing new parameters and thereby increases the predictiveness of the model enormously.

Using Eqs. (5.9) and (5.11)-(5.15) for the squarks $(mass)^2$ elements ($\delta_{LL,RR,LR}^{ij}$ etc.) as predicted in our model, the expressions given in Refs. [40, 84–86] for the SUSY contributions, and the values of m_s , m_c and the CKM elements (including $\bar{\rho}'_W$ and $\bar{\eta}'_W$) as obtained in the fits A and B given above (see Eqs. (5.16), (5.17)), we can now derive the values of the four entities listed in Eq. (5.1), treating separately the cases of the SO(10) and the G(224)-models. For reasons explained below Eq. (5.8), the SUSY contributions are reduced (in most cases) by about a factor of 2.5 in the amplitude for the case of G(224) compared to that of SO(10), being the effective symmetry in 4D. This distinction, as we will see, provides a way to distinguish between the SO(10) and the G(224)-models experimentally. The predictions of the model (corresponding to the fit shown in Eq. (5.16)) are shown in table 1. We have included both the SM' and the SUSY contributions in obtaining the total contributions (denoted by “Tot”).

In quoting the numbers we have fixed, for concreteness, $M^*/M_{GUT} \approx 3$ and thus $\xi \approx 0.4$, and have made a plausible choice for the SUSY spectrum - i.e. $m_{sq} \approx (0.8 - 1)$ TeV with $x = m_{\tilde{g}}^2/m_{sq}^2 \approx 0.8$, although a variation in these parameters with m_{sq} as low as about 600 GeV or $x = 0.5 - 0.6$ can still lead to the desired results for all four quantities especially for the case of G(224) (see remarks below).

$(m_o, m_{1/2})(\text{GeV})$	(800, 250)		(600, 300)	
	(a)	(b)	(c)	(d)
	SO(10)	G(224)	SO(10)	G(224)
$\Delta m_K^{s,d.} (\text{Tot} \approx SM')(\text{GeV})$	2.9×10^{-15}	2.9×10^{-15}	2.9×10^{-15}	2.9×10^{-15}
$\epsilon_K(SM')$	2.83×10^{-3}	2.83×10^{-3}	2.83×10^{-3}	2.83×10^{-3}
$\epsilon_K(\text{Tot})$	1.30×10^{-3}	2.32×10^{-3}	2.01×10^{-3}	2.56×10^{-3}
$\Delta m_{B_d} (\text{Tot} \approx SM')(\text{GeV})$	3.62×10^{-13}	3.56×10^{-13}	3.58×10^{-13}	3.55×10^{-13}
$S(B_d \rightarrow J/\psi K_S) (\text{Tot} \approx SM')$	0.740	0.728	0.732	0.726

$(m_o, m_{1/2})(\text{GeV})$	(450, 250)		(400, 300)	
	(a)	(b)	(c)	(d)
	SO(10)	G(224)	SO(10)	G(224)
$\Delta m_K^{s,d}(\text{Tot} \approx SM')(\text{GeV})$	2.9×10^{-15}	2.9×10^{-15}	2.9×10^{-15}	2.9×10^{-15}
$\epsilon_K(SM')$	2.83×10^{-3}	2.83×10^{-3}	2.83×10^{-3}	2.83×10^{-3}
$\epsilon_K(\text{Tot})$	1.89×10^{-3}	2.51×10^{-3}	2.33×10^{-3}	2.67×10^{-3}
$\Delta m_{B_d}(\text{Tot} \approx SM')(\text{GeV})$	3.58×10^{-13}	3.56×10^{-13}	3.56×10^{-13}	3.55×10^{-13}
$S(B_d \rightarrow J/\psi K_S) (\text{Tot} \approx SM')$	0.733	0.726	0.728	0.724

Tab. 5.1:

Table 1. Predictions of the SUSY SO(10) and G(224) models corresponding to the fit A for the fermion mass-parameters shown in Eq. (5.16), which incorporates CP violation. Either model with the fit as in Eq. (5.16) leads to the fermion masses and CKM mixings in good agreement with the data (see Eq. (5.17)). The total contribution (denoted by “Tot”) represents the sum of the SM' and the SUSY contributions. These values are to be compared with the experimental values: $\Delta m_K = 3.48 \times 10^{-15}$ GeV, $\epsilon_K = 2.27 \times 10^{-3}$, $\Delta m_{B_d} = (3.30 \pm 0.06) \times 10^{-13}$ GeV and $S(B_d \rightarrow J/\psi K_S) = 0.687 \pm 0.032$. Note that the SUSY contribution is important only for ϵ_K furthermore it is relatively negative (as desired) compared to the SM' contribution (see discussion in text). The superscript *s.d.* on Δm_K represents short distance contribution. The long distance contribution accounts for $\sim 25 - 30\%$ of the value of Δm_K [86].

In obtaining the entries for the K -system we have used central values of the matrix element \hat{B}_K and the loop functions η_i (see Refs. [74, 86] for definitions and values) characterizing short distance QCD effects - i.e. $\hat{B}_K = 0.86 \pm 0.13$, $f_K = 159$ MeV, $\eta_1 = 1.38 \pm 0.20$,¹⁵ $\eta_2 = 0.57 \pm 0.01$ and $\eta_3 = 0.47 \pm 0.04$. For the B -system we use the central values of the unquenched lattice results: $f_{B_d} \sqrt{\hat{B}_{B_d}} =$

¹⁵ We will be guided by the error of ± 0.20 on η_1 , used in [86], although that quoted in [74] is considerably larger (± 0.53).

$215(11)_{(-23)}^{(+0)}(15) \text{ MeV}$ and $f_{B_s}\sqrt{\hat{B}_{B_s}} = 245(10)_{(-2)}^{(+3)}_{(-0)}^{(+7)} \text{ MeV}$ [87].

Note that the uncertainties in some of these hadronic parameters are in the range of 15%; thus the predictions of our model as well as that of the SM would be uncertain at present to the same extent. Clearly as may be seen by comparing the entries in Table 1 with the observed values listed below it, we see that there are cases which agree well with all the observed data.

Using the same values of matrix elements and loop functions as above, we get for the case of Fit B:

$(m_o, m_{1/2})(\text{GeV})$	(450, 250)		(600, 300)	
	(a)	(b)	(c)	(d)
	SO(10)	G(224)	SO(10)	G(224)
$\Delta m_K^{s,d}(\text{Tot} \approx SM')(\text{GeV})$	2.9×10^{-15}	2.9×10^{-15}	2.9×10^{-15}	2.9×10^{-15}
$\epsilon_K(SM')$	2.83×10^{-3}	2.83×10^{-3}	2.83×10^{-3}	2.83×10^{-3}
$\epsilon_K(\text{Tot})$	2.17×10^{-3}	2.58×10^{-3}	2.45×10^{-3}	2.68×10^{-3}
$\Delta m_{B_d}(\text{Tot} \approx SM')(\text{GeV})$	3.12×10^{-13}	3.10×10^{-13}	3.09×10^{-13}	3.07×10^{-13}
$S(B_d \rightarrow J/\psi K_S) (\text{Tot} \approx SM')$	0.683	0.676	0.679	0.672

Tab. 5.2:

Table 2. Predictions of the SUSY SO(10) and G(224) models corresponding to the fit B for the fermion mass-parameters shown in Eq. (5.18), which incorporates CP violation. The total contribution (denoted by “Tot”) represents the sum of the SM' and the SUSY contributions. Note that the SUSY contribution is important only for ϵ_K , furthermore it is relatively negative (as desired) compared to the SM' contribution (see discussion in text). The superscript *s.d.* on Δm_K represents short distance contribution.

At this stage the following comments are in order.

(1) In the cases of Δm_K , Δm_{B_d} and $S(B_d \rightarrow J/\psi K_S)$, the SUSY contributions (with $m_{sq} \sim 0.8-1$ TeV and $x \sim 0.5-0.8$) are found to be rather small ($\sim 0.5\%$, 2% , and 3% respectively) compared to the SM' contribution. (The expressions for the amplitudes of these processes are presented in the appendices). As a result, for these three entities, the SM' contribution practically coincides with the total contribution, which is what is shown in the table. By contrast, for the same spectrum, *the SUSY-contribution to ϵ_K is found to be rather sizeable ($\sim 20-25\%$)¹⁶, and importantly enough, negative compared to the SM' -*

¹⁶ The fact that the SUSY contribution to ϵ_K (in contrast to those for Δm_K , Δm_{B_d} and $S(B_d \rightarrow J/\psi K_S)$) is relatively large is simply because the SM contribution to ϵ_K is strongly suppressed owing to the smallness of the relevant CKM mixings.

*contribution*¹⁷. The fact that it is relatively negative is an outcome of the model and, as it turns out, is most desirable (see below).

(2) Comparing the predicted values shown in Table 1 with the observed ones (see those listed below Eq. (5.2)), together with $\Delta m_K^{obs} = 3.47 \times 10^{-15} \text{ GeV}$, we see that all four entities including ϵ_K and the asymmetry parameter $S(B_d \rightarrow J/\psi K_S)$ agree with the data quite well, for the cases of SO(10) as well as G(224) shown in the last two columns (i.e. for $m_{sq} \approx 1 \text{ TeV}$, and $x \approx 0.8$), and also for the case of G(224) in the second column ($m_{sq} \approx 800 \text{ GeV}$, $x \approx 0.8$). In making this comparison we are allowing for plausible (at present theoretically uncertain but allowed) long distance contribution to $\Delta m_K (\sim \pm 15\%)$, and uncertainties in \hat{B}_K or $\eta_1 \lesssim 10\%$ (see entries for ϵ_K in the last three columns) and that in $f_{B_d} \sqrt{\hat{B}_{B_d}}$ by about 3%.

(3) We note that a choice of the SUSY-parameters, e.g. $(m_o, m_{1/2}) = (800, 250) \text{ GeV}$, shown in the table, is in accord with the WMAP-constraint on CMSSM-spectrum in the event that the lightest neu-

¹⁷ In as much as we require $\bar{\rho}'_W$ and $\bar{\eta}'_W$ to be close to the SM-based phenomenological values (as in Eq. (5.2)), in accord with the observed values of the fermion masses, CKM-elements and neutrino oscillation parameters, we find that the class of fits satisfying these requirements lead to SUSY-contribution to ϵ_K that is relatively negative compared to the SM' -contribution.

trino is the LSP and represents cold dark matter [88].

(4) It is crucial that the SUSY contribution to ϵ_K (as mentioned above) is significant and is negative relative to the SM' -contribution. Indeed this is what makes it possible for $\epsilon_K(Tot)$ to be desirably lower than the $\epsilon_K(SM') = 2.83 \times 10^{-3}$ and thereby to agree better in the last three columns¹⁸ (cases b, c and d) with $\epsilon_K^{obs} = 2.27 \times 10^{-3}$. Had the SUSY contribution been positive relative to the SM' contribution and still as significant as above, $\epsilon_K(Tot)$ would have been $(3.34, 3.53,$ and $3.10) \times 10^{-3}$ for the cases (b), (c), and (d) respectively, in strong disagreement with observation. *In short, the SUSY contribution of the model to ϵ_K has just the right sign and nearly the right magnitude to play the desired role. This seems to be an intriguing feature of the*

¹⁸ In the most recent calculations on Unitarity Triangle fit in the Standard model [89], the value of \hat{B}_K has reduced from 0.86 ± 0.13 used in our work, to $0.79 \pm 0.04 \pm 0.08$. This would lower the value of $\epsilon_K(SM')$ from 2.83×10^{-3} to 2.60×10^{-3} . This will, however, not change the nature of our results, especially since the errors in lattice calculations cannot be taken too seriously at present. The main point is that even with the lowered value of $\epsilon_K(SM')$, a negative (SUSY) contribution is desired for it to agree with the experimental value of 2.27×10^{-3} . Another point that we wish to make here is that once the matrix element \hat{B}_K and the coefficients η_i are determined to a high accuracy, the value of ϵ_K can help distinguish between the supersymmetric SO(10), supersymmetric G(224) and the standard model (see remarks below).

model.

(5) Since the values of the CKM elements including $\bar{\rho}'_W$ and $\bar{\eta}'_W$ obtained within our model (see Eq. (5.17)) are quite close to the SM based phenomenological values (see Ref. [74] and Eq. (5.2)), we would of course expect that the SM' contributions should nearly be the same as the SM contributions, for the same choice of the hadronic parameters (\hat{B}_K , η_i , $f_{B_d}\sqrt{\hat{B}_{B_d}}$ etc.). For instance, using the central values of the parameters given in the recent update of the CKM-triangle analysis by M. Bona et al. [75], that is, $\lambda = |V_{us}| = 0.2265$, $|V_{cb}| = 4.14 \times 10^{-2}$, $\bar{\rho}_W = 0.172$, $\bar{\eta}_W = 0.348$, $m_c = 1.3 \text{ GeV}$ and $f_K = 159 \text{ MeV}$, and the hadronic parameters as in our case - that is, $\hat{B}_K = 0.86$, $\eta_1 = 1.38$, $\eta_2 = 0.57$, and $\eta_3 = 0.47$ - one obtains $\epsilon_K(SM) = 2.72 \times 10^{-3}$ which is about 20% higher than the observed value. Contrast this with the predictions for $\epsilon_K(\text{Tot})$ of the SO(10) or G(224) models for the cases (b), (c) and (d) in Table 1 where the discrepancies between the predicted and observed value of ϵ_K range from 2 to 12% with varying signs. At present, such discrepancies, even as high as 20% for the SM, can of course be accommodated by allowing

for uncertainties in \hat{B}_K , η_1 , and also in λ .

(6) One main point we wish to stress here, however, is this: At present, the distinctions between the predictions of the SM (in particular for ϵ_K) versus those of the SUSY SO(10) or G(224) models on the one hand, and those between the predictions of the SUSY SO(10) versus the G(224) models on the other hand (compare columns (a), (b), (c) and (d) of Table 1) are marred in part because of uncertainties ($\sim 15\%$) in the hadronic parameters (\hat{B}_K , η_1 etc.) as well as that ($\sim 2\%$) in λ , and in part because SUSY is not discovered as yet, and thus the SUSY spectrum is unknown. But once (hopefully) SUSY is discovered at the LHC and thereby the SUSY parameters get fixed, and in addition the uncertainties in the hadronic parameters are reduced to a few percent level through improvements in the lattice calculations, we see from the analysis presented above that we can utilize the combined set of informations to distinguish experimentally between the SM versus the SUSY SO(10)-model versus the SUSY G(224)-model. It is intriguing to see that even low energy experiments involving CP and flavor violations can help distinguish between the

SO(10) versus the G(224) models, both of which nearly coincide as regards their predictions for fermion masses and neutrino oscillations. In this way they can shed light on physics at the super-heavy scale $M^* \gtrsim M_{GUT}$. The experimental distinctions will of course be even sharper once we include predictions for the other processes, some of which are presented below.

(7) $B_d \rightarrow \phi K_S$, Δm_{B_s} **and** $b \rightarrow s\gamma$: We now consider the CP violating asymmetry parameter $S(B_d \rightarrow \phi K_S)$. For a representative choice of $(m_o, m_{1/2}) = (600, 300)$ GeV, we get $\delta_{LL}^{23} = (1.40 - 0.012i) \times 10^{-2}$, $\delta_{RR}^{23} = -(5.39 + 6.27i) \times 10^{-3}$, $\delta_{LR}^{23} = -(0.29 + 3.08i) \times 10^{-4} / \tan \beta$ and $\delta_{RL}^{23} = -(1.92 + 2.70i) \times 10^{-4} / \tan \beta$ as predictions of our model (see Eqs. (5.9) and (5.15)). It is easy to verify that the SUSY-amplitude for this decay in our model is only of order 1% (or less) [90] compared to that in the SM. As a result, adding SM' and SUSY contributions to the decay amplitudes, we obtain:

$$S(B_d \rightarrow \phi K_S)_{Theory} \approx 0.728 \quad (\text{FitA, SO(10)/G(224)}) \quad (5.19)$$

Allowing for variant fits which also give fermion masses and CKM mixings in good agreement with observations, we find that $S(B_d \rightarrow$

ϕK_S) should lie in the range of $\approx +0.65$ (e.g. for the case of Fit B) to $+0.73$. Thus our model predicts that $S(B_d \rightarrow \phi K_S)$ is close to the SM prediction ($\approx 0.70 \pm 0.10$) and certainly not negative in sign. When we started writing the paper Ref. [28], BaBar and BELLE data were yielding widely differing values of $(0.45 \pm 0.43 \pm 0.07)$ and $(-0.96 \pm 0.50_{-0.07}^{+0.09})$ respectively for $S(B_d \rightarrow \phi K_S)$ [91]. Most recently, the two groups reported new values for the asymmetry parameter $S(B_d \rightarrow \phi K_S) = (+0.50 \pm 0.25_{-0.04}^{+0.07})_{BaBar}; (+0.50 \pm 0.21 \pm 0.06)_{BELLE}$ [91], at the Beijing International Conference on High Energy Physics. Meanwhile there have been many theoretical and phenomenological attempts [90,92] to obtain possible large deviations in $S(B_d \rightarrow \phi K_S)$ from the SM-value, including, in some cases, negative values for the same (as suggested by the earlier BELLE data). It will thus be extremely interesting from the viewpoint of the G(224)/SO(10)-framework presented here to see whether the true value of $S(B_d \rightarrow \phi K_S)$ will turn out to be close to the SM-prediction or not.

Including contributions from $\delta_{LL,RR}^{23}$ and $\delta_{LR,RL}^{23}$ (as predicted in

our model), we get:

$$(\Delta m_{B_s})_{Theory} \approx 19.8 \pm 4.9 \text{ ps}^{-1} \quad (\text{SO}(10)/\text{G}(224)). \quad (5.20)$$

where we have used $f_{B_s} \sqrt{\hat{B}_{B_s}} = 262 \pm 35 \text{ MeV}$ [89]. This is fully compatible with the present value $\Delta m_{B_s} = 17.35_{-0.21}^{+0.42} \text{ (stat)} \pm 0.07 \text{ (syst)} \text{ ps}^{-1}$ [89].

Using δ_{RL}^{23} given above, we obtain $A(b_L \rightarrow s_R \gamma)_{\tilde{g}} \approx (1 - 1.5) \times 10^{-10} \text{ GeV}^{-1} / \tan \beta$. Even allowing for variant fits, the SUSY-amplitude, in this case, is found to be only about (1.5-5)% of the SM amplitude. The same conclusion holds also for $A(b_R \rightarrow s_L \gamma)_{\tilde{g}}$. In short, our results for $(B_d \rightarrow \phi K_S)$, Δm_{B_s} and $b \rightarrow s \gamma$ nearly coincide with those of the SM.

(8) **Contribution of the A term to ϵ'_K :** Direct CP violation in $K_L \rightarrow \pi\pi$ receives a new contribution from the chromomagnetic operator $Q_g^- = (g/16\pi^2)(\bar{s}_L \sigma^{\mu\nu} t^a d_R - \bar{s}_R \sigma^{\mu\nu} t^a d_L) G_{\mu\nu}^a$, which is induced by the gluino penguin diagram. This contribution is proportional to $X_{21} \equiv \text{Im}[(\delta_{LR}^d)_{21} - (\delta_{LR}^d)_{12}^*]$, which is predictable in our model (see Eqs. (5.14) and (5.15)). Following Refs. [93] and [94], one obtains:

$$\text{Re}(\epsilon'/\epsilon)_{\tilde{g}} \approx 91 B_G \left(\frac{110 \text{ MeV}}{m_s + m_d} \right) \left(\frac{500 \text{ GeV}}{m_{\tilde{g}}} \right) X_{21} \quad (5.21)$$

where B_G is the relevant hadronic matrix element. Model-dependent considerations (allowing for m_K^2/m_π^2 corrections) indicate that $B_G \approx 1-4$, and that it is positive [93]. Using the prediction of our model (via Eqs. (5.14) and (5.15)), for a typical SUSY- spectrum used in previous considerations (e.g. $(m_o, m_{1/2}) = (600, 300) \text{ GeV}$), we obtain: $X_{21} \approx 2.1 \times 10^{-5}/\tan\beta$. Note that the sign of X_{21} , as derived in the model, is positive. Inserting this in Eq. (5.21), and putting $(m_s + m_d) \approx 110$ MeV, we get:

$$\text{Re}(\epsilon'/\epsilon)_{\tilde{g}} \approx +(8.8 \times 10^{-4})(B_G/4)(5/\tan\beta) . \quad (5.22)$$

We see that if the positive sign of B_G is confirmed by reliable lattice calculations, the gluino penguin contribution in our model can quite plausibly give a significant positive contribution to $\text{Re}(\epsilon'/\epsilon)_{\tilde{g}} \approx (4 - 14) \times 10^{-4}$, depending upon $B_G \approx 2 - 4$ and $\tan\beta \approx (3 - 10)$. At present the status of SM contribution to $\text{Re}(\epsilon'/\epsilon)$ is rather uncertain. For instance, the results of Ref. [95] and [96] based on quenched lattice calculations in the lowest order chiral perturbation theory suggest negative central values for $\text{Re}(\epsilon'/\epsilon)$. (To be specific Ref. [95] yields $\text{Re}(\epsilon'/\epsilon)_{SM} = (-4.0 \pm 2.3) \times 10^{-4}$, the errors being statistical

only.) On the other hand, using methods of partial quenching [97] and staggered fermions, positive values of $Re(\epsilon'/\epsilon)$ in the range of about $(3 - 13) \times 10^{-4}$ are obtained in [98]. In addition, a recent non-lattice calculation based on next-to-leading order chiral perturbation theory yields $Re(\epsilon'/\epsilon)_{SM} = (19 \pm 2_{-6}^{+9} \pm 6) \times 10^{-4}$ [99]. The systematic errors in these calculations are at present hard to estimate. The point we wish to note here is that the SUSY-contribution to $Re(\epsilon'/\epsilon)$, in our model, is significant, and when the dust settles, following a reliable calculation of $Re(\epsilon'/\epsilon)$ in the SM, it would be extremely interesting to check whether the SUSY-contribution obtained here is playing an important role in accounting for the observed value given by $Re(\epsilon'/\epsilon)_{obs} = (17 \pm 2) \times 10^{-4}$ [100] or not.

(9) **EDM of the neutron and the electron:** RG-induced A -terms of the model generate chirality-flipping sfermion mixing terms $(\delta_{LR}^{d,u,l})_{ij}$, whose magnitudes *and* phases are predictable in the model (see Eqs. (5.14) and (5.15)), for a given choice of the universal SUSY-parameters (m_o , $m_{1/2}$, *and* $\tan\beta$). These contribute to the EDM's of the quarks and the electron by utilizing dominantly the gluino and

the neutralino loops respectively. We will approximate the latter by using the bino-loop. These contributions are given by (see e.g. [101]):

$$(d_d, d_u)_{A_{ind}} = \left(-\frac{2}{9}, \frac{4}{9}\right) \frac{\alpha_s}{\pi} e \frac{m_{\tilde{g}}}{m_{sq}^2} f\left(\frac{m_{\tilde{g}}^2}{m_{sq}^2}\right) \text{Im}(\delta_{LR}^{d,u})_{11} \quad (5.23)$$

$$(d_e)_{A_{ind}} = -\frac{1}{4\pi} \frac{\alpha_{em}}{\cos^2\theta_W} e \frac{m_{\tilde{B}}}{m_{\tilde{l}}^2} f\left(\frac{m_{\tilde{B}}^2}{m_{\tilde{l}}^2}\right) \text{Im}(\delta_{LR}^l)_{11} .$$

For a representative choice $(m_o, m_{1/2}) = (600, 300) \text{ GeV}$ (i.e. $m_{sq} = 1 \text{ TeV}$, $m_{\tilde{g}} = 900 \text{ GeV}$, $m_{\tilde{l}} = 636 \text{ GeV}$ and $m_{\tilde{B}} = 120 \text{ GeV}$), using Eqs. (5.14) and (5.15), we get:

$$(d_d)_{A_{ind}} = \frac{4.15 \times 10^{-26}}{\tan\beta} \text{ ecm}; \quad (d_u)_{A_{ind}} = (-1.6 \times 10^{-26}) \text{ ecm}; \quad (5.24)$$

$$(d_e)_{A_{ind}} = \frac{1.1 \times 10^{-28}}{\tan\beta} \text{ ecm} .$$

The EDM of the neutron is given by $d_n = \frac{1}{3}(4d_d - d_u)$. Thus for SO(10), with the choice of $(m_o, m_{1/2})$ as above, we get

$$(d_n)_{A_{ind}} = (1.6, 1.08) \times 10^{-26} \text{ ecm for } \tan\beta = (5, 10) . \quad (5.25)$$

Note that these induced A -term contributions are larger for smaller $\tan\beta$. For an alternative choice $(m_o, m_{1/2}) = (800, 250) \text{ GeV}$, which as mentioned before is compatible with the WMAP/CDM-constraint [88], the predicted EDM of the neutron and the electron are reduced respectively by about 36% and a factor of 3.6. The predictions for the

G(224)-model are smaller than those for the SO(10)-model by nearly a factor of two in all cases.

We should also note that intrinsic SUSY phases denoted by $\phi_A = \arg(A_o^* m_{1/2})$ and $\phi_B = \arg(m_{1/2} \mu B^*)$, if present, would make additional contributions to EDM's through gluino and/or chargino/neutralino loops, which should be added to the contributions shown above. These contributions have been widely discussed in the literature (see e.g. [101]). As is well known, with $A_o = 0$ or small ($\lesssim 1$ GeV) at the scale M^* (as we have chosen, following the examples of Refs. [54] and [50]), these contributions are proportional to $(m_{d,e}) \mu \tan \beta (\sin \phi_B)$. They would be typically about 50-300 times larger than the values shown above (Eqs. (5.24) and (5.25)), *if* the relevant intrinsic SUSY phases are nearly unity. This is the familiar SUSY CP problem. The point of the present study is that even if the intrinsic SUSY phases are naturally zero or insignificantly small, as would be true in a theory

where the SUSY CP problem is naturally solved^{19, 20}, *the induced A-term contributions to EDM's (arising from GUT-scale physics) as presented above would still be present.* The interesting point is that these contributions are *completely determined* in magnitude and phase within our model (for a given choice of the SUSY universal parameters $(m_o, m_{1/2}, \tan \beta)$).

¹⁹ A possible solution to the SUSY CP problem could arise as follows. Assume that *CP violation arises spontaneously, only in the visible sector*, through the VEV's of fields at the GUT-scale, like those of $\mathbf{16}_H$, $\overline{\mathbf{16}}_H$, $\mathbf{45}_H$ and the singlet S . One can argue that the VEV's of at least some of these can be naturally complex or purely imaginary, consistent with the minimization of the potential, even if all parameters in the potential are real. In this case, intrinsic SUSY phases like those in $m_{1/2}$, A and B are, of course, zero. Now if the μ -term can be derived, through a satisfactory resolution of the μ -problem, for example, either by the Giudice-Masiero mechanism [41], or by the ideas suggested in [42], or by involving a coupling in the superpotential of the form [102]: $\kappa \mathbf{10}_H \mathbf{10}_H N + \lambda N^3 + \dots$, where the singlet N is not allowed to couple to the other fields mentioned above, and acquires a real VEV of order 1 TeV (as needed), with κ and λ being real, then the μ -term would also be real. In this case, all intrinsic SUSY phases would disappear. We plan to explore this possibility in a future work.

²⁰ An alternative resolution of the SUSY CP problem arises in a class of gaugino mediated SUSY-breaking (with the μ -problem being resolved for example as in [41]) in which all relevant SUSY parameters become proportional to $m_{1/2}$ [54]. A third resolution of the SUSY CP problem would arise in a model where both A and B terms are naturally zero or sufficiently small at the scale M^* . This is precisely what happens in, for example, the anomalous $U(1)_A$ model of SUSY-breaking that arises in the context of a three-family string-solution [50]. In this case, extra gauge symmetries of the model suppress both A and B terms at M^* .

Given the experimental limits $d_n < 6.3 \times 10^{-26}$ e cm [103] and $d_e < 4.3 \times 10^{-27}$ e cm [104], we see that the predictions of the model (arising only from the induced A -term contributions) especially for the EDM of the neutron is in an extremely interesting range suggesting that it should be discovered with an improvement of the current limit by a factor of about 10.

5.5 *Summary and Concluding Remarks*

In this chapter I, following work done with Babu and Pati [28], have explored the possibility that (a) fermion masses, (b) neutrino oscillations, (c) CP-non conservation and (d) flavor violations get intimately linked to each other within supersymmetric grand unification, especially that based on the symmetry $SO(10)$ or an effective symmetry $G(224) = SU(2)_L \times SU(2)_R \times SU(4)^c$. In this context, we extend the framework proposed previously in [25], which successfully described fermion masses and neutrino oscillations (see Chapter 4), to include CP violation. We assume, in the interest of predictiveness, that CP-violation, arising through the SM as well as SUSY interactions, has its

origin entirely (or primarily) through phases in the fermion mass matrices. We also assume that flavor-blind universal SUSY parameters (m_o , $m_{1/2}$ and $\tan\beta$ with A_o being small or real) characterize SUSY-breaking effects at a high scale $M^* \gtrsim M_{GUT}$. In this case, all the weak scale CP and/or flavor-violating as well as flavor-preserving sfermion transition-elements $\delta_{LL,RR,LR}^{ij}$, and the induced A-parameters, get fully determined within the model, in their magnitudes as well as in phases, simply by the entries in the SO(10)-based fermion mass-matrices, once the few soft parameters (m_o , $m_{1/2}$ and $\tan\beta$) are specified. This is how CP and flavor violations arising jointly from the SM and SUSY interactions, get intimately tied to fermion masses and neutrino oscillations, within a predictive SO(10)/G(224)-framework outlined above. The presence of GUT-scale physics induces enhanced flavor violation with and without CP violation, which provides a distinguishing feature of

the model²¹, relative to CMSSM or MSSM.²²

As mentioned in Secs. 1 and 4, the framework presented above faces, however, a prima-facie challenge. Including SM *and* SUSY contributions, the question arises, can the framework successfully describe the observed features of CP and flavor-violations including those listed in Eq. (5.1), while retaining the successes of the CP-preserving framework [25] as regards fermion masses and neutrino oscillations? Our work here shows that the SUSY SO(10)/G(224)-framework proposed here, which extends the framework of Ref. [25], indeed meets this challenge squarely. In the process, it makes several predictions, only some

²¹ Even in the case of CMSSM, all the parameters of MSSM at the electroweak scale (some 105 of them) are of course also all fully determined in terms of the SUSY-parameters (m_o , $m_{1/2}$ and $\tan\beta$) and those involving the fermion masses and mixings. However, in this case, as mentioned in Sec. 4, owing to the absence of GUT-scale physics in the interval $M^* \rightarrow M_{GUT}$, the most interesting effects on the entities considered here (e.g. those on ϵ_K , ϵ'_K and the EDM's) would be absent or negligibly small.

²² While we have focussed in this Chapter on the SO(10)/G(224)-model of Ref. [25], we note that generically such enhanced flavor and/or CP violations arising from GUT-scale physics would of course be present in alternative models of SUSY grand unification [105] as well, as long as the messenger scale M^* lies above M_{GUT} . The detailed predictions and *consistency* of any such model as regards flavor and/or CP violations can however depend (even sensitively) upon the model, and this is worth examining.

of which are considered here; these can eventually help distinguish the framework from other alternatives.

Our results can be summarized as follows:

(1) It is found that, with allowance for phases, there exists a fit to the parameters of the fermion mass-matrices (Eq. (5.3)) which successfully describes fermion masses, all the CKM elements and neutrino oscillations as in Ref. [25] (see Eq. (5.17)), and simultaneously yields the Wolfenstein parameters $(\bar{\rho}'_W, \bar{\eta}'_W)$ that are close to the phenomenological SM values (Eq. (5.2)). The merit of obtaining such values for $(\bar{\rho}'_W, \bar{\eta}'_W)$ in accounting for the data on CP and flavor violations in quantities such as those listed in Eq. (5.1) has been stressed in Sec. 4.

(2) With these values of $(\bar{\rho}'_W, \bar{\eta}'_W)$, and a plausible choice of the SUSY-spectrum²³ (i.e. $m_{sq} \approx (600-1000)$ GeV and $m_{\tilde{g}} \approx (500-900)$ GeV, say, it is found that the derived values of all four quantities (i.e. Δm_K , ϵ_K , Δm_{B_d} and $S(B_d \rightarrow J/\psi K_S)$) agree with the data quite well (allowing for up to 15% uncertainty in hadronic matrix elements), see

²³ Lighter masses for the SUSY particles like $m_{sq} \approx 600$ GeV and $m_{\tilde{g}} \approx 500$ GeV (say) are allowed for the case of G(224), though not for SO(10) (see discussion following Table 1).

Table 1.

(3) Although the SM' contributions (e.g., for the fit shown in Eq. (5.16)) nearly coincide with the SM contributions to all entities, and SUSY-contributions to entities such as Δm_K , Δm_{B_d} and $S(B_d \rightarrow J/\psi K_S)$ are rather small (\lesssim a few%), the contributions from SUSY, as a rule, are nevertheless prominent (of order 20-25%) especially when the SM (or SM') contributions are suppressed (for example due to smallness of the mixing angles). Such is precisely the case for ϵ_K , ϵ'_K and the edm's of the neutron and the electron, (as well as for lepton flavor violating processes [29] to be discussed in the next chapter). It is found that the SUSY-contribution to ϵ_K is sizable (of order 20-25%) and *negative* relative to the SM' contribution, just as desired, to yield better agreement between the predicted and the observed value (see Table 1).

(4) The sizable negative contribution of SUSY to ϵ_K in our model provides an important tool to help distinguish not only between the SM versus the SUSY SO(10)/G(224)-models, but also between the SO(10) and the G(224)-models themselves (see Table 1). Such dis-

tinctions would be possible once (hopefully) SUSY is discovered at the LHC and thereby the SUSY parameters get fixed, and in addition the uncertainties in the hadronic parameters (\hat{B}_K and η_1) are reduced to (say) a 5% level or better, through improved lattice calculations.

(5) The model predicts that $S(B_d \rightarrow \phi K_S)$ should lie in the range of $+(0.65-0.73)$, i.e. close to the SM-prediction. Given the present still significant disparities between the BaBar and BELLE results versus the SM-predictions, it would be interesting to see where the true value of $S(B_d \rightarrow \phi K_S)$ would turn out to lie.

(6) It is interesting that the quantity $X_{21} = Im[(\delta_{LR}^d)_{21} - (\delta_{LR}^d)_{12}^*]$, relevant for ϵ'_K , is found to be positive in the model. If the presently indicated sign of the relevant hadronic matrix element B_G being positive is confirmed, our model would give a positive contribution to $Re(\epsilon'/\epsilon)$ which quite plausibly can lie in the range of $+(4-14) \times 10^{-4}$. While this is in the interesting range, its relevance can be assessed only after the associated matrix elements are determined reliably.

(7) The model predicts that the EDM's of the neutron and the electron should be discovered with improvements in the current limits

by factors of 10 and 100 respectively. (Intrinsic SUSY-phases, even if present, would not alter this conclusion as long as there is no large cancellation between different contributions.)

(8) It would be most interesting to explore the consequences of the model, involving SUSY contributions, to other processes such as $B_s \rightarrow J/\psi\phi$, $B_s \rightarrow \phi K_S$, $B \rightarrow K\pi$, $B \rightarrow \pi\pi$, $B \rightarrow DK$, $K_L \rightarrow \pi\nu\bar{\nu}$, $K^+ \rightarrow \pi\nu\bar{\nu}$, and especially lepton violating processes (such as $\mu \rightarrow e\gamma$, $\tau \rightarrow \mu\gamma$, $\tau \rightarrow e\gamma$ etc.). We stress that the net ($SM' + \text{SUSY}$)-contributions to all these processes involving CP and/or flavor violations are completely determined within our model. They do not involve any new parameters. For this reason, the model turns out to be highly predictive and thoroughly testable. Some of these processes are discussed in the next chapter.

To conclude, the SUSY $SO(10)/G(224)$ framework, as proposed in Ref. [25] and extended here, subject to the assumption of universality of SUSY parameters, drastically reduces the parameters for SUSY-contributions to CP and flavor-violations. In effect, the extension proposed here ties in fermion masses, neutrino oscillations, CP and flavor

violations within a predictive and testable framework.

APPENDIX

.1 Appendix: Approximate diagonalization of mass matrices and

the CKM matrix for the BPW model

The mass matrices in the BPW model²⁴ for the up and the down sector

are given by

$$M_u = \begin{bmatrix} 0 & \epsilon' & 0 \\ -\epsilon' & \zeta_{22}^u & \sigma + \epsilon \\ 0 & \sigma - \epsilon & 1 \end{bmatrix} \quad M_d = \begin{bmatrix} 0 & \eta' + \epsilon' & 0 \\ \eta' - \epsilon' & \zeta_{22}^d & \eta + \epsilon \\ 0 & \eta - \epsilon & 1 \end{bmatrix} \quad (.26)$$

These matrices are defined in the gauge basis and are multiplied by $\bar{\Psi}_L$ on left and Ψ_R on right. For instance, the row and column indices of M_u are given by $(\bar{u}_L, \bar{c}_L, \bar{t}_L)$ and (u_R, c_R, t_R) respectively.

While it is easy to diagonalize these matrices numerically and obtain the CKM matrix, knowing the approximate analytic form of the diagonalizing matrices and the CKM matrix, can provide useful insight. In this section, we will diagonalize these matrices approximately, and obtain (approximate) analytic expression of the CKM elements in terms of the parameters of the mass matrices.

²⁴ While in the BPW model, the parameters $\zeta_{22}^{u,d}$ were set to zero for simplicity, they are being retained here for generality, and are chosen to be $\mathcal{O}(10^{-2})$, in accord with the hierarchical structure of the matrices

The parameters in the mass matrices in Eq. (.26) are in general, complex. We can absorb some of the phases in the matrices into the quark fields. Our goal is to diagonalize the mass matrices and bring the CKM matrix into the Wolfenstein form. This is done in a set of steps.

1. Let $\eta \pm \epsilon \equiv A_{\pm} e^{i\phi_{\pm}}$, and $\eta' \pm \epsilon' \equiv B_{\pm} e^{i\chi_{\pm}}$. The phases of the quarks can be redefined so that $\bar{Q}_L^d \equiv \bar{Q}'_L{}^d P_L^{d\dagger}$; $Q_R^d \equiv P_R^d Q'_R{}^d$ and $\bar{Q}_L^d M_d Q_R^d = \bar{Q}'_L{}^d P_L^{d\dagger} M_d P_R^d Q'_R{}^d = \bar{Q}'_L{}^d M_d^{(1)} Q'_R{}^d$, where

$$P_L^{d\dagger} = \begin{bmatrix} e^{-i(\chi_+ - \phi_-)} & 0 & 0 \\ 0 & e^{-i\phi_+} & 0 \\ 0 & 0 & 1 \end{bmatrix} \quad P_R^d = \begin{bmatrix} e^{i(\phi_+ - \chi_-)} & 0 & 0 \\ 0 & e^{-i\phi_-} & 0 \\ 0 & 0 & 1 \end{bmatrix} \quad (.27)$$

and

$$M_d^{(1)} = \begin{bmatrix} 0 & B_+ & 0 \\ B_- & \zeta_{22}^d e^{-i(\phi_+ + \phi_-)} & A_+ \\ 0 & A_- & 1 \end{bmatrix} \quad (.28)$$

For brevity of notation define $\zeta_{22}^d e^{-i(\phi_+ + \phi_-)} \equiv |\zeta_{2d}| e^{-i\hat{\phi}_d}$. The same procedure can be carried out for the up sector. Let $|\sigma \pm \epsilon| \equiv C_{\pm} e^{i\xi_{\pm}}$

and $\epsilon' \equiv |\epsilon'|e^{i\phi_{\epsilon'}}$. Proceeding as above we get

$$P_L^{u\dagger} = \begin{bmatrix} e^{i(\xi_- - \phi_{\epsilon'})} & 0 & 0 \\ 0 & e^{-i\xi_+} & 0 \\ 0 & 0 & 1 \end{bmatrix} \quad P_R^u = \begin{bmatrix} e^{i(\xi_+ - \phi_{\epsilon'})} & 0 & 0 \\ 0 & e^{-i\xi_-} & 0 \\ 0 & 0 & 1 \end{bmatrix} \quad (.29)$$

$$P_L^{u\dagger} P_L^d = e^{i(\chi_+ + \xi_- - \phi_{\epsilon'} - \phi_-)} \begin{bmatrix} 1 & 0 & 0 \\ 0 & e^{i\gamma} & 0 \\ 0 & 0 & e^{i\delta} \end{bmatrix} \quad (.30)$$

where $\gamma \equiv \phi_+ - \xi_+ - \chi_+ - \xi_- + \phi_- + \phi_{\epsilon'}$ and $\delta \equiv -(\chi_+ + \xi_- - \phi_{\epsilon'} - \phi_-)$.

The charged current Lagrangian is given by:

$$\begin{aligned} J^+ W_+ &= \left[\bar{u}_L^{(0)} d_L^{(0)} + \bar{c}_L^{(0)} s_L^{(0)} + \bar{t}_L^{(0)} b_L^{(0)} \right] W_- \\ &= W_+ \left[\bar{u}'_L d'_L e^{i[(\xi_- - \phi_{\epsilon'}) - (\phi_- - \chi_+)]} + \bar{c}'_L s'_L e^{i(\phi_+ - \xi_+)} + \bar{t}_L b_L \right] \\ &= \left[\bar{u}'_L d'_L + \bar{c}'_L s'_L e^{i[(\phi_- - \xi_-) - (\xi_+ - \phi_{\epsilon'})]} + \bar{t}_L b_L e^{-i(\chi_+ + \xi_- - \phi_{\epsilon'} - \phi_-)} \right] \\ &\quad \times e^{i(\chi_+ + \xi_- - \phi_{\epsilon'} - \phi_-)} W_+ \end{aligned} \quad (.31)$$

where $u_L^{(0)}$, $d_L^{(0)}$ etc. are defined in the gauge basis, and primed fields are defined as $\bar{Q}_L^u = \bar{Q}_L^{\prime u} P_L^{u\dagger}$ and $Q_L^d = P_L^d Q_L^{\prime d}$. The overall phase $e^{i\alpha} = e^{i(\chi_+ + \xi_- - \phi_{\epsilon'} - \phi_-)}$ in $P_L^{u\dagger} P_L^d$ can be absorbed into W_+ .

2. The next step is to diagonalize the the 23 sector of the down mass matrix $M_d^{(1)}$ to a very good approximation. Let $\sin \theta_L^{23} \equiv A_+$ and

$\sin \theta_R^{23} \equiv A_-$. Now $M_d^{(1)}$ is transformed by the following matrices to

give $M_d^{(2)} = U_L^{(1)\dagger} M_d^{(1)} U_R^{(1)}$ shown below:

$$U_L^{(1)\dagger} = \begin{bmatrix} 1 & 0 & 0 \\ 0 & \cos \theta_L^{23} & -\sin \theta_L^{23} \\ 0 & \sin \theta_L^{23} & \cos \theta_L^{23} \end{bmatrix} \quad U_R^{(1)} = \begin{bmatrix} 1 & 0 & 0 \\ 0 & \cos \theta_R^{23} & \sin \theta_R^{23} \\ 0 & -\sin \theta_R^{23} & \cos \theta_R^{23} \end{bmatrix} \quad (.32)$$

$$M_d^{(2)} \approx \begin{bmatrix} 0 & B_+ \cos \theta_R^{23} & B_+ \sin \theta_R^{23} \\ B_- \cos \theta_L^{23} & |X_d| e^{i\phi_{X_d}} & 0 \\ B_- \sin \theta_L^{23} & 0 & 1 + \frac{A_+^2}{2} + \frac{A_-^2}{2} \end{bmatrix} \quad (.33)$$

where $X_d \equiv -|\eta^2 - \epsilon^2| + |\zeta_{2d}| e^{-i\hat{\phi}_d} \equiv |X_d| e^{i\phi_{X_d}}$.

3. Now the phase in the 22 element can be rotated away by the transformation $M_d^{(3)} = U_L^{(2)\dagger} M_d^{(2)} U_R^{(2)}$, where $U_L^{(2)}$ and $U_R^{(2)}$ are defined

below:

$$U_L^{(2)\dagger} = \begin{bmatrix} 1 & 0 & 0 \\ 0 & e^{i\phi_{X_d}} & 0 \\ 0 & 0 & 1 \end{bmatrix} \quad U_R^{(2)} = \begin{bmatrix} e^{i\phi_{X_d}} & 0 & 0 \\ 0 & 1 & 0 \\ 0 & 1 & 1 \end{bmatrix} \quad (.34)$$

$$M_d^{(3)} \approx \begin{bmatrix} 0 & B_+ \cos \theta_R^{23} & B_+ \sin \theta_R^{23} \\ B_- \cos \theta_L^{23} & |X_d| & 0 \\ B_- \sin \theta_L^{23} e^{i\phi_{X_d}} & 0 & 1 + \frac{A_+^2}{2} + \frac{A_-^2}{2} \end{bmatrix} \quad (.35)$$

4. A Cabibbo rotation is now done in the 12 sector. Define $\sin \theta_L^{12} \equiv B_+ \cos \theta_R^{23} / |X_d|$ and $\sin \theta_R^{12} \equiv B_- \cos \theta_L^{23} / |X_d|$. Let $M_d^{(4)} = U_L^{(3)\dagger} M_d^{(3)} U_R^{(3)}$

where the relevant matrices are

$$U_L^{(3)\dagger} = \begin{bmatrix} \cos \theta_L^{12} & -\sin \theta_L^{12} & 0 \\ \sin \theta_L^{12} & \cos \theta_L^{12} & 0 \\ 0 & 0 & 1 \end{bmatrix} \quad U_R^{(3)} = \begin{bmatrix} \cos \theta_R^{12} & \sin \theta_R^{12} & 0 \\ -\sin \theta_R^{12} & \cos \theta_R^{12} & 0 \\ 0 & 0 & 1 \end{bmatrix} \quad (.36)$$

$$M_d^{(4)} \approx \begin{bmatrix} -B_+ B_- \cos \theta_L^{23} \cos \theta_R^{12} \sin \theta_L^{12} & 0 & B_+ \sin \theta_R^{23} \cos \theta_L^{12} \\ 0 & |X_d| & 0 \\ B_- \sin \theta_L^{23} \cos \theta_R^{12} e^{i\phi_{X_d}} & 0 & 1 + \frac{A_+^2}{2} + \frac{A_-^2}{2} \end{bmatrix} \quad (.37)$$

5. Finally, a rotation in the 13 sector will make the mass matrix approximately diagonal. This is done by the transformation $M_d^{(5)} = U_L^{(4)\dagger} M_d^{(4)} U_R^{(4)}$, with

$$U_L^{(4)\dagger} = \begin{bmatrix} 1 & 0 & -B_+ A_- \\ 0 & 1 & 0 \\ B_+ A_- & 0 & 1 \end{bmatrix} \quad U_R^{(4)} = \begin{bmatrix} 1 & 0 & B_- A_+ e^{-i\phi_{X_d}} \\ 0 & 1 & 0 \\ -B_- A_+ e^{i\phi_{X_d}} & 0 & 1 \end{bmatrix} \quad (.38)$$

$$M_d^{(5)} \approx \begin{bmatrix} -B_+ B_- \cos \theta_L^{23} \cos \theta_R^{12} \sin \theta_L^{12} & 0 & 0 \\ 0 & |X_d| & 0 \\ 0 & 0 & 1 + \frac{A_+^2}{2} + \frac{A_-^2}{2} \end{bmatrix} \quad (.39)$$

$$\approx \begin{bmatrix} -\frac{|\eta'^2 - \epsilon'^2|}{|X_d|} \cos \theta_L^{23} \cos \theta_R^{23} & 0 & 0 \\ 0 & |X_d| & 0 \\ 0 & 0 & 1 + \frac{A_+^2}{2} + \frac{A_-^2}{2} \end{bmatrix}$$

The mass matrix is now diagonal to a very good approximation. We have made use of the hierarchical structure of the matrix $1 \gg \sigma \sim \eta \sim \epsilon \gg \zeta_{22}^u \sim \zeta_{22}^d \gg \eta' > \epsilon'$ in neglecting small terms. Thus in going from the gauge basis to the mass basis, the left handed down quarks are transformed as $q_L^d \rightarrow P_L^d U_L^{(1)} U_L^{(2)} U_L^{(3)} U_L^{(4)} q_L^d$, and similarly for the right handed quarks. The net transformation matrices for the down quarks then are $X_L^d \equiv P_L^d U_L^{(1)} U_L^{(2)} U_L^{(3)} U_L^{(4)}$ and $X_R^d \equiv P_R^d U_R^{(1)} U_R^{(2)} U_R^{(3)} U_R^{(4)}$. One can similarly find the corresponding $X_{L,R}^u$ matrices for the up sector.

The CKM matrix is then given by $V_{CKM} = X_L^{u\dagger} X_L^d$.

$$\begin{aligned}
X_L^d &= P_L^d U_L^{(1)} U_L^{(2)} U_L^{(3)} U_L^{(4)} \\
&= P_L^d \begin{bmatrix} 1 & \frac{\eta'}{|X_d|} & \eta'|\eta - \epsilon| \\ -\frac{\eta'}{|X_d|} e^{i\phi_{X_d}} & e^{i\phi_{X_d}} & |\eta + \epsilon| \\ \frac{\eta'}{|X_d|} |\eta + \epsilon| e^{i\phi_{X_d}} - \eta'|\eta - \epsilon| & -|\eta + \epsilon| e^{i\phi_{X_d}} & 1 \end{bmatrix} \quad (.40)
\end{aligned}$$

similarly

$$\begin{aligned}
X_L^u &= P_L^u \begin{bmatrix} 1 & \frac{\epsilon'}{|X_u|} & \epsilon'|\sigma - \epsilon| \\ -\frac{\epsilon'}{|X_u|} e^{i\phi_{X_u}} & e^{i\phi_{X_u}} & |\sigma + \epsilon| \\ \frac{\epsilon'}{|X_u|} |\sigma + \epsilon| e^{i\phi_{X_u}} - \epsilon'|\sigma - \epsilon| & -|\sigma + \epsilon| e^{i\phi_{X_u}} & 1 \end{bmatrix} \quad (.41)
\end{aligned}$$

The CKM elements calculated as above are listed below:

$$\begin{aligned}
V_{ud} &\approx 1 + \left| \frac{\eta'}{X_d} \frac{\epsilon'}{X_u} \right| e^{i(\phi_{X_d} - \phi_{X_u} + \gamma)} \equiv |V_{ud}| e^{i\zeta_{ud}} \\
V_{us} &\approx \left| \frac{\eta'}{X_d} \right| - \left| \frac{\epsilon'}{X_u} \right| e^{i(\phi_{X_d} - \phi_{X_u} + \gamma)} \equiv |V_{us}| e^{i\zeta_{us}} \\
V_{cd} &\approx - \left| \frac{\eta'}{X_d} \right| e^{i(\phi_{X_d} - \phi_{X_u} + \gamma)} + \left| \frac{\epsilon'}{X_u} \right| \equiv |V_{cd}| e^{i\zeta_{cd}} \\
V_{cs} &\approx e^{i(\phi_{X_d} - \phi_{X_u} + \gamma)} + \left| \frac{\eta'}{X_d} \right| \left| \frac{\epsilon'}{X_u} \right| \equiv |V_{cs}| e^{i\zeta_{cs}} \\
V_{ub} &\approx \eta' |\eta - \epsilon| - \left| \frac{\epsilon'}{X_u} \right| |\eta + \epsilon| e^{i(\gamma - \phi_{X_u})} + \left| \frac{\epsilon'}{X_u} \right| |\sigma + \epsilon| e^{i(\delta - \phi_{X_u})} \\
&\equiv |V_{ub}| e^{i\zeta_{ub}} \\
V_{cb} &\approx |\eta + \epsilon| e^{i(\gamma - \phi_{X_u})} - |\sigma + \epsilon| e^{i(\delta - \phi_{X_u})} \equiv |V_{cb}| e^{i\zeta_{cb}} \\
V_{td} &\approx \left| \frac{\eta'}{X_d} \right| |\eta + \epsilon| e^{i(\delta + \phi_{X_d})} - \left| \frac{\eta'}{X_d} \right| |\sigma + \epsilon| e^{i(\gamma + \phi_{X_d})} - \eta' |\eta - \epsilon| e^{i\delta} \\
&\equiv |V_{td}| e^{i\zeta_{td}} \\
V_{ts} &\approx - |\eta + \epsilon| e^{i(\delta + \phi_{X_d})} + |\sigma + \epsilon| e^{i(\gamma + \phi_{X_d})} \equiv |V_{ts}| e^{i\zeta_{ts}} \\
V_{tb} &\approx e^{i\delta} \equiv |V_{tb}| e^{i\zeta_{tb}}
\end{aligned} \tag{.42}$$

Due to the hierarchical structure of the matrices, the phases in the CKM elements, listed above, can be estimated. For example, $\zeta_{ud} \lesssim 1/75$, $\zeta_{us} \sim 1/10$. The phases in V_{cd} , V_{cs} , V_{cb} , V_{ub} , V_{td} , V_{td} , V_{tb} can be sizable.

6. This CKM matrix is still not in the Wolfenstein basis. To do this one more transformation is required. Let the CKM matrix in the Wolfenstein basis be denoted by \widehat{V}_{CKM} . Then $\widehat{V}_{CKM} = \widehat{P}_u^\dagger V_{CKM} \widehat{P}_d$

where

$$\widehat{P}_u = \begin{bmatrix} 1 & 0 & 0 \\ 0 & e^{i(\zeta_{cs}-\zeta_{us})} & 0 \\ 0 & 0 & e^{i(\zeta_{cs}-\zeta_{us}-\zeta_{cb}+\delta)} \end{bmatrix} \quad \widehat{P}_d = \begin{bmatrix} 1 & 0 & 0 \\ 0 & e^{-i\zeta_{us}} & 0 \\ 0 & 0 & e^{i(\zeta_{cs}-\zeta_{us}-\zeta_{cb})} \end{bmatrix} \quad (.43)$$

With this the mass matrices have been diagonalized with positive real eigen values, and the CKM matrix is brought to the Wolfenstein form, with only V_{ub} and V_{td} being complex, and all other elements being real to a very good approximation (see the appendix II on Wolfenstein parametrization).

The approximate expressions for the CKM elements and the masses of quarks, agree very well with the exact numerical diagonalization. The magnitudes and phases of the parameters in the mass matrices are varied so as to fit the values of fermion masses and CKM elements.

.2 Appendix: Renormalization group running of A-terms from the SUSY messenger scale M^ to M_{GUT}*

In our work on CP and flavor violation, we assume that flavor-universal soft SUSY-breaking is transmitted to the SM-sector at a messenger scale M^* , where $M_{GUT} < M^* \leq M_{string}$. This may naturally be real-

ized e.g. in models of mSUGRA [46], or gaugino-mediation [54]. With the assumption of extreme universality as in CMSSM, supersymmetry introduces five parameters at the scale M^* :

$$m_o, m_{1/2}, A_o, \tan \beta \text{ and } \text{sgn}(\mu).$$

For most purposes, we will adopt this restricted version of SUSY breaking with the added restriction that $A_o = 0$ at M^* [54]. The analysis can easily be extended to include $A_o \neq 0$. Even if $A_o = 0$ at the scale M^* , the scale at which supersymmetry breaking is communicated to the standard model- sector, RG running from M^* to M_{GUT} induces A -parameters at M_{GUT} , involving the $\text{SO}(10)/\text{G}(224)$ gauginos and the relevant Yukawa couplings (see figs. 1, 2 and 3). These yield chirality flipping transitions ($\tilde{l}_{L,R}^i \rightarrow \tilde{l}_{R,L}^j$).

The RGEs of A -terms, A^{ijk} between fields $\phi_i \phi_j \phi_k$ are given by

$$\begin{aligned} \frac{dA^{ijk}}{dt} = & \frac{1}{16\pi^2} \left[\frac{1}{2} A^{ijl} Y_{lmn} Y^{mnk} + Y^{ijl} Y_{lmn} A^{mnk} \right. \\ & \left. - 2(A^{ijk} - 2MY^{ijk})g^2 C(k) \right] + (k \leftrightarrow i) + (k \leftrightarrow j) \end{aligned} \quad (.44)$$

where $C(i)$ is the Casimir of the representation of the field ϕ_i relative to the group. The Casimirs can be evaluated as

$$C(i) = l(i) \frac{N(\text{adj})}{N(i)} \quad (.45)$$

where $l(i)$ is the Dynkin index of the irreducible representation of ϕ_i , $N(\text{adj})$ is the dimension of the adjoint representation of the group, and $N(i)$ is the dimension of the irreducible representation i . For the group $\text{SO}(10)$, the adjoint is 45 dimensional, and the relevant Dynkin indices and Casimirs are given below:

Representation	Dynkin index	Casimir	
10	2	9	(.46)
16	4	45/4	
45	16	16	

When $A_o = 0$, the only relevant term in Eq. (.44) is the last term.

$$\frac{dA^{ijk}}{dt} = \frac{1}{16\pi^2} [4MY^{ijk} g^2 (C(i) + C(j) + C(k))] \quad (.47)$$

For the effective A -term $16\ 16\ 10_H$, given in fig. 1, $\sum C(i) = C(16) + C(16) + C(10) = 63/2$. Similarly for figs. 2 and 3, $\sum C(i) = 95/2$ and $90/2$ respectively.

Evaluated at the GUT scale, the A -parameters in figs 1, 2 and 3, induced respectively through the couplings yukawa h_{ij} , a_{ij} and g_{ij} (see the Yukawa couplings for the BPW model in Chapter 4), are given by:

$$\begin{aligned}
A_{ij}^{(1)} &= \frac{63}{2} \frac{1}{8\pi^2} h_{ij} g_{10}^2 M_\lambda \ln\left(\frac{M^*}{M_{10\mathbf{H}}}\right) & (i, j = 2, 3) \\
A_{ij}^{(2)} &= \frac{95}{2} \frac{1}{8\pi^2} \frac{a_{ij}(\mathbf{45}_{\mathbf{H}})}{M'} g_{10}^2 M_\lambda \ln\left(\frac{M^*}{M_{10\mathbf{H}}}\right) & (ij = 23, 12) \\
A_{ij}^{(3)} &= \frac{90}{2} \frac{1}{8\pi^2} \frac{g_{ij}(\mathbf{10}_{\mathbf{H}})}{M''} g_{10}^2 M_\lambda \ln\left(\frac{M^*}{M_{16\mathbf{H}}}\right) & (ij = 23, 22, 12)
\end{aligned} \tag{.48}$$

For the case of G(224), an effective A - term analogous to that in fig. 1 is generated between the fields $(2, 2, 1)_H$, $(2, 1, 4)$, $(1, 2, \bar{4})$. Similarly, in fig. 2 the A - term involves the representations $(2, 2, 1)_H, (2, 1, 4)$, $(1, 2, \bar{4})$, $(1, 1, 15)_H$ and in fig. 3 the A - term is between the representations $(2, 1, 4)_H(1, 2, \bar{4})_H(2, 1, 4)(1, 2, \bar{4})$. The Casimirs of the relevant fields are $C(2)_{SU(2)} = 3/2$, $C(4)_{SU(4)} = 15/4$, $C(15)_{SU(4)} = 8$. Thus $\sum C(i) = 27/2$, $43/2$ and 21 for figs. 1, 2 and 3 respectively for G(224). Thus in Eq. (.48), one can replace the coefficients $(\frac{63}{2}, \frac{95}{2}, \frac{90}{2})$ by $(\frac{27}{2}, \frac{43}{2}, \frac{42}{2})$ for the case of G(224).

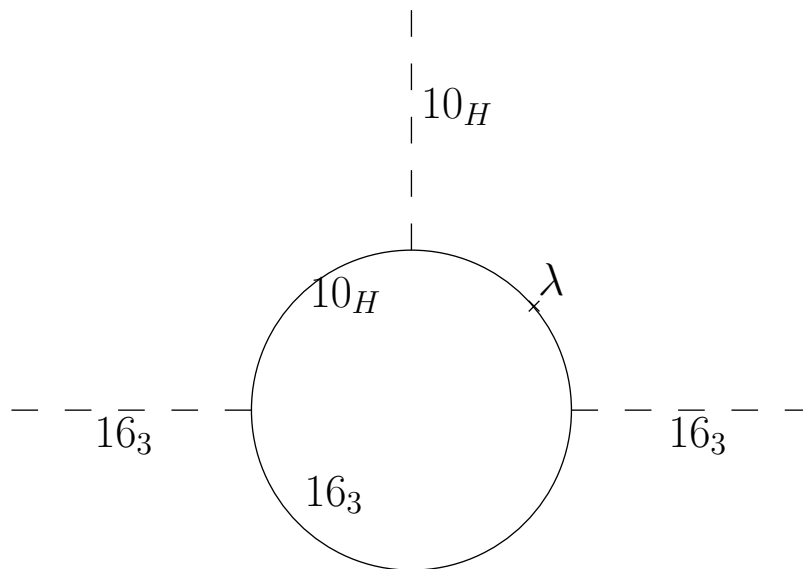


Figure 1.

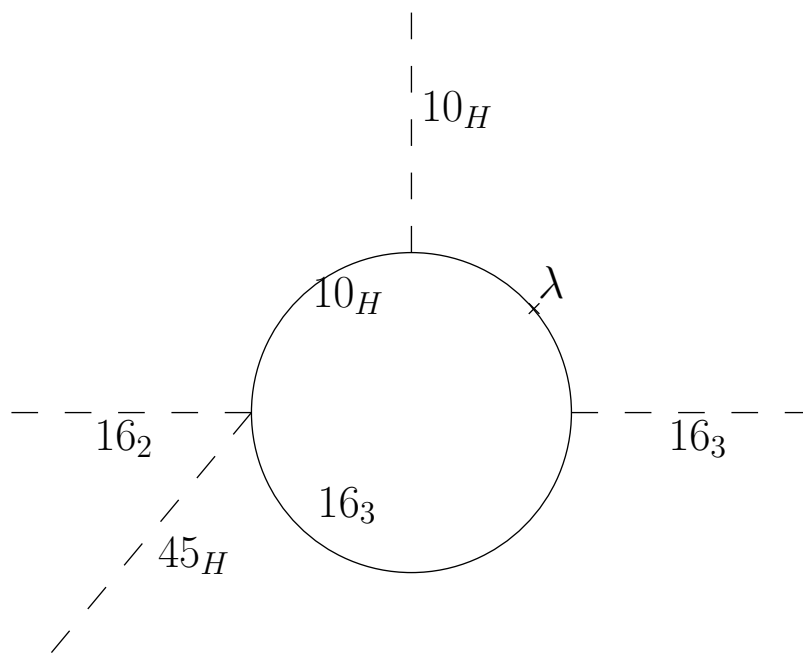


Figure 2.

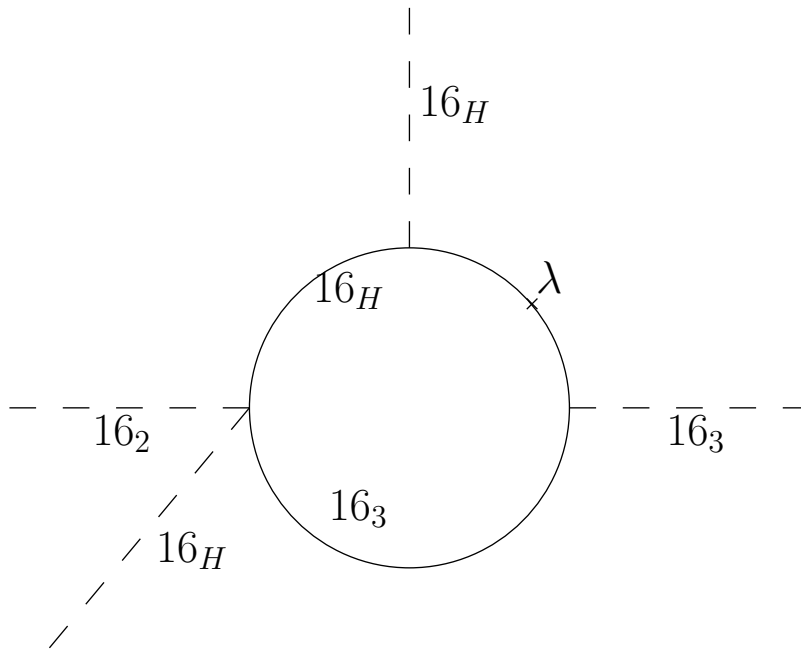


Figure 3.

.3 Appendix: CP Violation in the K Meson system

A general review can be found in Ref. [86].

.3.1 ϵ_K and ΔM_K

Standard Model Contribution

The off-diagonal element M_{12} in the $K^\circ - \overline{K}^\circ$ system is given by
(see Appendix III for definitions and background)

$$2m_K M_{12}^* = \langle \overline{K}^\circ | H_{\text{eff}}(\Delta S = 2) | K^\circ \rangle. \quad (.49)$$

The effective $\Delta S = 2$ Hamiltonian is

$$H_{\text{eff}}^{\Delta S=2} = \frac{G_F^2}{16\pi^2} M_W^2 \left(\lambda_c^2 \eta_1 S_0(x_c) + \lambda_t^2 \eta_2 S_0(x_t) + 2\lambda_c \lambda_t \eta_3 S_0(x_c, x_t) \right) \times (\bar{s}d)_{V-A} (\bar{s}d)_{V-A} + h.c. \quad (.50)$$

The matrix element of $H_{\text{eff}}^{\Delta S=2}$ is obtained from:

$$\langle \bar{K}^\circ | (\bar{s}d)_{V-A} (\bar{s}d)_{V-A} | K^\circ \rangle = \frac{8}{3} \widehat{B}_K f_K^2 m_K^2, \quad (.51)$$

where \widehat{B}_K describes the non-perturbative effects in the hadronic matrix element of the operator $(\bar{s}d)_{V-A} (\bar{s}d)_{V-A}$, $\lambda_c = V_{cs}^* V_{cd}$, $\lambda_t = V_{ts}^* V_{td}$, and the η_i describe the short distance QCD effects, and are numerically given by

$$\eta_1 = 1.38 \pm 0.20, \quad \eta_2 = 0.57 \pm 0.01, \quad \eta_3 = 0.47 \pm 0.04. \quad (.52)$$

The functions $S_0(x_{c,t})$ and $S_0(x_c, x_t)$ are the loop functions defined below, with $x_i = m_i^2/M_W^2$:

$$\begin{aligned} S_0(x_c) &= x_c \\ S_0(x_t) &= \frac{4x_t - 11x_t^2 + x_t^3}{4(1-x_t)^2} - \frac{3x_t^3 \ln x_t}{2(1-x_t)^3} \\ S_0(x_c, x_t) &= x_c \left[\ln \frac{x_t}{x_c} - \frac{3x_t}{4(1-x_t)} - \frac{3x_t^2 \ln x_t}{4(1-x_t)^2} \right] \end{aligned} \quad (.53)$$

Thus, from Eq. (.50),

$$M_{12} = \frac{G_F^2}{12\pi^2} M_W^2 \widehat{B}_K f_K^2 m_K \left(\lambda_c^2 \eta_1 S_0(x_c) + \lambda_t^2 \eta_2 S_0(x_t) + 2\lambda_c \lambda_t \eta_3 S_0(x_c, x_t) \right) \quad (.54)$$

The CP violation in the $K^\circ - \overline{K^\circ}$ mixing is parameterized by ϵ_K

defined as:

$$\epsilon_K = \frac{e^{i\pi/4}}{\sqrt{2}\Delta M_K} (\text{Im}M_{12} + 2\xi \text{Re}M_{12}); \quad \xi = \frac{\text{Im}A_0}{\text{Re}A_0}. \quad (.55)$$

The quantity A_0 is defined in terms of amplitudes of K° -meson decays:

$$\begin{aligned} A(K^\circ \rightarrow \pi^+\pi^-) &= \sqrt{\frac{2}{3}}A_0e^{i\delta^0} + \sqrt{\frac{1}{3}}A_2e^{i\delta^2} \\ A(K^\circ \rightarrow \pi^0\pi^0) &= \sqrt{\frac{2}{3}}A_0e^{i\delta^0} - 2\sqrt{\frac{1}{3}}A_2e^{i\delta^2} \end{aligned} \quad (.56)$$

The parameter ξ is small, therefore

$$\begin{aligned} \epsilon_K &\approx \frac{e^{i\pi/4}}{\sqrt{2}\Delta M_K} \text{Im}M_{12} \\ &= C_\epsilon \widehat{B}_K \text{Im}\lambda_t \left\{ \text{Re}\lambda_c \left[\eta_1 S_0(x_c) - \eta_3 S_0(x_c, x_t) \right] - \text{Re}\lambda_t \eta_2 S_0(x_t) \right\} e^{i\pi/4} \end{aligned} \quad (.57)$$

where

$$C_\epsilon = \frac{G_F^2 f_K^2 M_K M_W^2}{6\sqrt{2}\pi^2 (\Delta m_K)} \approx 3.84 \times 10^4 \quad (.58)$$

For details on $K^\circ - \overline{K^\circ}$ mixing in the standard model, see *e.g.* [86]

SUSY Contribution

The supersymmetric contribution to $K^\circ - \overline{K^\circ}$ mixing is given by

(see [40]):

$$\begin{aligned}
(M_{12})_K^{\text{SUSY}} &= \frac{-\alpha_s^2}{216m_q^2} \frac{1}{3} M_K f_K^2 \left\{ [(\delta_{12}^d)_{LL}^2 + (\delta_{12}^d)_{RR}^2] (24x f_6(x) + 66\tilde{f}_6(x)) \right. \\
&\quad + (\delta_{12}^d)_{LL} (\delta_{12}^d)_{RR} \left[(384 \left(\frac{M_K}{m_s+m_d}\right)^2 + 72) x f_6(x) \right. \\
&\quad \left. \left. + (-24 \left(\frac{M_K}{m_s+m_d}\right)^2 + 36) \tilde{f}_6(x) \right] \right. \\
&\quad + [(\delta_{12}^d)_{LR}^2 + (\delta_{12}^d)_{RL}^2] \left(-132 \left(\frac{M_K}{m_s+m_d}\right)^2 x f_6(x) \right) \\
&\quad \left. + (\delta_{12}^d)_{LR} (\delta_{12}^d)_{RL} \left[-144 \left(\frac{M_K}{m_s+m_d}\right)^2 - 84 \right] \tilde{f}_6(x) \right\} \tag{.59}
\end{aligned}$$

where $x = m_g^2/m_q^2$, and the loop functions $f_6(x)$ and $\tilde{f}_6(x)$ are defined

as:

$$f_6(x) = \frac{6(1+3x)\ln x + x^3 - 9x^2 - 9x + 17}{6(x-1)^5} \tag{.60}$$

$$\tilde{f}_6(x) = \frac{6x(1+x)\ln x - x^3 - 9x^2 + 9x + 1}{3(x-1)^5} \tag{.61}$$

The δ_{ij} in the above equations are defined as $\delta_{LL/RR}^{ij} \equiv (\Delta_{LL/RR}^{ij})/m_{sq}^2$,

where Δ_{LL}^{ij} denotes the $(mass)^2$ parameter for $\tilde{q}_{jL} \rightarrow \tilde{q}_{iL}$ transition in the SUSY basis.

.3.2 ϵ'_K/ϵ_K

The parameter ϵ'_K is defined as

$$\epsilon'_K = \frac{1}{\sqrt{2}} \text{Im} \left(\frac{A_2}{A_0} \right) e^{i\Phi} \quad \text{where} \quad \Phi = \frac{\pi}{2} + \delta_2 - \delta_0 \approx \frac{\pi}{4} \tag{.62}$$

The dimension four Hamiltonian giving rise to the $\bar{s}dZ$ vertex is:

$$H_{\text{eff}}^{d=4} = -\frac{G_F}{\sqrt{2}} \frac{e}{\pi^2} M_Z^2 \tan \theta_W \left(\lambda_t C_0(x_t) + ((\delta_{23}^u)_{LR} (\delta_{13}^d)_{RL}^*) H_0(x) \right) + h.c. \quad (.63)$$

where the first term is the contribution from the standard model, and the second from supersymmetry [93, 94]. The chromo- and electromagnetic dimension 5 operators are:

$$H_{\text{eff}}^{d=5} = \left(C_\gamma^+ Q_\gamma^+ + C_\gamma^- Q_\gamma^- + C_g^+ Q_g^+ + C_g^- Q_g^- \right) + h.c. \quad (.64)$$

where

$$Q_\gamma^\pm = \frac{Q_d e}{16\pi^2} \left(\bar{s}_L \sigma^{\mu\nu} F_{\mu\nu} d_R \pm \bar{s}_R \sigma^{\mu\nu} F_{\mu\nu} d_L \right) \quad (.65)$$

$$Q_g^\pm = \frac{g}{16\pi^2} \left(\bar{s}_L \sigma^{\mu\nu} t^a G_{\mu\nu}^a d_R \pm \bar{s}_R \sigma^{\mu\nu} t^a G_{\mu\nu}^a d_L \right)$$

The Wilson coefficients are given by :

$$C_\gamma^\pm(m_{\tilde{g}}) = \frac{\pi \alpha_s(m_{\tilde{g}})}{m_{\tilde{g}}} \left[(\delta_{21}^d)_{LR} \pm (\delta_{12}^d)_{LR}^* \right] F_0(x) \quad (.66)$$

$$C_g^\pm(m_{\tilde{g}}) = \frac{\pi \alpha_s(m_{\tilde{g}})}{m_{\tilde{g}}} \left[(\delta_{21}^d)_{LR} \pm (\delta_{12}^d)_{LR}^* \right] G_0(x)$$

where the functions are defined as:

$$C_0(x) = \frac{x}{8} \left[\frac{x-6}{x-1} + \frac{3x+2}{(x-1)^2} \ln x \right] \quad (.67)$$

$$H_0(x) = \frac{-x(x^3 - 6x^2 + 3x + 2 + 6x \ln x)}{48(1-x)^4} \quad (.68)$$

$$F_0(x) = \frac{4x(1 + 4x - 5x^2 + 4x \ln x + 2x^2 \ln x)}{3(1-x)^4} \quad (.69)$$

$$G_0(x) = \frac{x(22 - 20x - 2x^2 + 16x \ln x - x^2 \ln x + 9 \ln x)}{3(1-x)^4} \quad (.70)$$

The matrix elements of the chromo- and electro-magnetic operators $Q_{g,\gamma}^\pm$ between the states K° and $\pi\pi$ are:

$$\langle (\pi\pi)_{I=0} | Q_g^- | K^\circ \rangle = \sqrt{\frac{3}{2}} \frac{11}{16\pi^2} \frac{\langle \bar{q}q \rangle}{F_\pi^3} m_\pi^2 B_G \quad (.71)$$

$$\langle \pi^\circ | Q_\gamma^+ | K^\circ \rangle = \frac{Q_d e}{16\pi^2} \frac{i\sqrt{2}}{m_K} P_\pi^\mu P_K^\nu F_{\mu\nu} B_T \quad (.72)$$

$$\langle (\pi\pi)_{I=0} | Q_g^+ | K^\circ \rangle = \langle \pi^\circ | Q_\gamma^- | K^\circ \rangle = 0 \quad (.73)$$

Thus we can write

$$Re\left(\frac{\epsilon'}{\epsilon}\right)_{\text{SUSY}} = \frac{11\sqrt{3}}{64\pi} \frac{\omega}{|\epsilon| Re A_0} \frac{m_\pi^2 m_K^2}{F_\pi(m_s + m_d)} \frac{\alpha_s(m_{\tilde{g}})}{m_{\tilde{g}}} \eta B_G Im \Lambda_g^- \quad (.74)$$

where $\omega = Re A_2 / Re \bar{A}_0$ and Λ_g^- is the effective coupling $\left[(\delta_{21}^d)_{LR} - (\delta_{12}^d)_{LR}^* \right] G_0(x)$.

.4 Appendix: CP Violation in the B Meson system

For a review see Ref. [94].

.4.1 Calculation of $S(B_d \rightarrow \phi K_S)$

The amplitude for $B_d \rightarrow \phi K_S$ in the standard model is given by [90]:

$$A_{\phi K_S}^{\text{SM}} = \frac{G_F}{\sqrt{2}} V_{ts}^* V_{tb} \sum_{i=3}^6 C_i^{\text{SM}} \langle \phi \bar{K}^\circ | O_i | \bar{B}^\circ \rangle + C_g \langle \phi \bar{K}^\circ | O_g | \bar{B}^\circ \rangle + \frac{8}{9} P H. \quad (.75)$$

where the matrix elements of the O_i are:

$$\langle \phi \bar{K}^\circ | O_3 | \bar{B}^\circ \rangle = \frac{H}{3} \quad (.76)$$

$$\langle \phi \bar{K}^\circ | O_4 | \bar{B}^\circ \rangle = \frac{H}{3} \quad (.77)$$

$$\langle \phi \bar{K}^\circ | O_5 | \bar{B}^\circ \rangle = \frac{H}{4} \quad (.78)$$

$$\langle \phi \bar{K}^\circ | O_6 | \bar{B}^\circ \rangle = \frac{H}{12} \quad (.79)$$

$$\langle \phi \bar{K}^\circ | O_g | \bar{B}^\circ \rangle = \frac{4}{9\pi} \alpha_s \kappa H \quad (.80)$$

where $\kappa \approx -1.1$ and $H = 2(\epsilon \cdot p) f_\phi m_\phi F_{B \rightarrow K}^+(m_\phi^2)$, and the Wilson coefficients are $C_3^{\text{SM}} = 0.0114$, $C_4^{\text{SM}} = -0.0321$, $C_5^{\text{SM}} = 0.00925$, $C_6^{\text{SM}} = -0.0383$ and $C_g^{\text{SM}} = -0.188$.

The SUSY amplitude for the process is given below:

$$A_{\phi K_S}^{\text{SUSY}} = \frac{G_F}{\sqrt{2}} V_{ts}^* V_{tb} \sum_{i=3}^6 C_i^{\text{SUSY}} \langle \phi \bar{K}^\circ | O_i | \bar{B}^\circ \rangle + C_g^{\text{SUSY}} \langle \phi \bar{K}^\circ | O_g | \bar{B}^\circ \rangle \quad (.81)$$

$$+(L \leftrightarrow R)$$

The coefficients C_i^{SUSY} are given by:

$$C_3^{\text{SUSY}} = X \left(-\frac{1}{9}B_1(x) - \frac{5}{9}B_2(x) - \frac{1}{18}P_1(x) - \frac{1}{2}P_2(x) \right) \quad (.82)$$

$$C_4^{\text{SUSY}} = X \left(-\frac{7}{3}B_1(x) + \frac{1}{3}B_2(x) + \frac{1}{6}P_1(x) + \frac{3}{2}P_2(x) \right) \quad (.83)$$

$$C_5^{\text{SUSY}} = X \left(\frac{10}{9}B_1(x) + \frac{1}{18}B_2(x) - \frac{1}{18}P_1(x) - \frac{1}{2}P_2(x) \right) \quad (.84)$$

$$C_6^{\text{SUSY}} = X \left(-\frac{2}{3}B_1(x) + \frac{7}{6}B_2(x) + \frac{1}{6}P_1(x) + \frac{3}{2}P_2(x) \right) \quad (.85)$$

$$C_g^{\text{SUSY}} = \frac{\sqrt{2}\alpha_2\pi}{G_F V_{tb} V_{ts}^* m_{\tilde{q}}^2} \left((\delta_{LL}^d)_{23} \left[\frac{1}{3}M_3(x) + 3M_4(x) \right] \right. \\ \left. + (\delta_{LR}^d)_{23} \frac{m_{\tilde{g}}}{m_{\tilde{q}}} \left[\frac{1}{3}M_1(x) + 3M_2(x) \right] \right) \quad (.86)$$

where

$$X \equiv \frac{\sqrt{2}\alpha_s^2}{G_F V_{tb} V_{ts}^* m_{\tilde{q}}^2} (\delta_{LL}^d)_{23} \quad \text{and} \quad x = \frac{m_{\tilde{g}}^2}{m_{\tilde{q}}^2}.$$

The loop functions are given below [40]:

$$B_1(x) = \frac{1 + 4x - 5x^2 + 4x \ln x + 2x^2 \ln x}{8(1-x)^4} \quad (.87)$$

$$B_2(x) = x \frac{5 - 4x - x^2 + 2 \ln x + 4x \ln x}{2(1-x)^4} \quad (.88)$$

$$P_1(x) = \frac{1 - 6x + 18x^2 - 10x^3 - 3x^4 + 12x^3 \ln x}{18(x-1)^5} \quad (.89)$$

$$P_2(x) = \frac{7 - 18x + 9x^2 + 2x^3 + 3 \ln x - 9x^2 \ln x}{9(x-1)^5} \quad (.90)$$

$$M_1(x) = 4B_1(x) \quad (.91)$$

$$M_2(x) = -xB_2(x) \quad (.92)$$

$$M_3(x) = \frac{-1 + 9x + 9x^2 - 17x^3 + 18x^2 \ln x + 6x^3 \ln x}{12(x-1)^5} \quad (.93)$$

$$M_4(x) = \frac{-1 - 9x + 9x^2 + x^3 - 6x \ln x - 6x^2 \ln x}{6(x-1)^5} \quad (.94)$$

.5 Appendix: Renormalization Group Analysis of the CKM

Elements

A set of coupled differential equations, independent of the weak interaction basis, for the running of the CKM elements is derived in this appendix. These can be found in the literature in [106, 107].

The Yukawa coupling matrices for the up, down and the electron

sectors can be diagonalized by the biunitary transformations:

$$\begin{aligned}
U_R^u Y_u U_L^{u\dagger} &= D_u = \text{Diag}[y_u, y_c, y_t] \\
U_R^d Y_d U_L^{d\dagger} &= D_d = \text{Diag}[y_d, y_s, y_b] \\
U_R^e Y_e U_L^{e\dagger} &= D_e = \text{Diag}[y_e, y_\mu, y_\tau]
\end{aligned}
\tag{.95}$$

The CKM matrix is defined in term of the transformation matrices as:

$$V = U_L^u U_L^{d\dagger} \tag{.96}$$

Under a redefinition of the phases of the quarks, all physical observables remain unchanged, but the CKM matrix gets transformed as $V \rightarrow PVQ$ where P and Q are diagonal phase matrices. This rephasing has resulted in various parameterizations of V . However, if one chooses a parametrization of V at a momentum scale μ , then it does not remain of the same form at a different scale μ' . For studying the renormalization of the CKM elements, it is necessary to choose variables that are independent of parametrization. The magnitudes of the CKM elements are basis independent, as well as the quantity $J = \text{Im}(V_{ud}V_{cs}V_{us}^*V_{cd}^*)$, which is a basis independent measure of CP non conservation.

The Yukawa coupling matrices Y_u , Y_d and Y_e , evolve in MSSM according to the following equations:

$$\begin{aligned}
16\pi^2 \frac{dY_u}{dt} &= Y_u [3Y_u^\dagger Y_u + Y_d^\dagger Y_d + 3Tr(Y_u^\dagger Y_u) - G_u] \\
16\pi^2 \frac{dY_d}{dt} &= Y_d [3Y_d^\dagger Y_d + Y_u^\dagger Y_u + Tr(3Y_d^\dagger Y_d + Y_e^\dagger Y_e) - G_d] \quad (.97) \\
16\pi^2 \frac{dY_e}{dt} &= Y_e [3Y_e^\dagger Y_e + Tr(3Y_d^\dagger Y_d + Y_e^\dagger Y_e) - G_e]
\end{aligned}$$

where $t = \ln\left(\frac{\mu}{m_W}\right)$ and

$$\begin{aligned}
G_u &= \frac{13}{15}g_1^2 + 3g_2^2 + \frac{16}{3}g_3^2 \\
G_d &= \frac{7}{15}g_1^2 + 3g_2^2 + \frac{16}{3}g_3^2 \quad (.98) \\
G_e &= \frac{9}{5}g_1^2 + 3g_2^2
\end{aligned}$$

The CKM matrix V is composed of unitary matrices U_L^u and U_L^d , which diagonalize $Y_u^\dagger Y_u$ and $Y_d^\dagger Y_d$ respectively. It may thus be useful to consider the RGEs of $M \equiv Y_u^\dagger Y_u$, $M' \equiv Y_d^\dagger Y_d$, and $M'' \equiv Y_e^\dagger Y_e$ found from the above equations.

$$\begin{aligned}
16\pi^2 \frac{dM}{dt} &= 6M^2 + \{M, M'\} + 2M(3Tr(M) - G_u) \\
16\pi^2 \frac{dM'}{dt} &= 6M'^2 + \{M, M'\} + 2M'(3Tr(M') + Tr(M'') - G_d) \quad (.99) \\
16\pi^2 \frac{dM''}{dt} &= 6M''^2 + 2M''(3Tr(M') + Tr(M'') - G_e)
\end{aligned}$$

Let at momentum scale μ , M and M' be diagonalized by unitary matrices U_L^u and U_L^d respectively. Then the CKM matrix at the scale

μ is $V = U_L^u U_L^{d\dagger}$. As μ is changed the mass matrices are changed to $M + \Delta M$ and $M' + \Delta M'$, which are no longer diagonalized by U_L^u and U_L^d . The resultant change in the diagonal couplings are obtained by:

$$\begin{aligned}
U_L^u \Delta M U_L^{u\dagger} &= \frac{1}{16\pi^2} \left(6D_u^4 + (D_u^2 V D_d^2 V^\dagger + V D_d^2 V^\dagger D_u^2) \right. \\
&\quad \left. + 2D_u^2 (3Tr(M) - G_u) \right) \Delta t \\
U_L^d \Delta M' U_L^{d\dagger} &= \frac{1}{16\pi^2} \left(6D_d^4 + (D_u^2 V D_d^2 V^\dagger + V D_d^2 V^\dagger D_u^2) \right. \\
&\quad \left. + 2D_d^2 (3Tr(M') + Tr(M'') - G_d) \right) \Delta t
\end{aligned} \tag{.100}$$

The variation of the diagonal couplings is then given by:

$$\begin{aligned}
16\pi^2 \frac{dy_i^2}{dt} &= \left(6y_i^4 + 2 \sum_\alpha y_\alpha^2 |V_{i\alpha}|^2 + 2y_i^2 (3Tr(M) - G_u) \right) \\
16\pi^2 \frac{dy_\alpha^2}{dt} &= \left(6y_\alpha^4 + 2 \sum_i y_i^2 |V_{i\alpha}|^2 + 2y_\alpha^2 (3Tr(M') + Tr(M'') - G_d) \right) \tag{.101} \\
16\pi^2 \frac{dy_a^2}{dt} &= \left(6y_a^4 + 2y_a^2 (3Tr(M') + Tr(M'') - G_e) \right)
\end{aligned}$$

where $i = \{u, c, t\}$, $\alpha = \{d, s, b\}$ and $a = \{e, \mu, \tau\}$. The variation of the CKM matrix is obtained by considering the following. Let the matrix $U_L^u (M + \Delta M) U_L^{u\dagger}$ be diagonalized by the unitary matrix $(1 + \epsilon)$ and $U_L^d (M' + \Delta M') U_L^{d\dagger}$ by $(1 + \epsilon')$. Then the variation in the CKM matrix is given by:

$$\Delta V = \epsilon V - V \epsilon' . \tag{.102}$$

Unitarity requires $\epsilon^\dagger = -\epsilon$ and $\epsilon_{ii} = 0$. Using Eqs. (.100) and (.101),

and

$$(1 + \epsilon)(D_u^2 + U_L^u(M + \Delta M)U_L^{u\dagger})(1 - \epsilon) = D_u^2 + \Delta D_u^2 \quad (.103)$$

we can get the elements of the matrices ϵ and ϵ' as:

$$\epsilon_{ij} = \frac{1}{16\pi^2} \left[\frac{y_i^2 + y_j^2}{y_i^2 - y_j^2} \sum_{\alpha} y_{\alpha}^2 V_{i\alpha} V_{j\alpha}^* \right] \Delta t \quad (.104)$$

$$\epsilon'_{ij} = \frac{1}{16\pi^2} \left[\frac{y_{\alpha}^2 + y_{\beta}^2}{y_{\alpha}^2 - y_{\beta}^2} \sum_i y_i^2 V_{i\alpha} V_{i\beta}^* \right] \Delta t$$

Now Eq. (.104) together with Eq. (.102) yields the variation of the CKM elements:

$$16\pi^2 \frac{dV_{i\alpha}}{dt} = \left[\sum_{\beta, j \neq i} \frac{y_i^2 + y_j^2}{y_i^2 - y_j^2} y_{\beta}^2 V_{i\beta} V_{j\beta}^* V_{j\alpha} + \sum_{j, \beta \neq \alpha} \frac{y_{\alpha}^2 + y_{\beta}^2}{y_{\alpha}^2 - y_{\beta}^2} y_j^2 V_{j\beta}^* V_{j\alpha} V_{i\beta} \right] (.105)$$

Choosing basis independent parameters of V to be $X \equiv |V_{ud}|^2$, $Y \equiv |V_{us}|^2$, $Z \equiv |V_{cd}|^2$ and J , the other elements of the CKM matrix can be written as:

$$\begin{aligned} |V_{ub}|^2 &= (1 - X - Y) \\ |V_{cs}|^2 &= \frac{[XYZ + (1 - X - Y)(1 - X - Z) - 2K]}{(1 - X)^2} \\ |V_{cb}|^2 &= \frac{[XZ(1 - X - Y) + Y(1 - X - Z) + 2K]}{(1 - X)^2} \\ |V_{td}|^2 &= (1 - X - Z) \\ |V_{ts}|^2 &= \frac{[XY(1 - X - Z) + Z(1 - X - Y) - 2K]}{(1 - X)^2} \\ |V_{tb}|^2 &= \frac{[X(1 - X - Y)(1 - X - Z) + YZ + 2K]}{(1 - X)^2} \end{aligned} \quad (.106)$$

where $K = [XYZ(1 - X - Y)(1 - X - Z) - J^2(1 - X)^2]^{1/2}$.

The renormalization group evolution of X , Y , Z and K can be obtained from Eq. (.105).

$$\begin{aligned}
16\pi^2 \frac{dX}{dt} = & 2 \left[\frac{y_u^2 + y_c^2}{y_u^2 - y_c^2} \left\{ (y_d^2 - y_b^2)XZ + \frac{(y_b^2 - y_s^2)}{1-X} (XYZ - K) \right\} \right. \\
& + \frac{y_u^2 + y_t^2}{y_u^2 - y_t^2} \left\{ (y_d^2 - y_b^2)X(1 - X - Z) \right. \\
& \quad \left. + \frac{(y_b^2 - y_s^2)}{1-X} (XY(1 - X - Z) + K) \right\} \\
& + \frac{y_d^2 + y_s^2}{y_d^2 - y_s^2} \left\{ (y_u^2 - y_t^2)XY + \frac{(y_t^2 - y_c^2)}{1-X} (XYZ - K) \right\} \\
& + \frac{y_d^2 + y_b^2}{y_d^2 - y_b^2} \left\{ (y_u^2 - y_t^2)X(1 - X - Y) \right. \\
& \quad \left. + \frac{(y_t^2 - y_c^2)}{1-X} (XZ(1 - X - Y) + K) \right\} \left. \right] \tag{.107}
\end{aligned}$$

$$\begin{aligned}
16\pi^2 \frac{dY}{dt} = & 2 \left[\frac{y_u^2 + y_c^2}{y_u^2 - y_c^2} \left\{ \frac{(y_b^2 - y_d^2)}{1-X} (XYZ - K) \right. \right. \\
& \quad \left. + \frac{(y_s^2 - y_b^2)}{(1-X)^2} Y (XYZ + (1 - X - Y)(1 - X - Z) - 2K) \right\} \\
& + \frac{y_u^2 + y_t^2}{y_u^2 - y_t^2} \left\{ \frac{(y_d^2 - y_b^2)}{1-X} (XY(1 - X - Z) + K) \right. \\
& \quad \left. + \frac{(y_s^2 - y_b^2)}{(1-X)^2} Y (XY(1 - X - Z) + Z(1 - X - Y) + 2K) \right\} \\
& + \frac{y_s^2 + y_d^2}{y_s^2 - y_d^2} \left\{ (y_u^2 - y_t^2)XY + \frac{(y_t^2 - y_c^2)}{1-X} (XYZ - K) \right\} \\
& + \frac{y_s^2 + y_b^2}{y_s^2 - y_b^2} \left\{ (y_u^2 - y_t^2)Y(1 - X - Y) + \frac{(y_c^2 - y_t^2)}{(1-X)^2} (XYZ(1 - X - Y) \right. \\
& \quad \left. - Y(1 - X - Y)(1 - X - Z) - K(1 - X - 2Y)) \right\} \left. \right] \tag{.108}
\end{aligned}$$

$$\begin{aligned}
16\pi^2 \frac{dZ}{dt} &= 2 \left[\frac{y_c^2 + y_u^2}{y_c^2 - y_u^2} \left\{ (y_d^2 - y_b^2) XZ + \frac{(y_b^2 - y_s^2)}{1-X} (XYZ - K) \right\} \right. \\
&+ \frac{y_c^2 + y_t^2}{y_c^2 - y_t^2} \left\{ (y_d^2 - y_b^2) Z(1 - X - Z) + \frac{(y_s^2 - y_b^2)}{(1-X)^2} (XYZ(1 - X - Z) \right. \\
&\quad \left. \left. - Z(1 - X - Z)(1 - X - Z) - K(1 - X - 2Z)) \right\} \right. \\
&+ \frac{y_d^2 + y_s^2}{y_d^2 - y_s^2} \left\{ \frac{(y_u^2 - y_t^2)}{1-X} (K - XYZ) \right. \\
&\quad \left. + \frac{(y_c^2 - y_t^2)}{(1-X)^2} Z (XYZ + (1 - X - Y)(1 - X - Z) - 2K) \right\} \\
&+ \frac{y_d^2 + y_b^2}{y_d^2 - y_b^2} \left\{ \frac{(y_t^2 - y_u^2)}{1-X} (XZ(1 - X - Y) + K) \right. \\
&\quad \left. + \frac{(y_c^2 - y_t^2)}{(1-X)^2} Z (XZ(1 - X - Y) + Y(1 - X - Z) + 2K) \right\} \quad (.109)
\end{aligned}$$

$$\begin{aligned}
16\pi^2 \frac{dJ}{dt} &= -\frac{1}{2} J \left[\sum_{\alpha, j \neq i} \frac{y_i^2 + y_j^2}{y_i^2 - y_j^2} y_\alpha^2 (|V_{i\alpha}|^2 - |V_{j\alpha}|^2) \right. \\
&\quad \left. + \sum_{i, \alpha \neq \beta} \frac{y_\alpha^2 + y_\beta^2}{y_\alpha^2 - y_\beta^2} y_i^2 (|V_{i\alpha}|^2 - |V_{i\beta}|^2) \right] \quad (.110)
\end{aligned}$$

Equations (.107–.110) form a set of coupled differential equations for the evolution of the basis independent parameters of the CKM matrix. The evolution of the other elements of the CKM matrix can be obtained using the equations in (.106).

6. LEPTON FLAVOR VIOLATION WITHIN A REALISTIC SO(10)/G(224) FRAMEWORK

6.1 Introduction

Individual lepton numbers (L_e , L_μ and L_τ) being symmetries of the standard model (SM)(with $m_\nu^i = 0$), processes like $\mu \rightarrow e\gamma$, $\tau \rightarrow \mu\gamma$ and $\tau \rightarrow e\gamma$ are forbidden within this model. Even within simple extensions of the SM (that permit $m_\nu^i \neq 0$), they are too strongly suppressed to be observable. Experimental searches have put upper limits on the branching ratios of these processes: $\text{Br}(\mu \rightarrow e\gamma) \leq 1.2 \times 10^{-11}$ [108], $\text{Br}(\tau \rightarrow \mu\gamma) \leq 6.8 \times 10^{-8}$ [109] and $\text{Br}(\tau \rightarrow e\gamma) \leq 1.1 \times 10^{-7}$ [110]. The extreme smallness of these branching ratios poses a challenge for physics beyond the standard model, especially for supersymmetric grand unified (SUSY GUT) models, as these generically possess new sources of lepton flavor violation that could easily lead to rates even surpassing the current limits.

In this chapter, we study how lepton flavor violation (LFV) gets linked with fermion masses, neutrino oscillations and CP violation within a predictive SUSY grand unified framework, based on either SO(10) [18], or an effective (presumably string derived) symmetry $G(224) = SU(2)_L \times SU(2)_R \times SU(4)^c$ [12]. The desirability of having an effective symmetry as above that possesses SU(4)-color [12], has been stressed in Chapter 2.

A predictive framework based on supersymmetric SO(10) or G(224)-symmetry has been proposed by Babu, Pati and Wilczek (BPW) in [25], which successfully describes the masses and mixings of all fermions including neutrinos. In particular it makes seven predictions, all in good accord with observations. This framework was extended to describe the observed CP and flavor violations by allowing for phases in the fermion mass matrices [28] (see Chapter 5). Remarkably enough, this extension could successfully describe the masses of all the quarks and leptons (especially of the two heavier families), the CKM elements, the observed CP and flavor violations in the $K^\circ - \overline{K}^\circ$ system (yielding correctly Δm_K and ϵ_K) and the $B_d^\circ - \overline{B}_d^\circ$ system (yield-

ing the correct values of Δm_{B_d} and $S_{\psi K_S}$).

In this chapter, based on the work done with Babu and Pati [29], I consider lepton flavor violating processes, i.e. $\mu \rightarrow e\gamma$, $\tau \rightarrow \mu\gamma$, $\tau \rightarrow e\gamma$ and $\mu N \rightarrow eN$ within the BPW framework as extended in Chapter 5. The subject of LFV has been discussed widely in the literature within supersymmetric extensions of the standard model. (For earlier works see Ref. [26, 27, 111]). Our work based on SUSY SO(10) or G(224) differs from those based on either MSSM with right-handed neutrinos (RHN's) [27, 111, 112] or SUSY SU(5) [113], because for these latter cases the RHN's are singlets and thereby their Yukawa couplings are *a priori* arbitrary. By contrast, for G(224) or SO(10) the corresponding Yukawa couplings are determined in terms of those of the quarks at the GUT-scale (such as $h(\nu^\tau)_{Dirac} \approx h_{top}$) (see Ref. [25]). Thus the SUSY G(224)/SO(10)-framework is naturally more predictive than the MSSM or SUSY SU(5)-framework.

In addition, our work differs from all others, including those based on SUSY SO(10) [114] as well, in two other important respects: First, we work within a predictive and realistic framework [25, 28] which (as

mentioned above) successfully describes a set of phenomena – i.e. (a) fermion masses, (b) CKM mixings, (c) neutrino oscillations, (d) observed CP and flavor violations in the K and B systems, as well as (e) baryogenesis via leptogenesis [62]. As we will see, lepton flavor violation emerges as an important prediction of this framework, bringing no new parameters (barring the few flavor-universal SUSY-parameters).

Second, we do a comprehensive study of LFV processes by including contributions from three different sources: (i) the sfermion mass-insertions, $\hat{\delta}_{LL,RR}^{ij}$, arising from renormalization group (RG) running from M^* to $M_{GUT} \sim 2 \times 10^{16}$ GeV (where M^* denotes the presumed messenger-scale, with $M_{GUT} < M^* \leq M_{string}$, at which flavor-universal soft SUSY breaking is transmitted to the squarks and sleptons, like in a mSUGRA model [46]), (ii) the mass-insertions $(\delta_{LL}^{ij})^{RHN}$ arising from RG running from M_{GUT} to the right handed neutrino mass scales M_{R_i} , and (iii) the chirality-flipping mass-insertions $\delta_{LR,RL}^{ij}$ arising from A -terms that are induced solely through RG running from M^* to M_{GUT} involving gauginos in the loop. All the three types of mass-insertions: $\hat{\delta}_{LL,RR}^{ij}$, $(\delta_{LL}^{ij})^{RHN}$ and $\delta_{LR,RL}^{ij}$ are in fact fully deter-

mined in our model. (See Chapter 5 for details). Most previous works in this regard have included only the second contribution associated with the RH neutrinos in their analysis.¹ We find, however, that it is the first and the third contributions associated with post-GUT physics that typically dominate over the second in a SUSY unified framework.

The BPW framework and its extension were reviewed in Chapters 4 and 5 respectively. Some CP violating processes were studied within this framework in Chapter 5. Here we will present only the structure of the mass matrices of the framework and a fit to the parameters, which we will use to study lepton flavor violation.

6.2 Lepton Flavor Violation in the $SO(10)/G(224)$ Framework

The Dirac mass matrices of the sectors u, d, l and ν proposed in Ref. [25] in the context of $SO(10)$ or $G(224)$ -symmetry have the following structure:

¹ Barbieri, Hall and Strumia (in Ref. [26]) have discussed the relevance of the contributions from the mass-insertions $\hat{\delta}_{LL,RR}^{ij}$ and those from the induced A -terms, but without a realistic framework for light fermion masses and neutrino oscillations.

$$\begin{aligned}
M_u &= \begin{bmatrix} 0 & \epsilon' & 0 \\ -\epsilon' & \zeta_{22}^u & \sigma + \epsilon \\ 0 & \sigma - \epsilon & 1 \end{bmatrix} \mathcal{M}_u^0; & M_d &= \begin{bmatrix} 0 & \eta' + \epsilon' & 0 \\ \eta' - \epsilon' & \zeta_{22}^d & \eta + \epsilon \\ 0 & \eta - \epsilon & 1 \end{bmatrix} \mathcal{M}_d^0 \\
M_\nu^D &= \begin{bmatrix} 0 & -3\epsilon' & 0 \\ 3\epsilon' & \zeta_{22}^u & \sigma - 3\epsilon \\ 0 & \sigma + 3\epsilon & 1 \end{bmatrix} \mathcal{M}_u^0; & M_l &= \begin{bmatrix} 0 & \eta' - 3\epsilon' & 0 \\ \eta' + 3\epsilon' & \zeta_{22}^d & \eta - 3\epsilon \\ 0 & \eta + 3\epsilon & 1 \end{bmatrix} \mathcal{M}_d^0
\end{aligned} \tag{6.1}$$

These matrices are defined in the gauge basis and are multiplied by $\bar{\Psi}_L$ on left and Ψ_R on right.

In the BPW model of Ref. [25], the parameters σ, η, ϵ *etc.* were chosen to be real. To allow for CP violation, this framework was extended to include phases for the parameters in Ref. [28]. Remarkably enough, it was found that there exists a class of fits within the SO(10)/G(224) framework, which correctly describes not only (a) fermion masses, (b) CKM mixings and (c) neutrino oscillations [25,62], but also (d) the observed CP and flavor violations in the K and B systems (see Chapter 5 for the predictions in this regard). A repre-

representative of this class of fits (to be called fit A) is given by [28]:

$$\begin{aligned} \sigma &= 0.109 - 0.012i, & \eta &= 0.122 - 0.0464i, & \epsilon &= -0.103, \\ \eta' &= 2.4 \times 10^{-3}, & \epsilon' &= 2.35 \times 10^{-4} e^{i(69^\circ)}, & \zeta_{22}^d &= 9.8 \times 10^{-3} e^{-i(149^\circ)}, \end{aligned} \quad (6.2)$$

$$(\mathcal{M}_u^0, \mathcal{M}_d^0) \approx (100, 1.1) \text{ GeV}.$$

In this particular fit ζ_{22}^u is set to zero for the sake of economy in parameters. However, allowing for $\zeta_{22}^u \lesssim (1/3)(\zeta_{22}^d)$ (see e.g. Fit B in Chapter 5) would still yield the desired results. Because of the success of this class of fits in describing correctly all four features (a), (b), (c) and (d)-which is a non-trivial feature by itself - we will use fit A as a representative to obtain the mass-insertion parameters $\hat{\delta}_{LL,RR}^{ij}$, $(\delta_{LL}^{ij})^{RHN}$ and $\delta_{LR,RL}^{ij}$ in the lepton sector and thereby the predictions of our model for lepton flavor violation.

The fermion mass matrices M_u , M_d and M_l are diagonalized at the GUT scale $\approx 2 \times 10^{16}$ GeV by bi-unitary transformations (details can be found in the appendices):

$$M_{u,d,l}^{diag} = X_L^{(u,d,l)\dagger} M_{u,d,l} X_R^{(u,d,l)} \quad (6.3)$$

The analytic expressions for the matrices $X_{L,R}^d$ can be found in Chapter 5 and the appendices. The corresponding expressions for $X_{L,R}^l$ can

be obtained by letting $(\epsilon, \epsilon') \rightarrow -3(\epsilon, \epsilon')$.

We now discuss the sources of lepton flavor violation in our model.

We assume that flavor-universal soft SUSY-breaking is transmitted to the SM-sector at a messenger scale M^* , where $M_{GUT} < M^* \leq M_{string}$. This may naturally be realized e.g. in models of mSUGRA [46], or gaugino-mediation [54]. With the assumption of extreme universality as in CMSSM, supersymmetry introduces five parameters at the scale M^* :

$$m_o, m_{1/2}, A_o, \tan \beta \text{ and } \text{sgn}(\mu).$$

For most purposes, we will adopt this restricted version of SUSY breaking with the added restriction that $A_o = 0$ at M^* [54]. However, we will not insist on strict Higgs-squark-slepton mass universality. Even though we have flavor preservation at M^* , flavor violating scalar (mass)²-transitions arise in the model through RG running from M^* to the EW scale. As described below, we thereby have *three sources* of lepton flavor violation.

(1) RG Running of Scalar Masses from M^* to M_{GUT} .

With family universality at the scale M^* , all sleptons have the

mass m_o at this scale and the scalar (mass)² matrices are diagonal. Due to flavor dependent Yukawa couplings, with $h_t = h_b = h_\tau (= h_{33})$ being the largest, RG running from M^* to M_{GUT} renders the third family lighter than the first two (see e.g. [26]) by the amount:

$$\Delta \hat{m}_{\tilde{b}_L}^2 = \Delta \hat{m}_{\tilde{b}_R}^2 = \Delta \hat{m}_{\tilde{\tau}_L}^2 = \Delta \hat{m}_{\tilde{\tau}_R}^2 \equiv \Delta \approx -\left(\frac{30m_o^2}{16\pi^2}\right)h_t^2 \ln(M^*/M_{\text{GUT}}) \quad (6.4)$$

The factor $30 \rightarrow 12$ for the case of $G(224)$. The slepton (mass)² matrix thus has the form $\tilde{M}_i^{(o)} = \text{diag}(m_o^2, m_o^2, m_o^2 - \Delta)$. As mentioned earlier, the spin-1/2 lepton mass matrix is diagonalized at the GUT scale by the matrices $X_{L,R}^l$. Applying the same transformation to the slepton (mass)² matrix (which is defined in the gauge basis), i.e. by evaluating $X_L^{l\dagger}(\tilde{M}_i^{(o)})_{LL} X_L$ and similarly for $L \rightarrow R$, the transformed slepton (mass)² matrix is no longer diagonal. The presence of these off-diagonal elements (at the GUT-scale) given by:

$$(\hat{\delta}_{LL,RR}^l)_{ij} = \left(X_{L,R}^{l\dagger}(\tilde{M}_i^{(o)})X_{L,R} \right)_{ij} / m_i^2 \quad (6.5)$$

induces flavor violating transitions $\tilde{l}_{L,R}^i \rightarrow \tilde{l}_{L,R}^j$. Here m_i denotes an average slepton mass and the hat signifies GUT-scale values.

(2) RG Running of the A -parameters from M^* to M_{GUT} .

Even if $A_o = 0$ at the scale M^* (as we assume for concreteness, see also [54]). RG running from M^* to M_{GUT} induces A -parameters at M_{GUT} , involving the $\text{SO}(10)/\text{G}(224)$ gauginos; these yield chirality flipping transitions ($\tilde{l}_{L,R}^i \rightarrow \tilde{l}_{R,L}^j$).

Evaluated at the GUT scale, the A -parameters, induced respectively through the couplings h_{ij} , a_{ij} and g_{ij} , are given by (see Appendix .2 of Chapter 5):

$$\begin{aligned}
A_{ij}^{(1)} &= \frac{63}{2} \frac{1}{8\pi^2} h_{ij} g_{10}^2 M_\lambda \ln\left(\frac{M^*}{M_{10\mathbf{H}}}\right) & (i, j = 2, 3) \\
A_{ij}^{(2)} &= \frac{95}{2} \frac{1}{8\pi^2} \frac{a_{ij} \langle \mathbf{45}_{\mathbf{H}} \rangle}{M'} g_{10}^2 M_\lambda \ln\left(\frac{M^*}{M_{10\mathbf{H}}}\right) & (ij = 23, 12) \\
A_{ij}^{(3)} &= \frac{90}{2} \frac{1}{8\pi^2} \frac{g_{ij} \langle \mathbf{10}_{\mathbf{H}} \rangle}{M''} g_{10}^2 M_\lambda \ln\left(\frac{M^*}{M_{16\mathbf{H}}}\right) & (ij = 23, 22, 12)
\end{aligned} \tag{6.6}$$

The coefficients $(\frac{63}{2}, \frac{95}{2}, \frac{90}{2})$ are the sums of the Casimirs of the $\text{SO}(10)$ representations of the chiral superfields involved in the diagrams. For the case of $\text{G}(224)$, $(\frac{63}{2}, \frac{95}{2}, \frac{90}{2}) \rightarrow (\frac{27}{2}, \frac{43}{2}, \frac{42}{2})$. Thus, summing $A^{(1)}$, $A^{(2)}$ and $A^{(3)}$, the induced A matrix for the leptons is given

by:

$$A_{LR}^l = Z \left\{ K_{10} \begin{bmatrix} 0 & -285\epsilon' & 0 \\ 285\epsilon' & 63\zeta_{22}^u & -285\epsilon + 63\sigma \\ 0 & 285\epsilon + 63\sigma & 63 \end{bmatrix} \right. \quad (6.7)$$

$$+ Z \left\{ K_{16} \begin{bmatrix} 0 & 90\eta' & 0 \\ 90\eta' & 90(\zeta_{22}^d - \zeta_{22}^u) & 90(\eta - \sigma) \\ 0 & 90(\eta - \sigma) & 0 \end{bmatrix} \right\}$$

where $Z = (\frac{1}{16\pi^2})h_t g_{10}^2 M_\lambda$, $K_{10} = \ln(\frac{M^*}{M_{10H}})$ and $K_{16} = \ln(\frac{M^*}{M_{16H}})$. For simplicity if we let $M_{16H} \approx M_{10H} \approx M_{GUT}$, we can write the A matrix in the SUSY basis as:

$$A_{LR}^l = (X_L^l)^\dagger \begin{bmatrix} 0 & -285\epsilon' + 90\eta' & 0 \\ 285\epsilon' + 90\eta' & 90\zeta_{22}^d - 27\zeta_{22}^u & -285\epsilon + 90\eta - 27\sigma \\ 0 & 285\epsilon + 90\eta - 27\sigma & 63 \end{bmatrix} X_R^l$$

$$\times Z \ln\left(\frac{M^*}{M_{GUT}}\right) \quad (6.8)$$

Approximate analytic forms for $X_{L,R}^d$ are given in Chapter 5, and $X_{L,R}^l$ can be obtained from $X_{L,R}^d$ by the substitutions $(\epsilon, \epsilon') \rightarrow -3(\epsilon, \epsilon')$.

The chirality flipping transition angles are defined as :

$$(\delta_{LR}^l)_{ij} \equiv (A_{LR}^l)_{ij} \left(\frac{v_d}{m_{\tilde{l}}^2}\right) = (A_{LR}^l)_{ij} \left(\frac{v_u}{\tan\beta m_{\tilde{l}}^2}\right). \quad (6.9)$$

(3) RG Running of scalar masses from M_{GUT} to the RH neutrino mass scales:

We work in a basis in which the charged lepton Yukawa matrix Y_l and M_R^ν are diagonal at the GUT scale. The off-diagonal elements in the Dirac neutrino mass matrix Y_N in this basis give rise to lepton flavor violating off-diagonal components in the left handed slepton mass matrix through the RG running of the scalar masses from M_{GUT} to the RH neutrino mass scales M_{R_i} . The RH neutrinos decouple below M_{R_i} . (For RGEs for MSSM with RH neutrinos see e.g. Refs. [111] and [115].) In the leading log approximation, the off-diagonal elements in the left-handed slepton (mass)²-matrix, thus arising, are given by:

$$(\delta_{LL}^l)_{ij}^{RHN} = \frac{-(3m_o^2 + A_o^2)}{8\pi^2} \sum_{k=1}^3 (Y_N)_{ik} (Y_N^*)_{jk} \ln\left(\frac{M_{\text{GUT}}}{M_{R_k}}\right). \quad (6.10)$$

The superscript RHN denotes the contribution due to the presence of the RH neutrinos. We remind the reader that the masses M_{R_i} of RH neutrinos are well determined within our framework to within factors of 2 to 4 (see Chapter 4). The total LL contribution is thus:

$$(\delta_{LL}^l)_{ij}^{Tot} = (\hat{\delta}_{LL}^l)_{ij} + (\delta_{LL}^l)_{ij}^{RHN} \quad (6.11)$$

Now, most authors including those using SUSY SU(5) with RHN's

or SUSY SO(10) [113,114] have considered only the second term $(\delta_{LL}^l)^{RHN}$ that arises due to the right-handed neutrinos. As mentioned in the introduction, however, the first term $\hat{\delta}_{LL}^l$ and the contribution of the A -term $\delta_{LR,RL}^l$ (Eq. (6.9)) are found to dominate over the second term (as long as $\ln(M^*/M_{GUT}) \sim 1$). We obtain our results by including the contributions from all three sources listed above in Eqs. (6.5), (6.9) and (6.10). They are presented in the following section.

6.3 Results

The decay rates for the lepton flavor violating processes $l_i \rightarrow l_j \gamma$ ($i > j$) are given by (see Appendix .1):

$$\Gamma(l_i^+ \rightarrow l_j^+ \gamma) = \frac{e^2 m_{l_i}^3}{16\pi} \left(|A_L^{ji}|^2 + |A_R^{ji}|^2 \right) \quad (6.12)$$

Here A_L^{ji} is the amplitude for $(l_i)_L^+ \rightarrow (l_j)_L^+ \gamma$ decay, while $A_R^{ji} = A((l_i)_R^+ \rightarrow (l_j)_R^+ \gamma)$. The amplitudes $A_{L,R}^{ji}$ are evaluated in the mass insertion approximation using the $(\delta_{LL}^l)^{Tot}$, δ_{RR}^l , $\delta_{LR,RL}^l$ calculated as above. The general expressions for the amplitudes $A_{L,R}^{ji}$ in one loop can be found in e.g. Refs. [111] and [115]. We include the contributions from both chargino and neutralino loops with or without the

μ -term.

We evaluate the amplitudes by first going to a basis in which the chargino and the neutralino mass matrices are diagonal. Analytic expressions for this diagonalization can be obtained in the approximation $|M_2 \pm \mu|$ and $|\frac{5}{3}M_1 \pm \mu| \gg m_Z$ and $|M_2\mu| > m_W^2 \sin 2\beta$ [116]. This approximation holds for all the input values of $(m_o, m_{1/2})$ that we consider.

In Table 1 as well as in Fig. 1, we give the branching ratios of the processes $\mu \rightarrow e\gamma$, $\tau \rightarrow \mu\gamma$, $\tau \rightarrow e\gamma$ for the case of SO(10), with some sample choices of $(m_o, m_{1/2})$. For these calculations we set $\ln\left(\frac{M^*}{M_{GUT}}\right) = 1$, i.e. $M^* \approx 3M_{GUT}$, $\tan\beta = 10$, $M_{R_1} = 10^{10}$ GeV, $M_{R_2} = 10^{12}$ GeV and $M_{R_3} = 5 \times 10^{14}$ GeV (see chapter 4), and $A_o(\text{ at } M^*) = 0$. The corresponding values for G(224) are smaller approximately by a factor of 4 to 6 in the rate, provided $\ln(M^*/M_{GUT})$ is the same in both cases (see comments below Eqs. (6.4) and (6.6)).

$(m_o, m_{1/2})//\tan\beta$	$\text{Br}(\mu \rightarrow e\gamma)$		$\text{Br}(\tau \rightarrow \mu\gamma)$		$\text{Br}(\tau \rightarrow e\gamma)$	
	$\mu > 0$	$\mu < 0$	$\mu > 0$	$\mu < 0$	$\mu > 0$	$\mu < 0$
I (600, 300)//10	3.3×10^{-12}	9.8×10^{-12}	2.4×10^{-9}	3.1×10^{-9}	2.4×10^{-12}	3.3×10^{-12}
II (800, 250)//10	2.9×10^{-13}	1.7×10^{-12}	1.9×10^{-9}	1.9×10^{-9}	2.0×10^{-12}	2.0×10^{-12}
III (450, 300)//10	2.7×10^{-11}	4.6×10^{-11}	2.7×10^{-9}	5.6×10^{-9}	2.7×10^{-12}	6.1×10^{-12}
IV (500, 250)//10	5.9×10^{-12}	1.9×10^{-11}	4.8×10^{-9}	6.4×10^{-9}	5.0×10^{-12}	6.9×10^{-12}
V (100, 440)//10	1.02×10^{-8}	1.02×10^{-8}	8.3×10^{-8}	8.4×10^{-8}	1.0×10^{-10}	1.0×10^{-10}
VI (1000, 250)//10	1.6×10^{-13}	5.6×10^{-12}	9.5×10^{-10}	9.0×10^{-10}	1.0×10^{-12}	9.5×10^{-13}
VII (400, 300)//20	9.5×10^{-12}	3.8×10^{-11}	1.4×10^{-8}	1.8×10^{-8}	1.5×10^{-11}	1.9×10^{-11}

Tab. 6.1:

Table 1. Branching ratios of $l_i \rightarrow l_j \gamma$ for the SO(10) framework with $\kappa \equiv \ln(M^*/M_{GUT}) = 1$; $(m_o, m_{1/2})$ are given in GeV, which determine μ through radiative electroweak symmetry breaking conditions. The entries for $\text{Br}(\mu \rightarrow e \gamma)$ for the case of G(224) would be reduced by a factor $\approx 4 - 6$ compared to that of SO(10) (see text).

To give the reader an idea of the magnitudes of the various contributions, we exhibit in table 2 the amplitudes for the process $\mu \rightarrow e \gamma$ calculated individually from the four sources $\hat{\delta}_{LL}^{ji}$, $\delta_{LR,RL}^{ji}$ and $(\delta_{LL}^{ji})^{RHN}$ (see Eqs. (6.5), (6.9) and (6.10)), for a few cases of table 1.

$(m_o, m_{1/2})(\text{GeV})$	$A_L^{(1)}(\hat{\delta}_{LL})$	$A_L^{(2)}(\delta_{LR})$	$A_R(\delta_{RL})$	$A_L^{(3)}((\delta_{LL})^{RHN})$
I, (600, 300)	3.3×10^{-13}	-6.7×10^{-13}	-5.9×10^{-13}	2.4×10^{-14}
II, (800, 250)	2.9×10^{-13}	-1.8×10^{-13}	-1.6×10^{-13}	2.0×10^{-14}
IV, (500, 250)	4.8×10^{-13}	-9.7×10^{-13}	-8.5×10^{-13}	3.4×10^{-14}

Tab. 6.2:

Table 2. Comparison of the various contributions to the amplitude for $\mu \rightarrow e\gamma$ for cases I, II and IV, with $\mu > 0$. Each entry should be multiplied by a common factor a_o . Imaginary parts being small are not shown. Note that columns 2,3 and 4 arising from RG running from $M^* \rightarrow M_{GUT}$ (see text) dominate over the RHN contribution.

Glancing at tables 1 and 2, the following features of our results are worth noting:

(1) It is apparent from table 2 that the contribution due to the presence of the RH neutrinos² (fifth column) is about an order of magnitude smaller, *in the amplitude*, than those of the others (proportional to $\hat{\delta}_{LL}^{ij}$, δ_{LR}^{ij} and δ_{RL}^{ij}), listed in columns 2, 3 and 4. The latter arise from RG running of the scalar masses and the A -parameters in

² In the context of contributions due to the RH neutrinos alone, there exists an important distinction (partially observed by Barr, see Ref. [114]) between the hierarchical BPW form [25] and the lop-sided Albright-Barr (AB) form [30] of the mass-matrices. The amplitude for $\mu \rightarrow e\gamma$ from this source turns out to be proportional to the difference between the (23)-elements of the Dirac mass-matrices of the charged leptons and the neutrinos, with (33)-element being 1. This difference is (see Eq. (6.1)) is $\eta - \sigma \approx 0.041$, *which is naturally small for the hierarchical BPW model* (incidentally it is also V_{cb}), while it is order one for the lop-sided AB model. This means that the rate for $\mu \rightarrow e\gamma$ due to RH neutrinos would be about 600 times larger in the AB model than the BPW model (for the same input SUSY parameters). A comparison of the BPW and the AB models based on their predictions regarding CP and flavor violations is presented in Chapter 7.

the context of SO(10) or G(224) from M^* to M_{GUT} . It seems to us that the latter, which have commonly been omitted in the literature, should exist in any SUSY GUT model for which the messenger scale for SUSY-breaking is high ($M^* > M_{GUT}$), as in a mSUGRA model.

*The inclusion of these new contributions to LFV processes arising from post-GUT physics, that too in the context of a predictive and realistic framework, is the distinguishing feature of the present work.*³

(2) Again from table 2 we see that the two dominant contributions to $A_L = A(\mu_L^+ \rightarrow e^+\gamma)$, arising from δ_{LL} and δ_{LR} -insertions, partially cancel each other if $\mu > 0$; they would however add if $\mu < 0$. By contrast, A_R gets contribution dominantly only from δ_{RL} (column 4).⁴ As a result we find that in our model, typically, $|A_R| > |A_L|$ if $\mu > 0$ and $|A_L| > |A_R|$ if $\mu < 0$.

(3) Owing to the general prominence of the new contributions from

³ For the sake of comparison, should one drop the post-GUT contribution by setting $M^* = M_{GUT}$, however, the predicted $Br(\mu \rightarrow e\gamma)$ would be reduced in our model to e.g. (4.2, 2.9, and 8.6) $\times 10^{-15}$ for cases I, II and IV respectively.

⁴ Although $\hat{\delta}_{RR}$ is comparable to $\hat{\delta}_{LL}$, its contribution to A_R (via the bino loop) is typically suppressed compared to that of δ_{LL} to A_L (in part by the factor $(\alpha_1/\alpha_2)(M_1/M_2)$) in most of the parameter space.

post-GUT physics, we see from table 1 that case V, (with low m_o and high $m_{1/2}$) is clearly excluded by the empirical limit on $\mu \rightarrow e\gamma$ -rate (see Sec. 1). Case III is also excluded, for the case of SO(10), yielding a rate that exceeds the limit by a factor of about 2 (for $\kappa = \ln(M^*/M_{GUT}) \gtrsim 1$), though we note that for the case of G(224), Case III is still perfectly compatible with the observed limit (see remark below table 1). All the other cases (I, II, IV, VI, and VII), with medium heavy (~ 500 GeV) to moderately heavy sleptons (800-1000 GeV), are compatible with the empirical limit, even for the case of SO(10). The interesting point about these predictions of our model, however, is that $\mu \rightarrow e\gamma$ should be discovered, even with moderately heavy sleptons, both for SO(10) and G(224), with improvement in the current limit by a factor of 10–100. Such an improvement is being planned at the forthcoming MEG experiment at PSI.

(4) We see from table 1 that $\tau \rightarrow \mu\gamma$ (leaving aside case V, which is excluded by the limit on $\mu \rightarrow e\gamma$), is expected to have a branching ratio in the range of 2×10^{-8} (Case VII) to about $(1 \text{ or } 2) \times 10^{-9}$ (Case VI or II). The former may be probed at BABAR and BELLE, while

the latter can be reached at the LHC or a super B factory. The process $\tau \rightarrow e\gamma$ would, however, be inaccessible in the foreseeable future (in the context of our model).

(5) The WMAP-Constraint: Of the cases exhibited in table 1, Case V ($m_o = 100$ GeV, $m_{1/2} = 440$ GeV) would be compatible with the WMAP-constraint on relic dark matter density, in the context of CMSSM, assuming that the lightest neutralino is the LSP and represents cold dark matter (CDM), accompanying co-annihilation mechanism. (See e.g. [88]). As mentioned above (see table 1), a spectrum like Case V, with low m_o and higher $m_{1/2}$, is however excluded in our model by the empirical limit on $\mu \rightarrow e\gamma$. *Thus we infer that in the context of our model CDM cannot be associated with the co-annihilation mechanism.*

Several authors (see e.g. Refs. [117] and [118]), have, however considered the possibility that Higgs-squark-slepton mass universality need not hold even if family universality does. In the context of such non-universal Higgs mass (NUHM) models, the authors of Ref. [118] show that agreement with the WMAP data can be obtained over a

wide range of mSUGRA parameters. In particular, such agreement is obtained for (m_ϕ/m_o) of order unity (with either sign) for almost all the cases (I, II, III, IV, VI and VII)⁵, with the LSP (neutralino) representing CDM.⁶ (Here $m_\phi \equiv \text{sign}(m_{H_{u,d}}^2)\sqrt{|m_{H_{u,d}}^2|}$, see [118]). All these cases (including Case III for G(224)) are of course compatible with the limit on $\mu \rightarrow e\gamma$.

(6) Coherent $\mu - e$ conversion in nuclei: In our framework, $\mu - e$ conversion (i.e. $\mu^- + N \rightarrow e^- + N$) will occur when the photon emitted in the virtual decay $\mu \rightarrow e\gamma^*$ is absorbed by the nucleus (see e.g. [119]). In such situations, there is a rather simple relation connecting the $\mu - e$ conversion rate with $B(\mu \rightarrow e\gamma)$: $B(\mu \rightarrow e\gamma)/(\omega_{\text{conversion}}/\omega_{\text{capture}}) = R \simeq (230 - 400)$, depending on the nucleus. For example, R has been calculated to be $R \simeq 389$ for ^{27}Al , 238 for ^{48}Ti and 342 for ^{208}Pb in this type of models. (These numbers were computed in [119] for the specific model of [26], but they should approximately hold for our model as well.) With the branching ratios listed in Table 1 ($\sim 10^{-11}$ to

⁵ We thank A. Mustafayev and H. Baer for private communications in this regard.

⁶ We mention in passing that there may also be other possibilities for the CDM if we allow for either non-universal gaugino masses, or axino or gravitino as the LSP, or R-parity violation (with e.g. axion as the CDM).

10^{-13}) for our model, $\omega_{conversion}/\omega_{capture} \simeq (40-1) \times 10^{-15}$. The MECO experiment at Brookhaven is expected to have a sensitivity of 10^{-16} for this process, and thus will test our model.

(7) Parity odd asymmetry in $\mu^+ \rightarrow e^+\gamma$ decay: Parity violation can be observed by studying the correlation between the momentum \vec{p}_e of e^+ in $\mu^+ \rightarrow e^+\gamma$ decay and the polarization vector \vec{P} of positive muons (from π^+ decays). The distribution of e^+ is proportional to $(1 + \mathcal{A} \hat{p}_e \cdot \vec{P})$ where \mathcal{A} is the P -odd asymmetry parameter given by $\mathcal{A}(\mu^+ \rightarrow e^+\gamma) = (|A_L|^2 - |A_R|^2)/(|A_L|^2 + |A_R|^2)$. Here A_L is the amplitude for $\mu_L^+ \rightarrow e^+\gamma$ decay, while $A_R = A(\mu_R^+ \rightarrow e^+\gamma)$. In our model, as noted in (2), we typically have $|A_R| > |A_L|$ and thus $\mathcal{A}(\mu^+ \rightarrow e^+\gamma) < 0$ if $\mu > 0$, and $|A_L| > |A_R|$ and thus $\mathcal{A} > 0$ if $\mu < 0$. For example, with $(m_o, m_{1/2}) = (800, 250)$ GeV, $\mu > 0$ and $\tan \beta = 10$, we obtain $|A_L| = |A_L^{(1)}(\hat{\delta}_{LL}) + A_L^{(2)}(\delta_{LR}) + A_L^{(3)}| = 1.3 \times 10^{-13}$ (see table 2) while $|A_R| \simeq 1.6 \times 10^{-13}$, and thus $\mathcal{A} \simeq -0.25$, while for $(m_o, m_{1/2}) = (500, 250)$ GeV and $\tan \beta = 10$ we get, $|A_L| \simeq 4.7 \times 10^{-13}$ and $|A_R| \simeq 8.6 \times 10^{-13}$, yielding $\mathcal{A} \simeq -0.54$. The precise prediction of our model for \mathcal{A} would thus be definitive once the SUSY spectrum

is known.

We can compare the predictions of our model for \mathcal{A} with those of other SUSY models. In the MSSM with ν_R , since LFV arises through δ_{LL} type mixings, $A_L \gg A_R$, and thus $\mathcal{A}(\mu^+ \rightarrow e^+\gamma) \approx +1$, at least for $\tan\beta \leq 30$ or so, regardless of the choice of $(m_o, m_{1/2})$. In SUSY $SU(5)$ GUT, with or without ν_R , the GUT threshold effects realized in the regime $M_{GUT} \leq \mu \leq M_*$ generate δ_{RR} type mixings, and will lead to $A_R \gg A_L$ and thus $\mathcal{A} \simeq -1$. In the SUSY $SO(10)$ models with symmetric mass matrices, such as the ones studied in [26, 120], $A_L = A_R$ from GUT threshold effects, leading to a vanishing \mathcal{A} . Thus, we see that a determination of \mathcal{A} may help sort out the specific type of GUT that is responsible for LFV.

(8) Correlation between muon $g-2$ and $\mu \rightarrow e\gamma$: Currently there exists a discrepancy between theory and experiment in the anomalous magnetic moment of the muon: $\Delta a_\mu = a_\mu^{\text{expt}} - a_\mu^{\text{SM}} = 251(93) \times 10^{-11}$ [121]. This is a 2.7 sigma effect ⁷ and may be an indication of low energy supersymmetry. In our framework, this discrepancy can

⁷ This analysis is based on theory and data on $e^+e^- \rightarrow \text{hadron}$. If $\tau \rightarrow \nu_\tau + \text{hadron}$ data is used, this discrepancy reduces to 1.3 sigma; this may however be less reliable [121].

be considerably reduced for some, but not all, choices of the SUSY spectrum. When the sleptons are relatively light (≤ 500 GeV) with $\tan\beta = 10 - 20$, the SUSY contribution to a_μ is in the range $(50 - 200) \times 10^{-11}$. For example, following a recent numerical analysis (see [122] and references there in), we find $\Delta a_\mu^{SUSY} \approx 180 \times 10^{-11}$ for the cases of both IV and VII (see table 1). Note that when the SUSY contributions to Δa_μ becomes significant, $B(\mu \rightarrow e\gamma)$ is enhanced. Thus, a confirmation of new physics contribution to a_μ , for example by improved precision in the $e^+e^- \rightarrow$ hadron data and in the theoretical analysis, would imply (in the context of a SUSY-explanation) that $\mu \rightarrow e\gamma$ is just around the corner, within our framework.

In summary, lepton flavor violation is studied here within a predictive $SO(10)/G(224)$ -framework, possessing supersymmetry, that was proposed in Refs. [25, 28]. The framework seems most realistic in that it successfully describes five phenomena: (i) fermion masses and mixings, (ii) neutrino oscillations, (iii) CP violation, (iv) quark flavor-violations, as well as (v) baryogenesis via leptogenesis [16]. LFV emerges as an important prediction of this framework bringing no

new parameters, barring the few flavor-preserving SUSY parameters.

As mentioned before, the inclusion of contributions to LFV arising both from the presence of the RH neutrinos as well as those from the post-GUT regime, that too within a realistic framework, is the distinguishing feature of the present work. Typically, the latter contribution, which is commonly omitted in the literature, is found to dominate. Our results show that – (i) The decay $\mu \rightarrow e\gamma$ should be seen with improvement in the current limit by a factor of 10 – 100, even if sleptons are moderately heavy (~ 800 GeV, say); (ii) for the same reason, $\mu - e$ conversion ($\mu N \rightarrow eN$) should show in the planned MECO experiment, and (iii) $\tau \rightarrow \mu\gamma$ may be accessible at the LHC and a super B-factory. It is noted that the muon $(g - 2)$ -anomaly, if confirmed, would strongly suggest, within our model, that the discovery of the $\mu \rightarrow e\gamma$ decay is imminent. The significance of a measurement of the parity-odd asymmetry in polarized μ^+ decay into $e^+\gamma$ is also noted. In conclusion, the SO(10)/G(224) framework pursued here seems most successful on several fronts; it can surely meet further stringent tests through a search for lepton flavor violation.

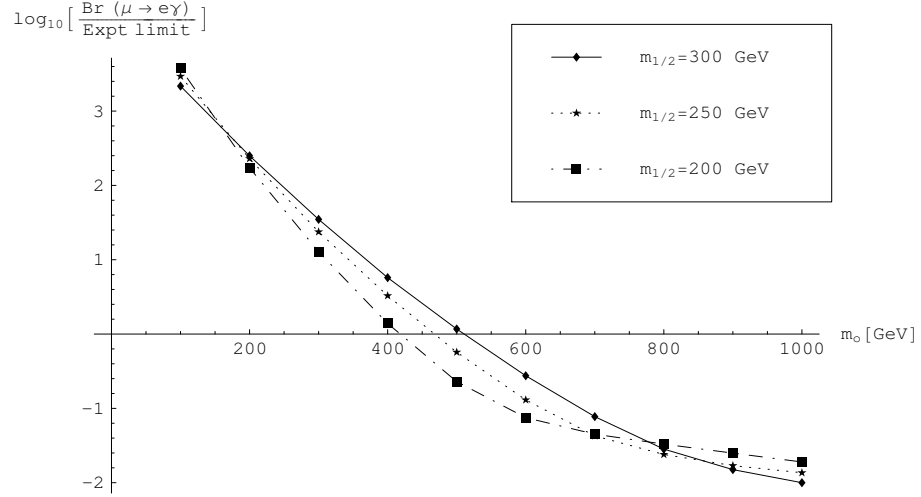


Fig. 6.1: Log of $Br(\mu \rightarrow e\gamma)$ divided by the experimental bound (1.2×10^{-11}) obtained for the SO(10) framework with $\ln(M^*/M_{GUT}) = 1$, $\tan\beta = 10$ and $\mu > 0$ vs m_o (in GeV) with $m_{1/2} = 200, 250$ and 300 GeV.

APPENDIX

.1 Appendix: Lepton Flavor violation: Amplitudes

The amplitude for the process $l_i^+ \rightarrow l_j^+ \gamma$ with $i > j$ (e.g. $\mu^+ \rightarrow e^+ \gamma$) is given by [111, 115]

$$\mathcal{A} = e\epsilon^{\alpha*}(q)\bar{v}_i(p)i\sigma_{\alpha\beta}q^\beta(A_L^{(ij)}P_L + A_R^{(ij)}P_R)v_j(p-q) \quad (.13)$$

The rate for this decay is given by

$$\Gamma = \frac{e^2}{16\pi^2}m_{l_i}^3(|A_L^{(ij)}|^2 + |A_R^{(ij)}|^2) \quad (.14)$$

In the context of MSSM, the diagrams that contribute to this process are

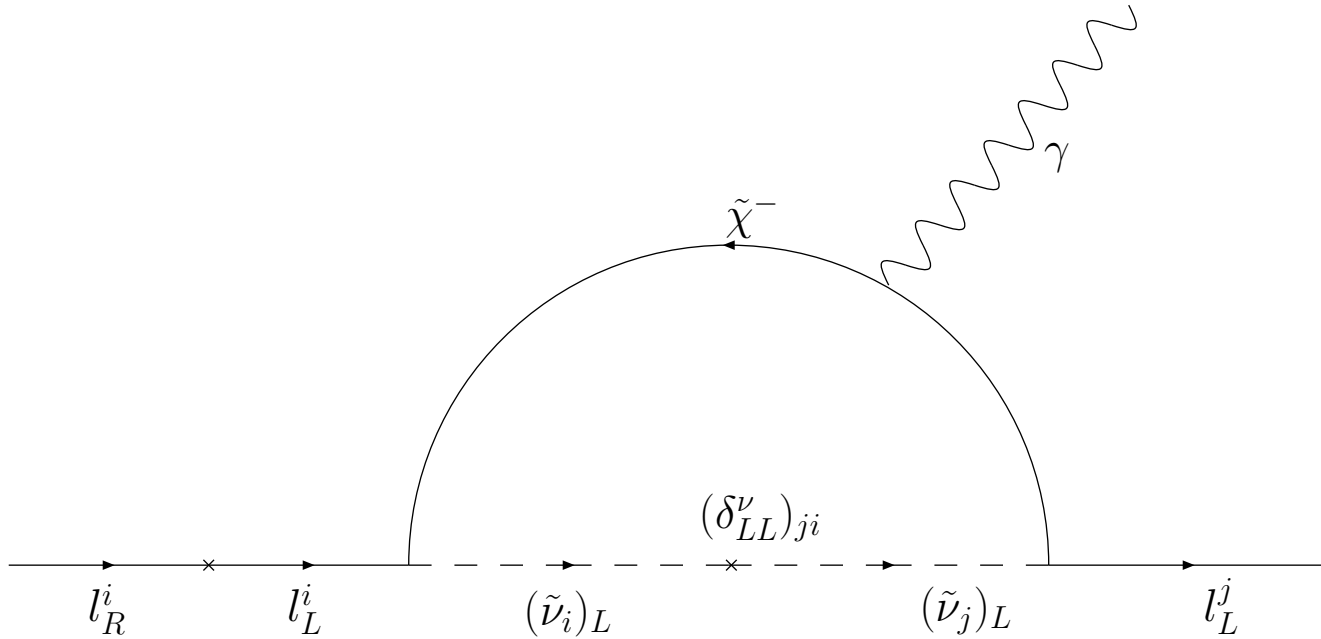


Figure 2.

The amplitude of the process in fig. 2 including one mass insertion is given by

$$(A_L)_1^C = m_{l_i} \frac{\alpha_2}{24\pi} (O_R)_{A1}^2 \frac{(\delta_{LL}^l)_{ji}}{m_{\tilde{\nu}}^4} g_{C_1}(x_{A\tilde{\nu}}) \quad (.15)$$

Here C stands for chargino, the matrices (O_L) and (O_R) are the matrices that diagonalize the chargino mass matrix, and g_{C_1} is a loop function defined below. A corresponding neutralino contribution is shown in fig. 3.

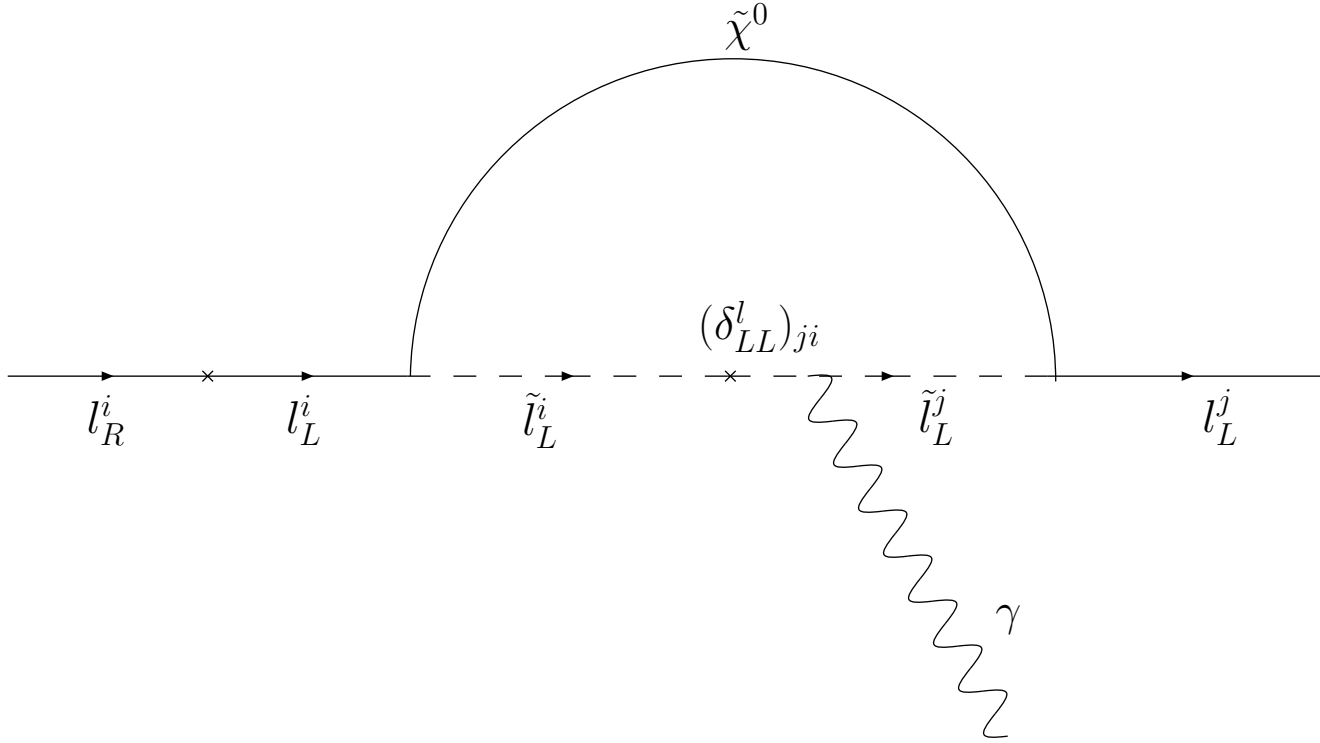


Figure 3.

The amplitude of the process in fig. 3 is

$$(A_L)_1^n = -m_{l_i} \frac{\alpha_2}{48\pi} \left((O_N)_{A2} + (O_N)_{A1} \tan \theta_W \right)^2 \frac{(\delta_{LL}^l)_{ji}}{m_{\tilde{l}}^4} g_{n_1}(x_{A\tilde{l}}) \quad (.16)$$

where n stands for neutralino, and θ_W is the weak angle. The matrix O_N is the matrix that diagonalizes the neutralino mixing matrix. Contributions to $l_i \rightarrow l_j \gamma$ also arise due to charged and neutral Higgsino exchange. These are given in figs. 4 and 5.

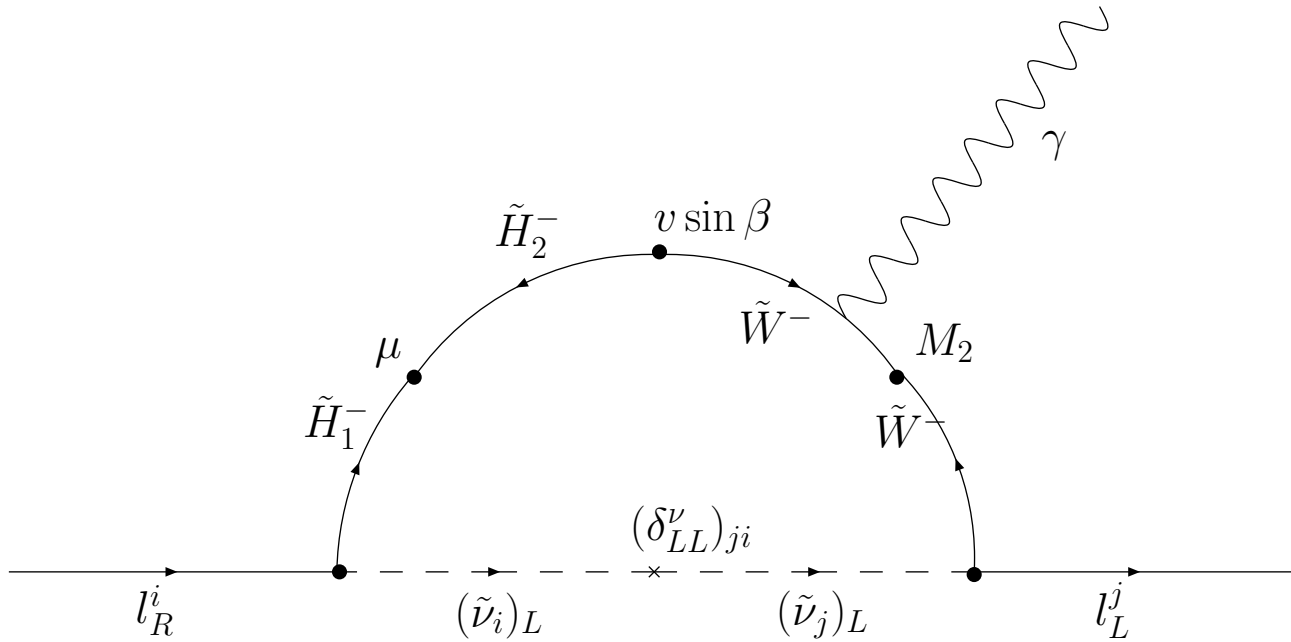


Figure 4.

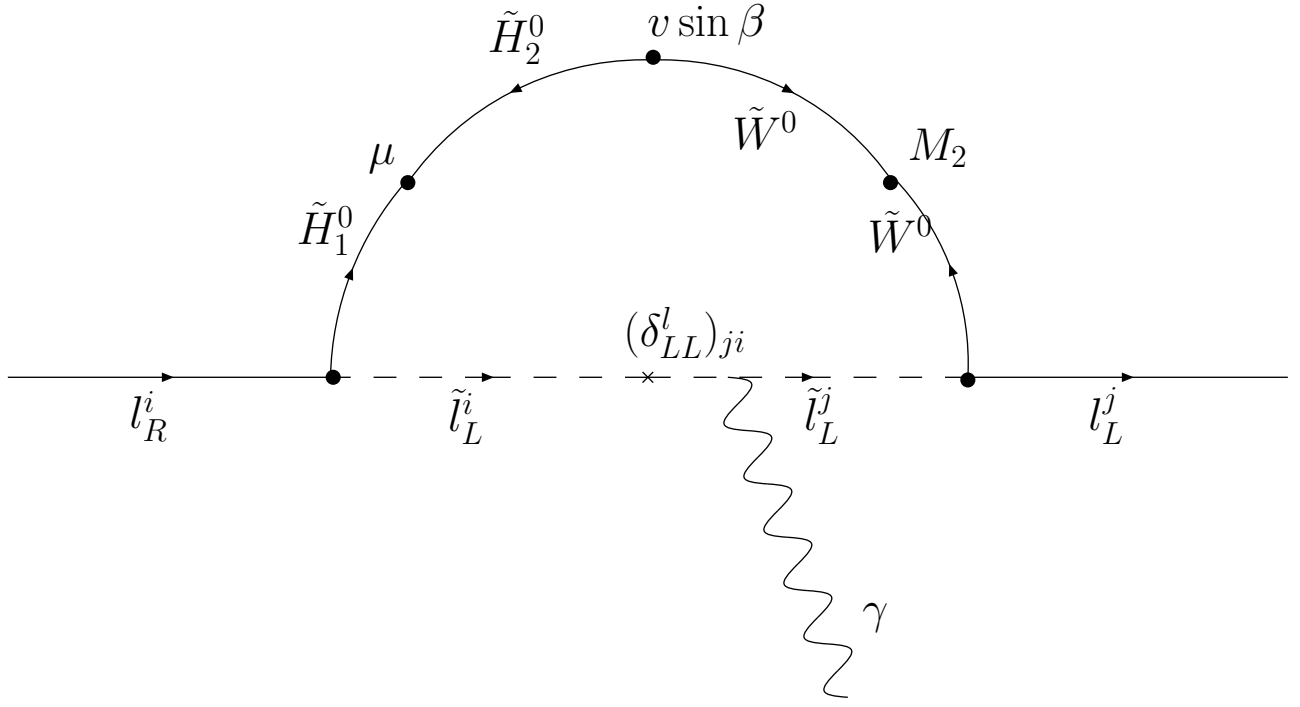


Figure 5.

The amplitudes to the processes in figs. 4 and 5 are respectively

$$(A_L)_2^C = -m_{l_i} \frac{\alpha_2}{4\pi} \frac{M_{\tilde{\chi}_A^-}}{\sqrt{2}m_W \cos \beta} (O_R)_{A1} (O_L)_{A2} \frac{(\delta_{LL}^l)_{ji}}{m_{\tilde{\nu}}^4} g_{C_2}(x_{A\tilde{\nu}}) \quad (.17)$$

$$(A_L)_2^n = m_{l_i} \frac{\alpha_2}{16\pi} \frac{M_{\tilde{\chi}_A^0}}{m_Z \cos \theta_W \cos \beta} (O_N)_{A3} ((O_N)_{A2} + (O_N)_{A1} \tan \theta_W) \times \frac{(\delta_{LL}^l)_{ji}}{m_{\tilde{l}}^4} g_{n_2}(x_{A\tilde{l}}) \quad (.18)$$

If we let $L \longleftrightarrow R$ in figs. 3 and 5, the corresponding processes contribute to A_R . These contributions are given by

$$(A_R)_1^n = -m_{l_i} \frac{\alpha_1}{12\pi} (O_N)_{A1}^2 \frac{(\delta_{RR}^l)_{ji}}{m_{\tilde{l}}^4} g_{n_1}(x_{A\tilde{l}}) \quad (.19)$$

$$(A_R)_2^n = -m_{l_i} \frac{\alpha_2}{8\pi} \frac{M_{\tilde{\chi}_A^0}}{m_Z \sin \theta_W \cos \beta} (O_N)_{A3} (O_N)_{A1} \frac{(\delta_{RR}^l)_{ji}}{m_{\tilde{l}}^4} g_{n_2}(x_{A\tilde{l}}) \quad (.20)$$

The chargino contributions to A_R are negligible as they involve $\tilde{\nu}_R$ insertions. In Eqs. (.15)–(.20), $x_{A\tilde{\nu}} = M_{\chi_A}^2/m_{\tilde{\nu}}^2$ and $x_{A\tilde{l}} = M_{\chi_A}^2/m_{\tilde{l}}^2$, where χ_A is the corresponding chargino or neutralino in figs. 2–5.

Finally, one can have chirality flipping mass insertions, which contribute to A_{LR} . Such a contribution is shown in fig. 6.

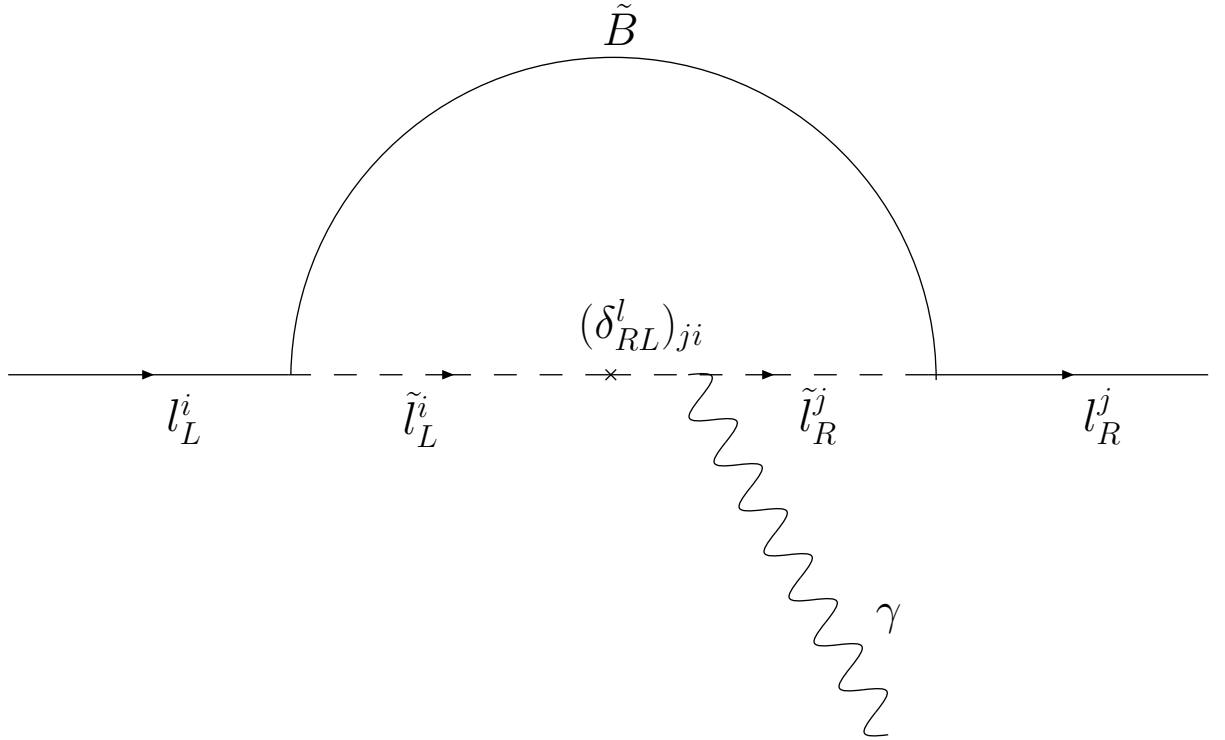


Figure 6.

The amplitude of the process in fig. 6 is given below

$$A_{LR} = \frac{3}{20\pi} \alpha_1 \frac{m_{\tilde{B}}}{m_{\tilde{l}}^2} (\delta_{RL}^l)_{ji} f(x); \quad x = \frac{m_{\tilde{B}}^2}{m_{\tilde{l}}^2} \quad (.21)$$

The loop functions in the amplitudes are defined below:

$$f(x) = \frac{1 - x^2 + 2x \ln x}{2(1 - x)^3} \quad (.22)$$

$$g_{C_1}(x) = \frac{-1 - 9x + 9x^2 + x^3 - 6x(1 + x) \ln x}{(x - 1)^5} \quad (.23)$$

$$g_{C_2}(x) = \frac{-5 + 4x + x^2 - 2(1 + 2x) \ln x}{2(x - 1)^4} \quad (.24)$$

$$g_{n_1}(x) = \frac{-1 + 9x + 9x^2 - 17x^3 + 6x^2(3 + x) \ln x}{2(x - 1)^5} \quad (.25)$$

$$g_{n_2}(x) = \frac{1 + 4x - 5x^2 + 2x(2 + x) \ln x}{(x - 1)^4} \quad (.26)$$

The mass term for the charginos in the Lagrangian is:

$$\mathcal{L}_m = -\frac{1}{2} \begin{pmatrix} \psi^+ & \psi^- \end{pmatrix} \begin{pmatrix} 0 & X^T \\ X & 0 \end{pmatrix} \begin{pmatrix} \psi^+ \\ \psi^- \end{pmatrix} \quad (.27)$$

where $\psi^+ = (-i\tilde{W}^+, \tilde{H}_2^+)$, $\psi^- = (-i\tilde{W}^-, \tilde{H}_1^-)$, and X is given

below.

$$X = \begin{pmatrix} M_2 & m_W \sqrt{2} \sin \beta \\ m_W \sqrt{2} \cos \beta & \mu \end{pmatrix} \quad (.28)$$

The diagonal mass matrix for the charginos is obtained by a bi-unitary transformation of X such that $O_L^* X O_R^{-1} = M_D$. In the approximation $|M_2 \pm \mu|$, $|\frac{5}{3}M_1 \pm \mu| \gg m_Z$ and $|M_2 \mu| > m_W^2 \sin 2\beta$, the

matrices O_L and O_R have the form [116]

$$O_R = \begin{bmatrix} 1 & \frac{m_W \sqrt{2}(M_2 \sin \beta + \mu \cos \beta)}{M_2^2 - \mu^2} \\ \frac{-m_W \sqrt{2}(M_2 \sin \beta + \mu \cos \beta) \text{sgn}(\mu)}{M_2^2 - \mu^2} & \text{sgn}(\mu) \end{bmatrix} \quad (.29)$$

$$O_L = \begin{bmatrix} 1 & \frac{m_W \sqrt{2}(M_2 \cos \beta + \mu \sin \beta)}{M_2^2 - \mu^2} \\ \frac{-m_W \sqrt{2}(M_2 \cos \beta + \mu \sin \beta)}{M_2^2 - \mu^2} & 1 \end{bmatrix} \quad (.30)$$

The mass matrix for the neutralinos in the basis $(\tilde{B}, \tilde{W}_3, \tilde{H}_1, \tilde{H}_2)$

is given by

$$N = \begin{pmatrix} M' & 0 & -m_{ZSW}c\beta & m_{ZSW}s\beta \\ 0 & M_2 & m_{ZCW}c\beta & -m_{ZCW}s\beta \\ -m_{ZSW}c\beta & m_{ZCW}c\beta & 0 & -\mu \\ m_{ZSW}s\beta & -m_{ZCW}s\beta & -\mu & 0 \end{pmatrix} \quad (.31)$$

In this basis, the matrix that diagonalizes N is given below.

$$O_N = \begin{bmatrix} 1 & \frac{m_Z^2 \sin 2\theta_W (M' + \mu \sin 2\beta)}{2(M' - M_2)(\mu^2 - M'^2)} & \frac{-m_Z s_W (M' c_\beta + \mu s_\beta)}{M'^2 - \mu^2} & \frac{m_Z s_W (M' s_\beta + \mu c_\beta)}{M'^2 - \mu^2} \\ \frac{m_Z^2 \sin 2\theta_W (M_2 + \mu \sin 2\beta)}{2(M_2 - M')(\mu^2 - M_2^2)} & 1 & \frac{m_Z c_W (M_2 c_\beta + \mu s_\beta)}{M_2^2 - \mu^2} & \frac{-m_Z c_W (M_2 s_\beta + \mu c_\beta)}{M_2^2 - \mu^2} \\ \frac{-m_Z s_W (s_\beta - c_\beta)}{\sqrt{2}(\mu - M')} & \frac{m_Z c_W (s_\beta - c_\beta)}{\sqrt{2}(\mu + M_2)} & \frac{1}{\sqrt{2}} & \frac{1}{\sqrt{2}} \\ \frac{-m_Z s_W (s_\beta + c_\beta)}{\sqrt{2}(\mu - M')} & \frac{m_Z c_W (s_\beta + c_\beta)}{\sqrt{2}(\mu - M_2)} & \frac{1}{\sqrt{2}} & -\frac{1}{\sqrt{2}} \end{bmatrix} \quad (.32)$$

where $s_W = \sin \theta_W$, $c_W = \cos \theta_W$, $s_\beta = \sin \beta$, $c_\beta = \cos \beta$ and $M' = \frac{5}{3}M_1$.

The expressions for the amplitudes for the process $l_i^+ \rightarrow l_j^+ \gamma$ are used to calculate the branching ratios for $\mu \rightarrow e\gamma$, $\tau \rightarrow \mu\gamma$ and $\tau \rightarrow e\gamma$ as discussed above.

7. DISTINGUISHING BETWEEN HIERARCHICAL AND LOP-SIDED SO(10) MODELS.

7.1 Introduction

In recent years, several models based on supersymmetric SO(10) GUT have emerged [123]. Two promising candidates have been proposed which have much similarity in their Higgs structure and yet important differences in the pattern of fermion mass-matrices. One is by Albright and Barr (AB) [30] and the other by Babu, Pati and Wilczek (BPW) [25]. Both models use low-dimensional Higgs multiplets (like $45_H, 16_H, \overline{16}_H$ and 10_H) to break SO(10) and generate fermion masses (see remarks later) as opposed to large-dimensional ones (like 126, $\overline{126}$, 210 and possibly 120). Both of these models work extremely well in making predictions regarding the masses of quarks and leptons, the CKM elements and neutrino masses and their mixings in good accord with observations. Nevertheless there is a significant difference

between these two models in the structure of their fermion mass matrices. In the BPW-model, the elements of the fermion mass-matrices (constrained by a U(1)-flavor symmetry [28, 62, 65]) are consistently family-hierarchical with “33” \gg “23” \sim “32” \gg “22” \gg “12” \sim “21” \gg “11” *etc.* By contrast, in the AB-model, the fermion mass-matrices are lopsided with “23” \sim “33” in the down quark mass-matrix and “32” \sim “33” in the charged lepton matrix. (The exact structure of the fermion mass-matrices will be presented in Sec. 2.) This difference in the structure of the mass matrices leads to two characteristically different explanations for the largeness of the $\nu_\mu - \nu_\tau$ oscillation angle in the two models. For the BPW model, both charged lepton and neutrino sectors give moderately large contributions to this mixing which, as they show, naturally add to give a nearly maximal $\sin^2 2\theta_{\nu_\mu - \nu_\tau}$, while simultaneously giving small V_{cb} as desired. The largeness of $\theta_{\nu_\mu - \nu_\tau}$, together with the smallness of V_{cb} (in the BPW model) turns out in fact to be a consequence of (a) the group theory of SO(10)/G(224) in the context of the minimal Higgs system, and (b) the hierarchical pattern of the mass-matrices. For the lopsided AB model, on the other hand,

the large (maximal) $\nu_\mu - \nu_\tau$ oscillation angle comes almost entirely from the charged lepton sector which has a “32” element comparable to the “33”.

The original work of Babu, Pati and Wilczek, (reviewed in Chapter 4) treated the entries in the mass matrices to be real for simplicity, thereby ignoring CP non-conservation. It was successfully extended to include CP violation by allowing for phases in the mass matrices in Ref. [28] and has been discussed in Chapter 5.

In this chapter based on the work done in Ref. [31], we do a comparative study between certain testable predictions of the AB model versus those of the BPW model allowing for the extension of the latter as in Ref. [28] (see Chapter 5). We find that while both models give similar predictions regarding fermion masses and mixings, they can be sharply distinguished by lepton flavor violation, especially by the rate of $\mu \rightarrow e\gamma$ and the edm of the electron.

We work in a scenario as in Refs. [28] and [29], in which flavor-universal soft SUSY breaking is transmitted to the sparticles at a messenger-scale M^* , with $M_{GUT} < M^* \leq M_{string}$ as in a mSUGRA

model [46]. Following the general analysis in Ref. [26] it was pointed out in Refs. [28] and [29] that in a SUSY-GUT model with a high messenger scale as above, post-GUT physics involving RG running from $M^* \rightarrow M_{GUT}$ leads to dominant flavor and CP violating effects. In the literature, however, post-GUT contribution has invariably been omitted, except for Refs. [28] and [29], where it has been included only for the BPW model. Lepton flavor violation in the AB model has been studied so far by many authors by including the contribution arising only through the RH neutrinos [124], without, however, the inclusion of post-GUT contributions. I therefore make a comparative study of the BPW and the AB models by including the contributions arising from both post-GUT physics, as well as those from the RH neutrinos through RG running below the GUT scale. For the sake of comparison and completeness, we will include the results obtained in Refs. [28] and [29] which deal with CP and flavor violation in the BPW model.

To calculate the branching ratio of lepton flavor violating processes we include contributions from three different sources: (i) the sfermion mass-insertions, $\hat{\delta}_{LL,RR}^{ij}$, arising from renormalization group

(RG) running from M^* to $M_{GUT} \sim 2 \times 10^{16}$ GeV, (ii) the mass-insertions $(\delta_{LL}^{ij})^{RHN}$ arising from RG running from M_{GUT} to the right handed neutrino mass scales M_{R_i} , and (iii) the chirality-flipping mass-insertions $\delta_{LR,RL}^{ij}$ arising from A -terms that are induced solely through RG running from M^* to M_{GUT} involving $SO(10)$ or $G(224)$ gauginos in the loop.

It was found in Ref. [29], that for the BPW-model (see Chapter 6), contributions to the rate of $\mu \rightarrow e\gamma$ from sources (i) and (iii) associated with post-GUT physics, were typically much larger than that from source (ii) associated with the RH neutrinos. For the AB-model, we find that the RH neutrino contribution is strongly enhanced compared to that in the BPW model; as a result all the three contributions to the amplitude of $\mu \rightarrow e\gamma$ are comparable. Including all three contributions, we find that for most of the SUSY parameter space, the branching ratio for $\mu \rightarrow e\gamma$ calculated in the AB-model is much larger than that in the BPW model and is in fact excluded by the experimental upper bound unless $(m_o, m_{1/2}) \gtrsim 1$ TeV. Thus one main result of this chapter is that, with all three sources of lepton flavor

violation included, the process $\mu \rightarrow e\gamma$ can provide a clear distinction between the BPW and the AB models. We also examine CP violation as well as flavor violation in the quark sector, including that reflected by electric dipole moments, in the AB model, and compare it with the corresponding results for the BPW-model, obtained in [28] (see chapter 5).

In the following section the patterns of the fermion mass matrices for the BPW and the AB models are presented.

7.2 *A brief description of the BPW and the AB models*

While the BPW model was reviewed in detail in Chapter 4, and its extension in Chapter 5, for the sake of convenience and completeness, we briefly describe it again in this section.

The Babu-Pati-Wilczek (BPW) model

The Dirac mass matrices of the sectors u, d, l and ν proposed in Ref. [25] in the context of SO(10) or G(224)-symmetry have the following structure:

$$M_u = \begin{bmatrix} 0 & \epsilon' & 0 \\ -\epsilon' & \zeta_{22}^u & \sigma + \epsilon \\ 0 & \sigma - \epsilon & 1 \end{bmatrix} \mathcal{M}_u^0; \quad M_d = \begin{bmatrix} 0 & \eta' + \epsilon' & 0 \\ \eta' - \epsilon' & \zeta_{22}^d & \eta + \epsilon \\ 0 & \eta - \epsilon & 1 \end{bmatrix} \mathcal{M}_d^0 \quad (7.1)$$

$$M_\nu^D = \begin{bmatrix} 0 & -3\epsilon' & 0 \\ 3\epsilon' & \zeta_{22}^u & \sigma - 3\epsilon \\ 0 & \sigma + 3\epsilon & 1 \end{bmatrix} \mathcal{M}_u^0; \quad M_l = \begin{bmatrix} 0 & \eta' - 3\epsilon' & 0 \\ \eta' + 3\epsilon' & \zeta_{22}^d & \eta - 3\epsilon \\ 0 & \eta + 3\epsilon & 1 \end{bmatrix} \mathcal{M}_d^0$$

These matrices are defined in the gauge basis and are multiplied by $\bar{\Psi}_L$ on left and Ψ_R on right. For instance, the row and column indices of M_u are given by $(\bar{u}_L, \bar{c}_L, \bar{t}_L)$ and (u_R, c_R, t_R) respectively. These matrices have a hierarchical structure which can be attributed to a presumed U(1)-flavor symmetry (see e.g. [28, 62]), so that in magnitudes $1 \gg \sigma \sim \eta \sim \epsilon \gg \zeta_{22}^u \sim \zeta_{22}^d \gg \eta' > \epsilon'$. Following the constraints of SO(10) and the U(1)-flavor symmetry, such a pattern of mass-matrices can be obtained using a *minimal* Higgs system consisting of $\mathbf{45}_H, \mathbf{16}_H, \overline{\mathbf{16}}_H, \mathbf{10}_H$ and a singlet S of SO(10)¹, which lead

¹ Both the BPW and the AB models bear similarities in the choice of the Higgs system, yet there are significant differences in the mass matrices. See text for details.

to effective couplings of the form [28, 62]:

$$\begin{aligned}
\mathcal{L}_{\text{Yuk}} = & \\
& h_{33} \mathbf{16}_3 \mathbf{16}_3 \mathbf{10}_H \\
& + h_{23} \mathbf{16}_2 \mathbf{16}_3 \mathbf{10}_H (S/M) \\
& + a_{23} \mathbf{16}_2 \mathbf{16}_3 \mathbf{10}_H (\mathbf{45}_H / M') (S/M)^p \\
& + g_{23} \mathbf{16}_2 \mathbf{16}_3 \mathbf{16}_H^d (\mathbf{16}_H / M'') (S/M)^q \\
& + h_{22} \mathbf{16}_2 \mathbf{16}_2 \mathbf{10}_H (S/M)^2 \tag{7.2} \\
& + g_{22} \mathbf{16}_2 \mathbf{16}_2 \mathbf{16}_H^d (\mathbf{16}_H / M'') (S/M)^{q+1} \\
& + g_{12} \mathbf{16}_1 \mathbf{16}_2 \mathbf{16}_H^d (\mathbf{16}_H / M'') (S/M)^{q+2} \\
& + a_{12} \mathbf{16}_1 \mathbf{16}_2 \mathbf{10}_H (\mathbf{45}_H / M') (S/M)^{p+2}
\end{aligned}$$

The powers of (S/M) are determined by flavor-charge assignments (see Refs. [62] and [28]). The mass scales M' , M'' and M are of order M_{string} or (possibly) of order M_{GUT} [67]. Depending on whether $M'(M'') \sim M_{GUT}$ or M_{string} (see [67]), the exponent $p(q)$ is either one or zero [69]. The VEVs of $\langle \mathbf{45}_H \rangle$ (which is along $B - L$), $\langle \mathbf{16}_H \rangle = \langle \overline{\mathbf{16}}_H \rangle$ (along $\langle \tilde{\nu}_{RH} \rangle$) and $\langle S \rangle$ are of the GUT-scale, while those of $\langle \mathbf{10}_H \rangle$ and $\langle \mathbf{16}_H^d \rangle$ are of the electroweak scale [25, 68]. The

combination $\mathbf{10}_H \cdot \mathbf{45}_H$ effectively acts like a $\mathbf{120}$ which is antisymmetric in family space and is along $B - L$. The hierarchical pattern is determined by the suppression of the couplings by appropriate powers of $M_{GUT}/(M, M' \text{ or } M'')$. The entry “1” in the matrices arises from the dominant $\mathbf{16}_3 \mathbf{16}_3 \mathbf{10}_H$ term. The entries ϵ and ϵ' arising from the $\mathbf{16}_i \mathbf{16}_j \mathbf{10}_H \mathbf{45}_H$ terms, are proportional to $B - L$ and are antisymmetric in family space. Thus $(\epsilon, \epsilon') \rightarrow -3(\epsilon, \epsilon')$ as $q \rightarrow l$. The parameter σ comes from the $\mathbf{16}_2 \mathbf{16}_3 \mathbf{10}_H$ term and contributes equally to the up and down sectors, whereas $\hat{\eta} \equiv \eta - \sigma$, arising from $\mathbf{16}_2 \mathbf{16}_3 \mathbf{16}_H^d \mathbf{16}_H$ operator, contributes only to the down and charged lepton sectors. Similarly, ζ_{22}^u arises from the $\mathbf{16}_2 \mathbf{16}_2 \mathbf{10}_H$ term while ζ_{22}^d gets contributions from both $\mathbf{16}_2 \mathbf{16}_2 \mathbf{10}_H$ and $\mathbf{16}_2 \mathbf{16}_2 \mathbf{16}_H^d \mathbf{16}_H$ operators. Finally, η' , which is present only in the down and charged lepton sectors, gets a contribution from $\mathbf{16}_1 \mathbf{16}_2 \mathbf{16}_H^d \mathbf{16}_H$ terms in the Yukawa Lagrangian (see Eq. (7.2)).

The right-handed neutrino masses arise from the effective couplings of the form [70]:

$$\mathcal{L}_{\text{Maj}} = f_{ij} \mathbf{16}_i \mathbf{16}_j \overline{\mathbf{16}}_H \overline{\mathbf{16}}_H / M \quad (7.3)$$

where the f_{ij} 's include appropriate powers of $\langle S \rangle / M$. The hierarchical form of the Majorana mass-matrix for the RH neutrinos is [25]:

$$M_R^\nu = \begin{bmatrix} x & 0 & z \\ 0 & 0 & y \\ z & y & 1 \end{bmatrix} M_R \quad (7.4)$$

Following flavor charge assignments (see [62]), we have $1 \gg y \gg z \gg x$. We expect $M_{st} \lesssim M \lesssim M_{Pl}$ where $M_{st} \approx 4 \times 10^{17}$ GeV and thus $M \approx 10^{18}$ GeV (1/2-2). The magnitude of M_R can now be estimated by putting $f_{33} \approx 1$, $\langle \overline{\mathbf{16}}_H \rangle \approx 2 \times 10^{16}$ GeV and $M \approx (1/2-2) 10^{18}$ GeV [25, 62]. This yields: $M_R = f_{33} \langle \overline{\mathbf{16}}_H \rangle^2 / M \approx (4 \times 10^{14} \text{ GeV})(1/2-2)$.

Thus the Majorana masses of the RH neutrinos are given by [25, 62]:

$$\begin{aligned} M_3 &\approx M_R \approx 4 \times 10^{14} \text{ GeV (1/2-2),} \\ M_2 &\approx |y^2| M_3 \approx 10^{12} \text{ GeV(1/2-2),} \\ M_1 &\approx |x - z^2| M_3 \sim (1/4-2) 10^{-4} M_3 \\ &\sim 4 \times 10^{10} \text{ GeV(1/8 - 4).} \end{aligned} \quad (7.5)$$

Note that both the RH neutrinos as well as the light neutrinos have hierarchical masses.

In the BPW model of Ref. [25], the parameters σ, η, ϵ *etc.* were chosen to be real. Setting $\zeta_{22}^d = \zeta_{22}^u = 0$, and with $m_t^{\text{phys}} = 174$ GeV, $m_c(m_c) = 1.37$ GeV, $m_s(1 \text{ GeV}) = 110 - 116$ MeV, $m_u(1 \text{ GeV}) = 6$ MeV, and the observed masses of e, μ , and τ as inputs, for this CP conserving case the following fit for the parameters was obtained in Ref. [25]:

$$\begin{aligned} \sigma &\approx 0.110, & \eta &\approx 0.151, & \epsilon &\approx -0.095, & |\eta'| &\approx 4.4 \times 10^{-3}, \\ \epsilon' &\approx 2 \times 10^{-4}, & \mathcal{M}_u^0 &\approx m_t(M_X) \approx 100 \text{ GeV}, \\ \mathcal{M}_d^0 &\approx m_\tau(M_X) \approx 1.1 \text{ GeV}. \end{aligned} \tag{7.6}$$

These output parameters remain stable to within 10% corresponding to small variations ($\lesssim 10\%$) in the input parameters of m_t, m_c, m_s , and m_u . These in turn lead to the following seven predictions for the quarks and light neutrinos [25], [62], described in Chapter 4 (see Eq. (4.12)): (i) $m_b(m_b) \approx (4.7\text{--}4.9)$ GeV, (ii) $\sqrt{\Delta m_{23}^2} \approx m(\nu_3) \approx (1/24 \text{ eV})(1/2\text{--}2)$, (iii) $V_{cb} \approx 0.044$, (iv) $\sin^2 2\theta_{\nu_\mu\nu_\tau}^{\text{osc}} \approx 0.993$, (v) $V_{us} \approx 0.20$, (vi) $\left| \frac{V_{ub}}{V_{cb}} \right| \approx \sqrt{\frac{m_u}{m_c}} \approx 0.07$, (vii) $m_d(1 \text{ GeV}) \approx 8$ MeV.

All seven predictions are in good agreement with observation (to within 10%) (see Chapter 4 for other predictions). To allow for CP violation, this framework can be extended to include phases for the

parameters in Ref. [28]. Remarkably enough, it was found that there exists a class of fits within the $SO(10)/G(224)$ framework, which correctly describes not only (a) fermion masses, (b) CKM mixings and (c) neutrino oscillations [25, 62], but also (d) the observed CP and flavor violations in the $K^\circ - \bar{K}^\circ$ and $B_d - \bar{B}_d$ systems (see Ref. [28] for the predictions in this regard). A representative of this class of fits (to be called fit A) is given by [28]:

$$\sigma = 0.109 - 0.012i, \quad \eta = 0.122 - 0.0464i, \quad \epsilon = -0.103,$$

$$\eta' = 2.4 \times 10^{-3}, \quad \epsilon' = 2.35 \times 10^{-4} e^{i(69^\circ)}, \quad \zeta_{22}^d = 9.8 \times 10^{-3} e^{-i(149^\circ)}, \quad (7.7)$$

$$(\mathcal{M}_u^0, \mathcal{M}_d^0) \approx (100, 1.1) \text{ GeV}.$$

In this particular fit ζ_{22}^u is set to zero for the sake of economy in parameters. However, allowing for $\zeta_{22}^u \lesssim (1/3)(\zeta_{22}^d)$ would still yield the desired results (see Fit B given in Chapter 5). Because of the success of this class of fits in describing correctly all four features (a), (b), (c) and (d) mentioned above - which is a non-trivial feature by itself - we will use fit A as a representative to obtain the sfermion mass-insertion parameters $\hat{\delta}_{LL,RR}^{ij}$, $(\delta_{LL}^{ij})^{RHN}$ and $\delta_{LR,RL}^{ij}$ in the lepton sector and thereby the predictions of the BPW model and its extension

(Ref. [28]) for lepton flavor violation.

The fermion mass matrices M_u , M_d and M_l are diagonalized at the GUT scale $\approx 2 \times 10^{16}$ GeV by bi-unitary transformations:

$$M_{u,d,l}^{diag} = X_L^{(u,d,l)\dagger} M_{u,d,l} X_R^{(u,d,l)} \quad (7.8)$$

The approximate analytic expressions for the matrices $X_{L,R}^d$ can be found in Chapter 5 and the appendices. The corresponding expressions for $X_{L,R}^l$ can be obtained by letting $(\epsilon, \epsilon') \rightarrow -3(\epsilon, \epsilon')$. For our calculations, the mass-matrices have been diagonalized numerically.

The Albright-Barr Model

The Dirac mass matrices of the u, d, l and ν sectors are given by [30]:

$$M_u = \begin{bmatrix} \tilde{\eta} & 0 & 0 \\ 0 & 0 & \tilde{\epsilon}/3 \\ 0 & -\tilde{\epsilon}/3 & 1 \end{bmatrix} \mathcal{M}_U; \quad M_d = \begin{bmatrix} 0 & \tilde{\delta} & \tilde{\delta}' e^{i\phi} \\ \tilde{\delta} & 0 & \tilde{\sigma} + \tilde{\epsilon}/3 \\ \tilde{\delta}' e^{i\phi} & -\tilde{\epsilon}/3 & 1 \end{bmatrix} \mathcal{M}_D \quad (7.9)$$

$$M_\nu^D = \begin{bmatrix} \tilde{\eta} & 0 & 0 \\ 0 & 0 & -\tilde{\epsilon} \\ 0 & \tilde{\epsilon} & 1 \end{bmatrix} \mathcal{M}_U; \quad M_l = \begin{bmatrix} 0 & \tilde{\delta} & \tilde{\delta}' e^{i\phi} \\ \tilde{\delta} & 0 & -\tilde{\epsilon} \\ \tilde{\delta}' e^{i\phi} & \tilde{\sigma} + \tilde{\epsilon} & 1 \end{bmatrix} \mathcal{M}_D$$

These matrices are defined with the convention that the left-handed fermions multiply them from the right, and the left handed antifermions from the left. The AB model involves a multitude of Higgs multiplets to generate fermion masses and mixings including a $\mathbf{45}_H$, two pairs of $\mathbf{16}_H + \overline{\mathbf{16}}_H$, two pairs of $\mathbf{10}_H$ and several singlets of SO(10). The “1” entry in the mass matrices arises from the dominant $\mathbf{16}_3 \mathbf{16}_3 \mathbf{10}_H$ operator. The $\tilde{\epsilon}$ entry arises from operators of the form $\mathbf{16}_2 \mathbf{16}_3 \mathbf{10}_H \mathbf{45}_H$ (as in the BPW model). Since $\langle \mathbf{45}_H \rangle \propto B - L$, the $\tilde{\epsilon}$ entry is antisymmetric, and brings in a factor of 1/3 in the quark sector. The $\tilde{\sigma}$ term comes from the operator $\mathbf{16}_2 \mathbf{16}_3 \mathbf{16}_H \mathbf{16}'_H$ by integrating out the $\mathbf{10}$ s of SO(10). (Note that the two $\mathbf{16}$ s of Higgs, $\mathbf{16}_H$

and $\mathbf{16}'_{\mathbf{H}}$, are distinct). The $\mathbf{16}'_{\mathbf{H}}$ breaks the electroweak symmetry but does not participate in the GUT scale breaking of $\text{SO}(10)$. The resulting operator is $\bar{\mathbf{5}}(\mathbf{16}_2)\mathbf{10}(\mathbf{16}_3)\langle\bar{\mathbf{5}}(\mathbf{16}'_{\mathbf{H}})\rangle\langle\mathbf{1}(\mathbf{16}_{\mathbf{H}})\rangle$, where the $\bar{\mathbf{5}}$, $\mathbf{10}$ and $\mathbf{1} \subset \text{SU}(5)$. Thus the $\tilde{\sigma}$ contributes “lopsidedly” to the l and d matrices. The entries $\tilde{\delta}$ and $\tilde{\delta}'$ arise from the operators $\mathbf{16}_i\mathbf{16}_j\mathbf{16}_{\mathbf{H}}\mathbf{16}'_{\mathbf{H}}$, like the $\tilde{\sigma}$ and contribute only to the l and d matrices. Finally, $\tilde{\eta}$, which enters the u and ν Dirac mass matrices, is of order 10^{-5} and arises from higher dimensional operators. The Majorana mass matrix for the right-handed neutrinos in the AB model is taken to have the following form:

$$M_R = \begin{bmatrix} c^2\tilde{\eta}^2 & -b\tilde{\epsilon}\tilde{\eta} & a\tilde{\eta} \\ -b\tilde{\epsilon}\tilde{\eta} & \tilde{\epsilon}^2 & -\tilde{\epsilon} \\ a\tilde{\eta} & -\tilde{\epsilon} & 1 \end{bmatrix} \Lambda_R \quad (7.10)$$

with $\Lambda_R = 2.5 \times 10^{14}$ GeV. The parameters a , b and c are of order one to give the LMA solution for neutrino oscillations. Given below is a fit to the parameters $\tilde{\sigma}$, $\tilde{\epsilon}$, $\tilde{\delta}$ *etc.* which gives the values of the fermion masses and the CKM elements in very good agreement with

observations [125, 126]:

$$\begin{aligned} \tilde{\sigma} = 1.78, \quad \tilde{\epsilon} = 0.145, \quad \tilde{\delta} = 8.6 \times 10^{-3}, \quad \tilde{\delta}' = 7.9 \times 10^{-3}, \\ \phi = 126^\circ, \quad \tilde{\eta} = 8 \times 10^{-6}, \quad (\mathcal{M}_u, \mathcal{M}_d) \approx (113, 1) \text{ GeV}. \end{aligned} \tag{7.11}$$

In the next section, we turn to lepton flavor violation.

7.3 The Three Sources of Lepton Flavor Violation

As done earlier in the study on CP and flavor violation (Chapters 5 and 6), we assume that flavor-universal soft SUSY-breaking is transmitted to the SM-sector at a messenger scale M^* , where $M_{GUT} < M^* \leq M_{string}$. This may naturally be realized e.g. in models of mSUGRA [46], or gaugino-mediation [54] or in a class of anomalous U(1) D-term SUSY breaking models [49, 50]. With the assumption of extreme universality as in CMSSM, supersymmetry introduces five parameters at the scale M^* :

$$m_o, m_{1/2}, A_o, \tan \beta \text{ and } \text{sgn}(\mu).$$

For most purposes, we will adopt this restricted version of SUSY breaking with the added restriction that $A_o = 0$ at M^* [54]. However, we will not insist on strict Higgs-squark-slepton mass universality.

Even though we have flavor preservation at M^* , flavor violating scalar (mass)²-transitions arise in the model through RG running from M^* to the EW scale. As described below, we thereby have *three sources* of lepton flavor violation [28, 29].

(1) RG Running of Scalar Masses from M^* to M_{GUT} .

With family universality at the scale M^* , all sleptons have the mass m_o at this scale and the scalar (mass)² matrices are diagonal. Due to flavor dependent Yukawa couplings, with $h_t = h_b = h_\tau (= h_{33})$ being the largest, RG running from M^* to M_{GUT} renders the third family lighter than the first two (see e.g. [26]) by the amount:

$$\Delta \hat{m}_{\tilde{b}_L}^2 = \Delta \hat{m}_{\tilde{b}_R}^2 = \Delta \hat{m}_{\tilde{\tau}_L}^2 = \Delta \hat{m}_{\tilde{\tau}_R}^2 \equiv \Delta \approx \left(\frac{30m_o^2}{16\pi^2}\right) h_t^2 \ln(M^*/M_{\text{GUT}}) \quad (7.12)$$

The factor $30 \rightarrow 12$ for the case of $G(224)$. The slepton (mass)² matrix thus has the form $\tilde{M}_i^{(o)} = \text{diag}(m_o^2, m_o^2, m_o^2 - \Delta)$. As mentioned earlier, the spin-1/2 lepton mass matrix is diagonalized at the GUT scale by the matrices $X_{L,R}^l$. Applying the same transformation to the slepton (mass)² matrix (which is defined in the gauge basis), i.e. by evaluating $X_L^{l\dagger} (\tilde{M}_i^{(o)})_{LL} X_L^l$ and similarly for $L \rightarrow R$, the transformed slepton (mass)² matrix is no longer diagonal. The presence of these

off-diagonal elements (at the GUT-scale) given by:

$$(\hat{\delta}_{LL,RR}^l)_{ij} = \left(X_{L,R}^{l\dagger}(\tilde{M}_l^{(o)})X_{L,R}^l \right)_{ij} / m_{\tilde{l}}^2 \quad (7.13)$$

induces flavor violating transitions $\tilde{l}_{L,R}^i \rightarrow \tilde{l}_{L,R}^j$. Here $m_{\tilde{l}}$ denotes an average slepton mass and the hat signifies GUT-scale values. Note that while the $(mass)^2$ -shifts given in Eq. (7.12) are the same for the BPW and the AB models, the mass insertions $\hat{\delta}_{LL,RR}$ would be different for the two models since the matrices $X_{L,R}^l$ are different. As mentioned earlier, the approximate analytic expressions for the matrices $X_{L,R}^d$ for the BPW-model can be found in [28]. The corresponding expressions for $X_{L,R}^l$ can be obtained by letting $(\epsilon, \epsilon') \rightarrow -3(\epsilon, \epsilon')$, though we use the exact numerical results in our calculations.

(2) RG Running of the A -parameters from M^* to M_{GUT} .

Even if $A_o = 0$ at the scale M^* (as we assume for concreteness, see also [54]). RG running from M^* to M_{GUT} induces A -parameters at M_{GUT} , involving the $\text{SO}(10)/\text{G}(224)$ gauginos; these yield chirality flipping transitions ($\tilde{l}_{L,R}^i \rightarrow \tilde{l}_{R,L}^j$). If we let $M_{16\text{H}} \approx M_{10\text{H}} \approx M_{\text{GUT}}$, following the general analysis given in [26], the induced A -parameter-matrix for the **BPW** model is given by (see Chapter 6 and Appendix

2 of Chapter 5 for details):

$$(A_{LR}^l)_{\text{BPW}} = (X_L^l)^\dagger \begin{bmatrix} 0 & -285\epsilon' + 90\eta' & 0 \\ 285\epsilon' + 90\eta' & 90\zeta_{22}^d - 27\zeta_{22}^u & -285\epsilon + 90\eta - 27\sigma \\ 0 & 285\epsilon + 90\eta - 27\sigma & 63 \end{bmatrix} X_R^l \times Z \ln\left(\frac{M^*}{M_{\text{GUT}}}\right) \quad (7.14)$$

where $Z = \left(\frac{1}{16\pi^2}\right)h_t g_{10}^2 M_\lambda$. The coefficients $(\frac{63}{2}, \frac{95}{2}, \frac{90}{2})$ are the sums of the Casimirs of the SO(10) representations of the chiral superfields involved in the diagrams. For the case of G(224), we need to use the substitutions: $(\frac{63}{2}, \frac{95}{2}, \frac{90}{2}) \rightarrow (\frac{27}{2}, \frac{43}{2}, \frac{42}{2})$. The $X_{L,R}^l$ are defined in Eq. (7.13). The A-term contribution is directly proportional to the SO(10) gaugino mass M_λ and thus to $m_{1/2}$.

For the **Albright-Barr** model, the induced A-matrix for the leptons is given by:

$$(A_{LR}^l)_{\text{AB}} = Z \ln\left(\frac{M^*}{M_{\text{GUT}}}\right) (X_L^l)^\dagger \begin{bmatrix} 0 & 90\tilde{\delta} & 90\tilde{\delta}'e^{i\phi} \\ 90\tilde{\delta} & 0 & -95\tilde{\epsilon} \\ 90\tilde{\delta}'e^{i\phi} & 90\tilde{\sigma} + 95\tilde{\epsilon} & 63 \end{bmatrix} X_R^l \quad (7.15)$$

$(A_{LR}^l)_{\text{AB}}$ is transformed to the SUSY basis by multiplying it with the matrices that diagonalize the lepton mass matrix i.e. $X_{L,R}^l$ as in Eq.

(7.14). The chirality flipping transition angles are defined as :

$$(\delta_{LR}^l)_{ij} \equiv (A_{LR}^l)_{ij} \left(\frac{v_d}{m_{\tilde{l}_i}^2} \right) = (A_{LR}^l)_{ij} \left(\frac{v_u}{\tan \beta m_{\tilde{l}_i}^2} \right). \quad (7.16)$$

(3) RG Running of scalar masses from M_{GUT} to the RH neutrino mass scales:

We work in a basis in which the charged lepton Yukawa matrix Y_l and M_R^ν are diagonal at the GUT scale. The off-diagonal elements in the Dirac neutrino mass matrix Y_N in this basis give rise to lepton flavor violating off-diagonal components in the left handed slepton mass matrix through the RG running of the scalar masses from M_{GUT} to the RH neutrino mass scales M_{R_i} [27, 127]. The RH neutrinos decouple below M_{R_i} . (For RGEs for MSSM with RH neutrinos see e.g. Ref. [111]). In the leading log approximation, the off-diagonal elements in the left-handed slepton (mass)²-matrix, thus arising, are given by:

$$(\delta_{LL}^l)_{ij}^{\text{RHN}} = \frac{-(3m_o^2 + A_o^2)}{8\pi^2} \sum_{k=1}^3 (Y_N)_{ik} (Y_N^*)_{jk} \ln\left(\frac{M_{\text{GUT}}}{M_{R_k}}\right). \quad (7.17)$$

The superscript RHN denotes the contribution due to the presence of the RH neutrinos. For the case of the AB-model, in the above expression, $(Y_N)_{ik} (Y_N^*)_{jk} \rightarrow (Y_N)_{kj} (Y_N^*)_{ki}$ because of the definition of the

mass-matrices. The masses M_{R_i} of RH neutrinos are determined from Eqs. (7.5) and (7.10) for the BPW and AB models respectively. The total LL contribution, including post-GUT contribution (Eq. (7.13)) and the RH neutrino contribution (Eq. (7.17)), is thus:

$$(\delta_{LL}^l)^{Tot} = (\hat{\delta}_{LL}^l)_{ij} + (\delta_{LL}^l)^{RHN} \quad (7.18)$$

We will see in the next section that this contribution to $\mu \rightarrow e\gamma$ is very different in the two models (noted in part in Ref. [129]) and provides a way to distinguish the two models. We find that this contribution in the AB model is a factor of $\sim 25 - 35$ larger in the the amplitude than that in the BPW model, and this difference arises entirely due to the structure of the mass matrices. We also find that this difference in the mass matrices, also gives rise to large differences in the edm of the electron between the two models.

We now present some results on lepton flavor violation. In the following section we will turn to CP violation, and see how the two models compare.

7.4 Results on Lepton Flavor Violation

The decay rates for the lepton flavor violating processes $l_i \rightarrow l_j \gamma$ ($i > j$) are given by (see the Appendix in Chapter 6):

$$\Gamma(l_i^+ \rightarrow l_j^+ \gamma) = \frac{e^2 m_{l_i}^3}{16\pi} \left(|A_L^{ji}|^2 + |A_R^{ji}|^2 \right) \quad (7.19)$$

Here A_L^{ji} is the amplitude for $(l_i)_L^+ \rightarrow (l_j)^+ \gamma$ decay, while $A_R^{ji} = \text{Amp}((l_i)_R^+ \rightarrow (l_j)^+ \gamma)$. The amplitudes $A_{L,R}^{ji}$ are evaluated in the mass insertion approximation using the $(\delta_{LL}^l)^{Tot}$, δ_{RR}^l and $\delta_{LR,RL}^l$ calculated as above. The general expressions for the amplitudes $A_{L,R}^{ji}$ in one loop can be found in e.g. Refs. [111] and [115]. We include the contributions from both chargino and neutralino loops with or without the μ -term.

In Table 1 we give the branching ratio of the process $\mu \rightarrow e \gamma$ and the individual contributions from the sources $\hat{\delta}_{LL}^{ji}$, $\delta_{LR,RL}^{ji}$ and $(\delta_{LL}^{ji})^{RHN}$ (see Eqs. (7.13), (7.16) and (7.17)) evaluated in the SO(10)-BPW model, with some sample choices of $(m_o, m_{1/2})$. For these calculations, to be concrete, we set $\ln\left(\frac{M^*}{M_{GUT}}\right) = 1$, i.e. $M^* \approx 3M_{GUT}$, $\tan\beta = 10$, $A_o(\text{ at } M^*) = 0$ and $\mu > 0$. In the BPW model, for concreteness, the RH neutrino masses are taken to be $M_{R_1} = 10^{10}$

GeV, $M_{R_2} = 10^{12}$ GeV and $M_{R_3} = 5 \times 10^{14}$ GeV (see Eq. (7.5)).

For the masses of the right-handed neutrinos in the AB model, we set $M_{R_1} = 7.5 \times 10^8$ GeV, $M_{R_2} = 7.5 \times 10^8$ GeV and $M_{R_3} = 2.6 \times 10^{14}$ GeV corresponding to $a = c = 4$ and $b = 6$ in Eq. (7.10). (The results on the rate of $\mu \rightarrow e\gamma$, presented in the following table do not change very much for other ($\mathcal{O}(1)$) values of a , b and c .) It should be noted that *the corresponding values for the $G(224)$ -BPW model are smaller than those for the $SO(10)$ -BPW model approximately by a factor of 4 to 6 in the rate, provided $\ln(M^*/M_{GUT})$ is the same in both cases (see comments below Eqs. (7.12) and (7.14)).* A pictorial representation of these results is depicted in Figs. 1 and 2.

$(m_o, m_{1/2})(\text{GeV})$	$A_L^{(1)}(\hat{\delta}_{LL})$	$A_L^{(2)}(\delta_{LR})$	$A_R(\delta_{RL})$	$A_L^{(3)}((\delta_{LL})^{RHN})$	$\text{Br}(\mu \rightarrow e\gamma)$
(100, 250) BPW	-1.2×10^{-10}	4.5×10^{-13}	-7.2×10^{-11}	3.7×10^{-14}	1.3×10^{-7}
(100, 250) AB	-8.5×10^{-11}	1.9×10^{-12}	-6.4×10^{-11}	1.3×10^{-12}	8.0×10^{-8}
(500, 250) BPW	-1.9×10^{-12}	1.0×10^{-12}	-1.6×10^{-12}	8.5×10^{-14}	2.2×10^{-11}
(500, 250) AB	-1.4×10^{-12}	4.4×10^{-12}	-1.4×10^{-12}	2.9×10^{-12}	2.6×10^{-10}
(800, 250) BPW	-3.5×10^{-13}	6.1×10^{-13}	-2.9×10^{-13}	4.9×10^{-14}	1.3×10^{-12}
(800, 250) AB	-2.6×10^{-13}	2.5×10^{-12}	-2.6×10^{-13}	1.7×10^{-12}	1.1×10^{-10}
(1000, 250) BPW	-1.5×10^{-13}	4.3×10^{-13}	-1.2×10^{-13}	3.5×10^{-14}	8.1×10^{-13}
(1000, 250) AB	-1.1×10^{-13}	1.8×10^{-12}	-1.1×10^{-13}	1.2×10^{-12}	5.9×10^{-11}
(600, 300) BPW	-1.3×10^{-12}	7.2×10^{-13}	-1.1×10^{-12}	5.9×10^{-14}	1.1×10^{-11}
(600, 300) AB	-9.8×10^{-13}	3.0×10^{-12}	-9.7×10^{-13}	2.0×10^{-12}	1.3×10^{-10}

$(m_o, m_{1/2})(\text{GeV})$	$A_L^{(1)}(\hat{\delta}_{LL})$	$A_L^{(2)}(\delta_{LR})$	$A_R(\delta_{RL})$	$A_L^{(3)}((\delta_{LL})^{RHN})$	$\text{Br}(\mu \rightarrow e\gamma)$
(100, 500) BPW	-5.4×10^{-11}	3.5×10^{-14}	-2.8×10^{-11}	2.8×10^{-15}	2.6×10^{-8}
(100, 500) AB	-4.0×10^{-11}	1.5×10^{-13}	-2.5×10^{-11}	9.7×10^{-14}	1.6×10^{-8}
(500, 500) BPW	-4.3×10^{-12}	3.1×10^{-13}	-3.3×10^{-12}	2.5×10^{-14}	1.9×10^{-10}
(500, 500) AB	-3.2×10^{-12}	1.3×10^{-12}	-3.0×10^{-12}	8.6×10^{-13}	7.5×10^{-11}
(1000, 500) BPW	-4.8×10^{-13}	2.6×10^{-13}	-3.9×10^{-13}	2.1×10^{-14}	1.4×10^{-12}
(1000, 500) AB	-3.5×10^{-13}	1.1×10^{-12}	-3.5×10^{-13}	7.3×10^{-13}	1.6×10^{-11}
(200, 1000) BPW	-1.3×10^{-11}	8.8×10^{-15}	-7.1×10^{-12}	7.2×10^{-16}	1.6×10^{-9}
(200, 1000) AB	-9.9×10^{-12}	3.7×10^{-14}	-6.4×10^{-12}	2.4×10^{-14}	1.0×10^{-9}
(1000, 1000) BPW	-1.1×10^{-12}	7.7×10^{-14}	-8.3×10^{-13}	6.3×10^{-15}	1.2×10^{-11}
(1000, 1000) AB	-7.9×10^{-13}	3.2×10^{-13}	-7.4×10^{-13}	2.2×10^{-13}	4.7×10^{-12}

Tab. 7.1:

Table 1. Comparison between the AB and the BPW models of the various contributions to the amplitude and of the branching ratio for $\mu \rightarrow e\gamma$ for the case of SO(10). Each of the entries for the amplitudes should be multiplied by a common factor a_o . Imaginary parts being small are not shown. Only the cases shown in **bold** typeface are in accord with experimental bounds; the other ones are excluded. The first three columns denote contributions to the amplitude from post-GUT physics arising from the regime of $M^* \rightarrow M_{GUT}$ (see Eqs. (7.13)–(7.16)), where for concreteness we have chosen $\ln(M^*/M_{GUT}) = 1$. The fifth column denotes the contribution from the right-handed neutrinos (RHN). Note that the entries corresponding to the RHN-contribution are much larger in the AB-model than those in the BPW-model; this is precisely because the AB-model is lopsided while the BPW model is hierarchical (see text). Note that for the BPW model, the post-GUT contribution far dominates over the RHN-contribution while for the AB model they are comparable. The last column gives the branching ratio of $\mu \rightarrow e\gamma$ including contributions from all four columns. The net result is that the AB model is compatible with the empirical limit on $\mu \rightarrow e\gamma$ only for rather heavy SUSY spectrum like $(m_o, m_{1/2}) \gtrsim (1000, 1000)$ GeV, whereas the BPW is fully compatible with lighter SUSY spectrum like $(m_o, m_{1/2}) \sim (600, 300)$ GeV (see text) for the case of SO(10), and $(m_o, m_{1/2}) \sim (400, 250)$ GeV for

G(224). These results are depicted graphically in Figs. 1 and 2.

Before discussing the features of this table, it is worth noting some distinguishing features of the BPW and the AB models. As can be inferred from Eqs. (7.14) and (7.15), for a given m_o , the post-GUT contribution for both the BPW and the AB models increases with increasing $m_{1/2}$ primarily due to the A-term contribution. It turns out that for $m_{1/2} \gtrsim 300$ GeV, this contribution becomes so large that $\text{Br}(\mu \rightarrow e\gamma)$ exceeds the experimental limit, unless one chooses $m_o \gtrsim 1000$ GeV, so that the rate is suppressed due to large slepton masses. This effect applies to both models.

For the hierarchical BPW model, however, it turns out that the RHN contribution is strongly suppressed both relative to that in the lopsided AB-model; and also relative to the post-GUT contributions (see discussion below). As a result the dominant contribution for the BPW model comes only from post-GUT physics, which decreases with decreasing $m_{1/2}$ for a fixed m_o . Such a dependence on $m_{1/2}$ is not so striking, however, for the AB model because in this case, owing to the lopsided structure, the RHN contribution (which is not

so sensitive to $m_{1/2}$) is rather important and is comparable to the post-GUT contribution.

Tables 1 and 2 bring out some very interesting distinctions between the two models:

(1) The experimental limit on $\mu \rightarrow e\gamma$ is given by: $\text{Br}(\mu \rightarrow e\gamma) < 1.2 \times 10^{-11}$ [108]. This means that for the case of the AB model, with dominant contribution coming not only from post-GUT physics but also from the RHN contribution, only rather heavy SUSY spectrum, $(m_o, m_{1/2}) \gtrsim (1000, 1000)$ GeV, is allowed. The BPW-model, on the other hand, allows for relatively low $m_{1/2}$ ($\lesssim 300$ GeV), with moderate to heavy m_o , which can be as low as about 600 GeV with $m_{1/2} \leq 300$ GeV. *As a result, whereas the AB model is consistent with $\mu \rightarrow e\gamma$ only for rather heavy sleptons ($\gtrsim 1200$ GeV) and heavy squarks ($\gtrsim 2.8$ TeV), the BPW model is fully compatible with much lighter slepton masses ~ 600 GeV, with squarks being 800 GeV to 1 TeV.* These results hold for the case of SO(10). For the G(224) case the BPW model would be consistent with the experimental limit on the rate of $\mu \rightarrow e\gamma$ for even lighter SUSY spectrum including values of $(m_o, m_{1/2}) \approx (400, 250)$

GeV, which corresponds to $m_{\tilde{q}} \sim 780$ GeV and $m_{\tilde{t}} \sim 440$ GeV.

(2) From the point of view of forthcoming experiments we also note that $\mu \rightarrow e\gamma$ for the BPW case, ought to be seen with an improvement in the current limit by a factor of 10–50. For the AB case, even with a rather heavy SUSY spectrum ($(m_o, m_{1/2}) \gtrsim (1000, 1000)$ GeV), $\mu \rightarrow e\gamma$ should be seen with an improvement by a factor of only 3–5. Such experiments are being planned at the MEG experiment at PSI [128]

(3) As has been noted in [129] and in [29] (see Chapter 6), the contribution to $A_L(\mu \rightarrow e\gamma)$ due to RH neutrinos in the BPW model is approximately proportional to $\eta - \sigma \approx 0.041$, which is naturally small because the entries η and σ are of $\mathcal{O}(1/10)$ in magnitude due to the hierarchical structure. In the AB-model on the other hand, this contribution is proportional to $\tilde{\sigma} + 2\tilde{\epsilon}/3 \approx 1.8$. Thus we expect that in amplitude, the RHN contribution in the BPW model is smaller by about a factor of 40 than that in the AB model. This has two consequences:

(a) First, there is a dramatic difference between the two mod-

els which becomes especially prominent if one drops the post-GUT contribution, that amounts to setting $M^* = M_{GUT}$. In this case the contribution to $(\mu \rightarrow e\gamma)$ comes entirely from the RHN contribution. In this case the branching ratio of $(\mu \rightarrow e\gamma)$ in the two models differs by a factor of about $(40)^2 \sim \mathcal{O}(10^3)$ as depicted in table 2.

$(m_o, m_{1/2})(\text{GeV})$	$\text{Br}(\mu \rightarrow e\gamma)_{AB}^{RHN}$	$\text{Br}(\mu \rightarrow e\gamma)_{BPW}^{RHN}$
(100, 250)	1.2×10^{-11}	9.7×10^{-15}
(800, 250)	2.1×10^{-11}	1.7×10^{-14}
(600, 300)	2.8×10^{-11}	2.5×10^{-14}
(500, 500)	5.3×10^{-12}	4.4×10^{-15}
(1000, 1000)	3.4×10^{-13}	2.8×10^{-16}

Table 2. Branching ratio for $(\mu \rightarrow e\gamma)$ based only on the RHN contribution (this corresponds to setting $M^* = M_{GUT}$) for the AB and BPW models for different choices of $(m_o, m_{1/2})$.

It can be seen from table 2 that with only the RHN contribution (which would be the total contribution if $M^* = M_{GUT}$), the AB model is consistent with the limit on $\mu \rightarrow e\gamma$ for light SUSY spectrum, e.g. for $(m_o, m_{1/2}) = (100, 250)$ GeV. A similar analysis for the AB model

was done in Ref. [126] (including the RHN contribution only), and our results agree with those of Ref. [126]. One may expect that for the same value of $m_{1/2}$, increasing m_o would result in decreasing the branching ratio. For example, from Eq. (7.17), one may expect the rate for $\mu \rightarrow e\gamma$ to be proportional to $(m_o^2/m_l^4)^2 \sim 1/m_o^4$. However, the associated loop function (see e.g. Ref. [115]) alters the dependence on $(m_o, m_{1/2})$ drastically; it increases with increasing m_o , for fixed $m_{1/2}$. *The net result of these two effects is that for the same $m_{1/2}$, a low $m_o \sim 100$ GeV and a high $m_o \sim 1000$ GeV, give nearly the same value of the branching ratio for $\mu \rightarrow e\gamma$ with the inclusion of only the RH neutrino contribution (see Fig. 3) .* This can also be seen in the results of Ref. [126] which analyzes the AB model. The RHN contribution in the case of the BPW model is extremely small because of its hierarchical structure, as explained above.

Of course, in the context of supersymmetry breaking as in mSUGRA or gaugino-mediation, we expect $M^* > M_{GUT}$, thus post-GUT contributions should be included at least in these cases. With the inclusion of post-GUT physics, as mentioned above, the AB model is

consistent with the experimental limit on $\mu \rightarrow e\gamma$, only for very heavy SUSY spectrum with $(m_o, m_{1/2}) \gtrsim (1000, 1000)$ GeV, i.e. $m_{\tilde{l}} \gtrsim 1200$ GeV and $m_{\tilde{q}} \gtrsim 2.8$ TeV; whereas the BPW model is fully compatible with the empirical limit for significantly lower values of $(m_o, m_{1/2}) \sim (600, 300)$ GeV, i.e. $m_{\tilde{l}} \sim 600$ GeV and $m_{\tilde{q}} \sim 1$ TeV (see table 1).

(b) Second, it was shown in Ref. [29] that the P-odd asymmetry parameter for the process $(\mu^+ \rightarrow e^+\gamma)$ defined as $\mathcal{A}(\mu^+ \rightarrow e^+\gamma) = (|A_L|^2 - |A_R|^2)/(|A_L|^2 + |A_R|^2)$ (where $|A_L| = |A_L^{(1)}(\hat{\delta}_{LL}) + A_L^{(2)}(\delta_{LR}) + A_L^{(3)}|$), is typically negative for the BPW model except for cases with very large $m_{1/2}$ e.g. $(m_o, m_{1/2}) = (1000, 1000)$ or $(500, 500)$ GeV. For the AB-case, due to the large RHN contribution, $|A_L| > |A_R|$ and therefore the P-odd asymmetry parameter \mathcal{A} would typically be positive. Thus the determination of \mathcal{A} in future experiments can help distinguish between the BPW and the AB models.

For the sake of completeness, we give the branching ratios of the processes $\tau \rightarrow \mu\gamma$ and $\tau \rightarrow e\gamma$ calculated in the two models in table 3.

$(m_o, m_{1/2})(\text{GeV})$	AB-model		BPW-model	
	$\text{Br}(\tau \rightarrow \mu\gamma)$	$\text{Br}(\tau \rightarrow e\gamma)$	$\text{Br}(\tau \rightarrow \mu\gamma)$	$\text{Br}(\tau \rightarrow e\gamma)$
(100, 250)	2.9×10^{-9}	3.8×10^{-11}	2.6×10^{-7}	1.6×10^{-9}
(800, 250)	1.0×10^{-8}	4.5×10^{-11}	1.6×10^{-9}	6.8×10^{-12}
(600, 300)	1.4×10^{-8}	6.4×10^{-11}	2.1×10^{-9}	8.4×10^{-12}
(500, 500)	2.4×10^{-9}	1.0×10^{-11}	3.9×10^{-10}	1.8×10^{-12}
(1000, 1000)	1.5×10^{-10}	6.5×10^{-13}	2.5×10^{-11}	1.1×10^{-13}

Table 3.

Table 3. Branching ratios for $(\tau \rightarrow \mu\gamma)$ and $(\tau \rightarrow e\gamma)$ evaluated in the two models for the case of SO(10), for some sample choices of $(m_o, m_{1/2})$. We have set $\tan\beta = 10$, $\mu > 0$ and $\ln\left(\frac{M^*}{M_{GUT}}\right) = 1$.

From table 3 we see that the predictions for the branching ratios for $(\tau \rightarrow \mu\gamma)$ and $(\tau \rightarrow e\gamma)$ in either model are well below the current experimental limits. The process $(\tau \rightarrow \mu\gamma)$ can be probed at BABAR and BELLE or at LHC in the forthcoming experiments; $(\tau \rightarrow e\gamma)$ seems to be out of the reach of the upcoming experiments.

In the following section we turn to CP violation in the two models.

7.5 Results on Fermion Masses, CKM Elements and CP Violation

CP violation in the BPW model [28] was studied in detail in Chapter 5. We will recapitulate some of those results and do a comparative study with the AB model. For any choice of the parameters in the mass matrices (η, σ, ϵ etc. for the BPW case, and $\tilde{\sigma}, \tilde{\epsilon}$ etc. for the AB case), one gets the SO(10)-model based values of ρ_W and η_W , which generically can differ widely from the SM-based phenomenological values. We denote the former by $(\rho'_W)_{BPW,AB}$ and $(\eta'_W)_{BPW,AB}$ and the

corresponding contributions from the SM-interactions (based on ρ'_W and η'_W) by SM'. In our calculations we include both the SM' contribution and the SUSY contributions involving the sfermion $(mass)^2$ -parameters($\delta_{LL,RR,LR}^{ij}$) which are in general CP violating. These parameters are completely determined in each of the two models for a given choice of flavor preserving SUSY-parameters (i.e. m_o , $m_{1/2}$, μ , and $\tan \beta$; we set $A_o = 0$ at M^*). Using the fits given in Eqs. (7.7) and (7.11), we get the following values for the CKM elements and fermion masses using $m_t(m_t) = 167 \text{ GeV}$ and $m_\tau(m_\tau) = 1.777 \text{ GeV}$ as inputs:

BPW:

$$\begin{aligned}
((V_{us}, V_{cb}, |V_{ub}|, |V_{td}|)(\leq m_Z))_{BPW} &\approx (0.2250, 0.0412, 0.0037, 0.0086) \\
(\bar{\rho}'_W)_{BPW} &= 0.150, \quad (\bar{\eta}'_W)_{BPW} = 0.374 \\
(m_b(m_b), m_c(m_c)) &\approx (4.97, 1.32) \text{ GeV} \\
(m_s(1\text{GeV}), m_\mu) &\approx (101, 109) \text{ MeV} \\
(m_u^\circ(1\text{GeV}), m_d^\circ(1\text{GeV}), m_e^\circ) &\approx (10.1, 3.7, 0.13) \text{ MeV}
\end{aligned} \tag{7.20}$$

AB:

$$\begin{aligned}
((V_{us}, V_{cb}, |V_{ub}|, |V_{td}|)(\leq m_Z))_{AB} &\approx (0.220, 0.041, 0.0032, 0.0081) \\
(\bar{\rho}'_W)_{AB} &= 0.148, \quad (\bar{\eta}'_W)_{AB} = 0.309 \\
(m_b(m_b), m_c(m_c)) &\approx (4.97, 1.15) \text{ GeV} \\
(m_s(1\text{GeV}), m_\mu) &\approx (177, 106) \text{ MeV} \\
(m_u^\circ(1\text{GeV}), m_d^\circ(1\text{GeV}), m_e^\circ) &\approx (3.2, 8.5, 0.56) \text{ MeV}
\end{aligned} \tag{7.21}$$

The predictions of both models for the CKM elements are in good agreement with the measured values, and $(\bar{\rho}'_W)$ and $(\bar{\eta}'_W)$ are close to the SM values in each case. It was remarked in Ref. [28] that for the BPW model, the masses of the light fermions (u, d and e) can be corrected by allowing for $\mathcal{O}(10^{-4} - 10^{-5})$ “11” entries in the mass matrices which can arise naturally through higher dimensional operators. Such small entries will not alter the predictions for the CKM mixings.² For the AB model, the masses of the bottom and

² The superscript “ \circ ” in Eq. (7.20), denotes that the masses of the light fermions (u,d and e) at the 1 GeV scale need corrections of few MeV to be in accord with the observations. It was noted in Ref. [28] that “11” entries in the mass matrices of order $10^{-4} - 10^{-5}$ arising from higher dimensional operators can lead to a needed reduction in m_u by 6-8 MeV and an increase in m_e and m_d by 0.36 and 2-3 MeV respectively at the GeV scale without altering the CKM elements. The “11” entries in the up sector can differ from those in the down sector in sign because of contributions through the operator $\mathbf{16}_1 \mathbf{16}_1 \mathbf{16}_H^d (\mathbf{16}_H/M)(S/M)^n$ which contributes only to m_e and m_d but not to m_u .

strange quarks have been lowered by the gluino loop contributions from 5.12 GeV and 183 MeV to 4.97 GeV and 177 MeV respectively. Thus from Eqs. (7.20) and (7.21), we see that both models are capable of yielding the gross pattern of fermion masses and especially the CKM mixings in good accord with observations; at the same time ($\bar{\rho}'_W$) and ($\bar{\eta}'_W$) are close to the phenomenological SM values.

We now present some results on CP violation. We include both the SM' and the SUSY contributions in obtaining the total contributions (denoted by “Tot”). The SUSY contribution is calculated using the squark mixing elements, $\delta_{LL,RR,LR}^{ij}$, which are completely determined in both models for any given choice of the SUSY breaking parameters m_o , $m_{1/2}$, A_o , $\tan\beta$ and $\text{sgn}(\mu)$. As emphasized earlier, in our calculations, the δ^{ij} s include contributions from both post-GUT physics as well as those coming from RG running in MSSM below the GUT scale. (For details, see Ref. [28] and Chapter 5). We set $A_o = 0$ for concreteness, as before. Listed below in Table 4 are the results on CP and flavor violations in the $K^\circ - \bar{K}^\circ$ and $B_d^\circ - \bar{B}_d^\circ$ systems for the two models. For these calculations we set $\ln(M^*/M_{GUT}) = 1$.

$(m_o, m_{1/2})(\text{GeV})$	$\Delta m_K^{s,d.}(\text{GeV})$ Tot \approx SM'	$\epsilon_K(\text{SM}')$	$\epsilon_K(\text{Tot})$	$\Delta m_{B_d}(\text{GeV})$ Tot \approx SM'	$S_{\psi K_S}$ Tot \approx SM'
(300, 300) BPW	2.9×10^{-15}	2.8×10^{-3}	2.6×10^{-3}	3.5×10^{-13}	0.73
(300, 300) AB	2.8×10^{-15}	2.2×10^{-3}	2.2×10^{-3}	3.1×10^{-13}	0.66
(600, 300) BPW	2.9×10^{-15}	2.8×10^{-3}	2.0×10^{-3}	3.6×10^{-13}	0.73
(600, 300) AB	2.8×10^{-15}	2.2×10^{-3}	1.4×10^{-3}	3.1×10^{-13}	0.66
(1000, 250) BPW	2.9×10^{-15}	2.8×10^{-3}	1.4×10^{-3}	3.6×10^{-13}	0.74
(1000, 250) AB	2.8×10^{-15}	2.2×10^{-3}	-4.0×10^{-3}	3.13×10^{-13}	0.656
(1000, 500) BPW	2.9×10^{-15}	2.83×10^{-3}	2.6×10^{-3}	3.6×10^{-13}	0.73
(1000, 500) AB	2.8×10^{-15}	2.2×10^{-3}	2.0×10^{-3}	3.1×10^{-13}	0.66
(1000, 1000) BPW	2.9×10^{-15}	2.8×10^{-3}	2.9×10^{-3}	3.5×10^{-13}	0.72
(1000, 1000) AB	2.8×10^{-15}	2.2×10^{-3}	2.3×10^{-3}	3.1×10^{-13}	0.66

Table 4.

Table 4. CP violation in the $K^\circ - \overline{K^\circ}$ and $B_d - \overline{B_d}$ systems as predicted in the BPW and the AB models for some sample choices of $(m_o, m_{1/2})$ and a generic fit of parameters (see Eq.(7.7) for the BPW case and Eq. (7.11) for the AB case). The superscript s.d. on Δm_K denotes the short distance contribution. The predictions in either model are in good agreement with experimental data for most of the cases displayed above, especially given the uncertainties in the matrix elements (see text). It may be noted that values of $S(B_d \rightarrow J/\psi K_S)$ as high as 0.74 in the AB model, and as low as 0.65 in the BPW model, can be achieved by varying the fit.

In obtaining the entries for the K -system we have used central values of the matrix element \hat{B}_K and the loop functions η_i (see Refs. [74, 86] for definitions and values) characterizing short distance QCD effects - i.e. $\hat{B}_K = 0.86 \pm 0.13$, $f_K = 159 \text{ MeV}$, $\eta_1 = 1.38 \pm 0.20$, $\eta_2 = 0.57 \pm 0.01$ and $\eta_3 = 0.47 \pm 0.04$. For the B -system we use the central values of the unquenched lattice results: $f_{B_d} \sqrt{\hat{B}_{B_d}} = 215(11)_{(-23)}^{(+0)}(15) \text{ MeV}$ [87] and $f_{B_s} \sqrt{\hat{B}_{B_s}} = 262 \pm 35 \text{ MeV}$ [89]. Note that the uncertainties in some of these hadronic parameters are in the range of 15%; thus the predictions of the two SO(10) models as well as those of the SM would be uncertain at present to the same extent.

Some points of distinctions and similarities between the two models are listed below.

(1) First note that the data point $(m_o, m_{1/2}) = (300, 300)$ GeV displayed above, though consistent with CP violation, gives too large a value for $\text{Br}(\mu \rightarrow e\gamma)$ for both BPW and AB models. All other cases shown in table 4 are consistent with the experimental limit on $\mu \rightarrow e\gamma$ for the BPW model. For the AB model on the other hand, as may be inferred from table 1, the choice $(m_o, m_{1/2}) = (1000, 1000)$ GeV is the only case that is consistent with the limit on $\mu \rightarrow e\gamma$ (see table 1). It is to be noted that for this case the squark masses are extremely high (~ 2.8 TeV), and therefore, in the AB model, once the $\mu \rightarrow e\gamma$ constraint is satisfied, the SUSY contributions are strongly suppressed for all four entities: Δm_K , ϵ_K , Δm_{B_d} and $S(B_d \rightarrow J/\psi K_S)$.

(2) For the BPW model on the other hand, there are good regions of parameter space allowed by the limit on the rate of $\mu \rightarrow e\gamma$ (e.g. $(m_o, m_{1/2}) = (600, 300)$ GeV), which are also in accord with ϵ_K . The SUSY contribution to ϵ_K for these cases is sizable ($\sim 20 - 30\%$) and negative, as desired.

(3) We have exhibited the case $(m_o, m_{1/2}) = (1000, 250)$ GeV to illustrate that this case does not work for either model as it gives too low a value for ϵ_K in the BPW model, and a negative value in the AB model. In this case the SUSY contribution, which is negative, is sizable because of the associated loop functions which are increasing functions of $(m_{sq}^2/m_{\tilde{g}}^2)$.

(4) The predictions regarding Δm_K , Δm_{B_d} and $S(B_d \rightarrow J/\psi K_S)$ are very similar in both the models, i.e they are both close to the SM value.

(5) As noted above, there are differences between the predictions of the BPW vs. the AB models for ϵ_K for a given $(m_o, m_{1/2})$. With uncertainties in \hat{B}_K and the SUSY spectrum, ϵ_K cannot, however, be used at present to choose between the two models, but if $(m_o, m_{1/2})$ get determined (e.g. following SUSY searches at the LHC) and \hat{B}_K is more precisely known through improved lattice calculations, ϵ_K can indeed distinguish between the BPW and the AB models, as also between SO(10) and G(224) models (for details on this see Ref. [28]). This distinction can be sharpened especially by searches for $\mu \rightarrow e\gamma$.

(6) $B_d \rightarrow \phi K_S$, Δm_{B_s} : Including the SM' and SUSY contributions to the decay $B_d \rightarrow \phi K_S$, we get the following results for the CP violating asymmetry parameter $S(B_d \rightarrow \phi K_S)$ in the two models:

$$\mathbf{BPW} : S(B_d \rightarrow \phi K_S) \approx +0.65 - 0.74 . \quad (7.22)$$

$$\mathbf{AB} : S(B_d \rightarrow \phi K_S) \approx +0.61 - 0.65 .$$

The values displayed above for the AB model are calculated for the fit given in Eq. (7.11). For variant fits in the AB model, values as high as $S(B_d \rightarrow \phi K_S) \approx 0.7$ may be obtained. The SUSY contribution to the amplitude for the decay $B_d \rightarrow \phi K_S$ in the BPW model is only of order 1%, whereas in the AB model it is nearly 5% for light SUSY spectrum ($(m_o, m_{1/2}) \sim (300, 300)$ GeV) and about 1% for large $(m_o, m_{1/2}) (\sim (1000, 500)$ GeV). The main point to note is that in both models $S(B_d \rightarrow \phi K_S)$ is positive in sign and close to the SM prediction. The current experimental values for the asymmetry parameter are $S(B_d \rightarrow \phi K_S) = (+0.50 \pm 0.25_{-0.04}^{+0.07})_{BaBar}; (+0.50 \pm 0.21 \pm 0.06)_{BELLE}$ [91]. It will thus be extremely interesting from the viewpoint of the two frameworks presented here to see whether the true value of $S(B_d \rightarrow \phi K_S)$ will turn out to be close to the SM-prediction or not.

Including SUSY contributions to $B_s - \overline{B}_s$ mixing coming from $\delta_{LL,RR,LR,RL}^{23}$ insertions we get:

$$\mathbf{BPW} : \Delta m_{B_s}(Tot \approx SM') \approx \mathbf{19.8 \pm 4.9} \text{ ps}^{-1}. \quad (7.23)$$

$$\mathbf{AB} : \Delta m_{B_s}(Tot \approx SM') \approx \mathbf{19.0 \pm 4.8} \text{ ps}^{-1}.$$

where we have used $f_{B_s} \sqrt{\hat{B}_{B_s}} = 262 \pm 35 \text{ MeV}$ [89]. Both predictions are compatible with the present value $\Delta m_{B_s} = 17.35_{-0.21}^{+0.42} \text{ (stat)} \pm 0.07 \text{ (syst)} \text{ ps}^{-1}$ [89].

(7) **Contribution of the A term to ϵ'_K** : Direct CP violation in $K_L \rightarrow \pi\pi$ receives a new contribution from the chromomagnetic operator $Q_g^- = (g/16\pi^2)(\bar{s}_L\sigma^{\mu\nu}t^a d_R - \bar{s}_R\sigma^{\mu\nu}t^a d_L)G_{\mu\nu}^a$, which is induced by the gluino penguin diagram. This contribution is proportional to $Im[(\delta_{LR}^d)_{21} - (\delta_{LR}^d)_{12}^*]$, which is known in both models (see Eqs. (7.14) and (7.15)). Following Refs. [93] and [94], one obtains:

$$Re(\epsilon'/\epsilon)_{\tilde{g}} \approx 91 B_G \left(\frac{110 \text{ MeV}}{m_s + m_d}\right) \left(\frac{500 \text{ GeV}}{m_{\tilde{g}}}\right) Im[(\delta_{LR}^d)_{21} - (\delta_{LR}^d)_{12}^*] \quad (7.24)$$

where B_G is the relevant hadronic matrix element. Model-dependent considerations (allowing for m_K^2/m_π^2 corrections) indicate that $B_G \approx 1 - 4$, and that it is positive [93]. Putting in the values of $\delta_{LR}^d)_{12,21}$ obtained in each model with $(m_o, m_{1/2}) =$ (a) (600, 300) GeV, and

(b) (1000, 1000) GeV, we get:

$$\begin{aligned}
\mathbf{BPW} : \quad Re(\epsilon'/\epsilon)_{\tilde{g}} &\approx +(3.7 \times 10^{-4})(B_G/4)(10/\tan\beta) \quad \text{Case (a)} . \\
&\approx +(4.5 \times 10^{-5})(B_G/4)(10/\tan\beta) \quad \text{Case (b)} . \\
\mathbf{AB} : \quad Re(\epsilon'/\epsilon)_{\tilde{g}} &\approx -(3.7 \times 10^{-5})(B_G/4)(10/\tan\beta) \quad \text{Case (a)} . \\
&\approx +(4.5 \times 10^{-6})(B_G/4)(10/\tan\beta) \quad \text{Case (b)} .
\end{aligned} \tag{7.25}$$

Whereas both cases (a) and (b) are consistent with the limit on $\mu \rightarrow e\gamma$ for the BPW model, only case (b) is in accord with $\mu \rightarrow e\gamma$ for the AB model. The observed value of $Re(\epsilon'/\epsilon)_{obs}$ is given by $Re(\epsilon'/\epsilon)_{obs} = (17 \pm 2) \times 10^{-4}$ [100]. At present the theoretical status of SM contribution to $Re(\epsilon'/\epsilon)$ is rather uncertain. For instance, the results of Ref. [95] and [96] based on quenched lattice calculations in the lowest order chiral perturbation theory suggest negative central values for $Re(\epsilon'/\epsilon)$. (To be specific Ref. [95] yields $Re(\epsilon'/\epsilon)_{SM} = (-4.0 \pm 2.3) \times 10^{-4}$, the errors being statistical only.) On the other hand, using methods of partial quenching [97] and staggered fermions, positive values of $Re(\epsilon'/\epsilon)$ in the range of about $(3 - 13) \times 10^{-4}$ are obtained in [98]. In addition, a recent non-lattice calculation based on next-to-leading order chiral perturbation theory yields $Re(\epsilon'/\epsilon)_{SM} = (19 \pm 2_{-6}^{+9} \pm 6) \times 10^{-4}$ [99].

The systematic errors in these calculations are at present hard to estimate. The point to note here is that the BPW model predicts a relatively large and positive SUSY contribution to $Re(\epsilon'/\epsilon)$, especially for case (a), which can eventually be relevant to a full understanding of the value of ϵ'_K , whereas this contribution in the AB model is rather small for both cases. Better lattice calculations can hopefully reveal whether a large contribution, as in the BPW model, is required or not.

(8) **EDM of the neutron and the electron:** RG-induced A -terms of the model generate chirality-flipping sfermion mixing terms $(\delta_{LR}^{d,u,l})_{ij}$, whose magnitudes *and* phases are predictable in the two models (see Eq. (7.16)), for a given choice of the universal SUSY-parameters (m_o , $m_{1/2}$, *and* $\tan\beta$). These contribute to the EDM's of the quarks and the electron by utilizing dominantly the gluino and the neutralino loops respectively. We will approximate the latter by using the bino-loop. These contributions are given by (see e.g. [101]):

$$\begin{aligned}
 (d_d, d_u)_{A_{ind}} &= \left(-\frac{2}{9}, \frac{4}{9}\right) \frac{\alpha_s}{\pi} e \frac{m_{\tilde{g}}}{m_{sq}^2} f\left(\frac{m_{\tilde{g}}^2}{m_{sq}^2}\right) \text{Im}(\delta_{LR}^{d,u})_{11} \\
 (d_e)_{A_{ind}} &= -\frac{1}{4\pi} \frac{\alpha_{em}}{\cos^2\theta_W} e \frac{m_{\tilde{B}}}{m_{\tilde{l}}^2} f\left(\frac{m_{\tilde{B}}^2}{m_{\tilde{l}}^2}\right) \text{Im}(\delta_{LR}^l)_{11} .
 \end{aligned}
 \tag{7.26}$$

The EDM of the neutron is given by $d_n = \frac{1}{3}(4d_d - d_u)$. The up sector

being purely real implies $d_u = 0$ in the AB model. In table 5 we give the values of d_n and d_e calculated in the two models for moderate and heavy SUSY spectrum and $\tan \beta = 10$.

$(m_o, m_{1/2})(\text{GeV})$	AB-model		BPW-model	
	d_n (e-cm)	d_e (e-cm)	d_n (e-cm)	d_e (e-cm)
I (600, 300)	4.0×10^{-26}	1.6×10^{-27}	1.1×10^{-26}	1.1×10^{-29}
II (1000, 500)	1.4×10^{-26}	5.9×10^{-28}	3.9×10^{-27}	4.1×10^{-30}
III (1000, 1000)	5.7×10^{-27}	1.1×10^{-27}	1.7×10^{-27}	7.7×10^{-30}
Expt. upper bound	6.3×10^{-26}	4.3×10^{-27}	6.3×10^{-26}	4.3×10^{-27}

Table 5.

Table 5. EDMs of neutron and electron calculated in the BPW and the AB models for moderate and heavy SUSY spectrum and $\tan\beta = 10$ arising only from the induced A-terms. While all cases are consistent with $\mu \rightarrow e\gamma$ for the BPW model, only case III is consistent for the AB model.

From the table above, we see that while both models predict that the EDM of the neutron should be seen within an improvement by a factor of 5–10 in the current experimental limit, their predictions regarding the EDM of the electron are quite different. While the AB model predicts that the EDM of the electron should be observed with an improvement by a factor of 5–10 in the current experimental limit, the prediction of the BPW model for the EDM of the electron is that it is 2 to 3 orders of magnitude smaller than the current upper bound. These predictions are in an extremely interesting range; while future experiments on edm of the neutron can provide support for or deny both models, those on the edm of the electron can clearly distinguish between the two models.

7.6 Conclusions

In summary, a comparative study of two realistic SO(10) models: the hierarchical Babu-Pati-Wilczek (BPW) model and the lop-sided Albright-Barr (AB) model is presented. Both models have been shown to successfully describe fermion masses, CKM mixings and neutrino oscillations. Here we compared the two models with respect to their predictions regarding CP and flavor violations in the quark and lepton sectors. CP violation is assumed to arise primarily through phases in fermion mass matrices (see e.g. Ref. [28]). For all processes we include the SM as well as SUSY contributions. For the SUSY contributions, assuming that the SUSY messenger scale M^* lies above M_{GUT} as in a mSUGRA model, we include contributions from both post-GUT physics as well as those arising due to RG running in MSSM below the GUT scale. While this has been done before for the BPW model in Refs. [28] and [29], this is the first time that flavor and CP violations have been studied in the AB model *including* both post-GUT and sub-GUT physics. This inclusion brings out important distinctions between the two models.

Previous works on lepton flavor violation in the AB model [124] have included only the RHN contribution associated with sub-GUT physics. It is important to note, however, that in both models the sfermion-transition elements $\delta_{LL,RR,LR,RL}^{ij}$ and the induced A parameters get fully determined for a given choice of soft SUSY-breaking parameters (m_o , $m_{1/2}$, A_o , $\tan\beta$ and $\text{sgn}(\mu)$) and thus both contributions are well determined. Including both contributions, we find the following similarities and distinctions between the two models.

Similarities:

- Both models are capable of yielding values of the Wolfenstein parameters (ρ'_W , η'_W) which are close to the SM values and simultaneously the right gross pattern for fermion masses, CKM elements and neutrino oscillations. For this reason, both models give the values of Δm_K , Δm_{B_d} and $S(B_d \rightarrow J/\psi K_S)$ that are close to the SM predictions and agree quite well with the data. The SUSY contribution to these processes is small ($\lesssim 3\%$).
- For the case of ϵ_K , it is found that for the BPW model, the SM' value is larger than the observed value by about 20% for central values of

\hat{B}_K and η_i , but the SUSY contribution is sizable and negative, so that the net value can be in good agreement with the observed value for most of the SUSY parameter space. For the AB model, for the choice of input parameters as in Eq. (7.11), the SM' value for ϵ_K is close to the observed value. For most of the soft-SUSY parameter space the AB model also yields ϵ_K in good agreement with the observed value once one allows for uncertainties in the matrix elements (see table 4).

- Both models predict that $S(B_d \rightarrow \phi K_S)$ should be $\approx +0.65 - 0.74$, close to the SM predictions.
- The predictions regarding Δm_{B_s} are similar and compatible with the experimental limit in both models.
- Both models predict the EDM of the neutron to be ($few \times 10^{-26} e - cm$) which should be observed with an improvement in the current limit by a factor of 5–10.

Thus a confirmation of these predictions on the edm of the neutron and $S(B_d \rightarrow \phi K_S)$, would go well with the two models, but cannot distinguish between them.

Distinctions:

- The lepton sector brings in impressive distinction between the two models through lepton flavor violation and through the EDM of the electron as noted below.

- The BPW model gives $\text{BR}(\mu \rightarrow e\gamma)$ in the range of $10^{-11} - 10^{-13}$ for slepton masses $\lesssim 500$ GeV with the restriction that $m_{1/2} \lesssim 300$ GeV (see remarks below table 1). Thus it predicts that $\mu \rightarrow e\gamma$ should be seen in upcoming experiments which will have a sensitivity of $10^{-13} - 10^{-14}$ [128]. The contribution to $\mu \rightarrow e\gamma$ in the AB model is generically much larger than that of the BPW model. For it to be consistent with the experimental upper bound on $\text{BR}(\mu \rightarrow e\gamma)$, the AB model would require a rather heavy SUSY spectrum, i.e. $(m_o, m_{1/2}) \gtrsim (1000, 1000)$ GeV, i.e. $m_{\tilde{l}} \gtrsim 1200$ GeV and $m_{\tilde{q}} \gtrsim 2.8$ TeV. With the constraints on $(m_o, m_{1/2})$ as noted above, both models predict that $\mu \rightarrow e\gamma$ should be seen with an improvement in the current limit which needs to be a factor of 10–50 for the BPW model and a factor of 3–5 for the AB model.

- An interesting distinction between the AB and the BPW models arises in their predictions for the EDM of the electron. The AB model

give d_e in the range $10^{-27} - 10^{-28} e \text{ cm}$ which is only a factor of 3–10 lower than the current limit. Thus the AB model predicts that the EDM of the electron should be seen in forthcoming experiments. The BPW model on the other hand predicts a value of d_e in the range $10^{-29} - 10^{-30} e \text{ cm}$ which is about 100–1000 times lower than the current limit.

- In the quark sector, another interesting distinction between the two models comes from ϵ'/ϵ . The BPW model predicts that $\text{Re}(\epsilon'/\epsilon)_{SUSY} \approx +5 \times 10^{-4} (B_G/4) (10/\tan \beta)$. Thus the BPW model predicts that SUSY will give rise to a significant positive contribution to ϵ'/ϵ , assuming B_G is positive [93]. The AB model gives $\text{Re}(\epsilon'/\epsilon)_{SUSY} \approx -5 \times 10^{-5} (B_G/4) (10/\tan \beta)$. Thus it predicts that the SUSY contribution is $\sim \mathcal{O}(1/10)$ the experimental value and is negative. Since the current theoretical status of the SM contribution to $\text{Re}(\epsilon'/\epsilon)$ is uncertain, the relevance of these contributions can be assessed only after the associated matrix elements are known reliably.

In conclusion, the Babu-Pati-Wilczek model and the Albright-Barr model have both been extremely successful in describing fermion

masses and mixings and neutrino oscillations. In this note, including all three important sources of flavor violation (two of which have been neglected in the past), we have seen that CP and flavor violation can bring out important distinctions between the two models, especially through studies of $\mu \rightarrow e\gamma$ and the edm of the electron. It will be extremely interesting to see how these two models fare against the upcoming experiments on CP and flavor violation.

7.7 *Figures*

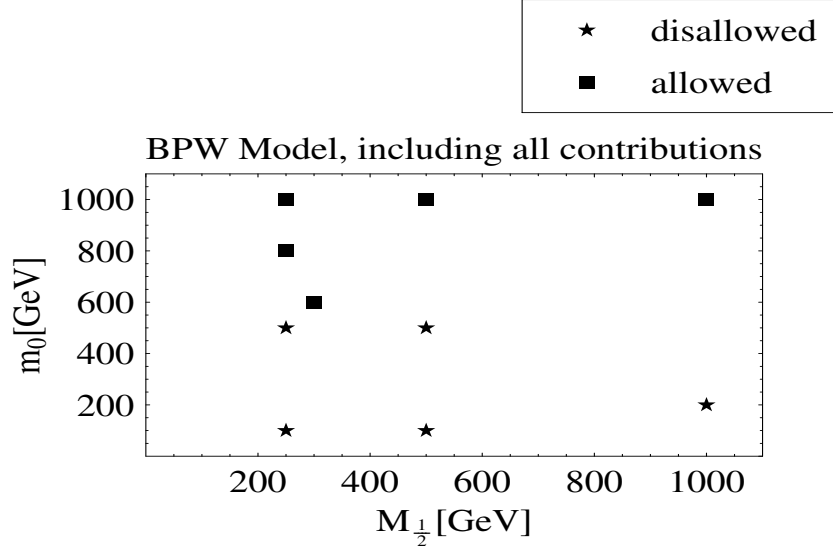


Fig. 7.1: Regions in the $(m_o, m_{1/2})$ plane allowed and disallowed by the current experimental limit on $\text{Br}(\mu \rightarrow e\gamma) = 1.2 \times 10^{-11}$ as obtained for the BPW model with $\ln(M^*/M_{GUT}) = 1$, $\tan \beta = 10$ and $\mu > 0$. The points allowed by the limit on $\text{Br}(\mu \rightarrow e\gamma)$ are marked with a box, while the points disallowed by this limit are marked with a star. The results include post-GUT and RHN contributions to the rate of $\mu \rightarrow e\gamma$. Note that a large region of parameter space is allowed.

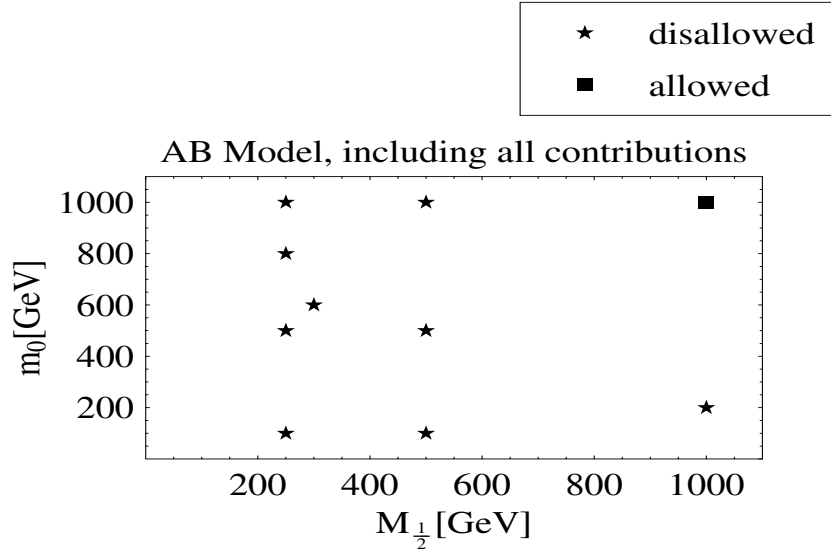


Fig. 7.2: Regions in the $(m_o, m_{1/2})$ plane allowed and disallowed by the current experimental limit on $\text{Br}(\mu \rightarrow e\gamma) = 1.2 \times 10^{-11}$ as obtained for the AB model with $\ln(M^*/M_{GUT}) = 1$, $\tan\beta = 10$ and $\mu > 0$. The points allowed by the limit on $\text{Br}(\mu \rightarrow e\gamma)$ are marked with a box, while the points disallowed by this limit are marked with a star. The results include post-GUT and RHN contributions to the rate of $\mu \rightarrow e\gamma$. Note that, only a rather heavy SUSY spectrum with $(m_o, m_{1/2}) \gtrsim (1000, 1000)$ GeV is allowed by the limit on $\mu \rightarrow e\gamma$. This corresponds to a squark mass of ~ 2.8 TeV and a slepton mass of ~ 1200 GeV.

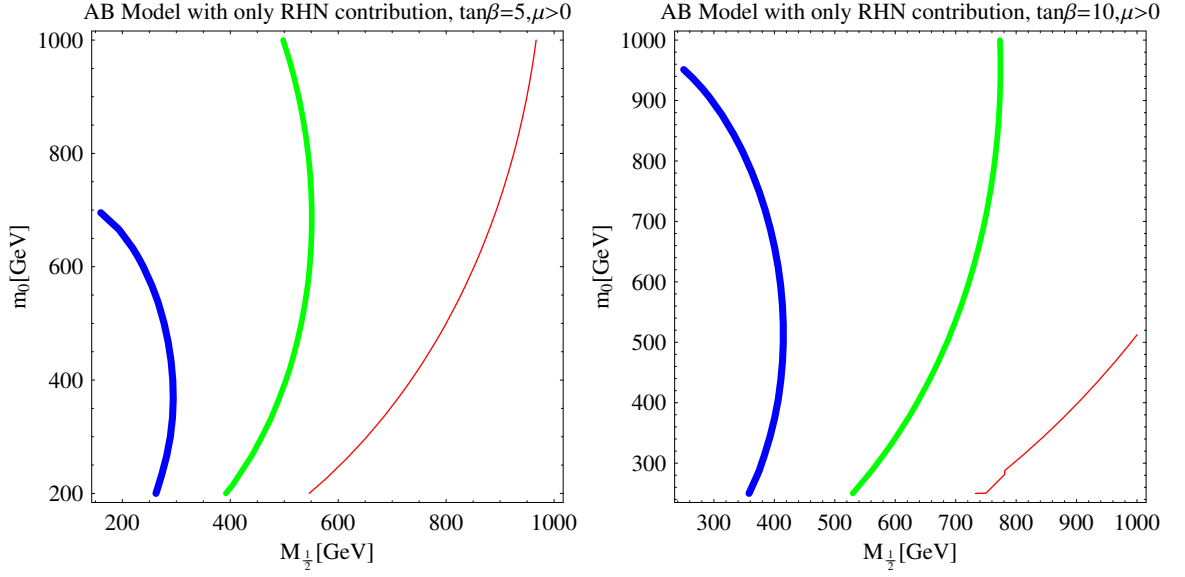


Fig. 7.3: Curves of constant $\text{Br}(\mu \rightarrow e\gamma)$ in the $(m_o, m_{1/2})$ plane with only the right handed neutrino contribution for the case of the AB model. The thickest (blue) line corresponds to the experimental limit of 1.2×10^{-11} , the medium (green) line to $\text{Br}(\mu \rightarrow e\gamma) = 10^{-12}$, and the thinnest (red) one to $\text{Br}(\mu \rightarrow e\gamma) = 10^{-13}$. A similar analysis was carried out in Ref. [126].

8. COUPLING UNIFICATION FOR AN EFFECTIVE G(224) OR G(214) SYMMETRY: COMPATIBILITY WITH STRING UNIFICATION

8.1 Introduction

It has been noted in Chapters 1 and 3 that the evidence in favor of supersymmetric grand unification is now rather strong, especially because of the observation that the three gauge couplings of the standard model unify at a scale $M_U \sim 10^{16}$ GeV, in the context of supersymmetry, and also because of the discovery of neutrino oscillations with $\sqrt{\Delta m^2(\nu)_{23}} \sim 1/20$ eV. It has been argued (see e.g. [62] and Chapter 3) that a set of facts including including (a) neutrino oscillations, (b) certain empirically favored relations between fermion masses: $m_b(\text{GUT}) \approx m_\tau$ and $m(\nu_{\text{Dirac}}^\tau) \approx m_{\text{top}}(\text{GUT})$ (needed for the success of the seesaw mechanism) and (c) baryogenesis via leptogenesis, strongly suggest that the symmetry above the unification

scale should maximally be either $SO(10)$ [18] (possibly E_6 [19]) or an effective $G(224) \equiv SU(2)_L \times SU(2)_R \times SU(4)^c$ symmetry [12] as opposed to other alternatives such as $SU(5)$ [13] or $[SU(3)]^3$ [21]. As noted in Chapter 3, the main advantages of $SO(10)$ or $G(224)$ arise because they contain the symmetry $SU(4)$ -color. Assuming that such an effective theory has its origin within an underlying unified theory that includes quantum gravity, it is natural to assume that it emerges from the compactification of string/M-theory defined in higher dimensions, $d=10/11$, near the string scale ($M_{st} \gtrsim M_{GUT}$) [36], and that effective symmetry $G(224)$ or $G(214) \equiv SU(2)_L \times U(1)_{I_{3R}} \times SU(4)^c$ or $SO(10)$ breaks spontaneously by the Higgs mechanism near the GUT scale $M_U \sim 2 \times 10^{16}$ GeV¹ into the standard model symmetry $G(213) \equiv SU(2)_L \times U(1)_Y \times SU(3)^c$. (For attempts at obtaining a string-derived $SO(10)$ solution see Ref. [61] and for a string $G(224)$ solution see Ref. [20]). The theory thus described should also possess weak scale supersymmetry so as to avoid unnatural fine tuning in

¹ Such a scale of breaking of $G(224)$, $G(214)$ or $SO(10)$ is suggested in part by the observed gauge coupling unification and in part by the observed scale of neutrino mass-splitting $\Delta m^2(\nu)_{23}$ (see chapters 3 and 4).

Higgs mass and to ensure gauge coupling unification.

The common advantages of the symmetries $SO(10)$ and $G(224)$, both viewed as having their origins in string/M-theory, were noted in Chapter 3. The two symmetries also lead to similar predictions regarding fermion masses and neutrino oscillations [25] as discussed in Chapter 4, as well as baryogenesis via leptogenesis [16]. Despite these similarities, they differ, however, as regards the issues of (a) doublet-triplet splitting, and (b) gauge coupling unification.

As noted by several authors [20, 34], a string derived $G(224)$ solution has the advantage over a $SO(10)$ -solution in that doublet-triplet splitting can emerge naturally for the former in 4D through string compactification, while for an $SO(10)$ -solution, this feature (needing something like the Dimopoulos-Wilczek mechanism [35, 130]) is yet to be realized in the context of string theory.

On the other hand, an $SO(10)$ -solution would have the *a priori* advantage in that it would preserve gauge coupling unification in the interval from M_{st} to M_{GUT} regardless of the gap between them. By contrast for a $G(224)$ -solution, coupling unification ($g_{2L} = g_{2R} = g_4$)

can hold only at the string scale M_{st} [36] through the constraints of string theory, even though $G(224)$ is semi-simple. One would be tempted to presume (see e.g. [62]) that such a string-scale unification may still be compatible with the observed gauge coupling unification if the string scale is not far above the conventional GUT-scale ², where $G(224)$ should break spontaneously to the standard model symmetry.

In view of the advantage of $G(224)$ (or $G(214)$) as regards the problem of doublet triplet splitting, it is important to examine concretely as to how well gauge coupling unification can be realized at the string scale ($M_{st} \gtrsim M_{GUT}$) for such a presumed string derived $G(224)$ or $G(214)$ solution. The purpose of this chapter is to examine precisely this issue.

In exploring this issue, I will consider two well-motivated low energy spectra, each of which can be tested at the LHC. One is the Minimal Supersymmetric Standard Model (MSSM) (defined in Chapter 2), and the other is the so called Extended Supersymmetric Standard

² $M_{st} \approx (2 - 3)M_{GUT}$, say, with $M_{GUT} \sim 2 \times 10^{16}$ GeV. Despite the small gap between M_{st} and M_{GUT} , one would still have the advantages of $G(224)$ by having the right-handed neutrino ν_R with the desired protection of its mass by $B - L$ and the $SU(4)$ -color relations for fermion masses: $m_b(\text{GUT}) \approx m_\tau$ and $m(\nu_{\text{Dirac}}^\tau) \approx m_{\text{top}}(\text{GUT})$ that are empirically favored.

Model (ESSM) [37]. The latter adds two vector-like families having the quantum numbers of $\mathbf{16}_V + \overline{\mathbf{16}}_V$ of SO(10) and masses of $\mathcal{O}(1 \text{ TeV})$ to the MSSM spectrum. It has been motivated *a priori* on several grounds [37]. Although less economical than MSSM, ESSM possesses certain advantages over MSSM: (a) It raises the unified coupling α_{Unif} to a semi-perturbative value of $0.2 - 0.3$ which may provide a better chance to stabilize the dilaton than the case of MSSM for which $\alpha_{\text{Unif}} \sim 0.04$ [37, 131]. (b) With enhanced two loop effects, ESSM raises the scale of unification, M_U to $(0.5-2) \times 10^{17} \text{ GeV}$ [37, 131], thus reducing the gap between the gauge and the string unification scales³. (c) The GUT prediction of $\alpha_3(m_Z)$ in ESSM is lowered compared to that in MSSM to about 0.122. This is in better agreement with data without needing large GUT-scale threshold corrections. (d) By raising the unification scale, it naturally enhances the GUT prediction for proton lifetime [25] compared to the case of MSSM embedded in a GUT, as needed by data. (e) Finally, it provides a simple reason for inter family mass hierarchy [37, 131, 132]. In addition, the ESSM

³ A perturbative value for the string scale is given by $M_{st} = \frac{e^{(1-\gamma)} 3^{-3/4}}{4\pi} g_{st} M_{Pl} \approx g_{st} \times 5.27 \times 10^{17} \text{ GeV}$, where γ is the Euler constant. For $g_{st} \sim \mathcal{O}(1)$, $M_{st} \approx 5 \times 10^{17} \text{ GeV}$ [36]

provides a simple explanation of the indicated $(g - 2)_\mu$ anomaly [133]. Such an explanation can be tested with improved searches for $\tau \rightarrow \mu\gamma$ and $\mu \rightarrow e\gamma$ decays.

With these advantages in mind, especially because of (b) and (c), one may *a priori* expect that gauge coupling unification at a presumed string scale exceeding the GUT scale ($M_{st} \gtrsim M_{GUT}$) may be realized more easily (without a need for extra Higgs multiplets at the GUT-scale) for the case of ESSM embedded in G(224) or G(214) than that of MSSM subject to the same embedding. I would, therefore, first consider the case of ESSM embedded in G(224) or G(214), and then that of MSSM with the same embedding.

I should clarify that ESSM, like MSSM, is based on the standard model gauge symmetry $G(213) = SU(2)_L \times U(1)_Y \times SU(3)^c$. Prior works [37, 131] have examined the issue of gauge coupling unification for the case of ESSM (thus G(213)) embedded directly into a GUT SO(10)-symmetry near the coupling unification scale ($M_U \lesssim M_{st}$). This case would, however, either face the familiar doublet-triplet (D-T) splitting problem in 4D if SO(10) emerges as an effective symmetry

at $M_{st} > M_U$, or would not necessarily have the advantages of SU(4)-color in 4D (i.e. a ν_R with desired mass-protection, $B - L$, and the desired fermion mass relations for the third generation, mentioned above) if $M_U = M_{GUT} = M_{st}$, i.e. if string theory directly yields the standard model symmetry G(213) in 4D at $M_{GUT} = M_{st}$. Motivated by the desire to avoid the D-T splitting problem and yet to retain the advantages of SU(4)-color in 4D, I would explore the issue of gauge coupling unification for the case of ESSM, based on the symmetry G(213), being embedded into a G(224) (or G(214)) symmetry near the conventional GUT-scale ($M_{GUT} \sim 2 \times 10^{16}$ GeV), and would examine if coupling unification would occur in this case at a scale $M_U (> M_{GUT})$; the scale M_U may then be identified with the string scale. In this sense my present work will directly explore the issue of coupling unification for an effective non-simple symmetry like G(224) or G(214) and its compatibility with string-unification. This distinguishes the present work from all prior works [37, 131].

In exploring the issue of coupling unification with ESSM or MSSM embedded in G(224) (or (G(214))) above the GUT scale, I will also

attempt to satisfy the following constraints simultaneously: (1) consistent electroweak symmetry breaking, (2) non-violation of color and charge, (3) a large enough Higgs mass with as little fine tuning as possible, (4) lightest neutralino mass constraint, (5) the right masses of the third generation fermions i.e. t , b and τ by allowing for $B - L$ dependent terms and (6) also consistent masses for the second generation masses and CKM mixings. We can see from the outset that it is a challenging task to meet all these goals simultaneously.

I find that with the ESSM embedded into $G(224)$, one can achieve gauge coupling unification for the case of an effective $G(224)$ symmetry at a scale of $\sim 1.1 \times 10^{17}$ GeV with consistent electroweak symmetry breaking and color and charge preservation. One obtains the mass of the lightest Higgs to be 142 GeV; the neutralino mass constraint can also be satisfied. This is encouraging. However, the masses of t , b and τ do not simultaneously turn out to be in the right range with the $G(224)$ mass-relations holding at the GUT scale. If, instead, we relax the $SU(2)_R$ symmetry, and consider the gauge symmetry $G(214) \equiv SU(2)_L \times U(1)_{I_{3R}} \times SU(4)^c$, we are able to meet all our

goals listed above simultaneously, including the masses of t , b and τ and the masses and mixings of the second generation. The embedding of ESSM into G(224) is discussed in section 2, and that into G(214) is discussed in section 3. In each case I attempt to achieve coupling unification, while satisfying all the constraints listed above.

Finally, I also study the case of MSSM embedded in G(224) near the conventional GUT-scale, with the aim of having G(224) unification holding in the entire region spanning from M_{GUT} to M_{st} . As is well known, with the MSSM spectrum, the standard model gauge couplings unify at about 2×10^{16} GeV. If MSSM is embedded into G(224), then the gauge couplings of G(224) will also unify at this scale. However, since G(224) is not a simple group, the three couplings of G(224) will ordinarily diverge above the GUT scale, making it inconsistent with unification at the string scale. To preserve G(224) unification above the GUT scale, I discuss how suitable Higgs multiplets can be introduced which preserve gauge couplings unification in the interval M_{GUT} to M_{st} . A well known issue with gauge coupling unification within MSSM is that it predicts $\alpha_3(m_Z) \approx 0.127 \pm 0.02$, which is

higher than the experimental value $\alpha_3(m_Z) = 0.1176 \pm 0.002$ [5]. It is shown that the GUT scale threshold corrections to α_3 due to the Higgs-multiplets (including the additional Higgs-multiplets mentioned above) and the super heavy gauge particles of $G(224)$, can give rise to a reduction in the value of $\alpha_3(m_Z)$, and thus a better agreement with the data. This result is presented in section 4.

8.2 The Extended Supersymmetric Standard Model and its embedding in $G(224)$

I will proceed by first recalling certain salient features of ESSM, and refer to Refs. [37, 131–133] for details. The ESSM contains, in addition to the particle content of MSSM, two vector like families, which have the quantum numbers of $\mathbf{16} + \overline{\mathbf{16}}$ of $SO(10)$, with $\mathbf{16} \equiv (Q_L | \overline{Q}'_R)$ and $\overline{\mathbf{16}} \equiv (\overline{Q}_R | Q'_L)$ where Q_L and Q_R transform as $(2, 1, 4)$ of $G(224)$ and Q'_L and Q'_R as $(1, 2, 4)$ of $G(224)$. In addition there are two singlet Higgs, H_S and H_λ . These vector like families are assumed to have masses in the range of 1 to a few TeV [37].

The addition of complete vector-like families satisfies the phe-

nomenological constraints of neutrino counting at LEP, measurement of the ρ -parameter as well as those of the oblique electroweak parameters (see e.g. [132]). Now the gauge couplings will still unify for the case of ESSM (just as for MSSM) at one loop, at the canonical scale of 2×10^{16} GeV, even after the addition of a complete set of vector-like families, because they are complete SO(10)-multiplets. However, with the addition of the two vector-like families, the unified coupling (α_{unif}) is raised, and thereby the two loop effects are enhanced. This in turn raises the unification scale [37]. For the case of ESSM, α_{Unif} lies in the semi-perturbative range of 0.25–0.3 providing, as mentioned above, a better chance to stabilize the dilaton. The scale of unification is increased to $(0.5\text{--}2) \times 10^{17}$ GeV, thus reducing the mismatch between the coupling unification and the string unification scales, while at the same time enhancing the proton lifetime, as desired. Other advantages of ESSM are mentioned in Sec. 1 of this chapter.

8.2.1 Yukawa couplings in ESSM and inter family mass hierarchy

Assuming that the chiral families receive their masses almost entirely through their mixing with the vector-like families (this may be justified by suitable flavor symmetries), the 5×5 Yukawa coupling matrix of the three chiral families and the two vector-like families is assumed to have the form:

$$\begin{array}{c} \overline{q_R^i} \\ \overline{Q_R} \\ \overline{Q'_R} \end{array} \begin{array}{c} q_L^i \quad Q_L \quad Q'_L \\ \left(\begin{array}{ccc} 0_{3 \times 3} & X_f H_f & Y_f H_c \\ Y_c'^{\dagger} H_c & z_c H_\lambda & 0 \\ X_f'^{\dagger} H_f & 0 & z_f H_\lambda \end{array} \right) \end{array} \quad (8.1)$$

The symbols q , Q and Q' stand for quarks as well as leptons, $i = 1, 2, 3$ is the generation index, the subscript f stands for u, d, e, ν , and c for q, l . The fields H_f are the usual H_u and H_d of MSSM, while H_c and H_λ are singlets of the standard model and acquire VEV $\sim 1\text{TeV}$. The couplings X_ν and Y_ν are zero as the right handed neutrinos are super heavy.

To see how ESSM can explain inter-family mass hierarchy, con-

sider the following. Let the Yukawa couplings X_f^T be denoted by $(x_1, x_2, x_3)_f$, and Y_f^T by $(y_1, y_2, y_3)_f$. It is always possible to rotate the basis vectors so that Y_f^T is transformed to $(0, 0, 1)y$, and simultaneously X_f^T to $(1, p_f, 1)x_f$, X'_f to $(0, p'_f, 1)x'_f$, and Y'_c to $(0, 0, 1)y'$. It is now evident that the first generation is almost massless, even if there is no hierarchy in the original basis. If, for simplicity we assume $x_f = x'_f$, $y = y'$ and $z = z'$ at the unification scale and no $B - L$ dependent contribution, we get $m_{t,b,\tau}^0 \approx (2x_f y (\langle H_S \rangle \langle H_f \rangle) / (z \langle H_V \rangle))$ and $m_{c,s,\mu}^0 \approx (p_f p'_f / 4) m_{t,b,\tau}^0$. For $p_f, p'_f = 1/2 - 1/7$, we can get a hierarchy between the second and the third family ranging from $1/16 - 1/200$. In short, the ESSM spectrum can plausibly lead to large inter-family mass hierarchy as observed, without introducing very small numbers by hand.

8.2.2 Gauge coupling unification with ESSM embedded into $G(224)$

As it stands ESSM has a large number of parameters because of the Yukawa couplings. A natural next step is to consider a larger gauge group above the unification scale, so that some of the yukawa cou-

plings get related to each other. In the introduction, we mentioned the advantages of having a symmetry that contains SU(4)-color. We are then led to consider the embedding of ESSM based on the symmetry G(213) into the symmetry group G(224). The idea is to achieve unification of the gauge couplings of G(224) at a scale $(few) \times M_4$ (where M_4 denotes the scale at which G(224) (or G(214)) breaks into the standard model gauge symmetry) [37]. This scale can then be identified as the string scale, and the emergent theory will have the advantages of both G(224) and ESSM.

If ESSM is embedded into G(224), there is a drastic reduction in the number of Yukawa coupling parameters at the scale M_4 . The Yukawa couplings are now related by G(224) symmetry. At M_4 we have: $x_u = x_d = x_l = x_\nu \equiv X$, $x'_u = x'_d = x'_l = x'_\nu \equiv X'$ (see comments below), $y_u = y_d = y_l = y_\nu \equiv Y$, $y'_q = y'_l \equiv Y'$, $z_q = z_l \equiv Z$ and $z'_u = z'_d = z'_l = z'_\nu \equiv Z'$. Since ν_R gets integrated out at the unification scale, $x_\nu = y_\nu = 0$. The Higgs potential has a form as in the Next to Minimal Supersymmetric Standard Model (NMSSM):

$$W_H = k_1 H_u H_d H_\lambda + \frac{k_2}{6} H_\lambda^3 + \frac{k_3}{6} H_c^3 \quad (8.2)$$

To break $G(224)$ to ESSM and then to the standard model, we make use of the following Higgs multiplets: $(2, 2, 1)$, $(1, 2, \bar{4})_H$, $(1, 2, 4)_H$ of $G(224)$ and to allow for $B-L$ dependence to obtain the right fermion masses, a $(1, 1, 15)$ is introduced. Due to a mixing between $(2, 2, 1)_d$ i.e. the “down” sector of $(2, 2, 1)$, and $(1, 2, 4)_H \oplus (1, 2, \bar{4})_H$ the down and lepton yukawa couplings x_d , x'_d , x_l and x'_l are multiplied with $\cos \gamma$ which is the mixing between $(2, 2, 1)_d$ and $(1, 2, 4)_H \oplus (1, 2, \bar{4})_H$ (see e.g. [25]). Thus at the unification scale $x_d = x_l = X \cos \gamma$ and $x'_d = x'_l = X' \cos \gamma$, while $x_u = X$ and $x'_u = x'_\nu = X'$. Therefore the top and bottom mass are related by $m_t/m_b = \tan \beta / \cos \gamma$ at the unification scale. The singlets H_c and H_λ are used to give masses to the vector like families, and get vacuum expectation values of a few TeV.

The values of the yukawa couplings are chosen with the goal of accomplishing the following tasks:

(1)**Unification of the couplings of $G(224)$** : The scale M_4 is defined to be the scale where $G(224)$ (or $G(214)$) breaks spontaneously to the standard model gauge symmetry, $G(213)$. Thus below M_4 , the

effective gauge symmetry is that of $G(213)$, and above it is that of $G(224)$. Based on observed gauge coupling unification as well as the scale of neutrino (mass)²-splitting (see Chapters 3 and 4), we will choose $M_4 \sim 2 \times 10^{16}$ GeV. Assuming that the low energy spectrum below the scale M_4 is given by that of ESSM, I now examine if the gauge couplings of $G(224)$ would unify at a scale $M_U > M_4$. The scale M_U may then be identified with the string scale. The gauge couplings of $G(224)$ are related to the standard model couplings at M_4 by the following relations:

$$g_1(M_4) = \frac{1}{\sqrt{\frac{3}{5g_{2R}^2(M_4)} + \frac{2}{5g_4^2(M_4)}}}; \quad g_2(M_4) = g_{2L}(M_4); \quad g_3(M_4) = g_4(M_4). \quad (8.3)$$

The values of $g_1(M_4)$, $g_2(M_4)$ and $g_3(M_4)$ are chosen so that when they are run down using the RGEs of ESSM (see Appendix .1), their values at m_Z are close to the observed values. The gauge couplings of $G(224)$ are run upward above M_4 by using the RGEs of $G(224)$ (see Appendix .2) after matching them at M_4 to the standard model couplings as in Eq. (8.3).

(2)**Consistent electroweak symmetry breaking:** Soft mass parameters and yukawa couplings are chosen so as to ensure consistent

electroweak symmetry breaking. The Higgs potential of ESSM (see Eq. (8.2)) is like that for NMSSM. The Higgs potential has to be consistently minimized with respect to H_u , H_d and H_λ . The following equations must be satisfied:

$$\begin{aligned}
k_1^2 v_\lambda^2 + m_{H_d}^2 &= -(k_2 v_\lambda + A_1)(k_1 v_\lambda) \tan \beta - \frac{m_Z^2}{2} \cos 2\beta \\
k_1^2 v_\lambda^2 + m_{H_u}^2 &= -(k_2 v_\lambda + A_1)(k_1 v_\lambda) \cot \beta + \frac{m_Z^2}{2} \cos 2\beta \\
\sin 2\beta &= 2v_\lambda \frac{m_{H_\lambda}^2 + k_2 A_2 v_\lambda + k_1^2 v^2 + 2k_2^2 v_\lambda^2}{k_1 A_1 v^2 + 2k_1 k_2 v^2 v_\lambda}
\end{aligned} \tag{8.4}$$

In these equations, A_1 and A_2 are the A -terms corresponding to the yukawa couplings k_1 and k_2 , v_λ is the VEV of H_λ , $v^2 = \langle H_u \rangle^2 + \langle H_d \rangle^2$ and $\tan \beta = \langle H_u \rangle / \langle H_d \rangle$. The μ -term, as in NMSSM, is effectively given by $k_1 v_\lambda$ and the B -term = $k_2 v_\lambda + A_1$.

(3) Color and charge preservation: Not only must there be consistent electroweak symmetry breaking, but also, we must ensure that color and electric charge are not broken. For this, the (mass)² of squarks and sleptons (including the ones belonging to the vector like families) must remain positive as the soft masses (assumed universal) are run down from the unification scale to the weak scale.

(4) Neutralino mass constraint: The universal gaugino mass

at the unification scale, $M_{1/2}$, is chosen so that the RG evolved lightest neutralino mass is consistent with the current experimental bound of 48 GeV.

(5) **Higgs mass limit:** The mass of the lightest Higgs should turn out to be larger than the LEP lower bound of 114 GeV [5]. Our goal is to try to make it as large as possible with minimum fine tuning between the μ -term and the soft mass m_{H_u} . This problem is partly resolved with the NMSSM like Higgs structure. The masses of the neutral Higgs bosons are calculated from the eigen values of the 3×3 matrix formed from the second derivatives of the potential with respect to H_u , H_d and H_λ . The details of this procedure, including one loop corrections, can be found in e.g. [135].

(6) **Masses of the third generation:** The magnitude of the Yukawa couplings of ESSM should be chosen at the GUT/string scale, so that masses of the third generation quarks and leptons i.e. top, bottom and tau-lepton, turn out to be close to the observed values. We find that for the case of G(224), even with $B - L$ contributions from the $(1, 1, 15)_H$, we are able to obtain right masses only for t and

τ or t and b , but not all three together. Either the bottom mass turns out to be too high or the τ mass too low. If instead of $G(224)$, the group $SU(2)_L \times U(1)_{I_{3R}} \times SU(4)^c \equiv G(214)$ is used, one is able to obtain all masses correctly. The group $G(214)$ is also able to satisfy all the other requirements mentioned above. We will present the results for $G(224)$ in this section and for $G(214)$ in the next section.

(7) Masses of the second family: Finally, we also want the second generation masses m_c , m_s and m_μ to come out in the right range. In addition, the mixing of the second and third families, i.e. the values of $V_{cb} \approx -V_{ts}$ should be close to the observed value of ~ 0.04 . For the second generation masses and mixings, we introduce the parameters p_u , p'_u , p_d , p'_d , p_l and p'_l as mentioned in section 2.1. The masses of c , s and μ are obtained by diagonalizing the 4×4 mass matrix given in Eq. (8.1).

We now proceed to give the results of our study for the case of $G(224)$.

(1) Renormalization group analysis: We perform a two loop analysis of gauge coupling renormalization group equations and a one loop analysis for the Yukawa couplings. The running of the RGEs is mass dependent with corrections for smooth crossover of beta functions at the threshold of each particle. The renormalization group equations can be found in the appendices. The yukawa couplings we have chosen are much smaller compared to the gauge couplings (this may be compared to the study in [37] where the yukawa couplings were chosen to be $\sqrt{4\pi}$ at the unification scale. See also [131]), therefore one loop analysis of yukawa couplings is justified.

(2) The vector like family masses are chosen so that the vector like quarks have a mass ~ 3 TeV, while the vector like leptons have masses ~ 1 TeV. The difference by a factor of 3 between the vector-like quarks and lepton masses represents QCD renormalization effects. The superpartner masses for the vector like particles are taken to be at the same scale as the corresponding fermion, i.e. $\tilde{m}_Q \sim M_Q$ and $\tilde{m}_L \sim M_L$, so that the scale of supersymmetry breaking is ~ 1 TeV,

while the vector like family scale is ~ 3 TeV. Because of the vector-like matter contribution to the beta functions, the gauge couplings run faster and meet at a higher value of α_{Unif} . We choose a scale M_4 slightly below the ESSM unification scale. The effective symmetry above the scale M_4 is assumed to be G(224). Thus G(224) is presumed to break spontaneously into the standard model symmetry G(213) at the scale M_4 , by the Higgs mechanism. As mentioned above, guided by observed gauge coupling unification and neutrino-mass considerations (see Chapters 3 and 4), M_4 is chosen within a factor of two (say) of the conventional MSSM unification scale $M_{GUT} = 2 \times 10^{16}$ GeV. For the results presented here, we choose $M_4 = 4 \times 10^{16}$ GeV. The matching conditions Eq. (8.3) between the gauge couplings of ESSM and G(224) are applied at this scale.

The Higgs multiplets above M_4 for the symmetry G(224) are chosen to be $(2, 2, 1)$, $(1, 2, 4)_H$ and $(1, 2, \bar{4})_H$. To get $B - L$ dependence, especially to get correct masses for t , b and τ , I add a $(1, 1, 15)$. The $(1, 1, 15)$ contributes only to the $SU(4)$ -color beta function and makes the g_4 coupling grow faster above M_4 . We are able to achieve G(224)

unification both with and without the $(1, 1, 15)$. If we let M_4 take the value of the conventional GUT scale i.e. 2×10^{16} GeV, without $(1, 1, 15)$, the $G(224)$ couplings unify at $\alpha_{224} \sim 0.35 - 0.4$ at a scale of $\sim 10^{17}$ GeV. When the $(1, 1, 15)$ is added, with $M_4 = 4 \times 10^{16}$ GeV, the $G(224)$ couplings unify at $\alpha_{224} \approx 0.39$ at a scale of 1.14×10^{17} GeV. If however, we had set $M_4 = 2 \times 10^{16}$ GeV, i.e. the conventional GUT scale, because g_4 runs faster due to the presence of $(1, 1, 15)$, the $G(224)$ couplings meet at a value of $\alpha_{224} \sim 0.7$ which tends to be non-perturbative. The meeting of $G(224)$ gauge couplings when run upward from $M_4 = 4 \times 10^{16}$ GeV is shown in figure 8.1. The input values for the gauge and yukawa couplings at M_4 are taken to be:

$$\begin{aligned}
M_4 &\approx 4 \times 10^{16}; & g_4 &= 1.89; & g_{2L} &= 1.63; & g_{2R} &= 1.45; \\
X = X' &= 0.26; & Y &= 0.7; & Y' &= 0.8; & Z &= 0.2; & Z' &= 0.5; \quad (8.5) \\
k_1 &= 1.04; & k_2 &= 0.84; & k_3 &= 1.32.
\end{aligned}$$

Below M_4 , the standard model gauge couplings are run down to about m_Z using the RGEs of ESSM. The inputs at M_4 are obtained

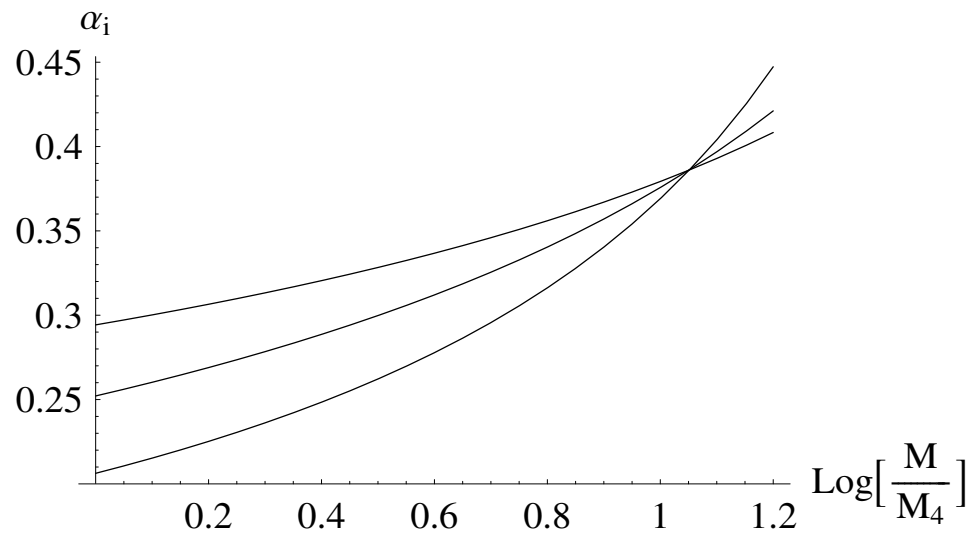


Fig. 8.1: Gauge coupling unification for ESSM embedded in $G(224)$ at the scale $M_4 = 4 \times 10^{16}$ GeV. The $G(224)$ couplings unify with $\alpha_{224} \approx 0.39$ at a scale $M_U \approx 1.14 \times 10^{17}$ GeV, which may be identified with the string scale. The curves from top to bottom are α_4 , α_{2L} and α_{2R} respectively.

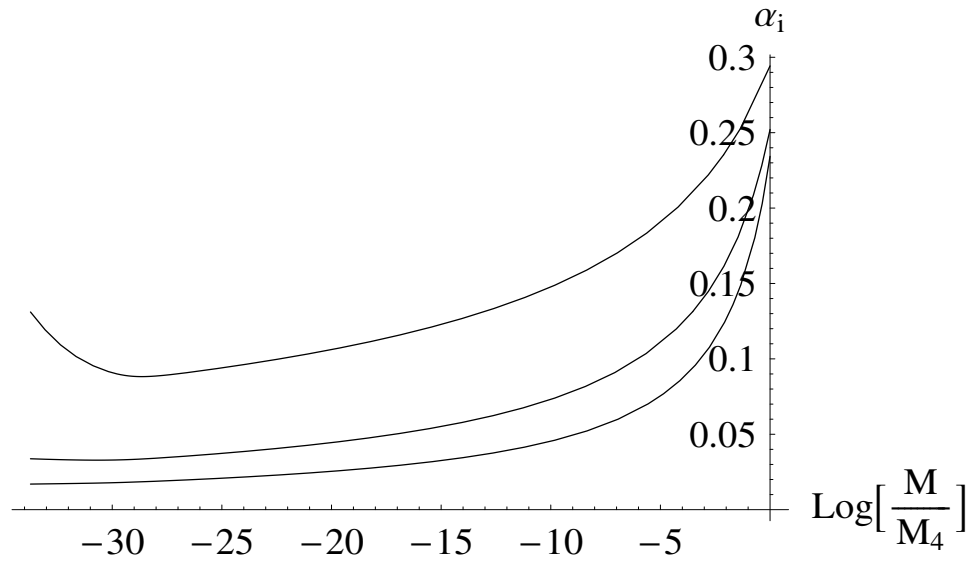


Fig. 8.2: Gauge coupling running below $M_4 = 4 \times 10^{16}$ GeV down to m_Z for ESSM embedded in G(224) at the scale $M_4 = 4 \times 10^{16}$ GeV. The curves from top to bottom are α_3 , α_{2L} and α_1 respectively.

by using G(224) relations:

$$\begin{aligned}
 M_4 &\approx 4 \times 10^{16}; & g_3 = g_4 = 1.89; & & g_2 = g_{2L} = 1.63; \\
 g_{2R} = 1.45 &\Rightarrow g_1 = 1.59; \\
 X = X' = 0.26; & & Y = 0.7; & & Y' = 0.8; & & Z = 0.2; & & Z' = 0.5; \\
 k_1 = 1.04; & & k_2 = 0.84; & & k_3 = 1.32.
 \end{aligned} \tag{8.6}$$

The running of the gauge couplings for the low energy regime (1 TeV to M_4) with ESSM spectrum is shown in figure 8.2.

(3) The next task is to satisfy the electroweak symmetry breaking conditions given in Eq. (8.4). For this, the values of v_λ , A_1 and A_2

are obtained by choosing the values of m_Z , k_1 , k_2 and $m_{H_u, H_d, H_\lambda}^2$. We then run A_1 and A_2 from 1 TeV up to M_4 to get A_0 . The values of $m_{H_u, H_d, H_\lambda}^2$ are obtained by running the relevant soft mass RGEs from the scale M_4 to lower momenta starting from a value of m_0^2 at M_4 . The choice of m_0 is restricted by requiring that Eqs. (8.4) be satisfied and imposing that the fine-tuning between $m_{H_u}^2$ and $|\mu|^2$ be as small as possible. We find that for $\tan\beta = 5$ and $\mathcal{O}(1\%)$ fine tuning, we are able to satisfy the electroweak symmetry breaking conditions for $m_0 \approx 500$ GeV and $A_0 \approx 800$ GeV.

(4) Neutralino mass constraint: Due to the addition of vector-like matter, the gauge couplings g_1 , g_2 and g_3 run much faster compared to the case of MSSM. Because of enhanced renormalization effects, we find (see also [131]) that $M_{1/2}/M_2 \approx 9$ and $M_2/M_1 \approx 1.6$. If the lightest neutralino has to be heavier than the current experimental limit of ~ 46 GeV, one needs a rather large $M_{1/2} \sim 750 - 800$ GeV.

(5) Color and Charge preservation: We have to make sure that all scalar (squark and slepton) (mass)² are positive. We find that with our choice of universal soft terms i.e. m_0 , A_0 and $\tan\beta$ and the

yukawa couplings, all squark/slepton scalar (mass)² turn out to be positive, with exact diagonalization of mass matrices.

(6) Top mass: To get the top mass in the right range, one needs rather large values of x_u and x'_u . We take $x_u = x'_u = 0.26$ at M_4 . This has the effect that $m_{H_u}^2$ turns negative at a high scale ($\sim 10^{14}$ GeV) and is $\approx -(1000)^2 \text{ GeV}^2$ at the electroweak scale. To break electroweak symmetry consistently, $m_{H_u}^2$ must cancel $|\mu|^2$ up to $m_Z^2/2$. This is found to correspond to approximately 1% fine-tuning⁴. If we start with lower values of x_u and x'_u at M_4 then the top mass turns out to be $\sim 40 \text{ GeV}$, which is too low. Thus while we can get the top mass correctly, we cannot do better than 1% fine-tuning in the Higgs mass. This is, of course, not very different from the case of MSSM (see Chapter 2).

(7) Mass of the b-quark and the τ lepton: Without including $B - L$ dependent terms in the mass-matrices, we cannot get the right values of m_b and m_τ unless we choose a very small $\cos \gamma$ (~ 0.04) ($\cos \gamma \approx \tan \beta \frac{m_b(GUT)}{m_t(GUT)}$). This would mean that $\tan \beta \sim 1.2$ which is

⁴ A measure of fine-tuning is defined in Chapter 2. A rough estimate of fine-tuning is $\left| \frac{|\mu|^2 + m_{H_u}^2}{m_{H_u}^2} \right| \sim \frac{m_Z^2}{|m_{H_u}^2|} \approx 0.01$ for the above case.

excluded⁵. Even if we did allow for such small $\cos\gamma$ but no $B - L$ dependence, we can get the right mass for the b-quark, but the mass of the τ -lepton turns out to be 0.65 GeV, which is smaller than the experimental value by a factor of nearly 2.7. Thus we are forced to include $B - L$ dependent terms contributing to the masses of the third family for the case of ESSM. If we have a $(1, 1, 15)$ of $G(224)$, we can have the following yukawa couplings:

$$\begin{aligned}
& h(2, 1, 4)_V(2, 1, \bar{4})'_V(1, 1, 15)_H 1'_V/M \\
& h'(1, 2, 4)_V(1, 2, \bar{4})'_V(1, 1, 15)_H 1'_V/M \\
& \xi(2, 1, 4)_V(1, 2, \bar{4})_i(1, 1, 15)_H(2, 2, 1)_H/M \\
& \xi'(1, 2, \bar{4})'_V(2, 1, 4)_i(1, 1, 15)_H(2, 2, 1)_H/M
\end{aligned} \tag{8.7}$$

The inclusion of these terms has the effect of changing the yukawa couplings as follows:

$$\begin{aligned}
z_q &\rightarrow z_q(1 + \kappa_1); & z'_{u,d} &\rightarrow z'_{u,d}(1 + \kappa_2) \\
x_{u,d} &\rightarrow x_{u,d}(1 + \delta_1); & x'_{u,d} &\rightarrow x'_{u,d}(1 + \delta_2)
\end{aligned} \tag{8.8}$$

where,

$$\begin{aligned}
z_q\kappa_1 &= h\langle(1, 1, 15)_H\rangle/M; & z'_{u,d}\kappa_2 &= h'\langle(1, 1, 15)_H\rangle/M \\
x_{u,d}\delta_1 &= \xi\langle(1, 1, 15)_H\rangle/M; & x'_{u,d}\delta_2 &= \xi'\langle(1, 1, 15)_H\rangle/M
\end{aligned} \tag{8.9}$$

⁵ Values of $0.5 < \tan\beta < 2.4$ are excluded by Higgs boson searches [134].

For the lepton sector, $(\kappa, \delta) \rightarrow -3(\kappa, \delta)$. To get the masses of b and τ in the right range, we choose, at the scale M_4 , the following values $\kappa_1 = 0.1$, $\kappa_2 = 0.2$, $\delta_1 = \delta_2 = -0.9$. However, to get all three m_t , m_b and m_τ correctly, we still need to choose a very small value of $\cos \gamma$ (~ 0.03). We will see in the next section that if we relax the $SU(2)_R$ relations on the yukawa couplings and consider the group $G(214)$, we are able to get the value of all three masses correctly.

(8) Higgs mass bound: The ESSM Higgs structure is like that of NMSSM. Thus the mass of the lightest Higgs scalar is expected to be larger than that in MSSM. To calculate the Higgs mass, we include the radiative corrections due to top and stop loops. The masses of the Higgs scalars are then obtained by diagonalizing the 3×3 (mass)² matrix given by

$$M_{ij}^2 = \frac{\partial^2 V_0}{\partial \phi_i \partial \phi_j} + \frac{\partial^2 V_1}{\partial \phi_i \partial \phi_j} \quad (8.10)$$

where V_0 is the tree level scalar potential and V_1 are the radiative corrections to the scalar potential, $\phi_{i,j} \equiv H_u, H_d, H_\lambda$. The detailed analysis can be found in [135]. For the lightest Higgs scalar we get $m_H = 140 - 142$ GeV, which is well above the LEP lower bound of

114 GeV.

(9) Second family masses and mixing: As described in section 2.1, the second family masses are obtained by introducing the parameters p_f and p'_f . Choosing $p_u = p'_u = -0.155$ and $p_d = p'_d = -0.41$, we get $m_c = 1.47$ GeV, $m_s = 88$ MeV (at m_c and 1 GeV respectively) and $V_{cb} = 0.046$. These value are reasonably close to the observed values (The mass of the muon can be obtained by appropriately choosing p_l and p'_l . We, however, do not quote it here as the mass of the tau lepton turned out to be too low (see Table 1)). The results for this

section are summarized in Table 1.

Quantity	Value
$\alpha_1^{-1}(m_Z), \alpha_2^{-1}(m_Z), \alpha_3(m_Z)$	58.5, 29.7, 0.121
$m_t(m_t), m_b(m_b), m_\tau$	166, 4.4, 0.65 GeV
$m_c(m_c), m_s(1 \text{ GeV}), V_{cb}$	1.47 GeV, 88 MeV, 0.046
m_h	142 GeV
$M_{Q_{L,R}}^{(\prime)}, M_{L_{L,R}}^{(\prime)}$	3.7 TeV, 880 GeV
$m_{\tilde{g}}$	276 GeV
Neutralino masses	(48, 94, 1062, 1065) GeV
$m_{\tilde{q}}, m_{\tilde{u}}, m_{\tilde{d}}$	785, 776, 901 GeV
$m_{\tilde{l}}, m_{\tilde{e}_R}$	466, 522 GeV
A_t, A_b	-301, -69 GeV
$A_{k_1}, A_{k_2}, v_\lambda$	947, 1054, 4094 GeV

Table 1. Low energy spectrum for the case of ESSM embedded in G(224) above the scale

$M_4 = 4 \times 10^{16}$ GeV with input parameters as in Eq. (8.6), including $B - L$ contributions.

Note that the value of m_τ is too low.

In the next section, we will describe the embedding of ESSM in G(214), which turns out to satisfy all constraints together with gauge

coupling unification.

8.3 Gauge Coupling Unification with ESSM embedded into $G(214)$

In the previous section we saw that ESSM embedded in the group $G(224)$ turns out to be a plausible mechanism to reduce the mismatch between the string and the unification scales, with the gauge couplings of $G(224)$ unifying at a scale of about 10^{17} GeV. The model can satisfy the constraints of (i) electroweak symmetry breaking, (ii) Higgs mass, (iii) lightest neutralino mass, (iv) color and charge preservation and (v) the masses and mixings of the second family, but it does not give the right masses of t , b and τ simultaneously. This is due to the fact that the yukawa couplings x_u and x_d are constrained by the relation $x_d = x_u \cos \gamma$ at M_4 due to the $G(224)$ symmetry. The same applies to the couplings x'_u and x'_d . If instead of the symmetry $G(224)$, we had $G(214)$ above the scale M_4 , these relations no longer hold. The gauge group $G(214)$ contains $SU(4)$ -color, and therefore has all the advantages associated with it (see chapter 3). It still has the advantage that there is no problem of doublet-triplet splitting as the triplets can

be projected out by string compactification as in the case of G(224). In this section, we will study the case of ESSM embedded in G(214) at about the conventional GUT-scale. We find that for this case, one can achieve the unification of the G(214) gauge couplings at a scale $\sim 10^{17}$ GeV, satisfying all the constraints listed above, *and* get the right masses of t , b and τ .

8.3.1 Yukawa couplings in G(214)

The low energy spectrum for the case of ESSM embedded in G(214) remains the same as in the previous section. Above the scale M_4 , the symmetry $SU(2)_R$ is replaced by I_{3R} . Thus all multiplets that were doublets of $SU(2)_R$ in G(224) are now replaced by two different multiplets of $U(1)_{I_{3R}}$ carrying $\pm 1/2$ of I_{3R} each. Therefore, $(1, 2, 4)$ of G(224) is replaced by $(1, 1/2, 4)$ and $(1, -1/2, 4)$ of G(214); $(2, 2, 1)$ of G(224) is replaced by $(2, 1/2, 1)$ and $(2, -1/2, 1)$ of G(214), and so on. Thus, the yukawa coupling X , which coupled $(2, 1, 4)_V$, $(1, 2, \bar{4})$ and $(2, 2, 1)$ in the case of G(224), is now replaced by X_1 and X_2 coupling $(2, 1, 4)_V$ with $(1, 1/2, \bar{4})$, $(2, 1/2, 1)$ and $(1, -1/2, \bar{4})$, $(2, -1/2, 1)$ re-

spectively. The yukawa couplings in the case of $G(214)$ are listed below:

$$\begin{array}{ll}
G(224) & G(214) \\
X & \rightarrow X1, X2 \\
X' & \rightarrow X1', X2' \\
Y & \rightarrow Y \\
Y' & \rightarrow Y1', Y2' \\
Z & \rightarrow Z \\
Z' & \rightarrow Z1', Z2'
\end{array} \tag{8.11}$$

With this pattern of Yukawa couplings, x_u and x_d are independent of each other at M_4 (the same is true for x'_u and x'_d as well). This will help in getting the masses of the top and bottom quarks correctly at the low scale. We still need the $B - L$ dependent couplings to get the masses of b relative to τ correctly. The $B - L$ dependent contributions for the case of $G(224)$ are listed in Eq. (8.7). For the case of $G(214)$, we should have $h' \rightarrow h'_1, h'_2, \xi \rightarrow \xi_1, \xi_2$ and $\xi' \rightarrow \xi'_1, \xi'_2$ at M_4 as for the case of the X, X', Y' and Z' couplings. For the sake of concreteness and economy of parameters, however, we will keep $h'_1 = h'_2 = h'$,

$\xi_1 = \xi_2 = \xi$, and $\xi'_1 = \xi'_2 = \xi'$ as in the case of G(224). Allowing for $h'_1 \neq h'_2$, $\xi_1 \neq \xi_2$ *etc.* would not alter the main features of our results.

8.3.2 Results for the case of ESSM embedded in G(214)

As in the case of G(224), we do two loop renormalization group running of G(214) couplings. The RGEs of G(214) are presented in Appendix .3. We find that we are able to achieve G(214) coupling unification at a scale of $M_U \sim 7.1 \times 10^{16}$ GeV, with $\alpha_{214} \approx 0.31$, taking M_4 to be 4×10^{16} GeV (see figure 8.3). The input values of G(214) gauge couplings and the yukawa couplings at M_4 are given below:

$$\begin{aligned}
M_4 &\approx 4 \times 10^{16}; & g_4 &= 1.843; & g_{2L} &= 1.78; & g_{I_{3R}} &= 1.61; \\
X1 &= X1' = 0.56; & X2 &= X2' = 0.138; \\
Y &= 0.7; & Y1' &= Y2' = 0.8; & Z &= 0.2; & Z1' &= Z2' = 0.5; \quad (8.12) \\
k_1 &= 1.4; & k_2 &= 0.87; & k_3 &= 1.34; \\
h &= 0.02; & h' &= 0.1; & \xi &= -0.24; & \xi' &= -0.24.
\end{aligned}$$

At M_4 , the standard model couplings are related to the G(214) gauge couplings by the relations given in Eq. (8.3), with g_{2R} replaced by $g_{I_{3R}}$. The ESSM yukawa couplings are matched with the G(214)

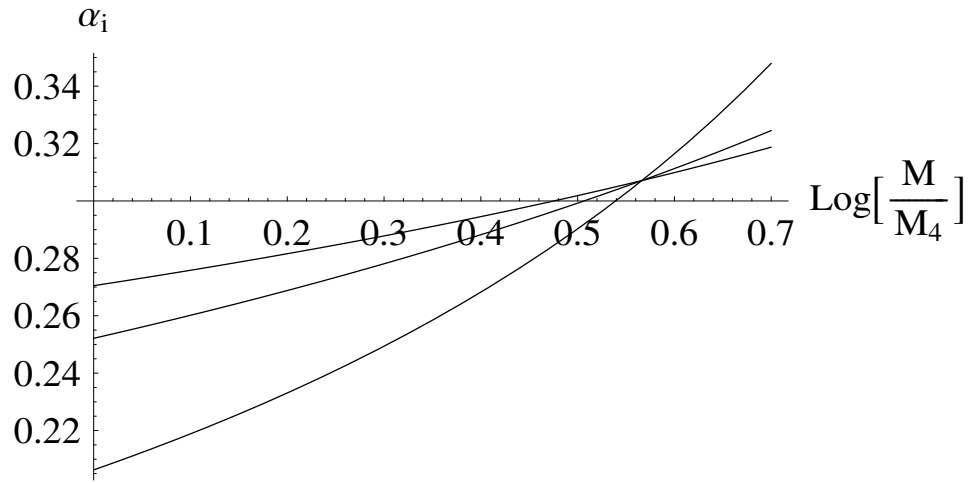


Fig. 8.3: Gauge coupling unification for ESSM embedded in $G(214)$ at the scale $M_4 = 4 \times 10^{16}$ GeV. The $G(214)$ couplings unify at a scale of 7.1×10^{16} GeV with $\alpha_{224} \approx 0.31$. The curves from top to bottom are α_4 , α_{2L} and $\alpha_{I_{3R}}$ respectively.

yukawa couplings at M_4 and are run down to m_Z along with the gauge couplings. Including the effects of the $B - L$ terms, the inputs

for ESSM at M_4 are:

$$\begin{aligned}
z_q &= 0.22; & z_l &= 0.14; & z_u &= z_d = 0.6; & z_e &= z_\nu = 0.2; \\
y_u &= y_d = y_l = 0.7; & y'_q &= y'_l = 0.8; \\
x_u &= x'_u = 0.336; & x_d &= x'_d = 0.01; \\
x_l &= x'_l = 0.038; & x_\nu &= 1.23; \\
k_1 &= 1.4; & k_2 &= 0.87; & k_3 &= 1.34; \\
\tan \beta &= 5; & \cos \gamma &= 0.125; \\
m_0 &= 500 \text{ GeV}; & A_0 &= 800 \text{ GeV}; & m_{1/2} &= 750 \text{ GeV}.
\end{aligned} \tag{8.13}$$

With these inputs we get $\alpha_3(m_Z) = 0.118$ which is in excellent agreement with data. The results are very similar to the case of G(224) except for the masses of the third family. The only shortcoming of the model with ESSM embedded in G(224) was that it could not give the right masses of the third family. This problem is rectified with the case of ESSM embedded in G(214). We are able to get the values of all three masses m_t , m_b and m_τ , in the right range. With the given soft masses as in Eq. (8.13), consistent breaking of electroweak symmetry is achieved along with color and charge conservation. The lightest neutralino mass constraint is satisfied as in the case of G(224). The

lightest Higgs scalar mass in this model is predicted to be ≈ 140 GeV with $\sim 1\%$ fine-tuning (see footnote 1). Lastly, the second family masses and mixings also turn out to be in the right range. Using $p_u = p'_u = -0.155$ and $p_d = p'_d = -0.41$, we get $m_c = 1.46$ GeV, $m_s = 84$ MeV and $V_{cb} = 0.046$. For the mass of the muon, we choose $p_l = p'_l = 0.23$, to get $m_\mu = 106$ MeV. The results of this section are

summarized in Table 2.

Quantity	Value
$\alpha_1^{-1}(m_Z), \alpha_2^{-1}(m_Z), \alpha_3(m_Z)$	58.9, 29.7, 0.118
$m_t(m_t), m_b(m_b), m_\tau$	165, 4.38, 1.73 GeV
$m_c(m_c), m_s(1 \text{ GeV}), m_\mu, V_{cb}$	1.46 GeV, 84 MeV, 106 MeV, 0.046
m_h	140 GeV
$M_{Q_{L,R}}^{(\prime)}, M_{L_{L,R}}^{(\prime)}$	3.4 TeV, 900 GeV
$m_{\tilde{g}}$	290 GeV
Neutralino masses	(57, 104, 1058, 1062) GeV
$m_{\tilde{q}}, m_{\tilde{u}}, m_{\tilde{d}}$	833, 823, 955 GeV
$m_{\tilde{l}}, m_{\tilde{e}_R}$	650, 616 GeV
A_t, A_b	-312, -67 GeV
$A_{k_1}, A_{k_2}, v_\lambda$	981, 922, 3654 GeV

Table 2. Low energy spectrum for the case of ESSM embedded in G(214) above the scale $M_4 = 4 \times 10^{16}$ GeV with input parameters as in Eq. (8.13). Note that this spectrum is very similar to the one in Table 1, except for the value of m_τ , which is close to the observed value in this case.

To conclude this section, the case of ESSM embedded in G(214)

provides a perfectly viable solution to the issue of matching coupling unification (for G(214)) with a presumed string unification, in accord with all phenomenological constraints. It has the advantages of both ESSM and SU(4)-color. We are able to achieve G(214) coupling unification at a scale $M_U \sim 7 \times 10^{16}$ GeV, with the unified coupling $\alpha_{214} \approx 0.31$ in the semi-perturbative range. The constraints of electroweak symmetry breaking, color and charge conservation, lightest neutralino mass bound and lightest Higgs mass limit are satisfied at the same time. We are able to obtain consistently the masses and mixings of the second and the third family fermions, providing an explanation of inter-family mass hierarchy. The result of $\alpha_3(m_Z) = 0.118$ is in excellent agreement with the data, which is an improvement over the MSSM prediction of 0.127 (without GUT-scale threshold corrections).

In the next section, we study the embedding of MSSM into G(224). Our goal is to see if we can achieve G(224) unification by including GUT scale threshold corrections.

8.4 Gauge Coupling Unification with MSSM embedded into $G(224)$

Lastly, we consider the embedding of MSSM into $G(224)$ at the conventional GUT scale of 2×10^{16} GeV. MSSM is the simplest supersymmetric extension of the standard model which includes only the superpartners of the existing standard model fields and an extra Higgs-doublet and its superpartner. If the gauge couplings of the standard model are extrapolated from low energy data within MSSM, they are known to unify at a scale of $M_{GUT} \approx 2 \times 10^{16}$ GeV [24], providing support for the idea of grand unification as well as supersymmetry. However, with MSSM, the gauge couplings unify for $\alpha_3(m_Z) \approx 0.127$ (if one ignores GUT-scale threshold corrections) which is somewhat higher than the experimental value $\alpha_3(m_Z)|_{expt} = 0.1176 \pm 0.002$ [5]. In the following, I examine if GUT scale threshold corrections due to the embedding of MSSM in $G(224)$ can reduce the predicted value of $\alpha_3(m_Z)$, while coupling unification is preserved above M_{GUT} up to a presumed string-scale.

The case of MSSM has been studied thoroughly by several authors. The constraints of (i) consistent electroweak symmetry break-

ing, (ii) non-violation of color and charge, (iii) desired SU(4)-color fermion mass relations: $m_b(\text{GUT}) \approx m_\tau$ and $m(\nu_{\text{Dirac}}^\tau) \approx m_{\text{top}}(\text{GUT})$, are all known to be satisfied in accord with observations. Thus I will have nothing new to add in this regard. We start with the following spectrum above M_{GUT} . Since the low energy theory is that of MSSM, we have three generations of quarks and leptons. We choose the following Higgs system above the GUT scale:

$$\begin{aligned}
& 2 \times (1, 1, 15)_H, (2, 1, 4)_H \oplus (2, 1, \bar{4})_H \\
& (1, 2, 4)_H \oplus (1, 2, \bar{4})_H \\
& \text{and } 2 \times (2, 2, 1)_H
\end{aligned} \tag{8.14}$$

With this choice of Higgs-multiplets, the one loop beta functions of the G(224) couplings for g_{2L} , g_{2R} and g_4 (including the gauge, Higgs and matter contributions) are equal, with

$$b_{2L} = b_{2R} = b_4 = 6. \tag{8.15}$$

Thus, in this case, we expect the three gauge couplings to run together even above $M_4 = M_{GUT}$ up to the scale which may be identified with the string scale $(M_{st})^6$. This would ensure G(224) unification at the

⁶ As α_U (≈ 0.04) is small in this case, we expect that two loop corrections will not alter coupling unification substantially.

string scale consistent with the observed gauge coupling unification. Our task now is to evaluate the threshold corrections to $\alpha_3(m_Z)$ due to super heavy gauge particles and Higgs multiplets of G(224).

8.4.1 *Threshold corrections to $\alpha_3(m_Z)$ due to gauge and Higgs multiplets of G(224)*

Denoting the one loop threshold corrections to $\alpha_i^{-1}(m_Z)$ by $-\Delta_i$, so that $\alpha_i^{-1}(m_Z) = \alpha_U^{-1} - (b_i/2\pi) \ln(m_Z/M_U) - \Delta_i$, we obtain $\Delta_i = \Sigma_\alpha(-b_i^\alpha)/(2\pi) \ln(m_Z/M_U)$. Here α_U is the unified coupling, $b_i = (33/5, 1, -3)$ yield the one loop beta functions of the three gauge couplings ($i = 1, 2, 3$) for the MSSM spectrum, and b_i^α is the contribution to the evolution due to the α th sub-multiplet with mass m_α . The threshold correction to $\alpha_3(m_Z)$ is given by:

$$\Delta\alpha_3(m_Z) = [\alpha_3(m_Z)]^2 \left(\frac{5}{7}\Delta_1 - \frac{12}{7}\Delta_2 + \Delta_3 \right) \quad (8.16)$$

The decomposition of the various G(224) Higgs multiplets under the standard model symmetry $G(213) = SU(2)_L \times U(1)_Y \times SU(3)^c$ is

given below:

$$\begin{aligned}
G(224) & \quad \textit{StandardModel} \\
(1, 1, 15) & \quad (8, 1, 0) + (1, 1, 0) + (3, 1, 2/3) + (\bar{3}, 1, -2/3) \\
(1, 2, 4) & \quad (3, 1, 2/3) + (3, 2, -1/3) + (1, 1, 0) + (1, 1, -1) \\
(1, 2, \bar{4}) & \quad (\bar{3}, 1, -2/3) + (\bar{3}, 2, 1/3) + (1, 1, 0) + (1, 1, 1) \quad (8.17) \\
(2, 1, 4) & \quad (3, 2, 1/6) + (3, 2, -1/2) \\
(2, 1, \bar{4}) & \quad (\bar{3}, 2, -1/6) + (\bar{3}, 2, 1/2) \\
(2, 2, 1) & \quad (1, 2, 1/2) + (1, 2, -1/2)
\end{aligned}$$

Using Eq. (8.16) and the decompositions of $G(224)$ multiplets into standard model multiplets given above, the threshold corrections to $\alpha_3(m_Z)$ can easily be calculated. The correction to $\alpha_3(m_Z)$ due to super heavy gauge particles is given by:

$$\Delta\alpha_3(m_Z)_{\text{Gauge}} = \frac{-3 \alpha_3^2(m_Z)}{28\pi} \left[15 \ln \frac{M^2(3, 1, 2/3)}{M_U^2} + 6 \ln \frac{M^2(1, 1, \pm 1)}{M_U^2} \right] \quad (8.18)$$

Defining the VEVs of $M(3, 1, 2/3)$ and $M(1, 1, \pm 1)$ as $M^2(3, 1, 2/3) = 4g^2(c^2 + a^2)$ and $M^2(1, 1, \pm 1) = 4g^2c^2$ and letting $M_U^2 = g^2a^2$, the above equation can be written as

$$\Delta\alpha_3(m_Z)_{\text{Gauge}} = \frac{-3 \alpha_3^2(m_Z)}{28\pi} \left[15 \ln(4 + p^2) + 6 \ln p^2 \right] \quad (8.19)$$

where $p = 4c^2/a^2$. For $p = 1, 2$, the correction to $\alpha_3(m_Z)$ from super heavy gauge particles is $\approx -0.011, -0.024$ respectively.

As mentioned above, the Higgs system consists of $2 \times (1, 1, 15)_H$, $(2, 1, 4)_H \oplus (2, 1, \bar{4})_H$, $(1, 2, 4)_H \oplus (1, 2, \bar{4})_H$ and $2 \times (2, 2, 1)_H$. Out of these, one $(2, 2, 1)_H$ remains light to give H_u and H_d of MSSM. The threshold corrections to $\alpha_3(m_Z)$ due to the Higgs multiplets getting GUT scale VEVs is given below:

$$\begin{aligned} \Delta\alpha_3(m_Z)_{\text{Higgs}} = & \frac{\alpha_3^2(m_Z)}{14\pi} \left[30 \ln \frac{M(3,1,2/3)_{15}}{M_U} + 15 \ln \frac{M(3,1,2/3)_{16}}{M_U} \right. \\ & + 2 \ln \frac{M(3,1,-1/3)}{M_U} + 6 \ln \frac{M(1,1,\pm 1)}{M_U} - 21 \ln \frac{M(3,2,1/6)}{M_U} \\ & \left. - 13 \ln \frac{M(3,2,-1/2)}{M_U} - 9 \ln \frac{M(1,2,1/2)}{M_U} + 42 \ln \frac{M(8,1,0)}{M_U} + 7 \ln \frac{M(3,1,-1/3)_{16}}{M_U} \right] \end{aligned} \quad (8.20)$$

Setting all superheavy Higgs masses to M in Eq. (8.20) for the sake of simplicity, we get

$$\Delta\alpha_3(m_Z)_{\text{Higgs}} = \frac{59\alpha_3^2(m_Z)}{14\pi} \ln \frac{M}{M_U} \quad (8.21)$$

Combining the effects in Eqs. (8.19) and (8.21), we find that for $p = 1 - 2$ and $M/M_U = 1 - 3$, we can get corrections to $\alpha_3(m_Z)$ ranging between $-(0.006-0.012)$, which gives $\alpha_3(m_Z)$ within one standard deviation of the observed value, $\alpha_3(m_Z)|_{\text{expt}} = 0.1176 \pm 0.002$. Thus MSSM embedded in G(224), gives rise to improved GUT prediction

for $\alpha_3(m_Z)$ when threshold corrections to gauge couplings due to the super heavy gauge particles and the Higgs multiplets (as chosen above) are taken into account. The gauge couplings of $G(224)$ are guaranteed to be unified in one loop, from the GUT scale, all the way up to the string scale by the choice of the Higgs system. We expect that two loop corrections will not alter coupling unification substantially, as in this case α_U is small ≈ 0.04 . This model demonstrates that gauge unification can be consistently achieved together with string unification for the case of MSSM embedded in $G(224)$, for a suitable choice of the Higgs system, with a clear benefit as regards the predicted value of $\alpha_3(m_Z)$.

8.5 Conclusion

It is well known that when the gauge couplings of the standard model are extrapolated upward within the context of supersymmetry, they unify at a scale $\sim 2 \times 10^{16}$ GeV. There are empirical reasons to believe that the effective symmetry above the unification scale contains $SU(4)$ -color. Thus this symmetry could be $G(224)$ or $G(214)$ or maximally

SO(10). The group $G(224)/G(214)$ has the advantage over SO(10), that within the context of string theory, the super heavy triplets are projected out through the process of string compactification. A suitable doublet-triplet splitting mechanism has not been realized for the case of SO(10) in the context of string theory. It has also been shown that for the case of a string derived $G(224)$, its gauge couplings can unify at the string scale. However, since $G(224)$ is semi-simple, we expect the gauge couplings to diverge above the unification scale. The question of interest then is how to reconcile observed gauge coupling unification with string unification for the cases of the standard model gauge symmetry being embedded in $G(224)$ or $G(214)$ near the conventional GUT scale. This was the purpose of my study in this chapter. I have considered two kinds of low energy spectra: MSSM, as well as a well motivated extension of MSSM, called the extended supersymmetric standard model, ESSM. The ESSM includes two vector like families that transform as $16 + \overline{16}$ of SO(10), in addition to the particle content of MSSM. Motivations for the case of ESSM have been noted in the introduction in Sec 8.1.

I have first considered the case of ESSM embedded into $G(224)$ above the conventional GUT scale. In doing so, our goals are:

- (1) to achieve gauge coupling unification for the case of $G(224)$ above the GUT scale,
- (2) ensure consistent electroweak symmetry breaking,
- (3) make sure that color and charge are not violated,
- (4) obtain a large enough Higgs mass with as little fine tuning as possible,
- (5) satisfy the lightest neutralino mass constraint,
- (6) obtain the right masses of the third generation particles i.e. t , b and τ by allowing for $B - L$ dependent terms in the mass matrices, and
- (7) obtain the second generation masses and their CKM mixings with the third family in accord with observations.

We find that with ESSM embedded in $G(224)$ the gauge couplings of $G(224)$ unify at a scale of 1.14×10^{17} GeV providing a plausible mechanism to reduce the mismatch between the string and the unification scales. The model, of course, has all the advantages of

ESSM mentioned in the introduction. It satisfies the constraints of (i) electroweak symmetry breaking, (ii) Higgs mass limit, (iii) lightest neutralino mass constraint, (iv) color and charge preservation and (v) explaining the masses and mixings of the second family. However, this model cannot give the right masses of t , b and τ simultaneously as the yukawa couplings x_u and x_d are constrained by the relation $x_d = x_u \cos \gamma$, at M_4 due to the G(224) symmetry relations. The same applies to the couplings x'_u and x'_d .

I next examine the case of ESSM embedded into G(214) at about the GUT scale. This case turns out to satisfy all the constraints listed above including the masses of the third family, together with gauge coupling unification. The G(214) couplings unify at 7.1×10^{16} GeV with the unified coupling $\alpha_{214} \approx 0.31$ being in the semi-perturbative range. The constraints of electroweak symmetry breaking, color and charge conservation, lightest neutralino mass bound and lightest Higgs mass limit are satisfied. The masses and mixings of the second and the third family turn out to be close to the observed values, providing an explanation of inter-family mass hierarchy. The strong coupling,

$\alpha_3(m_Z)$ is predicted to be around 0.118 in excellent agreement with data, and an improvement over the MSSM prediction of 0.127.

Finally, we considered the case of MSSM spectrum at low energy with the effective symmetry above the GUT scale being $G(224)$. With an appropriate choice of Higgs multiplets that break $G(224)$ to MSSM, we can ensure that the three couplings of $G(224)$ remain unified from the GUT scale all the way up to the string scale. The effect of GUT scale threshold corrections on $\alpha_3(m_Z)$ with the given choice of Higgs is calculated. It is found that these corrections can lower the GUT prediction for the value of $\alpha_3(m_Z)$ to $0.115 - 0.121$. This range lies within one standard deviation of the measured value.

The three cases studied above lead us to conclude that it is possible to achieve gauge coupling unification at a scale $M_U \sim 10^{17}$ GeV exceeding the conventional GUT scale $M_{GUT} \approx 2 \times 10^{16}$ GeV within an effective symmetry that contains $SU(4)$ -color above the scale M_{GUT} such as $G(224)$ or $G(214)$. The coupling unification scale M_U may quite plausibly be identified with the string unification scale [36]. While providing coupling unification, this case provides all the advan-

tages of SU(4)-color as regards an understanding of neutrino masses (via the seesaw mechanism) and implementing baryogenesis via leptogenesis, but without the problem of doublet-triplet splitting.

APPENDIX

.1 Renormalization group analysis of ESSM

The renormalization group equations of the gauge couplings below the unification scale with the addition of two vectorlike families and Yukawa couplings as in Eq. (8.1) are given by:

$$\frac{d\alpha_i}{dt} = \frac{b_i}{2\pi}\alpha_i^2 + \sum_{j=1}^3 \frac{b_{ij}}{8\pi^2}\alpha_i^2\alpha_j - \frac{\alpha_i^2}{2\pi} \frac{1}{16\pi^2} b_i^{\text{Yuk}} \quad (.22)$$

where

$$b_i = \begin{pmatrix} 2n_g + \frac{3}{5}n_H \\ -6 + 2n_g + n_H \\ -9 + 2n_g \end{pmatrix} = \begin{pmatrix} \frac{53}{5} \\ 5 \\ 1 \end{pmatrix} \quad (.23)$$

$$b_{ij} = \begin{pmatrix} \frac{38}{15}n_g + \frac{9}{25}n_H & \frac{6}{5}n_g + \frac{9}{5}n_H & \frac{88}{15}n_g \\ \frac{2}{5}n_g + \frac{3}{5}n_H & -24 + 14n_g + 7n_H & 8n_g \\ \frac{11}{15}n_g & 3n_g & -54 + \frac{68}{3}n_g \end{pmatrix} = \begin{pmatrix} \frac{977}{75} & \frac{39}{5} & \frac{88}{3} \\ \frac{13}{5} & 53 & 40 \\ \frac{11}{3} & 15 & \frac{178}{3} \end{pmatrix} \quad (.24)$$

Here n_g is the number of generations. Including the vectorlike generations, this number is 5. The number of pairs of light Higgs doublets is n_H , which for the case of ESSM is one. The contribution due to the

Yukawa couplings is given by:

$$\begin{aligned}
b_1^{\text{Yuk}} &= \frac{26}{5}(x_u'^2 + x_u^2) + \frac{14}{5}(x_d'^2 + x_d^2) + \frac{18}{5}(x_l'^2 + x_l^2) + \frac{2}{5}(y_q'^2 + z_q^2) \\
&\quad + \frac{6}{5}(y_l'^2 + z_l^2 + k_1^2) + \frac{16}{5}(z_u'^2 + y_u^2) + \frac{4}{5}(z_d'^2 + y_d^2) + \frac{12}{5}(z_l'^2 + y_l^2) \\
b_2^{\text{Yuk}} &= 6(x_u'^2 + x_u^2) + 6(x_d'^2 + x_d^2) + 2(x_l'^2 + x_l^2) + 6(y_q'^2 + z_q^2) \\
&\quad + 2(y_l'^2 + z_l^2 + k_1^2) \\
b_3^{\text{Yuk}} &= 4(x_u'^2 + x_u^2) + 4(x_d'^2 + x_d^2) + 4(y_q'^2 + z_q^2) + 2(z_u'^2 + y_u^2) \\
&\quad + 2(z_d'^2 + y_d^2)
\end{aligned} \tag{.25}$$

The one loop renormalization group equations for the ESSM

Yukawa couplings are given below:

$$\begin{aligned}
\frac{dx'_u}{dt} &= \frac{x'_u}{16\pi^2} [6x_u'^2 + x_d'^2 + y_q'^2 + z_u'^2 + 3x_u^2 + x_\nu'^2 + k_1^2 \\
&\quad - \frac{13}{15}g_1^2 - 3g_2^2 - \frac{16}{3}g_3^2] \\
\frac{dx'_d}{dt} &= \frac{x'_d}{16\pi^2} [6x_d'^2 + x_u'^2 + y_q'^2 + z_d'^2 + 3x_d^2 + x_l^2 + x_l'^2 + k_1^2 \\
&\quad - \frac{7}{15}g_1^2 - 3g_2^2 - \frac{16}{3}g_3^2] \\
\frac{dx_u}{dt} &= \frac{x_u}{16\pi^2} [6x_u^2 + x_d^2 + y_u^2 + z_q^2 + 3x_u'^2 + x_\nu'^2 + k_1^2 \\
&\quad - \frac{13}{15}g_1^2 - 3g_2^2 - \frac{16}{3}g_3^2] \\
\frac{dx_d}{dt} &= \frac{x_d}{16\pi^2} [6x_d^2 + x_u^2 + y_d^2 + z_q^2 + 3x_d'^2 + x_l^2 + x_l'^2 + k_1^2 \\
&\quad - \frac{7}{15}g_1^2 - 3g_2^2 - \frac{16}{3}g_3^2] \\
\frac{dy'_q}{dt} &= \frac{y'_q}{16\pi^2} [8y_q'^2 + x_u'^2 + x_d'^2 + 2y_l'^2 + z_q^2 + 3y_u^2 + 3y_d^2 + y_l^2 + \frac{1}{2}k_3^2 \\
&\quad - \frac{1}{15}g_1^2 - 3g_2^2 - \frac{16}{3}g_3^2] \\
\frac{dy_u}{dt} &= \frac{y_u}{16\pi^2} [5y_u^2 + 6y_q'^2 + 2x_u^2 + 2y_l'^2 + z_u'^2 + 3y_d^2 + y_l^2 + \frac{1}{2}k_3^2 \\
&\quad - \frac{16}{15}g_1^2 - \frac{16}{3}g_3^2] \\
\frac{dy_d}{dt} &= \frac{y_d}{16\pi^2} [5y_d^2 + 6y_q'^2 + 2x_d^2 + 2y_l'^2 + z_d'^2 + 3y_d^2 + y_l^2 + \frac{1}{2}k_3^2 \\
&\quad - \frac{4}{15}g_1^2 - \frac{16}{3}g_3^2] \\
\frac{dz_q}{dt} &= \frac{z_q}{16\pi^2} [8z_q^2 + x_u^2 + x_d^2 + 2z_l^2 + z_l'^2 + z_\nu'^2 + y_q'^2 + 3z_d'^2 + 3z_u'^2 \\
&\quad + y_l^2 + 2k_1^2 + \frac{1}{2}k_2^2 - \frac{1}{15}g_1^2 - 3g_2^2 - \frac{16}{3}g_3^2] \\
\frac{dz'_u}{dt} &= \frac{z'_u}{16\pi^2} [5z_u'^2 + 6z_q^2 + 2x_u'^2 + y_u^2 + 2z_l^2 + z_l'^2 + 3z_d'^2 + z_\nu'^2 \\
&\quad + 2k_1^2 + \frac{1}{2}k_3^2 - \frac{16}{15}g_1^2 - \frac{16}{3}g_3^2] \\
\frac{dz'_d}{dt} &= \frac{z'_d}{16\pi^2} [5z_d'^2 + 6z_q^2 + 2x_d'^2 + y_d^2 + 2z_l^2 + z_l'^2 + 3z_u'^2 + z_\nu'^2 \\
&\quad + 2k_1^2 + \frac{1}{2}k_3^2 - \frac{16}{15}g_1^2 - \frac{16}{3}g_3^2] \\
\frac{dx'_\nu}{dt} &= \frac{x'_\nu}{16\pi^2} [4x_\nu'^2 + x_l'^2 + y_l'^2 + z_\nu'^2 + 3x_u^2 + 3x_u'^2 + k_1^2 - \frac{3}{5}g_1^2 - 3g_2^2]
\end{aligned} \tag{.26}$$

$$\begin{aligned}
\frac{dz'_l}{dt} &= \frac{z'_l}{16\pi^2} \left[3z'_l{}^2 + 2x'_l{}^2 + y'_l{}^2 + 2z_l{}^2 + 6z_q{}^2 + z'_\nu{}^2 + 3z'_u{}^2 + 3z'_d{}^2 \right. \\
&\quad \left. + 2k_1{}^2 + \frac{1}{2}k_2{}^2 - \frac{12}{5}g_1{}^2 \right] \\
\frac{dz'_\nu}{dt} &= \frac{z'_\nu}{16\pi^2} \left[3z'_\nu{}^2 + 2x'_\nu{}^2 + 2z_l{}^2 + 6z_q{}^2 + z'_l{}^2 + 3z'_u{}^2 + 3z'_d{}^2 + 2k_1{}^2 + \frac{1}{2}k_2{}^2 \right] \\
\frac{dk_1}{dt} &= \frac{k_1}{16\pi^2} \left[4k_1{}^2 + 3x_u{}^2 + 3x'_u{}^2 + x'_\nu{}^2 + 3x_d{}^2 + 3x'_d{}^2 + x_l{}^2 + x'_l{}^2 \right. \\
&\quad \left. + 6z_q{}^2 + 3z'_u{}^2 + 3z'_d{}^2 + 2z_l{}^2 + z'_l{}^2 + z'_\nu{}^2 + \frac{1}{2}k_2{}^2 - \frac{3}{5}g_1{}^2 - 3g_2{}^2 \right] \\
\frac{dk_2}{dt} &= \frac{k_2}{16\pi^2} \left[\frac{1}{2}k_2{}^2 + 2k_1{}^2 + 6z_q{}^2 + 3z'_u{}^2 + 3z'_d{}^2 + 2z_l{}^2 + z'_l{}^2 + z'_\nu{}^2 \right] \\
\frac{dk_3}{dt} &= \frac{k_3}{16\pi^2} \left[\frac{1}{2}k_3{}^2 + 6y_q{}^2 + 3y_u{}^2 + 3y_d{}^2 + 2y_l{}^2 + y'_l{}^2 \right]
\end{aligned} \tag{.27}$$

.2 $G(224)$ renormalization group equations

The renormalization group equations for the group $G(224)$ with two vector like families and $(2, 2, 1)$, $(1, 2, \bar{4})_H$, $(1, 2, 4)_H$ and $(1, 1, 15)_H$ of Higgs are given by:

$$\begin{aligned}
\frac{g_{2L}}{dt} &= \frac{g_{2L}^3}{16\pi^2} \left[5 + \frac{1}{16\pi^2} (53g_{2L}^2 + 3g_{2R}^2 + 75g_4^2 - (16(X^2 + X'^2 + \xi^2 + \xi'^2) \right. \\
&\quad \left. + 8(Y^2 + Z^2 + h^2) + 4k_1^2)) \right] \\
\frac{g_{2R}}{dt} &= \frac{g_{2R}^3}{16\pi^2} \left[9 + \frac{1}{16\pi^2} (3g_{2L}^2 + 81g_{2R}^2 + 105g_4^2 - (16(X^2 + X'^2 + \xi^2 + \xi'^2) \right. \\
&\quad \left. + 8(Y'^2 + Z'^2 + h'^2) + 4k_1^2)) \right] \\
\frac{g_4}{dt} &= \frac{g_4^3}{16\pi^2} \left[4 + \frac{1}{16\pi^2} (15g_{2L}^2 + 21g_{2R}^2 + 152g_4^2 - (8(X^2 + X'^2 + \xi^2 + \xi'^2) \right. \\
&\quad \left. + 4(Y^2 + Y'^2 + Z^2 + Z'^2 + h^2 + h'^2))) \right] \\
\frac{X}{dt} &= \frac{X}{16\pi^2} \left[8X^2 + 4X'^2 + Y^2 + Z^2 + k_1^2 + h^2 + 2\xi^2 \right. \\
&\quad \left. - \left(\frac{15}{2}g_4^2 + 3g_{2L}^2 + 3g_{2R}^2 \right) \right] \\
\frac{X'}{dt} &= \frac{X'}{16\pi^2} \left[8X'^2 + 4X^2 + Y'^2 + Z'^2 + k_1^2 + h'^2 + 2\xi'^2 \right. \\
&\quad \left. - \left(\frac{15}{2}g_4^2 + 3g_{2L}^2 + 3g_{2R}^2 \right) \right] \\
\frac{Y}{dt} &= \frac{Y}{16\pi^2} \left[10Y^2 + 8Y'^2 + 2X^2 + Z'^2 + \frac{1}{2}k_3^2 + h^2 + 2\xi'^2 \right. \\
&\quad \left. - \left(\frac{15}{2}g_4^2 + 3g_{2L}^2 \right) \right] \\
\frac{Y'}{dt} &= \frac{Y'}{16\pi^2} \left[10Y'^2 + 8Y^2 + 2X'^2 + Z^2 + \frac{1}{2}k_3^2 + h'^2 + 2\xi^2 \right. \\
&\quad \left. - \left(\frac{15}{2}g_4^2 + 3g_{2R}^2 \right) \right] \tag{.28} \\
\frac{Z}{dt} &= \frac{Z}{16\pi^2} \left[10Z^2 + 8Z'^2 + 2X^2 + Y'^2 + \frac{1}{2}k_2^2 + 4k_1^2 + h^2 + 2\xi^2 \right. \\
&\quad \left. - \left(\frac{15}{2}g_4^2 + 3g_{2L}^2 \right) \right] \\
\frac{Z'}{dt} &= \frac{Z'}{16\pi^2} \left[10Z'^2 + 8Z^2 + 2X'^2 + Y^2 + \frac{1}{2}k_2^2 + 4k_1^2 + h'^2 + 2\xi'^2 \right. \\
&\quad \left. - \left(\frac{15}{2}g_4^2 + 3g_{2R}^2 \right) \right] \\
\frac{h}{dt} &= \frac{h}{16\pi^2} \left[4h^2 + 2h'^2 + 2X^2 + Y^2 + 2Z^2 - \frac{15}{2}g_4^2 \right] \\
\frac{h'}{dt} &= \frac{h'}{16\pi^2} \left[4h'^2 + 2h^2 + 2X'^2 + Y'^2 + 2Z'^2 - \frac{15}{2}g_4^2 \right] \\
\frac{\xi}{dt} &= \frac{\xi}{16\pi^2} \left[8\xi^2 + 4\xi'^2 + 4X^2 + Y^2 + Z^2 - \left(\frac{15}{2}g_4^2 + 3g_{2L}^2 + 3g_{2R}^2 \right) \right]
\end{aligned}$$

.3 $G(214)$ renormalization group equations

The renormalization group equations for the group $G(214)$ with two vector like families and $(2, 2, 1)$, $(1, 2, \bar{4})_H$, $(1, 2, 4)_H$ and $(1, 1, 15)_H$ of

Higgs are given by:

$$\begin{aligned}
\frac{g_{2L}}{dt} &= \frac{g_{2L}^3}{16\pi^2} \left[5 + \frac{1}{16\pi^2} (53g_{2L}^2 + 3g_{2R}^2 + 75g_4^2 \right. \\
&\quad \left. - (8(X1^2 + X1'^2 + X2^2 + X2'^2 + \xi_1^2 + \xi_1'^2 + \xi_2^2 + \xi_2'^2) \right. \\
&\quad \left. + 8(Y^2 + Z^2 + h^2) + 4k_1^2) \right] \\
\frac{g_{2R}}{dt} &= \frac{g_{2R}^3}{16\pi^2} \left[9 + \frac{1}{16\pi^2} (3g_{2L}^2 + 81g_{2R}^2 + 105g_4^2 \right. \\
&\quad \left. - (8(X1^2 + X1'^2 + X2^2 + X2'^2 + \xi_1^2 + \xi_1'^2 + \xi_2^2 + \xi_2'^2) \right. \\
&\quad \left. + 4(Y1'^2 + Y2'^2 + Z1'^2 + Z2'^2 + h1'^2 + h2'^2) + 4k_1^2) \right] \\
\frac{g_4}{dt} &= \frac{g_4^3}{16\pi^2} \left[4 + \frac{1}{16\pi^2} (15g_{2L}^2 + 21g_{2R}^2 + 152g_4^2 \right. \\
&\quad \left. - (4(X1^2 + X1'^2 + X2^2 + X2'^2 + \xi_1^2 + \xi_1'^2 + \xi_2^2 + \xi_2'^2) \right. \\
&\quad \left. + 4(Y^2 + Z^2 + h^2) \right. \\
&\quad \left. + 2((Y1'^2 + Y2'^2 + Z1'^2 + Z2'^2 + h1'^2 + h2'^2))) \right] \\
\frac{X1}{dt} &= \frac{X1}{16\pi^2} \left[4(X1^2 + X2^2) + 2(X1'^2 + X2'^2) + Y^2 + Z^2 + k_1^2 \right. \\
&\quad \left. + h^2 + (\xi_1^2 + \xi_2^2) - \left(\frac{15}{2}g_4^2 + 3g_{2L}^2 + 3g_{2R}^2 \right) \right] \\
\frac{X2}{dt} &= \frac{X2}{16\pi^2} \left[4(X1^2 + X2^2) + 2(X1'^2 + X2'^2) + Y^2 + Z^2 + k_1^2 \right. \\
&\quad \left. + h^2 + (\xi_1^2 + \xi_2^2) - \left(\frac{15}{2}g_4^2 + 3g_{2L}^2 + 3g_{2R}^2 \right) \right] \\
\frac{X1'}{dt} &= \frac{X1'}{16\pi^2} \left[4(X1'^2 + X2'^2) + 2(X1^2 + X2^2) \right. \\
&\quad \left. + (Y1'^2 + Y2'^2 + Z1'^2 + Z2'^2)/2 \right. \\
&\quad \left. + k_1^2 + (h1'^2 + h2'^2)/2 + (\xi_1'^2 + \xi_2'^2) - \left(\frac{15}{2}g_4^2 + 3g_{2L}^2 + 3g_{2R}^2 \right) \right] \\
\frac{X2'}{dt} &= \frac{X2'}{16\pi^2} \left[4(X1'^2 + X2'^2) + 2(X1^2 + X2^2) \right. \\
&\quad \left. + (Y1'^2 + Y2'^2 + Z1'^2 + Z2'^2)/2 \right. \\
&\quad \left. + k_1^2 + (h1'^2 + h2'^2)/2 + (\xi_1'^2 + \xi_2'^2) - \left(\frac{15}{2}g_4^2 + 3g_{2L}^2 + 3g_{2R}^2 \right) \right] \\
\frac{Y}{dt} &= \frac{Y}{16\pi^2} \left[10Y^2 + 4(Y1'^2 + Y2'^2) + (X1^2 + X2^2) + (Z1'^2 + Z2'^2)/2 \right.
\end{aligned} \tag{.29}$$

$$\begin{aligned}
\frac{Z1'}{dt} &= \frac{Z1'}{16\pi^2} [5(Z1'^2 + Z2'^2) + 8Z^2 + (X1'^2 + X2'^2) + Y^2 \\
&\quad + \frac{1}{2}k_2^2 + 4k_1^2 + (h1'^2 + h2'^2)/2 + (\xi_1'^2 + \xi_2'^2) - (\frac{15}{2}g_4^2 + 3g_{2R}^2)] \\
\frac{Z2'}{dt} &= \frac{Z2'}{16\pi^2} [5(Z1'^2 + Z2'^2) + 8Z^2 + (X1'^2 + X2'^2) + Y^2 \\
&\quad + \frac{1}{2}k_2^2 + 4k_1^2 + (h1'^2 + h2'^2)/2 + (\xi_1'^2 + \xi_2'^2) - (\frac{15}{2}g_4^2 + 3g_{2R}^2)] \\
\frac{h}{dt} &= \frac{h}{16\pi^2} [4h^2 + (h1'^2 + h2'^2) + (X1^2 + X2^2) + Y^2 + 2Z^2 - \frac{15}{2}g_4^2] \\
\frac{h1'}{dt} &= \frac{h1'}{16\pi^2} [2(h1'^2 + h2'^2) + 2h^2 + (X1'^2 + X2'^2) \\
&\quad + (Y1'^2 + Y2'^2)/2 + (Z1'^2 + Z2'^2) - \frac{15}{2}g_4^2] \\
\frac{h2'}{dt} &= \frac{h2'}{16\pi^2} [2(h1'^2 + h2'^2) + 2h^2 + (X1'^2 + X2'^2) \\
&\quad + (Y1'^2 + Y2'^2)/2 + (Z1'^2 + Z2'^2) - \frac{15}{2}g_4^2] \\
\frac{\xi_1}{dt} &= \frac{\xi_1}{16\pi^2} [4(\xi_1^2 + \xi_2^2) + 2(\xi_1'^2 + \xi_2'^2) + 2(X1^2 + X2^2) \\
&\quad + Y^2 + Z^2 - (\frac{15}{2}g_4^2 + 3g_{2L}^2 + 3g_{2R}^2)] \\
\frac{\xi_2}{dt} &= \frac{\xi_2}{16\pi^2} [4(\xi_1^2 + \xi_2^2) + 2(\xi_1'^2 + \xi_2'^2) + 2(X1^2 + X2^2) \\
&\quad + Y^2 + Z^2 - (\frac{15}{2}g_4^2 + 3g_{2L}^2 + 3g_{2R}^2)] \\
\frac{\xi_1'}{dt} &= \frac{\xi_1'}{16\pi^2} [4(\xi_1'^2 + \xi_2'^2) + 2(\xi_1^2 + \xi_2^2) + 2(X1'^2 + X2'^2) + (Y1'^2 + Y2'^2)/2 \\
&\quad + (Z1'^2 + Z2'^2)/2 - (\frac{15}{2}g_4^2 + 3g_{2L}^2 + 3g_{2R}^2)] \\
\frac{\xi_2'}{dt} &= \frac{\xi_2'}{16\pi^2} [4(\xi_1'^2 + \xi_2'^2) + 2(\xi_1^2 + \xi_2^2) + 2(X1'^2 + X2'^2) + (Y1'^2 + Y2'^2)/2 \\
&\quad + (Z1'^2 + Z2'^2)/2 - (\frac{15}{2}g_4^2 + 3g_{2L}^2 + 3g_{2R}^2)] \\
\frac{k_1}{dt} &= \frac{k_1}{16\pi^2} [4k_1^2 + \frac{1}{2}k_2^2 + 4(X1^2 + X2^2 + X1'^2 + X2'^2) \\
&\quad + 8Z^2 + 4(Z1'^2 + Z2'^2) - (3g_{2L}^2 + 3g_{2R}^2)] \\
\frac{k_2}{dt} &= \frac{k_2}{16\pi^2} [\frac{1}{2}k_2^2 + 4k_1^2 + 8Z^2 + 4(Z1'^2 + Z2'^2)] \\
\frac{k_3}{dt} &= \frac{k_3}{16\pi^2} [\frac{1}{2}k_3^2 + 8Y^2 + 4(Y1'^2 + Y2'^2)]
\end{aligned} \tag{.30}$$

I. APPENDIX: RENORMALIZATION GROUP ANALYSIS OF MSSM

I.1 Renormalization Group Equations of Gauge Couplings and Gaugino masses with softly broken supersymmetry

The running of gauge couplings at two loops in a supersymmetric theory is scheme independent. The two loop running of gauge couplings is given by [137]:

$$\frac{dg}{dt} = \frac{1}{16\pi^2}\beta_g^{(1)} + \frac{1}{(16\pi^2)^2}\beta_g^{(2)} \quad (\text{I.1})$$

$$\beta_g^{(1)} = g^3 [S(R) - 3C(G)] \quad (\text{I.2})$$

$$\beta_g^{(2)} = g^5 [-6C(G)^2 + 2C(G)S(R) + 4S(R)C(R)] \quad (\text{I.3})$$

$$-g^3 Y^{ijk} Y_{ijk} C(k) / d(G)$$

where $C(R)$ is the quadratic Casimir invariant for the representation R and $S(R)$ is the Dynkin index. The Y^{ijk} are the Yukawa couplings of the superfields $\Phi_i \Phi_j \Phi_k$, and $Y_{ijk} = (Y^{ijk})^*$, and $d(G)$ is the dimension

of the adjoint. The β -function of the gaugino masses in the $\overline{\text{DR}}$ scheme

are as follows:

$$\frac{dM}{dt} = \frac{1}{16\pi^2}\beta_M^{(1)} + \frac{1}{(16\pi^2)^2}\beta_M^{(2)} \quad (\text{I.4})$$

$$\beta_M^{(1)} = g^2 M [2S(R) - 6C(G)] \quad (\text{I.5})$$

$$\beta_M^{(2)} = g^4 M [-24C(G)^2 + 8C(G)S(R) + 16S(R)C(R)] \quad (\text{I.6})$$

$$+ 2g^2 (A^{ijk} - MY^{ijk}) Y_{ijk} C(k) / d(G)$$

The A^{ijk} are the scalar trilinear couplings between the fields $\phi_i \phi_j \phi_k$, and have mass dimension one. For the case of the standard model gauge group $SU(3) \times SU(2) \times U(1)$, the running of the gauge couplings (including supersymmetry) is given by:

$$\frac{dg_a}{dt} = \frac{g_a^3}{16\pi^2} B_a^{(1)} + \frac{g_a^3}{(16\pi^2)^2} \left[\sum_{b=1}^3 B_{ab}^{(2)} g_b^2 - \sum_{x=u,d,e} C_a^x \text{Tr}(Y_x^\dagger Y_x) \right] \quad (\text{I.7})$$

where the indices a, b run over the three gauge couplings, $B_a^{(1)} = (\frac{33}{5}, 1, -3)$, and

$$B_{ab}^{(2)} = \begin{bmatrix} \frac{199}{25} & \frac{27}{5} & \frac{88}{5} \\ \frac{9}{5} & 25 & 24 \\ \frac{11}{5} & 9 & 14 \end{bmatrix} \quad C_a^{u,d,e} = \begin{bmatrix} \frac{26}{5} & \frac{14}{5} & \frac{18}{5} \\ 6 & 6 & 2 \\ 4 & 4 & 0 \end{bmatrix} \quad (\text{I.8})$$

The two loop gaugino mass RGEs can be written in terms of the

$B_a^{(1)}$, $B_{ab}^{(2)}$ and $C_a^{u,d,e}$ as:

$$\begin{aligned} \frac{dM_a}{dt} = & \frac{2g_a^2}{16\pi^2} B_a^{(1)} M_a + \frac{2g_a^2}{(16\pi^2)^2} \left[\sum_{b=1}^3 B_{ab}^{(2)} g_b^2 (M_a + M_b) \right. \\ & \left. + \sum_{x=u,d,e} C_a^x (Tr(Y_x^\dagger A_x) - M_a Tr(Y_x^\dagger Y_x)) \right] \end{aligned} \quad (\text{I.9})$$

I.2 Renormalization group equations of Yukawa couplings and

A-terms

The one loop renormalization group equations for the Yukawa couplings Y^{ijk} and the trilinear couplings A^{ijk} are given by:

$$\frac{dY^{ijk}}{dt} = \frac{Y^{ijp}}{16\pi^2} \left(\frac{1}{2} Y_{prs} Y^{krs} - 2\delta_p^k g^2 C(p) \right) + (k \leftrightarrow i) + (k \leftrightarrow j) \quad (\text{I.10})$$

$$\begin{aligned} \frac{dA^{ijk}}{dt} = & \frac{1}{16\pi^2} \left[\frac{1}{2} A^{ijl} Y_{lmn} Y^{mnk} + Y^{ijl} Y_{lmn} A^{mnk} \right. \\ & \left. - 2(A^{ijk} - 2MY^{ijk}) g^2 C(k) + (k \leftrightarrow i) + (k \leftrightarrow j) \right] \end{aligned} \quad (\text{I.11})$$

Applying this to the case of MSSM we get:

$$\begin{aligned}
\frac{dY_u}{dt} &= \frac{Y_u}{16\pi^2} \left[3Tr(Y_u Y_u^\dagger) + 3Y_u^\dagger Y_u + Y_d^\dagger Y_d - \frac{16}{3}g_3^2 - 3g_2^2 - \frac{13}{15}g_1^2 \right] \\
\frac{dY_d}{dt} &= \frac{Y_d}{16\pi^2} \left[Tr(3Y_d Y_d^\dagger + Y_e Y_e^\dagger) + 3Y_d^\dagger Y_d + Y_u^\dagger Y_u - \frac{16}{3}g_3^2 - 3g_2^2 - \frac{7}{15}g_1^2 \right] \\
\frac{dY_e}{dt} &= \frac{Y_e}{16\pi^2} \left[Tr(3Y_d Y_d^\dagger + Y_e Y_e^\dagger) + 3Y_e^\dagger Y_e - 3g_2^2 - \frac{9}{5}g_1^2 \right] \\
\frac{dA_u}{dt} &= \frac{A_u}{16\pi^2} \left[3Tr(Y_u Y_u^\dagger) + 5Y_u^\dagger Y_u + Y_d^\dagger Y_d - \frac{16}{3}g_3^2 - 3g_2^2 - \frac{13}{15}g_1^2 \right] \\
&\quad + \frac{Y_u}{16\pi^2} \left[6Tr(A_u Y_u^\dagger) + 4Y_u^\dagger A_u + 2Y_d^\dagger A_d \right. \\
&\quad \left. + \frac{32}{3}g_3^2 M_3 + 6g_2^2 M_2 + \frac{26}{15}g_1^2 M_1 \right] \\
\frac{dA_d}{dt} &= \frac{A_d}{16\pi^2} \left[Tr(3Y_d Y_d^\dagger + Y_e Y_e^\dagger) + 5Y_d^\dagger Y_d + Y_u^\dagger Y_u - \frac{16}{3}g_3^2 - 3g_2^2 - \frac{7}{15}g_1^2 \right] \\
&\quad + \frac{Y_d}{16\pi^2} \left[Tr(6A_d Y_d^\dagger + 2A_e Y_e^\dagger) + 4Y_d^\dagger A_d + 2Y_u^\dagger A_u \right. \\
&\quad \left. + \frac{32}{3}g_3^2 M_3 + 6g_2^2 M_2 + \frac{14}{15}g_1^2 M_1 \right] \\
\frac{dA_e}{dt} &= \frac{A_e}{16\pi^2} \left[Tr(3Y_d Y_d^\dagger + Y_e Y_e^\dagger) + 5Y_e^\dagger Y_e - 3g_2^2 - \frac{9}{5}g_1^2 \right] \\
&\quad + \frac{Y_e}{16\pi^2} \left[Tr(6A_d Y_d^\dagger + 2A_e Y_e^\dagger) + 4Y_e^\dagger A_e + 6g_2^2 M_2 + \frac{18}{5}g_1^2 M_1 \right]
\end{aligned} \tag{I.12}$$

I.3 Renormalization group equations of scalar (mass)² terms

The renormalization group equations of scalar mass² couplings of fields

$\phi_i^* \phi_j$ are given by:

$$\begin{aligned}
\frac{d(m^2)_i^j}{dt} &= \frac{1}{16\pi^2} \left[\frac{1}{2}Y_{ipq} Y^{pqn} (m^2)_n^j + 2Y_{ipq} Y^{jpr} (m^2)_r^q + \frac{1}{2}Y^{jpq} Y_{pqn} (m^2)_i^n \right. \\
&\quad \left. + A_{ipq} A^{jpq} - 8\delta_i^j M M^\dagger g^2 C(i) + 2g^2 T_i^{Aj} Tr(T^A m^2) \right]
\end{aligned} \tag{I.13}$$

The RGEs of the soft masses can then be calculated:

$$\begin{aligned}
\frac{dm_{H_u}^2}{dt} &= \frac{6Tr}{16\pi^2} [(m_{H_u}^2 + m_Q^2)Y_u^\dagger Y_u + Y_u^\dagger m_u^2 Y_u + A_u^\dagger A_u] \\
&\quad - 6g_2^2 |M_2|^2 - \frac{6}{5}g_1^2 |M_1|^2 + \frac{3}{5}g_1^2 \mathcal{S} \\
\frac{dm_{H_d}^2}{dt} &= \frac{Tr}{16\pi^2} [6(m_{H_d}^2 + m_Q^2)Y_d^\dagger Y_d + 6Y_d^\dagger m_d^2 Y_d + 2(m_{H_d}^2 + m_L^2)Y_e^\dagger Y_e \\
&\quad + 2Y_e^\dagger m_e^2 Y_e + 6A_d^\dagger A_d + 2A_e^\dagger A_e] \\
&\quad - 6g_2^2 |M_2|^2 - \frac{6}{5}g_1^2 |M_1|^2 - \frac{3}{5}g_1^2 \mathcal{S} \\
\frac{dm_Q^2}{dt} &= \frac{1}{16\pi^2} [(2m_{H_u}^2 + m_Q^2)Y_u^\dagger Y_u + (2m_{H_d}^2 + m_Q^2)Y_d^\dagger Y_d \\
&\quad + (Y_u^\dagger Y_u + Y_d^\dagger Y_d)m_Q^2 + 2Y_u^\dagger m_u^2 Y_u + 2Y_d^\dagger m_d^2 Y_d \\
&\quad + 2A_u^\dagger A_u + A_d^\dagger A_d - \frac{32}{3}g_3^2 |M_3|^2 - 6g_2^2 |M_2|^2 - \frac{2}{15}g_1^2 |M_1|^2 + \frac{1}{5}g_1^2 \mathcal{S}] \\
\frac{dm_u^2}{dt} &= \frac{1}{16\pi^2} [(4m_{H_u}^2 + 2m_u^2)Y_u Y_u^\dagger + 4Y_u m_Q^2 Y_u^\dagger \\
&\quad + 2Y_u Y_u^\dagger m_u^2 + 4A_u A_u^\dagger - \frac{32}{3}g_3^2 |M_3|^2 - \frac{32}{15}g_1^2 |M_1|^2 - \frac{4}{5}g_1^2 \mathcal{S}] \\
\frac{dm_d^2}{dt} &= \frac{1}{16\pi^2} [(4m_{H_d}^2 + 2m_d^2)Y_d Y_d^\dagger + 4Y_d m_Q^2 Y_d^\dagger + 2Y_d Y_d^\dagger m_d^2 \\
&\quad + 4A_d A_d^\dagger - \frac{32}{3}g_3^2 |M_3|^2 - \frac{8}{15}g_1^2 |M_1|^2 + \frac{2}{5}g_1^2 \mathcal{S}] \\
\frac{dm_L^2}{dt} &= \frac{1}{16\pi^2} [(2m_{H_d}^2 + m_L^2)Y_e^\dagger Y_e + 2Y_e^\dagger m_e^2 Y_e + Y_e^\dagger Y_e m_L^2 + 2A_e^\dagger A_e \\
&\quad - 6g_2^2 |M_2|^2 - \frac{6}{5}g_1^2 |M_1|^2 - \frac{3}{5}g_1^2 \mathcal{S}] \\
\frac{dm_e^2}{dt} &= \frac{1}{16\pi^2} [(4m_{H_d}^2 + 2m_e^2)Y_e Y_e^\dagger + 4Y_e m_L^2 Y_e^\dagger + 2Y_e Y_e^\dagger m_e^2 \\
&\quad + 4A_e A_e^\dagger - \frac{24}{5}g_1^2 |M_1|^2 + \frac{6}{5}g_1^2 \mathcal{S}]
\end{aligned} \tag{I.14}$$

Finally, the renormalization group equations of the supersymmet-

ric μ -parameters and the corresponding soft parameter B are given by:

$$\frac{d\mu}{dt} = \frac{\mu}{16\pi^2} [Tr(3Y_u Y_u^\dagger + 3Y_d Y_d^\dagger + Y_e Y_e^\dagger) - 3g_2^2 - \frac{3}{5}g_1^2] \quad (\text{I.15})$$

$$\frac{dB}{dt} = \frac{B}{16\pi^2} [Tr(3Y_u Y_u^\dagger + 3Y_d Y_d^\dagger + Y_e Y_e^\dagger) - 3g_2^2 - \frac{3}{5}g_1^2] \quad (\text{I.16})$$

$$+ \frac{\mu}{16\pi^2} [Tr(6A_u Y_u^\dagger + 6A_d Y_d^\dagger + 2A_e Y_e^\dagger) + g_2^2 M_2 + \frac{6}{5}g_1^2 M_1]$$

II. APPENDIX: WOLFENSTEIN PARAMETERIZATION OF THE CKM MATRIX AND THE UNITARY TRIANGLE

The Cabibbo-Kobayashi-Maskawa (CKM) matrix connects the weak eigenstates (d', s', b') to the corresponding mass eigenstates (d, s, b) through

$$\begin{pmatrix} d' \\ s' \\ b' \end{pmatrix} = \begin{pmatrix} V_{ud} & V_{us} & V_{ub} \\ V_{cd} & V_{cs} & V_{cb} \\ V_{td} & V_{ts} & V_{tb} \end{pmatrix} \begin{pmatrix} d \\ s \\ b \end{pmatrix} = V_{CKM} \begin{pmatrix} d \\ s \\ b \end{pmatrix} \quad (\text{II.1})$$

The CKM matrix is a 3×3 unitary matrix, which in general, can be parameterized by three real rotational angles and six complex phases. Out of these six phases, five can be rotated away by redefinition of quark fields. Thus, the CKM matrix can be parameterized by three angles and a single phase. This phase leading to an imaginary part of the CKM matrix is a necessary ingredient to describe CP violation within the standard model.

II.1 Wolfenstein Parametrization of the CKM Matrix

The Wolfenstein parametrization is an approximate parametrization of the CKM matrix in which each element is expanded as a power series in the small parameter $\lambda = |V_{us}| \approx 0.22$ [77, 136].

$$V_{CKM} = \begin{pmatrix} 1 - \frac{\lambda^2}{2} & \lambda & A\lambda^3(\rho - i\eta) \\ -\lambda & 1 - \frac{\lambda^2}{2} & A\lambda^2 \\ A\lambda^3(1 - \rho - i\eta) & -A\lambda^2 & 1 \end{pmatrix} + \mathcal{O}(\lambda^4). \quad (\text{II.2})$$

II.1.1 Wolfenstein Parametrization beyond the leading order

The higher order corrections to the Wolfenstein parametrization are found by the requirement of unitarity. The corrections to Eq. (II.2)

in higher powers of λ are given by the following expressions:

$$\begin{aligned}
V_{ud} &= 1 - \frac{\lambda^2}{2} - \frac{1}{8}\lambda^4 + \mathcal{O}(\lambda^6) \\
V_{us} &= \lambda + \mathcal{O}(\lambda^7) \\
V_{ub} &= A\lambda^3(\rho - i\eta) \\
V_{cd} &= -\lambda + \frac{1}{2}A^2\lambda^5[1 - 2(\rho + i\eta)] + \mathcal{O}(\lambda^7) \\
V_{cs} &= 1 - \frac{\lambda^2}{2} - \frac{1}{8}\lambda^4(1 + 4A^2) + \mathcal{O}(\lambda^6) \\
V_{cb} &= A\lambda^2 + \mathcal{O}(\lambda^8) \\
V_{td} &= A\lambda^3[1 - (\rho + i\eta)(1 - \frac{\lambda^2}{2})] + \mathcal{O}(\lambda^7) \\
V_{ts} &= -A\lambda^2 + \frac{1}{2}A(1 - 2\rho)\lambda^4 - i\eta A\lambda^4 + \mathcal{O}(\lambda^6) \\
V_{tb} &= 1 - \frac{1}{2}A^2\lambda^4 + \mathcal{O}(\lambda^6)
\end{aligned} \tag{II.3}$$

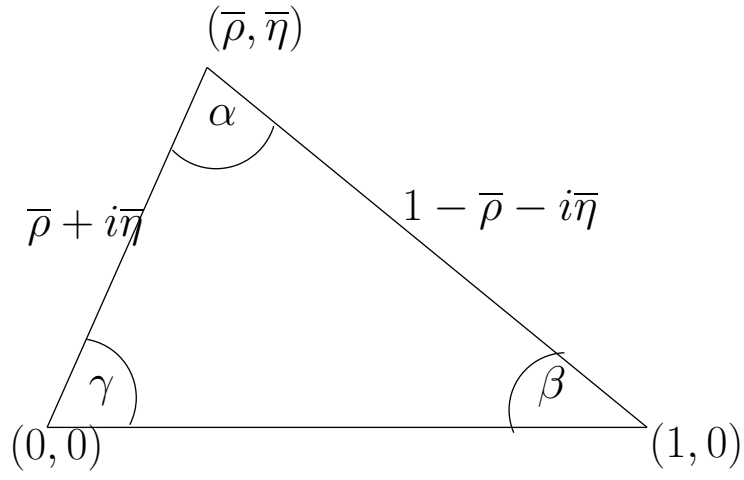
The quantities $\rho(1 - \frac{\lambda^2}{2})$ and $\eta(1 - \frac{\lambda^2}{2})$ are often represented by $\bar{\rho}$ and $\bar{\eta}$ respectively.

II.2 The Unitarity Triangle

The unitarity of the CKM matrix give rise to the following relation:

$$V_{ud}V_{ub}^* + V_{cd}V_{cb}^* + V_{td}V_{tb}^* = 0. \tag{II.4}$$

This relation can be represented as a “unitarity” triangle in the complex $(\bar{\rho}, \bar{\eta})$ plane.



The unitarity triangle.

The invariance of Eq. (II.4) under any phase transformations implies that the corresponding triangle is rotated in the $(\bar{\rho}, \bar{\eta})$ plane under such transformations. Since the angles and the sides in these triangles remain unchanged, they are phase convention independent, and are physical observables. The area of the unitarity triangle is related to the measure of CP violation $J_{CP} \equiv V_{ts}^* V_{cd}^* V_{cs} V_{td}$:

$$|J_{CP}| = 2A_{\Delta}, \quad (\text{II.5})$$

where A_{Δ} denotes the area of the unitarity triangle. The construction of the unitarity triangle is done as follows: 1. The term $V_{cd}V_{cb}^*$ in Eq. (II.4), is real to an excellent accuracy ($\mathcal{O}(\lambda^7)$), with $|V_{cd}V_{cb}^*| = A\lambda^3$. We can scale the other terms in Eq. (II.4) by $A\lambda^3$. Keeping $\mathcal{O}(\lambda^5)$

terms

$$\frac{1}{A\lambda^3}V_{ud}V_{ub}^* = \bar{\rho} + i\bar{\eta}; \quad \frac{1}{A\lambda^3}V_{td}V_{tb}^* = 1 - (\bar{\rho} + i\bar{\eta}). \quad (\text{II.6})$$

2. Thus Eq. (II.4) represents a triangle in the complex $(\bar{\rho}, \bar{\eta})$ plane.

3. The triangle gives rise to the following formulae:

$$\sin(2\alpha) = \frac{2\bar{\eta}(\bar{\eta}^2 + \bar{\rho}^2 - \bar{\rho})}{(\bar{\rho}^2 + \bar{\eta}^2)((1 - \bar{\rho})^2 + \bar{\eta}^2)} \quad (\text{II.7})$$

$$\sin(2\beta) = \frac{2\bar{\eta}(1 - \bar{\rho})}{((1 - \bar{\rho})^2 + \bar{\eta}^2)} \quad (\text{II.8})$$

$$\sin(2\gamma) = \frac{2\bar{\rho}\bar{\eta}}{\bar{\rho}^2 + \bar{\eta}^2} = \frac{2\rho\eta}{\rho^2 + \eta^2} \quad (\text{II.9})$$

The lengths CA and BA in the triangle, to be denoted by R_c and R_t respectively are given by:

$$R_b \equiv \frac{|V_{ud}V_{ub}^*|}{|V_{cd}V_{cb}^*|} = \sqrt{\bar{\rho}^2 + \bar{\eta}^2} = \left(1 - \frac{\lambda^2}{2}\right) \frac{1}{\lambda} \left| \frac{V_{ub}}{V_{cb}} \right| \quad (\text{II.10})$$

$$R_t \equiv \frac{|V_{td}V_{tb}^*|}{|V_{cd}V_{cb}^*|} = \sqrt{(1 - \bar{\rho})^2 + \bar{\eta}^2} = \frac{1}{\lambda} \left| \frac{V_{td}}{V_{cb}} \right| \quad (\text{II.11})$$

The angle β and γ of the unitarity triangle are related directly to the complex phases of the CKM elements V_{td} and V_{ub} respectively, through:

$$V_{td} = |V_{td}|e^{-i\beta}, \quad V_{ub} = |V_{ub}|e^{-i\gamma} \quad (\text{II.12})$$

The angle α can be found using the relation:

$$\alpha + \beta + \gamma = 180^\circ. \quad (\text{II.13})$$

The unitarity triangle gives a full description of the CKM matrix, as also a measure of CP violation within the standard model, indicating that quark mixing and CP violation are closely related.

III. APPENDIX: CP VIOLATION IN THE K MESON SYSTEM

For an extensive review see Ref. [136].

III.1 $K^0 - \bar{K}^0$ mixing

In the standard model, the strong interaction conserves strangeness, while the weak interaction does not. The strong interaction eigenstates K^0 and \bar{K}^0 can mix through weak interactions such as $K^0 \rightleftharpoons 2\pi \rightleftharpoons \bar{K}^0$. In this $K^0 - \bar{K}^0$ system the \bar{K}^0 state is defined as the CP conjugate of K^0 .

$$CP|K^0\rangle = -|\bar{K}^0\rangle \quad \text{and} \quad CP|\bar{K}^0\rangle = -|K^0\rangle \quad (\text{III.1})$$

In the absence of mixing, the time evolution of $|K^0(t)\rangle$ is given by:

$$|K^0(t)\rangle = |K^0(0)\rangle e^{-iHt} \quad (\text{III.2})$$

where H is a 2×2 matrix which can be decomposed into real and imaginary parts as $H = M - i\Gamma/2$. The time evolution of \overline{K}° can be written similarly. In the presence of mixing, the time evolution of the $K^\circ - \overline{K}^\circ$ system is described by:

$$i\frac{d\psi(t)}{dt} = \widehat{H}\psi(t); \quad \psi(t) = \begin{pmatrix} |K^\circ(t)\rangle \\ |\overline{K}^\circ(t)\rangle \end{pmatrix} \quad (\text{III.3})$$

where

$$\widehat{H} = \widehat{M} - i\widehat{\Gamma}/2 = \begin{pmatrix} M_{11} - i\frac{\Gamma_{11}}{2} & M_{12} - i\frac{\Gamma_{12}}{2} \\ M_{21} - i\frac{\Gamma_{21}}{2} & M_{22} - i\frac{\Gamma_{22}}{2} \end{pmatrix} \quad (\text{III.4})$$

Hermiticity of \widehat{H} requires $M_{12} = M_{21}^*$ and $\Gamma_{12} = \Gamma_{21}^*$, where as CPT invariance requires $M_{11} = M_{22} = M$ and $\Gamma_{11} = \Gamma_{22} = \Gamma$.

The eigenstates of K_L and K_S of \widehat{H} are defined in terms of $\bar{\epsilon}$:

$$K_{L,S} = \frac{(1 + \bar{\epsilon})K^\circ + (1 - \bar{\epsilon})\overline{K}^\circ}{\sqrt{2(1 + |\bar{\epsilon}|^2)}} \quad (\text{III.5})$$

where $\bar{\epsilon}$ is given by

$$\frac{1 - \bar{\epsilon}}{1 + \bar{\epsilon}} = \sqrt{\frac{M_{12}^* - i\frac{\Gamma_{12}^*}{2}}{M_{12} - i\frac{\Gamma_{12}}{2}}} \quad (\text{III.6})$$

and the eigenvalues are

$$M_{L,S} = M \pm \text{Re}(Q), \quad \Gamma_{L,S} = \Gamma \mp 2 \text{Im}(Q) \quad (\text{III.7})$$

where

$$Q = \sqrt{(M_{12} - i\frac{\Gamma_{12}}{2})(M_{12}^* - i\frac{\Gamma_{12}^*}{2})} \quad (\text{III.8})$$

We can rewrite

$$\frac{1 - \bar{\epsilon}}{1 + \bar{\epsilon}} = \frac{\Delta M - i\Delta\Gamma/2}{2M_{12} - i\Gamma_{12}} \equiv r e^{i\kappa} \quad (\text{III.9})$$

where $\Delta M = M_L - M_S = 2\text{Re}(Q)$, $\Delta\Gamma = \Gamma_L - \Gamma_S = -4\text{Im}(Q)$, and

$$r = 1 + \frac{2|\Gamma_{12}|^2}{4|M_{12}|^2 + |\Gamma_{12}|^2} \text{Im}\left(\frac{M_{12}}{\Gamma_{12}}\right) \quad (\text{III.10})$$

For the $K^\circ - \bar{K}^\circ$ system, $\text{Im}M_{12} \ll \text{Re}M_{12}$ and $\text{Im}\Gamma_{12} \ll \text{Re}\Gamma_{12}$,

therefore to a very good approximation,

$$\Delta M_K = 2\text{Re}M_{12}, \quad \Delta\Gamma_K = 2\text{Re}\Gamma_{12}. \quad (\text{III.11})$$

III.2 ϵ_K and ΔM_K

Standard Model Contribution

The off-diagonal element M_{12} in the $K^\circ - \bar{K}^\circ$ system is given by

$$2m_K M_{12}^* = \langle \bar{K}^\circ | H_{\text{eff}}(\Delta S = 2) | K^\circ \rangle. \quad (\text{III.12})$$

The effective $\Delta S = 2$ Hamiltonian is

$$H_{\text{eff}}^{\Delta S=2} = \frac{G_F^2}{16\pi^2} M_W^2 \left(\lambda_c^2 \eta_1 S_0(x_c) + \lambda_t^2 \eta_2 S_0(x_t) + 2\lambda_c \lambda_t \eta_3 S_0(x_c, x_t) \right) \quad (\text{III.13})$$

$$\times (\bar{s}d)_{V-A} (\bar{s}d)_{V-A} + h.c.$$

The matrix element of $H_{\text{eff}}^{\Delta S=2}$ is obtained from:

$$\langle \overline{K^0} | (\overline{s}d)_{V-A} (\overline{s}d)_{V-A} | K^0 \rangle = \frac{8}{3} \widehat{B}_K f_K^2 m_K^2, \quad (\text{III.14})$$

where \widehat{B}_K describes the non-perturbative effects in the hadronic matrix element of the operator $(\overline{s}d)_{V-A} (\overline{s}d)_{V-A}$, $\lambda_c = V_{cs}^* V_{cd}$, $\lambda_t = V_{ts}^* V_{td}$, and the η_i describe the short distance QCD effects, and are numerically given by

$$\eta_1 = 1.38 \pm 0.20, \quad \eta_2 = 0.57 \pm 0.01, \quad \eta_3 = 0.47 \pm 0.04. \quad (\text{III.15})$$

The functions $S_0(x_{c,t})$ and $S_0(x_c, x_t)$ are the loop functions defined below, with $x_i = m_i^2/M_W^2$:

$$\begin{aligned} S_0(x_c) &= x_c \\ S_0(x_t) &= \frac{4x_t - 11x_t^2 + x_t^3}{4(1-x_t)^2} - \frac{3x_t^3 \ln x_t}{2(1-x_t)^3} \\ S_0(x_c, x_t) &= x_c \left[\ln \frac{x_t}{x_c} - \frac{3x_t}{4(1-x_t)} - \frac{3x_t^2 \ln x_t}{4(1-x_t)^2} \right] \end{aligned} \quad (\text{III.16})$$

Thus, from Eq. (III.13),

$$M_{12} = \frac{G_F^2}{12\pi^2} M_W^2 \widehat{B}_K f_K^2 m_K \left(\lambda_c^2 \eta_1 S_0(x_c) + \lambda_t^2 \eta_2 S_0(x_t) + 2\lambda_c \lambda_t \eta_3 S_0(x_c, x_t) \right) \quad (\text{III.17})$$

The CP violation in the $K^0 - \overline{K^0}$ mixing is parameterized by ϵ_K defined as:

$$\epsilon_K = \frac{e^{i\pi/4}}{\sqrt{2}\Delta M_K} (\text{Im} M_{12} + 2\xi \text{Re} M_{12}); \quad \xi = \frac{\text{Im} A_0}{\text{Re} A_0}. \quad (\text{III.18})$$

The quantity A_0 is defined in terms of amplitudes of K° -meson decays:

$$\begin{aligned} A(K^\circ \rightarrow \pi^+\pi^-) &= \sqrt{\frac{2}{3}}A_0e^{i\delta^0} + \sqrt{\frac{1}{3}}A_2e^{i\delta^2} \\ A(K^\circ \rightarrow \pi^0\pi^0) &= \sqrt{\frac{2}{3}}A_0e^{i\delta^0} - 2\sqrt{\frac{1}{3}}A_2e^{i\delta^2} \end{aligned} \quad (\text{III.19})$$

The parameter ξ is small, therefore

$$\begin{aligned} \epsilon_K &\approx \frac{e^{i\pi/4}}{\sqrt{2}\Delta M_K} \text{Im}M_{12} \\ &= C_\epsilon \widehat{B}_K \text{Im}\lambda_t \left\{ \text{Re}\lambda_c \left[\eta_1 S_0(x_c) - \eta_3 S_0(x_c, x_t) \right] - \text{Re}\lambda_t \eta_2 S_0(x_t) \right\} e^{i\pi/4} \end{aligned} \quad (\text{III.20})$$

where

$$C_\epsilon = \frac{G_F^2 f_K^2 M_K M_W^2}{6\sqrt{2}\pi^2(\Delta m_K)} \approx 3.84 \times 10^4 \quad (\text{III.21})$$

For details on $K^\circ - \overline{K^\circ}$ mixing in the standard model, see *e.g.* [136]

SUSY Contribution

The supersymmetric contribution to $K^\circ - \overline{K^\circ}$ mixing comes from the following diagrams (see [40]):

These give:

$$\begin{aligned} (M_{12})_K^{\text{SUSY}} &= \frac{-\alpha_s^2}{216m_q^2} \frac{1}{3} M_K f_K^2 \left\{ [(\delta_{12}^d)_{LL}^2 + (\delta_{12}^d)_{RR}^2] (24x f_6(x) + 66\tilde{f}_6(x)) \right. \\ &\quad + (\delta_{12}^d)_{LL} (\delta_{12}^d)_{RR} \left[(384 \left(\frac{M_K}{m_s+m_d}\right)^2 + 72) x f_6(x) \right. \\ &\quad \left. \left. + (-24 \left(\frac{M_K}{m_s+m_d}\right)^2 + 36) \tilde{f}_6(x) \right] \right. \\ &\quad + [(\delta_{12}^d)_{LR}^2 + (\delta_{12}^d)_{RL}^2] \left(-132 \left(\frac{M_K}{m_s+m_d}\right)^2 x f_6(x) \right) \\ &\quad \left. + (\delta_{12}^d)_{LR} (\delta_{12}^d)_{RL} \left[-144 \left(\frac{M_K}{m_s+m_d}\right)^2 - 84 \right] \tilde{f}_6(x) \right\} \end{aligned} \quad (\text{III.22})$$

where $x = m_{\tilde{g}}^2/m_{\tilde{q}}^2$, and the loop functions $f_6(x)$ and $\tilde{f}_6(x)$ are defined

as:

$$f_6(x) = \frac{6(1+3x)\ln x + x^3 - 9x^2 - 9x + 17}{6(x-1)^5} \quad (\text{III.23})$$

$$\tilde{f}_6(x) = \frac{6x(1+x)\ln x - x^3 - 9x^2 + 9x + 1}{3(x-1)^5} \quad (\text{III.24})$$

III.3 ϵ'_K/ϵ_K

The parameter ϵ'_K is defined as

$$\epsilon'_K = \frac{1}{\sqrt{2}} \text{Im} \left(\frac{A_2}{A_0} \right) e^{i\Phi} \quad \text{where} \quad \Phi = \frac{\pi}{2} + \delta_2 - \delta_0 \approx \frac{\pi}{4} \quad (\text{III.25})$$

The dimension four Hamiltonian giving rise to the $\bar{s}dZ$ vertex is:

$$H_{\text{eff}}^{d=4} = -\frac{G_F}{\sqrt{2}} \frac{e}{\pi^2} M_Z^2 \tan \theta_W \left(\lambda_t C_0(x_t) + ((\delta_{23}^u)_{LR} (\delta_{13}^d)_{RL}^*) H_0(x) \right) + h.c. \quad (\text{III.26})$$

where the first term is the contribution from the standard model, and the second from supersymmetry [93, 94]. The chromo- and electromagnetic dimension 5 operators are:

$$H_{\text{eff}}^{d=5} = \left(C_\gamma^+ Q_\gamma^+ + C_\gamma^- Q_\gamma^- + C_g^+ Q_g^+ + C_g^- Q_g^- \right) + h.c. \quad (\text{III.27})$$

where

$$Q_\gamma^\pm = \frac{Q_d e}{16\pi^2} \left(\bar{s}_L \sigma^{\mu\nu} F_{\mu\nu} d_R \pm \bar{s}_R \sigma^{\mu\nu} F_{\mu\nu} d_L \right) \quad (\text{III.28})$$

$$Q_g^\pm = \frac{g}{16\pi^2} \left(\bar{s}_L \sigma^{\mu\nu} t^a G_{\mu\nu}^a d_R \pm \bar{s}_R \sigma^{\mu\nu} t^a G_{\mu\nu}^a d_L \right)$$

The Wilson coefficients are given by :

$$C_\gamma^\pm(m_{\tilde{g}}) = \frac{\pi\alpha_s(m_{\tilde{g}})}{m_{\tilde{g}}} \left[(\delta_{21}^d)_{LR} \pm (\delta_{12}^d)_{LR}^* \right] F_0(x) \quad (\text{III.29})$$

$$C_g^\pm(m_{\tilde{g}}) = \frac{\pi\alpha_s(m_{\tilde{g}})}{m_{\tilde{g}}} \left[(\delta_{21}^d)_{LR} \pm (\delta_{12}^d)_{LR}^* \right] G_0(x)$$

where the functions are defined as:

$$C_0(x) = \frac{x}{8} \left[\frac{x-6}{x-1} + \frac{3x+2}{(x-1)^2} \ln x \right] \quad (\text{III.30})$$

$$H_0(x) = \frac{-x(x^3 - 6x^2 + 3x + 2 + 6x \ln x)}{48(1-x)^4} \quad (\text{III.31})$$

$$F_0(x) = \frac{4x(1 + 4x - 5x^2 + 4x \ln x + 2x^2 \ln x)}{3(1-x)^4} \quad (\text{III.32})$$

$$G_0(x) = \frac{x(22 - 20x - 2x^2 + 16x \ln x - x^2 \ln x + 9 \ln x)}{3(1-x)^4} \quad (\text{III.33})$$

The matrix elements of the chromo- and electro-magnetic operators $Q_{g,\gamma}^\pm$ between the states K° and $\pi\pi$ are:

$$\langle (\pi\pi)_{I=0} | Q_g^- | K^\circ \rangle = \sqrt{\frac{3}{2}} \frac{11}{16\pi^2} \frac{\langle \bar{q}q \rangle}{F_\pi^3} m_\pi^2 B_G \quad (\text{III.34})$$

$$\langle \pi^\circ | Q_\gamma^+ | K^\circ \rangle = \frac{Q_d e}{16\pi^2} \frac{i\sqrt{2}}{m_K} P_\pi^\mu P_K^\nu F_{\mu\nu} B_T \quad (\text{III.35})$$

$$\langle (\pi\pi)_{I=0} | Q_g^+ | K^\circ \rangle = \langle \pi^\circ | Q_\gamma^- | K^\circ \rangle = 0 \quad (\text{III.36})$$

Thus we can write

$$Re\left(\frac{\epsilon'}{\epsilon}\right)_{\text{SUSY}} = \frac{11\sqrt{3}}{64\pi} \frac{\omega}{|\epsilon| Re A_0} \frac{m_\pi^2 m_K^2}{F_\pi(m_s + m_d)} \frac{\alpha_s(m_{\tilde{g}})}{m_{\tilde{g}}} \eta B_G Im \Lambda_g^- \quad (\text{III.37})$$

where $\omega = ReA_2/Re\bar{A}_0$ and Λ_g^- is the effective coupling $\left[(\delta_{21}^d)_{LR} - (\delta_{12}^d)_{LR}^* \right] G_0(x)$.

IV. APPENDIX: CP VIOLATION IN THE B MESON SYSTEM

For a review see Ref. [94].

IV.1 $B_d - \overline{B}_d$ mixing

Defining the phase convention of the CP transformation of neutral B mesons as

$$CP|B^\circ\rangle = \omega_B|\overline{B}^\circ\rangle, \quad CP|\overline{B}^\circ\rangle = \omega_B^*|B^\circ\rangle \quad \text{with } |\omega_B| = 1, \quad (\text{IV.1})$$

the B meson mass eigenstates can be written as:

$$|B_L\rangle = p|B^\circ\rangle + q|\overline{B}^\circ\rangle \quad (\text{IV.2})$$

$$|B_H\rangle = p|B^\circ\rangle - q|\overline{B}^\circ\rangle \quad (\text{IV.3})$$

where $|p|^2 + |q|^2 = 1$. The time evolution of the mass eigenstates is given by:

$$|B_H(t)\rangle = e^{-iM_H t} e^{-\Gamma_H t/2} |B_H\rangle \quad (\text{IV.4})$$

$$|B_L(t)\rangle = e^{-iM_L t} e^{-\Gamma_L t/2} |B_L\rangle \quad (\text{IV.5})$$

where as the time evolution of the strong interaction states is governed by

$$i \frac{d}{dt} \begin{pmatrix} B \\ \bar{B} \end{pmatrix} = \left(M - i \frac{\Gamma}{2} \right) \begin{pmatrix} B \\ \bar{B} \end{pmatrix} \quad (\text{IV.6})$$

with $(M - i\Gamma/2)$ being Hermitian, and $M = \frac{M_H + M_L}{2}$ and $\Gamma = \frac{\Gamma_H + \Gamma_L}{2}$.

Solving the eigen value equation gives

$$\begin{aligned} (\Delta m)^2 - \frac{1}{4}(\Delta \Gamma)^2 &= (4|M_{12}|^2 - |\Gamma_{12}|^2) \\ \Delta m \Delta \Gamma &= 4 \text{Re}(M_{12} \Gamma_{12}^*); \end{aligned} \quad (\text{IV.7})$$

$$\frac{q}{p} = \frac{-\Delta m - i \Delta \Gamma / 2}{2M_{12} - i \Gamma_{12}}$$

where $\Delta m = M_H - M_L$ and $\Delta \Gamma = \Gamma_H - \Gamma_L$. For the B system,

$|\Gamma_{12}| \ll |M_{12}|$, therefore

$$\Delta m_b \approx 2|M_{12}|, \quad \Delta \Gamma_B = 2 \frac{\text{Re}(M_{12} \Gamma_{12}^*)}{|M_{12}|} \quad (\text{IV.8})$$

$$\text{and } \frac{q}{p} \approx -\frac{M_{12}^*}{|M_{12}|} \left[1 - \frac{1}{2} \text{Im} \left(\frac{\Gamma_{12}}{M_{12}} \right) \right]$$

IV.2 CP violation in decay

Let the final state be denoted by f , such that

$$CP|f\rangle = \omega_f|\bar{f}\rangle, \quad CP|\bar{f}\rangle = \omega_f^*|f\rangle \quad \text{with } |\omega_f| = 1, \quad (\text{IV.9})$$

and the decay amplitudes be given by

$$A_f = \langle f|H_d|B^\circ\rangle; \quad \bar{A}_f = \langle f|H_d|\bar{B}^\circ\rangle \quad (\text{IV.10})$$

The amplitudes A_f and \bar{A}_f are related by CP. If the strong phases in the amplitudes are δ_i and the weak phases ϕ_i , then

$$\left| \frac{\bar{A}_f}{A_f} \right| = \left| \frac{\sum_i A_i e^{i(\delta_i - \phi_i)}}{\sum_i A_i e^{i(\delta_i - \phi_i)}} \right| \quad (\text{IV.11})$$

To discuss CP violation, let us define a quantity

$$\lambda_f = \frac{q \bar{A}_f}{p A_f}. \quad (\text{IV.12})$$

The effective Hamiltonian that is relevant to M_{12} is of the form

$$H_{\text{eff}}^{\Delta b=2} \propto e^{2i\phi_B} [\bar{d}\gamma^\mu(1 - \gamma_5)b]^2 + e^{-2i\phi_B} [\bar{b}\gamma^\mu(1 - \gamma_5)d]^2 \quad (\text{IV.13})$$

where $2\phi_B$ is the CP violating weak phase. Then with $|\Gamma_{12}| \ll |M_{12}|$,

we get

$$\frac{q}{p} = \omega_B \omega_b^* \omega_d e^{-2i\phi_B}. \quad (\text{IV.14})$$

For the decay of the B meson (*e.g.* $b \rightarrow q\bar{q}d$), the Hamiltonian is of the form:

$$H_{\text{Decay}} \propto e^{i\phi_f} [\bar{q}\gamma^\mu(1 - \gamma_5)d] \bar{b}\gamma^\mu(1 - \gamma_5)q \quad (\text{IV.15})$$

$$+ e^{-i\phi_f} [\bar{q}\gamma^\mu(1 - \gamma_5)b] \bar{d}\gamma^\mu(1 - \gamma_5)q.$$

In this case,

$$\frac{\bar{A}_f}{A_f} = \omega_f \omega_B^* \omega_b \omega_d^* e^{-2i\phi_f}, \quad (\text{IV.16})$$

and for a final CP eigenstate we get

$$\lambda = \frac{q \bar{A}_f}{p A_f} = \omega_f e^{-2i(\phi_f + \phi_B)}. \quad (\text{IV.17})$$

IV.3 Three types of CP violations in meson decays

IV.3.1 CP violation in mixing

This happens for the case when $|q/p| \neq 1$. This type of CP violation results from the mass eigenstates being different from the CP eigenstates, and requires a relative phase between M_{12} and Γ_{12} . For the B_d^0 system, this effect could be observed through semi-leptonic decays:

$$a_{SL} = \frac{\Gamma(\overline{B^0}(t) \rightarrow l^+ \nu X) - \Gamma(B^0(t) \rightarrow l^- \nu X)}{\Gamma(\overline{B^0}(t) \rightarrow l^+ \nu X) + \Gamma(B^0(t) \rightarrow l^- \nu X)} \quad (\text{IV.18})$$

$$a_{SL} = \frac{1 - |q/p|^4}{1 + |q/p|^4} = \text{Im}(\Gamma_{12}/M_{12}). \quad (\text{IV.19})$$

IV.3.2 CP violation in decay

This happens when $|\overline{A}_f/A_f| \neq 1$. In this case, a measure of CP violation is the parameter:

$$\begin{aligned} a_{f^\pm} &= \frac{\Gamma(B^+ \rightarrow f^+) - \Gamma(B^- \rightarrow f^-)}{\Gamma(B^+ \rightarrow f^+) + \Gamma(B^- \rightarrow f^-)} \\ &= \frac{1 - |\overline{A}_f/A_f|^2}{1 + |\overline{A}_f/A_f|^2}. \end{aligned} \quad (\text{IV.20})$$

IV.3.3 CP violation in the interference between decays, with and without mixing

This happens when $\text{Im}\lambda_f \neq 0$. This is the effect of interference between a direct decay amplitude and a first mix then decay path to the same final state.

$$\begin{aligned} a_{f_{CP}}(t) &= \frac{\Gamma(\overline{B}^\circ_{\text{phys}}(t) \rightarrow f_{CP}) - \Gamma(B^\circ_{\text{phys}}(t) \rightarrow f_{CP})}{\Gamma(\overline{B}^\circ_{\text{phys}}(t) \rightarrow f_{CP}) + \Gamma(B^\circ_{\text{phys}}(t) \rightarrow f_{CP})} \\ &= \frac{1 - |\lambda_f|^2}{1 + |\lambda_f|^2} \cos(\Delta m_B t) + \frac{2\text{Im}\lambda_f}{1 + |\lambda_f|^2} \sin(\Delta m_B t). \end{aligned} \quad (\text{IV.21})$$

In decays with $|\lambda_f| = 1$,

$$a_{f_{CP}}(t) = \frac{2\text{Im}\lambda_f}{1 + |\lambda_f|^2} \sin(\Delta m_B t) \quad (\text{IV.22})$$

Often the time independent quantity $a_{f_{CP}} = \frac{2Im\lambda_f}{1+|\lambda_f|^2}$ is used.

IV.3.4 Application to the specific case of $B_d \rightarrow \phi K_S$

In the standard model, for $B_d^0 \rightarrow \phi K_S$,

$$\begin{aligned} \frac{q}{p} &= \frac{V_{tb}^* V_{td}}{V_{tb} V_{td}^*} \\ \Rightarrow (S_{\phi K_S})_{SM} &= \sin 2\beta \end{aligned} \quad (\text{IV.23})$$

In the above expression, we have ignored $\mathcal{O}\left(\frac{\Gamma_{12}}{M_{12}}\right)$ terms as they are small.

When we include supersymmetric contributions from the box diagram, then

$$M_{12} = M_{12}^{\text{SM}} + M_{12}^{\text{SUSY}} \quad (\text{Box}) \quad (\text{IV.24})$$

$$\begin{aligned} \text{Let } \sqrt{\frac{M_{12}}{M_{12}^{\text{SM}}}} &\equiv r_d e^{i\theta_d} \\ \text{then } \frac{q}{p} &= e^{-2i\theta_d} e^{-2i\beta} \end{aligned} \quad (\text{IV.25})$$

We need to consider the interference between decay and mixing.

Therefore, we must include $\Delta B = 1$ transitions. Let

$$A^{\text{SM}}(\phi K_S) = |A^{\text{SM}}| e^{i\delta_{\text{SM}}}; \quad A^{\text{SUSY}}(\phi K_S) = |A^{\text{SUSY}}| e^{i\delta_{\text{SUSY}}} e^{i\theta_{\text{SUSY}}} \quad (\text{IV.26})$$

$$\overline{A}^{\text{SM}}(\phi K_S) = |A^{\text{SM}}| e^{i\delta_{\text{SM}}}; \quad \overline{A}^{\text{SUSY}}(\phi K_S) = |A^{\text{SUSY}}| e^{i\delta_{\text{SUSY}}} e^{-i\theta_{\text{SUSY}}} \quad (\text{IV.27})$$

where $\delta_{\text{SM/SUSY}}$ is the strong CP conserving phase, and θ_{SUSY} is the CP violating phase. Then,

$$\frac{A^{\text{Tot}}}{A^{\text{SM}}} = 1 + \left| \frac{A^{\text{SUSY}}}{A^{\text{SM}}} \right| e^{i(\theta_{\text{SUSY}} + \delta_{\text{SUSY}} - \delta_{\text{SM}})}. \quad (\text{IV.28})$$

Let $\left| \frac{A^{\text{SUSY}}}{A^{\text{SM}}} \right| = x$ and $-(\delta_{\text{SUSY}} - \delta_{\text{SM}}) = \delta_{12}$.

$$\frac{\overline{A}^{\text{Tot}}}{A^{\text{SM}}} = 1 + x e^{-i(\theta_{\text{SUSY}} + \delta_{12})} \quad (\text{IV.29})$$

$$\text{Let } \rho = \frac{\overline{A}^{\text{Tot}}}{A^{\text{Tot}}} = \frac{1 + x e^{-i(\theta_{\text{SUSY}} + \delta_{12})}}{1 + x e^{i(\theta_{\text{SUSY}} + \delta_{12})}} \quad (\text{IV.30})$$

$$= \frac{1 + 2x \cos \delta_{12} e^{-i\theta_{\text{SUSY}}} + x^2 e^{-2i\theta_{\text{SUSY}}}}{1 + 2x \cos(\theta_{\text{SUSY}} - \delta_{12}) + x^2}. \quad (\text{IV.31})$$

Using $q/p = e^{-2i\beta}$, where β includes the contribution from the SUSY box diagram as well, $\lambda = \rho q/p$, and that the SUSY contribution is small compared to the standard model, so that $|x| \ll 1$, we get:

$$S_{\phi K_S} = \frac{2\text{Im}\lambda}{1 + |\lambda|^2} = \frac{\sin 2\beta + 2x \cos \delta_{12} \sin(\theta_{\text{SUSY}} + 2\beta) + \mathcal{O}(x^2)}{1 + 2x \cos \delta_{12} \cos \theta_{\text{SUSY}} + x^2} \quad (\text{IV.32})$$

$$C_{\phi K_S} = -\frac{2x \sin \delta_{12} \sin \theta_{\text{SUSY}}}{1 + 2x \cos \delta_{12} \cos \theta_{\text{SUSY}} + x^2} \quad (\text{IV.33})$$

IV.4 Calculation of $S(B_d \rightarrow \phi K_S)$

The amplitude for $B_d \rightarrow \phi K_S$ in the standard model is given by [90]:

$$A_{\phi K_S}^{\text{SM}} = \frac{G_F}{\sqrt{2}} V_{ts}^* V_{tb} \sum_{i=3}^6 C_i^{\text{SM}} \langle \phi \overline{K}^{\circ} | O_i | \overline{B}^{\circ} \rangle + C_g \langle \phi \overline{K}^{\circ} | O_g | \overline{B}^{\circ} \rangle + \frac{8}{9} PH \quad (\text{IV.34})$$

where the matrix elements of the O_i are:

$$\langle \phi \overline{K^0} | O_3 | \overline{B^0} \rangle = \frac{H}{3} \quad (\text{IV.35})$$

$$\langle \phi \overline{K^0} | O_4 | \overline{B^0} \rangle = \frac{H}{3} \quad (\text{IV.36})$$

$$\langle \phi \overline{K^0} | O_5 | \overline{B^0} \rangle = \frac{H}{4} \quad (\text{IV.37})$$

$$\langle \phi \overline{K^0} | O_6 | \overline{B^0} \rangle = \frac{H}{12} \quad (\text{IV.38})$$

$$\langle \phi \overline{K^0} | O_g | \overline{B^0} \rangle = \frac{4}{9\pi} \alpha_s \kappa H \quad (\text{IV.39})$$

where $\kappa \approx -1.1$ and $H = 2(\epsilon \cdot p) f_\phi m_\phi F_{B \rightarrow K}^+(m_\phi^2)$, and the Wilson coefficients are $C_3^{\text{SM}} = 0.0114$, $C_4^{\text{SM}} = -0.0321$, $C_5^{\text{SM}} = 0.00925$, $C_6^{\text{SM}} = -0.0383$ and $C_g^{\text{SM}} = -0.188$.

The SUSY amplitude for the process is given below:

$$A_{\phi K_S}^{\text{SUSY}} = \frac{G_F}{\sqrt{2}} V_{ts}^* V_{tb} \sum_{i=3}^6 C_i^{\text{SUSY}} \langle \phi \overline{K^0} | O_i | \overline{B^0} \rangle + C_g^{\text{SUSY}} \langle \phi \overline{K^0} | O_g | \overline{B^0} \rangle \quad (\text{IV.40})$$

+ ($L \leftrightarrow R$)

The coefficients C_i^{SUSY} are given by:

$$C_3^{\text{SUSY}} = X \left(-\frac{1}{9}B_1(x) - \frac{5}{9}B_2(x) - \frac{1}{18}P_1(x) - \frac{1}{2}P_2(x) \right) \quad (\text{IV.41})$$

$$C_4^{\text{SUSY}} = X \left(-\frac{7}{3}B_1(x) + \frac{1}{3}B_2(x) + \frac{1}{6}P_1(x) + \frac{3}{2}P_2(x) \right) \quad (\text{IV.42})$$

$$C_5^{\text{SUSY}} = X \left(\frac{10}{9}B_1(x) + \frac{1}{18}B_2(x) - \frac{1}{18}P_1(x) - \frac{1}{2}P_2(x) \right) \quad (\text{IV.43})$$

$$C_6^{\text{SUSY}} = X \left(-\frac{2}{3}B_1(x) + \frac{7}{6}B_2(x) + \frac{1}{6}P_1(x) + \frac{3}{2}P_2(x) \right) \quad (\text{IV.44})$$

$$C_g^{\text{SUSY}} = \frac{\sqrt{2}\alpha_2\pi}{G_F V_{tb} V_{ts}^* m_{\tilde{q}}^2} \left((\delta_{LL}^d)_{23} \left[\frac{1}{3}M_3(x) + 3M_4(x) \right] \right. \quad (\text{IV.45})$$

$$\left. + (\delta_{LR}^d)_{23} \frac{m_{\tilde{g}}}{m_{\tilde{q}}} \left[\frac{1}{3}M_1(x) + 3M_2(x) \right] \right) \quad (\text{IV.46})$$

where

$$X \equiv \frac{\sqrt{2}\alpha_s^2}{G_F V_{tb} V_{ts}^* m_{\tilde{q}}^2} (\delta_{LL}^d)_{23} \quad \text{and} \quad x = \frac{m_{\tilde{g}}^2}{m_{\tilde{q}}^2}.$$

The loop functions are given below [40]:

$$B_1(x) = \frac{1 + 4x - 5x^2 + 4x \ln x + 2x^2 \ln x}{8(1-x)^4} \quad (\text{IV.47})$$

$$B_2(x) = x \frac{5 - 4x - x^2 + 2 \ln x + 4x \ln x}{2(1-x)^4} \quad (\text{IV.48})$$

$$P_1(x) = \frac{1 - 6x + 18x^2 - 10x^3 - 3x^4 + 12x^3 \ln x}{18(x-1)^5} \quad (\text{IV.49})$$

$$P_2(x) = \frac{7 - 18x + 9x^2 + 2x^3 + 3 \ln x - 9x^2 \ln x}{9(x-1)^5} \quad (\text{IV.50})$$

$$M_1(x) = 4B_1(x) \quad (\text{IV.51})$$

$$M_2(x) = -xB_2(x) \quad (\text{IV.52})$$

$$M_3(x) = \frac{-1 + 9x + 9x^2 - 17x^3 + 18x^2 \ln x + 6x^3 \ln x}{12(x-1)^5} \quad (\text{IV.53})$$

$$M_4(x) = \frac{-1 - 9x + 9x^2 + x^3 - 6x \ln x - 6x^2 \ln x}{6(x-1)^5} \quad (\text{IV.54})$$

BIBLIOGRAPHY

- [1] S. Weinberg, Phys. Rev. Lett. **19**, 1269 (1967); A. Salam, in Elementary Particle Theory Nobel Symposium, ed. by N. Svartholm (Almqvist, Stockholm, 1968), p. 367; S. L. Glashow, Nucl. Phys. **22**, 570 (1961).
- [2] The idea of QCD evolved over a span of seven years (1965-1972). It received a decisive boost with the discovery of asymptotic freedom by D. Gross and F. Wilczek, Phys. Rev. Lett. **30**, 1343 (1973); and by H. D. Politzer, Phys. Rev. Lett. **30**, 1346 (1973).
- [3] P. W. Higgs, Phys. Rev. Lett. **12**, 132 (1964), Phys. Rev. Lett. **13**, 508 (1964), Phys. Rev. **145**, 1156 (1966), R. Brout and F. Englert, Phys. Rev. Lett. **13**, 321 (1964), G. S. Guralnik, C. R. Hagen and T. W. B. Kibble, Phys. Rev. Lett. **13**, 585 (1964).
- [4] G. 't Hooft and M. J. G. Veltman, Nucl.Phys. **B 44**, 189 (1972), Nucl.Phys. **B 50**, 318 (1972).
- [5] W. M. Yao *et al*, Journal of Physics, **G33**, 1 (2006), Review of Particle Physics, Particle Data Group, <http://pdg.lbl.gov>.
- [6] Y. Fukuda et al. (Super-Kamiokande), Phys. Rev. Lett. **81**, 1562 (1998), hep-ex/9807003; K. Nishikawa (K2K) Talk at Neutrino 2002, Munich, Germany.
- [7] Q. R. Ahmad et al (SNO), Phys. Rev. Lett. **81**, 011301 (2002); B. T. Cleveland et al (Homestake), Astrophys. J. **496**, 505 (1998); W. Hampel et al. (GALLEX), Phys. Lett. **B447**, 127, (1999); J. N. Abdurashitov et al (SAGE) (2000), astro-ph/0204245; M. Altmann et al. (GNO), Phys. Lett. **B 490**, 16 (2000); S. Fukuda et al. (SuperKamiokande), Phys. Lett. **B 539**, 179 (2002). Disappearance of $\bar{\nu}_e$'s produced in earth-based reactors is established by the KamLAND data: K. Eguchi et al., hep-ex/0212021. For a recent review including analysis of several authors see, for example, S. Pakvasa and J. W. F. Valle, hep-ph/0301061.
- [8] WMAP Three Year Results: D. N. Spergel et al., astro-ph/0603449, and references therein, <http://map.gsfc.nasa.gov>.

- [9] See e.g. E. W. Kolb and M. S. Turner, *The Early Universe* (Frontiers in Physics), Perseus Books Group; New Ed edition (January 1993).
- [10] A. H. Guth, *Phys. Rev.* **D 23**, 347 (1981), A. D. Linde, *Phys. Lett.* **B 108**, 389 (1982), A. Albrecht and P. J. Steinhardt, *Phys. Rev. Lett.* **48**, 1220 (1982).
- [11] J. C. Pati and A. Salam, Proc. 15th High energy Conference, Batavia, reported by J. D. Bjorken, Vol. 2 p 301 (1972); *Phys. Rev.* **8**, 1240 (1973).
- [12] J.C. Pati and A. Salam, *Phys. Rev. Lett.* **31**, 661 (1973); *Phys. Rev.* **D 10**, 275 (1974).
- [13] H. Georgi and S. L. Glashow, *Phys. Rev. Lett.* **32**, 438 (1974).
- [14] H. Georgi, H. Quinn and S. Weinberg, *Phys. Rev. Lett.* **33**, 451 (1974).
- [15] M. Fukugita and T. Yanagida *Phys. Lett.* **B174**, 45 (1986); G. Lazarides and Q. Shafi, *Phys. Lett.* **B258**, 305 (1991); M.A. Luty, *Phys. Rev.* **D45**, 455 (1992). In the context of the model to be presented here, see J.C. Pati, *Phys. Rev.* **D68**, 072002 (2003), hep-ph/0209160.
- [16] For a discussion of leptogenesis, and its success, in a predictive SO(10)/G(224) framework, see J. C. Pati, *Phys. Rev.* **D 68**, 072002 (2003).
- [17] P. Minkowski, *Phys. Lett.* **B67**, 421 (1977); M. Gell-Mann, P. Ramond and R. Slansky, in: *Supergravity*, eds. F. van Nieuwenhuizen and D. Freedman (Amsterdam, North Holland, 1979) p. 315; T. Yanagida, in: *Workshop on the Unified Theory and Baryon Number in the Universe*, eds. O. Sawada and A. Sugamoto (KEK, Tsukuba) 95 (1979); S.L. Glashow, in *Quarks and Leptons*, Cargese 1979, eds. M. Levy et al. (Plenum 1980) p. 707; R. N. Mohapatra and G. Senjanovic, *Phys. Rev. Lett.* **44**, 912 (1980).
- [18] H. Georgi, in *Particles and Fields*, Ed. by C. Carlson (AIP, NY, 1975), p.575; H. Fritzsch and P. Minkowski, *Ann. Phys.* **93**, 193 (1975).
- [19] F. Gursev, P. Ramond and P. Sikivie, *Phys. Lett.* **B 60**, 177 (1976).
- [20] Promising string-theory solutions yielding the G(224)-symmetry in 4D have been obtained using different approaches, by a number of authors. They include: I. Antoniadis, G. Leontaris, and J Rizos, *Phys. Lett.* **B245**, 161 (1990); G. K. Leontaris, *Phys. Lett.* **B 372**, 212 (1996), hep-ph/9601337; A. Murayama and T. Toon, *Phys. Lett.* **B318**, 298 (1993); Z. Kakushadze, *Phys. rev.* **D58**, 101901

- (1998); G. Aldazabal, L. I. Ibanez and F. Quevedo, hep-th/9909172; C. Kokorelis, hep-th/0203187, hep-th/0209202; M. Cvetič, G. Shiu, and A. M. Uranga, Phys. Rev. Lett. **87**, 201801 (2001), hep-th/0107143, and Nucl. Phys. **B 615**, 3 (2001), hep-th/0107166; M. Cvetič and I. Papadimitriou, hep-th/0303197; R. Blumenhagen, L. Gorlich and T. Ott, hep-th/0211059. For a type I string-motivated scenario leading to the $G(224)$ symmetry in 4D, see L. I. Everett, G. L. Kane, S. F. King, S. Rigolin and L. T. Wang, hep-th/0202100. A promising class of four dimensional three-family $G(224)$ -string models has recently been obtained by T. Kobayashi, S. Raby, and R. J. Zhang, hep-ph/0409098. Another class of solutions leading to the $G(224)$ -symmetry from Type II-A orientifolds with interesting D6-branes is obtained in M. Cvetič, T. Li and T. Liu, hep-th/0403061. For alternative attempts based on flux compactification of Type II-B string theory leading to the $G(224)$ -symmetry, see F. Marchesano and G. Shiu, hep-th/0409132.
- [21] F. Gursev, P. Ramond and R. Slansky, Phys. Lett, **B60**, 177 (1976); Y. Achiman and B. Stech, Phys. Lett. **B77**, 389 (1978); Q. Shafi, Phys. Lett. **B79**, 301 (1978); A. deRujula, H. Georgi and S. L. Glashow, 5th Workshop on Grand Unification, edited by K. Kang et al., World Scientific, 1984, p88.
- [22] Y. A. Golfand and E. S. Likhtman, JETP Lett. **13**, 323 (1971); J. Wess and B. Zumino, Nucl. Phys. **B 70**, 139 (1974); D. Volkov and V. P. Akulov, JETP Lett. **16**, 438 (1972).
- [23] M. Green and J. H. Schwarz, Phys. Lett. 149B, 117 (1984); D. J. Gross, J. A. Harvey, E. Martinec and R. Rohm, Phys. Rev. Lett. 54, 502 (1985); P. Candelas, G. T. Horowitz, A. Strominger and E. Witten, Nucl. Phys. B258, 46 (1985). For detailed exposition, see M. B. Green, J. H. Schwarz and E. Witten, Superstring Theory (Cambridge Monographs on Mathematical Physics) Vol. 1 and 2, Cambridge University Press; New Ed edition (July 29, 1988) and J. Polchinski, String Theory (Cambridge Monographs on Mathematical Physics) Vol. 1 and 2, Cambridge University Press; New Ed edition (June 2, 2005).
- [24] S. Dimopoulos, S. Raby and F. Wilczek, Phys. Rev. **D 24**, 1681 (1981); W. Marciano and G. Senjanovic, Phys. Rev. **D 25**, 3092 (1982) and M. Einhorn and D.R.T. Jones, Nucl. Phys. **B 196**, 475 (1982). For work in recent years, see P. Langacker and M. Luo, Phys. Rev. **D 44**, 817 (1991); U. Maldi, W. de Boer and H. Furtenau, Phys. Rev. Lett. **B 260**, 131 (1991); F. Anselmo, L. Cifarelli, A. Peterman and A. Zichichi, Nuov. Cim. **A 104**, 1817 (1991).
- [25] K. S. Babu, J. C. Pati and F. Wilczek, “*Fermion masses, neutrino oscillations, and proton decay in the light of SuperKamiokande*” hep-ph/9812538, Nucl. Phys. **B566**, 33 (2000).

- [26] R. Barbieri, L. J. Hall and A. Strumia, Nucl. Phys. **B445**, 219 (1995); hep-ph/9501334.
- [27] F. Borzumati and A. Masiero, Phys. Rev. Lett. **57**, 961 (1986).
- [28] K. S. Babu, J. C. Pati, P. Rastogi, “*Tying in CP and flavor violations with fermion masses and neutrino oscillations*”, hep-ph/0410200; Phys. Rev. **D 71**, 015005 (2005).
- [29] K. S. Babu, J. C. Pati, P. Rastogi, “*Lepton Flavor Violation within a Realistic $SO(10)/G(224)$ Framework*”, Phys. Lett. **B 621**, 160 (2005), hep-ph/0502152.
- [30] C. H. Albright and S. M. Barr, Phys. Rev. **D 58**, 013002 (1998), C. H. Albright, K. S. Babu and S. M. Barr, Phys. Rev. Lett. **81**, 1167 (1998), C. H. Albright and S. M. Barr, Phys. Lett. **B 452**, 287 (1999), Phys. Lett. **B 461**, 218 (1999).
- [31] P. Rastogi, Phys. Rev. **D 72**, 075002 (2005).
- [32] P. Candelas, G.T. Horowitz, A. Strominger and E. Witten, Nucl. Phys. **B258**, 46 (1985); E. Witten, Nucl. Phys. **B258**, 75 (1985).
- [33] I. Antoniadis, G. Leontaris and J. Rizos, Phys. Lett. **B245**, 161 (1990).
- [34] A. Faraggi, Phys. Lett. **B 278**, 131 (1992); Phys. Lett. **B 274**, 47 (1992); Nucl. Phys. **B 403**, 101 (1993); A. Faraggi and E. Halyo, Nucl. Phys. **B 416**, 63 (1994).
- [35] S. Dimopoulos and F. Wilczek, report No NSF-ITP-82-07 (1981), in *The Unity of Fundamental Interactions*, Proc. Erice School (1981), Plenum Press (Ed. A. Zichichi).
- [36] P. Ginsparg, Phys. Lett. **B 197**, 139 (1987); V. S. Kaplunovsky, Nucl. Phys. **B 307**, 145 (1988); Erratum: *ibid.* **B 382**, 436 (1992). For a recent discussion, see K. Dienes, Phys. Rep. **287**, 447 (1997), hep-th/9602045 and references therein.
- [37] K. S. Babu and J. C. Pati, Phys. Lett. **B 384**, 140 (1996). Subsequent papers include: K. S. Babu and J. C. Pati, hep-ph/0203029, Int. J. Mod. Phys. **A 20**, 6403 (2005). See also Refs. [132] and [133].
- [38] See e.g. J. Wess and J. Bagger, *Supersymmetry and Supergravity*, Princeton University Press; 2nd Rev. a edition (1992); R. N. Mohapatra, *Unification and supersymmetry: The frontiers of quark-lepton physics* (Graduate texts in contemporary physics), Springer-Verlag; 2nd ed edition (1992).

- [39] S. P. Martin, hep-ph/9709356 provides a general review of the supersymmetric standard model.
- [40] F. Gabbiani, E. Gabrielli, A. Masiero, L. Silvestrini, Nucl. Phys. **B 477**, 321 (1996), hep-ph/9604387.
- [41] See e.g. G. F. Giudice and A. Masiero, Phys. Lett. **B206**, 480 (1988).
- [42] For alternative solutions to the μ -problem based on gauged $B - L$ symmetry, see: S. King and Q. Shafi, Phys.Lett. **B422**, 135 (1998); S. Jeannerot, S. Khalil, G. Lazarides and Q. Shafi, JHEP **0010**, 012 (2000); K. S. Babu, B. Dutta and R. N. Mohapatra, Phys. Rev. D **65**, 016005 (2002); R. Kitano and N. Okada, Prog. Theor. Phys. **106**, 1239 (2001); L. J. Hall, Y. Nomura and A. Pierce, Phys. Lett. B **538**, 359 (2002); J. Ellis, J. F. Gunion, H. E. Haber, L. Roszkowski and F. Zwirner, Phys. Rev. **D39**, 844 (1989); L. Durand and J. L. Lopez, Phys. Lett. **B217**, 463 (1989).
- [43] N. Arkani-Hamed, S. Dimopoulos and G.R. Dvali, Phys. Lett. **B 429**, 263 (1998).
- [44] See, for example, R. Harnik, G. D. Kribs, D. T. Larson and H. Murayama, Phys. Rev. **D 70**, 015002 (2004); A. Birkedal, Z. Chacko and Y. Nomura, Phys. Rev. **D 71**, 015006 (2005).
- [45] For a review see M. Luty, hep-th/0509029.
- [46] A. H. Chamseddine, R. Arnowitt and P. Nath, Phys. Rev. Lett. **49**, 970 (1982); R. Barbieri, S. Ferrara and C. A. Savoy, Phys. Lett. **B119**, 343 (1982); L. J. Hall, J. Lykken and S. Weinberg, Phys. Rev. **D27**, 2359 (1983); L. Alvarez-Gaume, J. Polchinski and M. B. Wise, Nucl. Phys. **B221**, 495 (1983), N. Ohta, Prog. Theor. Phys. **70**, 542, 1983.
- [47] For a review see M. Dine, hep-th/0003175.
- [48] M. Dine and A. Nelson, Phys. rev. **D 48**, 1277 (1993), M. Dine, A. Nelson and Y. Shirman, Phys. Rev. **D 51**, 1362 (1995), M. Dine, A. Nelson, Y. Nir and Y. Shirman, Phys. Rev. **D 53**, 2658 (1996)
- [49] G. Dvali and A. Pomarol, Phys. Rev. Lett. **77**, 3728 (1996); P. Binetruy and E. Dudas, Phys. Lett. **B389**, 503 (1996).
- [50] For a concrete realization of anomalous U(1) SUSY breaking in the context of a semi-realistic string model see A. Faraggi and J.C. Pati, Nucl. Phys. **B256**, 526 (1998); hep-ph/9712516v3.

- [51] For a link between the SUSY breaking via anomalous U(1) D-term and via induced dilaton F-term, see [50] and N. Arkani-Hamed, M. Dine and S. P. Martin, hep-ph/9803432, Phys. Lett. **B431**, 329 (1998).
- [52] L. Randall and R. Sundrum, Nucl. Phys. **B 557**, 79 (1999), G. F. Giudice, M. A. Luty, H. Murayama and R. Rattazzi, JHEP **9812**, 027 (1998).
- [53] See, for example, D. E. Kaplan and G. D. Kribs, JHEP **0009**, 48 (2000); Z. Chacko and M. A. Luty, JHEP **0205**, 047 (2002); R. Sundrum, Phys. Rev. **D 71**, 085003 (2005); N. Arkani-Hamed, D. E. Kaplan, H. Murayama and Y. Nomura, JHEP **0102**, 041 (2001).
- [54] Z. Chacko, M. A. Luty, A. E. Nelson and E. Ponton, JHEP, **0001**, 003 (2000); D. E. Kaplan, G. D. Kribs and M. Schmaltz, Phys. Rev. **D62**, 035010 (2000).
- [55] S. Raby, Rep. Prog. Phys. **67**, 755 (2004).
- [56] S. M. Barr, Phys. Lett. **B112**, 219 (1982); J. P. Derendinger, J. E. Kim and D. V. Nanopoulos, Phys. Lett. **B139**, 170 (1984); I. Antoniadis, J. Ellis, J. Hagelin and D. V. Nanopoulos, Phys. Lett. **B194**, 231 (1987).
- [57] R. N. Mohapatra and R. E. Marshak, Phys. Rev. Lett, **44**, 1316 (1980).
- [58] Jogesh C. Pati, hep-ph/0606089.
- [59] J. C. Pati and A. Salam, Phys. Rev. **D10**, 275 (1974); R. N. Mohapatra and J. C. Pati, Phys. Rev. **D11**, 566 and 2558 (1975).
- [60] G. Senjanovic and R. N. Mohapatra, Phys. Rev. **D 12**, 1502 (1975).
- [61] See e.g. D. Lewellen, Nucl. Phys. **B 337**, 61 (1990); A. Font, L. Ibanez and F. Quevedo, Nucl. Phys. **B 345**, 389 (1990); S. Chaudhari, G. Hockney and J. Lykken, Nucl. Phys. **B 456**, 89 (1995) and hep-th/9510241; G. Aldazabal, A. Font, L. Ibanez and A. Uranga, Nucl. Phys. **B 452**, 3 (1995); *ibid.* **B 465**, 34 (1996); D. Finnell, Phys. Rev. **D 53** 5781 (1996); A. A. Maslikov, I. Naumov and G. G. Volkov, Int. J. Mod. Phys. **A 11**, 1117 (1996); J. Erler, hep-th/9602032; G. Cleaver, hep-th/9604183; Z. Kakushadze and S. H. Tye, hep-th/9605221 and hep-th/9609027; Z. Kakushadze *et al.*, hep-ph/9705202.
- [62] J.C. Pati, “*Neutrino Masses: Shedding light on Unification and Our Origin*”, Talk given at the Fujihara Seminar, KEK Laboratory, Tsukuba, Japan, February 23-25, 2004, hep-ph/0407220, to appear in the proceedings.

- [63] See e.g. K. S. Babu and R. N. Mohapatra, Phys. Rev. Lett. **70**, 2845 (1993); C. S. Aulakh, B. Bajc, A. Melfo, A. Rasin and G. Senjanovic, hep-ph/0004031; M. C. Chen and K. T. Mahanthappa, Phys. Rev. **D 62**, 113007 (2000); H. S. Goh, R. N. Mohapatra and S. P. Ng, Phys. Lett. **B 570**, 215 (2003); B. Dutta, Y. Mimura, R.N. Mohapatra, Phys. Rev. **D 69**, 115014 (2004); M. Bando, S. Kaneko, M. Obara and M. Tanimoto, Phys. Lett. **B 580**, 229 (2004), hep-ph/0405071; T. Fukuyama, A. Ilakovac, T. Kikuchi and S. Meljanac, hep-ph/0411282.
- [64] See e.g., K.R. Dienes and J. March- Russell, hep-th/9604112; K.R. Dienes, hep-ph/ 9606467.
- [65] These have been introduced in various forms in the literature. For a sample, see e.g., C. D. Froggatt and H. B. Nielsen, Nucl. Phys. **B147**, 277 (1979); L. Hall and H. Murayama, Phys. Rev. Lett. **75**, 3985 (1995); P. Binetruy, S. Lavignac and P. Ramond, Nucl. Phys. **B477**, 353 (1996). In the string theory context, see e.g., A. Faraggi, Phys. Lett. **B278**, 131 (1992).
- [66] For $G(224)$, one can choose the corresponding sub-multiplets – that is $(1, 1, 15)_H$, $(1, 2, \bar{4})_H$, $(1, 2, 4)_H$, $(2, 2, 1)_H$ – together with a singlet S , and write a superpotential analogous to Eq. (4.3).
- [67] If the effective non-renormalizable operator like $\mathbf{16}_2\mathbf{16}_3\mathbf{10}_H\mathbf{45}_H/M'$ is induced through exchange of states with GUT-scale masses involving renormalizable couplings, rather than through quantum gravity, M' would, however, be of order GUT-scale. In this case $\langle\mathbf{45}_H\rangle/M' \sim 1$, rather than $1/10$.
- [68] While $\mathbf{16}_H$ has a GUT-scale VEV along the SM singlet, it turns out that it can also have a VEV of EW scale along the “ $\tilde{\nu}_L$ ” direction due to its mixing with $\mathbf{10}_H^d$, so that the H_d of MSSM is a mixture of $\mathbf{10}_H^d$ and $\mathbf{16}_H^d$. This turns out to be the origin of non-trivial CKM mixings (See Ref. [25]).
- [69] The flavor charge(s) of $\mathbf{45}_H(\mathbf{16}_H)$ would get determined depending upon whether $p(q)$ is one or zero.
- [70] These effective non-renormalizable couplings can of course arise through exchange of (for example) $\mathbf{45}$ in the string tower, involving renormalizable $\mathbf{16}_i\bar{\mathbf{16}}_H\mathbf{45}$ couplings. In this case, one would expect $M \sim M_{\text{string}}$.
- [71] J. C. Pati, “A Unified picture with neutrino as a central feature”, hep-ph/0507307.
- [72] J. C. Pati, “Confronting The Conventional ideas on Grand Unification With Fermion Masses, Neutrino Oscillations and Proton Decay”, hep-ph/0204240;

- [73] For a review, see P. Vogel, Phys. Rev. **D 66**, 010001 (2002).
- [74] See e.g. M. Ciuchini, E. Franco, F. Parodi, V. Lubicz, L. Silvestrini, and A. Stocchi, Talk at “Workshop on the CKM Unitarity Triangle”, Durham, April 2003, hep-ph/0307195.
- [75] An extensive analysis appears in the Proceedings of “The CKM Matrix and the Unitarity Triangle”, ed. by M. Battaglia, A. J. Buras, P. Gambino and A. Stochhi, hep-ph/0304132. For a very recent update, see M. Bona et al., hep-ph/0408079.
- [76] B. Aubert et al. (BaBar Collaboration), hep-ex/0408127; K. Abe et al. (BELLE Collaboration), hep-ex/0507037.
- [77] L. Wolfenstein, Phys. Rev. Lett. **51**, 1945 (1983).
- [78] See L. J. Hall, V. A. Kostelecky and S. Raby, Nucl. Phys **B267**, 415 (1986).
- [79] M. Carena, M. Olechowski, S. Pokorski, and C. E. M. Wagner, Nucl. Phys. **B419**, 213 (1994); hep-ph/9311222.
- [80] H. S. Goh, R. N. Mohapatra and Siew-Phang Ng, Phys. Rev. **D68** 115008 (2003), hep-ph/0308197.
- [81] For a partial list of refereces for works along these lines see e.g. H. Arason et al. Phys. Rev. D **46**, 3945 (1992); D. J. Castano, E. J. Pirad, P. Ramond, Phys. Rev. **D49**, 4882 (1994); K. S. Babu, C. N. Leung and J. Pantaleone, Phys. Lett. **B319**, 191 (1993); H. Fusaoka, Y. Koide, Phys. Rev. **D57**, 3986 (1998); C. R. Das, M. K. Parida, Eur. Phys. J. **C20**, 121 (2001).
- [82] For very recent improved lattice results on light quark masses, see C. Aubin et al. (HPQCD, MILC and UKQCD collaboration), Phys. Rev. **D70** 031504 (2004), hep-lat/0405022, and C. Aubin et al. (MILC collaboration), hep-lat/0407028. These papers give: $m_s^{\overline{MS}}(2 \text{ GeV}) = 76(0)(3)(7)(0)\text{MeV}$, $1/2(m_u + m_d)^{\overline{MS}}(2 \text{ GeV}) = 2.8(0)(1)(3)(0) \text{ MeV}$ and $m_u/m_d = 0.43(0)(1)(8)$. Using these results and extrapolating to 1 GeV, one gets: $m_u(1 \text{ GeV}) \approx 2.1 \pm 0.5 \text{ MeV}$, $m_d(1 \text{ GeV}) \approx 4.9 \pm 0.6 \text{ MeV}$ and $m_s(1 \text{ GeV}) \approx 95 \pm 10 \text{ MeV}$. Note that these values are considerably smaller than those commonly used in literature. Somewhat larger values of the masses are quoted in a paper, also based on

improved lattice-calculation, by M. Goeckeler et al. (QCDSF-UKQCD Collaboration) hep-ph/0409312, which appeared on the web just before the completion of Ref. [28].

- [83] For CKM elements, see e.g. Ref. [74] or most recent update by M. Bona et al. hep-ph/0408079 in Ref. [75]. The bottom quark mass quoted in C. W. Bauer et al. (Phys. Rev. **D67**, 054012 (2003)) is: $m_b(m_b) = 4.22 \pm 0.09 \text{ GeV}$, which is lower than our value given in Eq.(5.17) by about 10-12%. Gluino-loop corrections to m_b for $\mu < 0$ and $\tan\beta = 10$ (say) can, however, reduce m_b by about 6-7%.
- [84] M. Ciuchini et al., JHEP 9810:008 (1998), hep-ph/9808328.
- [85] S. Khalil and E. Kou, Phys. Rev. **D67**, 055009 (2003); hep-ph/0212023.
- [86] A. J. Buras, Proceedings of the International School of Subnuclear Physics, Erice, Italy 2000, p 200-337, edited by A. Zichichi, Publ. by World Scientific; hep-ph/0101336.
- [87] S. Aoki et al., JLQCD Collaboration, Phys. Rev. Lett. **91**, 212001 (2003), hep-ph/0307039.
- [88] For a recent analysis, that allows for uncertainties in (m_t, m_b) , and for the relevant references, see e.g. J. Ellis, K. Olive, Y. Santoso and V. Spanos, Phys. Rev. **D69**, 095004 (2004), hep-ph/0310356.
- [89] UTfit Collaboration, M. Bona et al., hep-ph/0606167.
- [90] E. Lunghi, D. Wyler, Phys. Lett. **B521** 320 (2001), hep-ph/0109149; S. Khalil and E. Kou, Phys. Rev. **D67**, 055009 (2003); hep-ph/0212023; R. Harnik, D. T. Larson, H. Murayama, A. Pierce, Phys. Rev. **D69**, 094024 (2004), hep-ph/0212180.
- [91] B. Aubert et al. (BaBar Collaboration), hep-ex/0403026; K. Abe et al. (BELLE Collaboration), Phys. Rev. Lett. **91**, 261602 (2003); The most recent results on $S(B_d \rightarrow \phi K_S)$ appear in the papers of B. Aubert et al. (BaBar Collaboration), hep-ex/0408072, and K. Abe et al. (BELLE Collaboration), hep-ex/0608039.
- [92] See e.g. D. Chang, A. Masiero and H. Murayama, Phys. Rev. **D67**, 075013 (2003), hep-ph/0205111; T. Moroi, Phys. Lett. **B493**, 366 (2000), hep-ph/0007328; G.L. Kane, P. Ko, H. Wang, C. Kolda, J. Park, L. Wang, Phys. Rev. **D70**, 035015 (2004), hep-ph/0212092; J. Park, hep-ph/0312118; J. Hisano and Y. Shimizu, Phys. Lett. **B565**, 183 (2003), hep-ph/0303071; T. Goto, Y.

- Okada, Y. Shimizu, T. Shindou and M. Tanaka, Phys. Rev. **D70**, 0305012 (2004), hep-ph/0306093.
- [93] A. J. Buras, G. Colangelo, G. Isidori, A. Romanino, and L. Silvestrini, Nucl. Phys. **B566**,3 (2000); hep-ph/9908371.
- [94] Y. Nir, Lectures Given at Scottish Univ. Summer School, Scotland 2001; hep-ph/0109090.
- [95] T. Blum et al. (RBC collab.), Phys. Rev. **D68**, 114506 (2003), hep-lat/0110075. See A. Soni, Talk at Pascos 2003 Conference, Mumbai (India), Pramana **62** 415 (2004), hep-ph/0307107, for a critical review of this and similar works.
- [96] J. Noaki et al., Phys. Rev. **D68**, 014501 (2003).
- [97] M. Golterman and E. Pallante, JHEP **0110**, 037 (2001), Phys. Rev. **D69**, 074503 (2004).
- [98] T. Bhattacharya, G. T. Fleming, R. Gupta, G. Kilcup, W. Lee and S. Sharpe, hep-lat/0409046.
- [99] A. Pich, hep-ph/0410215; E. Pallante, A. Pich and I. Scimemi, Nucl. Phys. **B617**, 441 (2001); E. Pallante and A. Pich, Phys. Rev. Lett. **84**, 2568 (2000), Nucl. Phys. **B592**, 294 (2000).
- [100] A. Alavi-Harari et al. (KTev collab.), Phys. Rev. Lett **83**, 22 (1999); A. Lai et al. (NA48 collab.), Eur. Phys. J. **C 22**, 231 (2001).
- [101] T. Ibrahim and P. Nath, Phys. Rev. **D57**, 478 (1998), Phys. Rev. **D58**, 111301 (1998).
- [102] See e.g. J. Ellis, J. F. Gunion, H. E. Haber, L. Roszkowski and F. Zwirner, Phys. Rev. **D39**, 844 (1989); L. Durand and J. L. Lopez, Phys. Lett. **B217**, 463 (1989).
- [103] P. Harris et al. Phys. Rev. Lett. **82**, 94 (1999).
- [104] E. D. Commins et al, Phys. Rev. **A50**, 2960 (1994).
- [105] For a sample see: C. H. Albright, K. S. Babu and S. M. Barr, Phys. Rev. Lett. **81**, 1167 (1998) J. Sato and T. Yanagida, Phys. Lett. B **430**, 127 (1998) N. Irges, S. Lavignac and P. Ramond, Phys. Rev. D **58**, 035003 (1998); C. H. Albright and S. M. Barr, Phys. Lett. B **461**, 218 (1999); G. Altarelli and F. Feruglio,

- Phys. Lett. B **451**, 388 (1999); T. Blazek, S. Raby and K. Tobe, Phys. Rev. **D62**, 055001 (2000), hep-ph/9912482; K. Hagiwara and N. Okamura, Nucl. Phys. B **548**, 60 (1999); M. C. Chen and K. T. Mahanthappa, Int. J. Mod. Phys. A **18**, 5819 (2003); C. S. Huang, T. j. Li and W. Liao, Nucl. Phys. B **673**, 331 (2003); N. Maekawa, arXiv:hep-ph/0402224.
- [106] K. S. Babu, Z. Phys. **C 35**, 69 (1987).
- [107] V. D. Barger, M.S. Berger, P. Ohmann, Phys. Rev. **D 47**, 2038 (1993).
- [108] M. L. Brooks *et al* [MEGA collaboration] Phys. Rev. Lett. **83**, 1521 (1999).
- [109] B. Aubert *et al* [BaBar Collaboration], Phys. Rev. Lett. **95**, 041802 (2005).
- [110] B. Aubert *et al* [BaBar Collaboration], Phys. Rev. Lett. **96**, 041801 (2006).
- [111] J. Hisano, T. Moroi, K. Tobe, M. Yamaguchi, Phys. Rev. **D 53**, 2442 (1996).
- [112] See e.g. S. F. King and M. Oliveira, Phys. Rev. **D 60**, 035003 (1999), J. Hisano and D. Nomura, Phys. Rev. **D 59**, 116005 (1999), W. Buchmuller, D. Delepine and F. Vissani, Phys. Lett. **B 459**, 171 (1999), K. S. Babu, B. Dutta and R. N. Mohapatra, Phys. Lett. **B 458**, 93 (1999); Phys. Rev. **D 67**, 076006 (2003), A. Belyaev *et al*, Eur. Phys. J. C **22**, 715 (2002), J. Sato, K. Tobe and T. Yanagida, Phys. Lett. **B 498**, 189 (2001), S. Lavignac, I. Masina and C. A. Savoy, Phys. Lett. **B 510**, 197 (2001), S. Baek *et al* Phys. Rev. **D 64**, 095001 (2001), J. Ellis *et al*, Nucl. Phys. **B 621**, 208 (2002), S. T. Petcov *et al*, Nucl. Phys. **B 676**, 453 (2004), A. Masiero *et al*, JHEP **0403**, 046 (2004), G. G. Ross, L. Velasco-Sevilla and O. Vives, Nucl. Phys. **B 692**, 50 (2004).
- [113] See e.g. J. Hisano *et al*, Phys. Lett. **B 391**, 341 (1997) [Erratum-ibid. **B 397**, 357 (1997)], J. Hisano, D. Nomura and T. Yanagida, Phys. Lett. **B 437**, 351 (1998), M. Ciuchini *et al*, Nucl. Phys. **B 548**, 60 (1999), Y. Okada, K. I. Okumura and Y. Shimizu, Phys. Rev. **D 61**, 094001 (2000).
- [114] See e.g. X. J. Bi, Y. B. Dai and X. Y. Qi, Phys. Rev. **D 63**, 096008 (2001), X. J. Bi and Y. B. Dai, Phys. Rev. **D 66**, 076006 (2002), S. M. Barr, Phys. Lett. **B 578**, 394 (2004), B. Dutta and R.N. Mohapatra, Phys. Rev. **D 68**, 113008 (2003), Phys. Rev. **D 68**, 056006 (2003), B. Dutta, Y. Mimura, R.N. Mohapatra, Phys. Rev. **D 69**, 115014 (2004), Int. J. Mod. Phys. **A 20**, 1180 (2005), E. Jankowski and D. W. Maybury, Phys. Rev. **D 70**, 035004 (2004), M. Bando *et al*, hep-ph/0405071, M. C. Chen and K. T. Mahanthappa, hep-ph/0409096, T. Fukuyama *et al*, hep-ph/0411282.
- [115] J. Hisano and D. Nomura, Phys. Rev. **D 59**, 116005 (1999).

- [116] J. F. Gunion and H. E. Haber, Phys. Rev. **D 37**, 2515 (1988).
- [117] K. A. Olive, hep-ph/0412054.
- [118] H. Baer, A. Mustafayev, S. Profumo, A. Belyaev, X. Tata, hep-ph/0412059.
- [119] See e.g. A. Czarnecki, W. J. Marciano and K. Melnikov, hep-ph/9801218.
- [120] See e.g. B. Dutta *et al* (Ref. [114]) and Y. Okada *et al* (Ref. [113]).
- [121] For a review see e.g. W. J. Marciano, hep-ph/0411179 and references there in.
- [122] H. Baer, C. Balazs, A. Belyaev, T. Krupovnickas and X. Tata, JHEP **0306**, 054 (2003).
- [123] See e.g. K. S. Babu and R. N. Mohapatra, Phys. Rev. Lett. **70**, 2845 (1993); T. Blazek, M. Carena, S. Raby and C. Wagner, Phys. Rev. **D 56**, 6919 (1997); T. Blazek, S. Raby, K. Tobe, Phys. Rev. **D 60**, 113001 (1999), Phys. Rev. **D 62**, 055001 (2000); H. Nishiura, K. Matsuda, T. Fukuyama, Phys. Rev. **D 60**, 013006 (1999), Phys. Rev. **D 61**, 053001 (2000); R. Dermisek and S. Raby, Phys. Rev. **D 62**, 015007 (2000); C. S. Aulakh, B. Bajc, A. Melfo, A. Rasin and G. Senjanovic, hep-ph/0004031; M. C. Chen and K. T. Mahanthappa, Phys. Rev. **D 62**, 113007 (2000); T. Fukuyama, N. Okada, hep-ph/0205066; H. S. Goh, R. N. Mohapatra and S. P. Ng, Phys. Lett. **B 570**, 215 (2003); B. Dutta, Y. Mimura, R.N. Mohapatra, Phys. Rev. **D 69**, 115014 (2004); M. Bando, S. Kaneko, M. Obara and M. Tanimoto, Phys. Lett. **B 580**, 229 (2004), hep-ph/0405071; T. Fukuyama, A. Ilakovac, T. Kikuchi and S. Meljanac, hep-ph/0411282.
- [124] X. J. Bi, Eur. Phys. J. **C 27**, 399 (2003); S. Pascoli, S.T. Petcov, C.E. Yaguna, Phys. Lett. **B 564**, 241 (2003); S.T. Petcov, S. Profumo, Y. Takanishi, C.E. Yaguna, Nucl. Phys. **B 676**, 453 (2004); See also Refs. [129] and [126].
- [125] C. H. Albright and S. M. Barr, Phys. Rev. **D 64**, 073010 (2001).
- [126] E. Jankowski and D. W. Maybury, Phys. Rev. **D 70**, 035004 (2004).
- [127] G. K. Leontaris, K. Tamavakis and J. D. Verdagos, Phys. Lett. **B171**, 412 (1986).
- [128] Web Page: <http://meg.psi.ch>
- [129] S. M. Barr, Phys. Lett. **B 578**, 394 (2004), hep-ph/0307372.

- [130] K. S. Babu and S. M. Barr, Phys. Rev. **D48**, 5354 (1993).
- [131] M. Bastero-Gil and B. Brahmachari, Nucl. Phys. **B 575**,35 (2000).
- [132] K. S. Babu, J. C. Pati and H. Stremnitzer, Phys. Rev. **D 51**,2451 (1995).
- [133] K. S. Babu and J. C. Pati, Phys. Rev. **D 68**, 035004 (2003).
- [134] ALEPH, DELPHI, L3 and Opal Collaborations and the LEP Higgs working group, hep-ex/0107030; ALEPH Collaboration, hep-ex/0201014.
- [135] T. Elliott, S.F. King and P.L. White, Phys. Rev. **D 49**, 2435 (1994).
- [136] An extensive review is presented in A. J. Buras, hep-ph/9806471.
- [137] S. P. Martin and M. T. Vaughn, Phys. Rev. **D 50**, 2282